DISSERTATION

SYSTEMATIC ANALYSIS OF BENEFICIAL REUSE IN UNCONVENTIONAL OIL AND GAS WASTEWATER MANAGEMENT

Submitted by

Cristian A. Robbins

Department of Civil and Environmental Engineering

In partial fulfillment of the requirements

For the Degree of Doctor of Philosophy

Colorado State University

Fort Collins, Colorado

Spring 2021

Doctoral Committee:

Advisor: Tiezheng Tong
Co-Advisor: Kenneth Carlson

Sybil Sharvelle
Todd Bandhauer

ABSTRACT

SYSTEMATIC ANALYSIS OF BENEFICIAL REUSE IN UNCONVENTIONAL OIL AND GAS WASTEWATER MANAGEMENT

Wastewater management within the unconventional oil and gas (UOG) sector has continued to grow in importance in correlation with the rising water footprint of hydraulic fracturing (HF). The predominant UOG wastewater management method in the U.S. is to dispose of the wastewater deep underground in geologically stable formations by deep-well injection (DWI). However, this method has been plagued with concerns such as induced seismicity and decreasing capacity for DWI in various UOG regions. Further, when the wastewater is disposed of via DWI this potential resource is no longer available for beneficial purposes. An alternative method to DWI is UOG wastewater treatment for beneficial reuse which repurposes the treated wastewater for end uses such as surface discharge. The main objective of this dissertation is to analyze key aspects of UOG wastewater management to include topics within technology, logistics, regulations, and economics in order to further facilitate increased wastewater treatment and beneficial reuse.

At the core of UOG wastewater treatment and beneficial reuse is an advanced treatment technology that can effectively treat hypersaline and complex UOG wastewater. For my work, I focused on membrane distillation (MD), a hybrid thermal-membrane desalination process well-suited to treat UOG wastewater. An advantage of using MD is its inherent ability to use low grade waste heat as an energy source to power treatment. I investigated the availability and sufficiency of waste heat at the well-pad to power MD for on-site UOG wastewater treatment in

Weld County, Colorado. Additionally, I also investigate the availability and sufficiency of natural gas at the well-pad to power MD. The analysis showed that well-pad waste heat is insufficient while natural gas is sufficient for long term on-site MD treatment.

Next, the impact of logistics, specifically transportation distance and costs, was researched for DWI and centralized wastewater treatment (CWT) powered by natural gas compressor station (NGCS) waste heat. Unlike on-site treatment, wastewater needs to be transported for DWI or CWT and thus incurs a transportation cost. Using ArcGIS software, transportation distances and associated costs were analyzed for Weld County, Colorado at various scales. At the county scale, DWI was economically favored based on transportation, however, when the scale of operation was reduced for certain areas (i.e., county to local) the economic advantage shifted towards CWT. Additionally, NGCS waste heat for Weld County was quantified and the MD treatment demand was correlated to MD treatment capacity provided by NGCS waste heat for CWT. This analysis emphasized the importance of matching treatment demand with capacity provided by waste heat.

Further, MD treatment of UOG wastewater has been constrained by surfactant-induced membrane pore wetting. Surfactants, commonly found in HF fluid, reduce the surface tension of membranes inducing wetting. We investigated two mitigation strategies, pretreatment via coagulation-adsorption and fabrication of omniphobic membranes. UOG wastewater sourced from the Denver-Julesburg Basin that induced exceptional wetting of a hydrophobic polyvinylidene fluoride membrane during MD treatment was used. Both strategies proved effective at mitigating surfactant-induced wetting, however, flux decline with the use of omniphobic membrane was unacceptable due to the effects of fouling thus hindering its viability. To better understand the surfactant composition in the UOG wastewater, ultrahigh pressure

liquid chromatography (UHPLC) coupled with quadrupole time-of-flight mass spectrometry (QToF/MS) was implemented to identify surfactants in the UOG wastewater and qualify the effect of pretreatment in reducing surfactants. In the UOG wastewater, 192 surfactants were identified with 91 being reduced by full pretreatment.

Finally, an in-depth perspective on the motivations and barriers to increased future treatment and beneficial reuse of UOG wastewater was provided. This analysis moved beyond technology, which receives the majority of research interest, to explore and better understand other non-treatment aspects. Four major barriers to beneficial reuse were identified which are technology, economics, regulations, and social. These barriers were clearly elucidated providing insight into ways to overcome them to facilitate increased beneficial reuse. A systems-level approach requiring broad collaborations across multiple disciplines pertaining to technology, policy, legislation, economics, and social science to shift UOG wastewater management towards treatment and beneficial reuse was proposed.

ACKNOWLEDGEMENTS

I would like to express a debt of gratitude to my advisor, Dr. Tiezheng Tong. His diligence, hard work, and keen attention to detail kept me on track and enabled the completion of this dissertation.

I am very grateful to have Dr. Kenneth Carlson to serve as my co-advisor. Dr. Carlson provided his profound insight and expertise for my research and helped guide it in the right direction. I would like to thank Dr. Sybil Sharvelle and Dr. Todd Bandhauer for serving on my committee. I greatly benefited from both of their academic acumen and appreciate the valuable time they provided to improve my research.

For the opportunity to pursue a PhD degree, I would like to thank the United States Army and specifically the Department of Geography and Environmental Engineering at the United States Military Academy. I appreciate those within the department who supported and selected me to return as faculty at my alma mater.

Last but most importantly, I would like to express my undying gratitude to my wife, Tracy, and my three children: Cameron, Landon, and Gwendolyn. Without your unwavering support and resiliency through my Army career and specifically during my time pursuing a PhD degree, this would not have been possible. I can always count on all of you to help get me through challenging times and motivate me to achieve my goals.

TABLE OF CONTENTS

LIST OF TABLES

LIST OF FIGURES

1.0 Introduction

In the past decade, the United States has witnessed a rapid growth of unconventional oil and gas (UOG) exploration and production. Meanwhile, the water use and wastewater production of hydraulic fracturing (HF) in major shale oil and gas regions have steadily increased (Kondash et al., 2018). During HF activities, large volumes of freshwater along with fracturing fluids and sand are injected under high pressure to fracture the underlying reservoir rock to stimulate hydrocarbon production (Barati and Liang, 2014) and subsequently produce substantial amounts of wastewater. For example, in the Niobrara shale formation situated in northeastern Colorado and parts of Wyoming, Nebraska, and Kansas, the volume of wastewater generated within the first 12 months of well completion increased from 1,823 m^3 (481,586 gallons)/well in 2011 to 2,959 m^3 (781,685 gallons)/well in 2016 (Kondash et al., 2018). In 2016 alone, ~45.4 million m^3 (~12 billion gallons) of wastewater were produced from oil and gas wells in Colorado (Dolan et al., 2018). From 2015 to 2019, the amount of water used for HF has steadily increased which in turn will lead to the generation of increasingly larger volumes of UOG wastewater (Figure 1-1). In four states with large shale oil and gas plays (Colorado, Texas, Pennsylvania, and North Dakota), the amount of water used for HF per well increased between 57.1% and 153.3% from 2015 to 2019 (Figure 1-1).

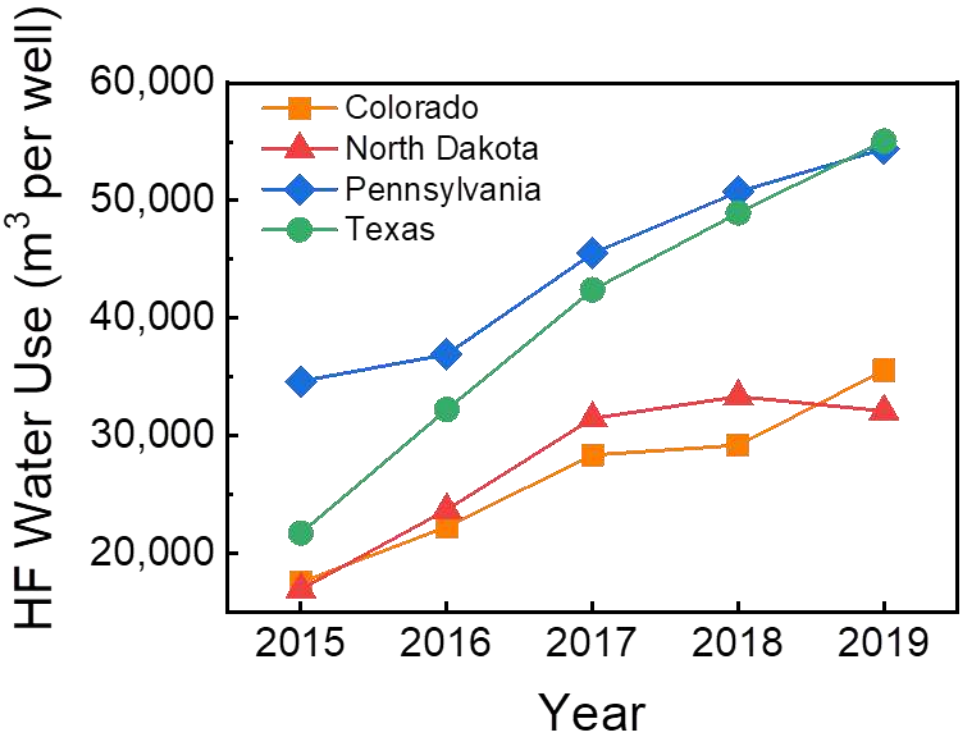

Figure 1-1. HF water use in four major oil and gas producing states in the U.S. from 2015 to 2019 (data collected from the FracFocus registry, 2020).

The current management practices for UOG wastewater rely heavily on injection into Class II Underground Injection Control (UIC) disposal wells (Brantley et al., 2014; Rahm and Riha, 2014; USEPA, 2018). Although deep-well injection (DWI) is technically mature, the availability of disposal wells has become increasingly limited (Whitfield, 2017). Multiple concerns such as induced seismicity, potential groundwater contamination, and the lack of available reservoir capacity continue to hinder DWI, leaving its future viability in doubt (Ellsworth, 2013; Shaffer et al., 2013 Gregory and Mohan, 2015; Tavakkoli et al., 2017; Hincks et al., 2018; Scanlon et al., 2018). Specifically, the concern regarding induced seismicity has grown as evidenced by the increase of earthquakes with a magnitude greater than 3.0 in the central U.S. over the last decade (Figure 1-2). The growing concern has resulted in updated regulations and policies in some states limiting DWI as a UOG wastewater management method.

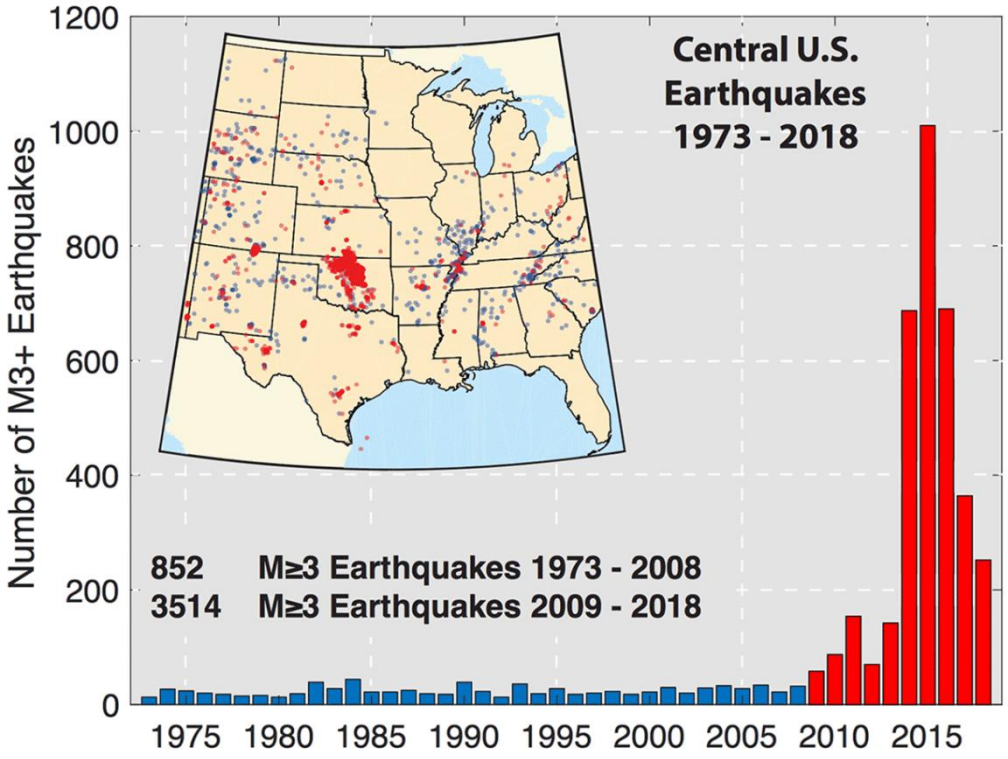

Figure 1-2. Annual number of earthquakes with a magnitude of 3.0 or larger in the central and eastern United States, 1973-2018 (United States Geological Survey, 2019).

In recent years, alternative approaches to manage UOG wastewater have gained increasing popularity, as highlighted by the extensive research activities associated with the treatment and beneficial reuse of such wastewater (e.g. discharge into surface waters and agricultural irrigation) (Rahm et al., 2013; Akob et al., 2016; Butkovskyi et al., 2017; Dolan et al., 2018; Jimenez et al., 2018; Ma et al., 2018; Chang et al., 2019a). UOG wastewater is characterized as having high salinity (often higher than seawater) along with various organic and inorganic contaminants such as petroleum-associated compounds, heavy metals, and radioactive materials (Kahrilas et al., 2016; Butkovskyi et al., 2017; Silva et al., 2017; Chang et al., 2019b; Sun et al., 2019). An important consideration in regards to treatment and beneficial reuse of UOG wastewater is the use of a core advanced treatment technology to attain a high quality water product. Membrane distillation (MD), a hybrid thermal-membrane desalination process, has emerged as a suitable

technology to treat complex and hypersaline wastewater such as UOG wastewater (Boo et al., 2016; Lokare et al., 2017; Tavakkoli et al., 2017; Tong et al., 2019; Zhang et al., 2019; Robbins et al., 2020; Robbins et al., 2021). MD is driven by a vapor pressure difference generated between the warmer feedwater and cooler permeate stream (Lawson and Lloyd, 1997). MD is only slightly sensitive to the feed salinity, which ranges between ~10,000-360,000 mg L^{-1} total dissolved solids (TDS) for UOG wastewater (Chang et al., 2019a), improving the viability of treating hypersaline UOG wastewater (Shaffer et al., 2013; Xu et al., 2013). Also, the feedwater only needs to be heated to a moderate temperature (60-80°C) and thus MD may utilize low-grade waste heat as an energy source to improve the economic viability of UOG wastewater treatment (Deshmukh et al., 2018; Robbins et al., 2020).

However, conventional hydrophobic MD membranes are constrained by membrane pore wetting, especially in the treatment of UOG wastewater. Surfactant-induced wetting is a major concern in MD desalination (Wang and Lin, 2017; Horseman et al., 2021). In UOG wastewater, high levels of surfactants along with other low surface tension contaminants such as oil, grease, and organic solvents have been reported (Lester et al., 2015; Thurman et al., 2015; Boo et al., 2016; Butkovskyi et al., 2017). Surfactants are a typical component of hydraulic fracturing (HF) fluids to facilitate the recovery of shale oil and gas (Butkovskyi et al., 2017). When treating surfactant-laden UOG wastewater, wetting may be induced constraining MD performance. Thus, the mitigation of surfactant-induced wetting is a necessity for the viability of MD treatment of UOG wastewater.

Waste heat has been proposed in previous work to power MD for the treatment of UOG and other hypersaline wastewater (Dow et al., 2016; Tavakkoli et al., 2016; Dow et al., 2017; Tavakkoli et al., 2017; Lai et al., 2018; Schwantes et al., 2018; Yuan et al., 2020). However, the

availability of waste heat at individual oil and gas well-pads or off-pad locations (i.e., natural gas compressor stations) along with the correlation of treatment demand with MD treatment capacity with waste heat as the energy source has not been rigorously investigated. Natural gas which is plentiful (Geary, 2019) and sometimes flared during the initial stages of oil and gas production (Magill, 2016) provides another intriguing energy source to power MD treatment that, like waste heat, has not been rigorously investigated.

Despite the extensive research activities associated with treatment and beneficial reuse, wastewater treatment and reuse (except for internal reuse for HF) has not been widely adopted by the UOG industry. Current efforts of research are still focused on improving the performance and energy efficiency of treatment technologies, which will remarkably enhance the viability of UOG wastewater treatment. However, treatment technology is not the only barrier to the shift of the wastewater management paradigm towards treatment and reuse in the UOG industry. Other aspects beyond treatment technology, including regulation and policy, economics, social acceptance, as well as system logistics, play equally or more important roles collectively in the selection and deployment of wastewater management practices. Such non-treatment aspects, which have been rarely discussed in the literature, have created significant barriers that prohibit practical implementation of newly developed wastewater treatment technologies. One of these non-treatment aspects, system logistics, could play an equally important role as compared to treatment costs in determining the economic feasibility of UOG wastewater treatment and reuse. Specifically, logistical considerations such as transportation distance and costs tailored to the UOG region of interest could be a determining factor for the selected UOG wastewater management strategy (Tavakkoli et al., 2020). Further research is needed in all aspects of UOG wastewater treatment and reuse to enhance its future viability as a management strategy.

In this dissertation, a review of literature for important topics within unconventional oil and gas wastewater management beneficial reuse such as treatment technologies, energy sources for treatment, along with logistical and regulatory considerations are provided in Chapter 2. An outline of research questions and objectives are presented in Chapter 3. Chapter 4 provides analysis on the use of waste heat or natural gas to power on-site membrane distillation treatment of UOG wastewater in Weld County, Colorado. In Chapter 5, a spatial analysis is conducted to compare membrane distillation treatment powered by natural gas compressor station waste heat to the predominant UOG wastewater management practice of DWI in Weld County, Colorado based on logistical considerations. Chapter 6 compares the effectiveness of pretreating UOG wastewater with coagulation and walnut shell filtration versus fabricating an omniphobic membrane in the mitigation of membrane wetting for MD treatment of UOG wastewater at the laboratory scale. Finally, Chapter 7 presents a thorough understanding of the motivations and barriers for UOG wastewater treatment and reuse along with presenting ways to overcome these barriers in the future to enable increased beneficial reuse.

References

Akob, D.M., Mumford, A.C., Orem, W., Engle, M.A., Klinges, J.G., Kent, D.B, Cozzarelli, I.M., 2016. Wastewater disposal from unconventional oil and gas development degrades stream quality at a West Virginia injection facility. *Environ. Sci. Technol.* 50 (11), 5517-5525.

Barati, R., Liang, J.T., 2014. A review of fracturing fluid systems used for hydraulic fracturing of oil and gas wells. *J. Appl. Poly. Sci.* 131 (16), 40735.

Boo, C., Lee, J., Elimelech, M., 2016. Omniphobic polyvinylidene fluoride (PVDF) membrane for desalination of shale gas produced water by membrane distillation. *Environ. Sci. Technol. 50* (22), 12275-12282.

Brantley, H.L., Thoma, E.D., Eisele, A.P., 2015. Assessment of volatile organic compound and hazardous air pollutant emissions from oil and natural gas well pads using mobile remote and on-site direct measurements. *J. Air Waste Manage. Assoc.* 65 (9), 1072-1082.

Brantley, S.L., Yoxtheimer, D., Arjmand, S., Grieve, P., Vidic, R., Pollak, J., Llewellyn, G.T., Abad, J., Simon, C., 2014. Water resource impacts during unconventional shale gas development: The Pennsylvania experience. *Int. J. Coal Geo.* 126, 140-156.

Butkovskyi, A., Bruning, H., Kools, S.A.E., Rijnaarts, H.H.M., Van Wezel, A.P., 2017. Organic pollutants in shale gas flowback and produced waters: Identification, potential ecological impact, and implications for treatment strategies. *Environ. Sci. Technol.* 51 (9), 4740-4754.

Chang, H., Li., T., Liu, B., Vidic, R.D., Elimelech, M., Crittenden, J.C., 2019a. Potential and implemented membrane-based technologies for the treatment and reuse of flowback and produced water from shale gas and oil plays: A review. *Desalination* 455, 34-57.

Chang, H., Liu, B., Yang, B., Yang, X., Guo, C., He, Q., Liang, S., Chen, S., Yang, P., 2019b. An integrated coagulation-ultrafiltration-nanofiltration process for internal reuse of shale gas flowback and produced water. *Sep. Purification Tech.* 211, 310-321.

Deshmukh, A., Boo, C., Karanikola, V., Lin, S.H., Straub, A.P., Tong, T.Z., Warsinger, D.M., Elimelech, M., 2018. Membrane distillation at the water-energy nexus: Limits, opportunities, and challenges. *Energy Environ. Sci.* 11, 1177-1196.

Dolan, F.C., Cath, T.Y., Hogue, T.S., 2018. Assessing the feasibility of using produced water for irrigation in Colorado. *Sci. Total Environ.* 640-641, 619-628.

Dow, N., Gray, S., Jun-de, L., Zhang, J., Ostarcevic, E., Liubinas, A., Atherton, P., Roeszler, G., Gibbs, A., Duke, M., 2016. Pilot trial of membrane distillation driven by low grade waste heat: Membrane fouling and energy assessment. *Desalination* 391, 30-42.

Dow, N ., Villalobos Garcia, J., Niadoo, L., Milne, N., Zhang, J., Gray, S., Duke, M., 2017. Demonstration of membrane distillation on textile waste water: Assessment of long term performance, membrane cleaning and waste heat integration. *Environ. Sci.: Water Res. Technol.* 3, 433-449.

Ellsworth, W.L., 2013. Injection-induced earthquakes. *Science* 341 (6142), 1225942.

FracFocus, 2020. FracFocus Data Download. FracFocus web site. https://fracfocus.org/node/356/done?sid=20424 (accessed April 26, 2020).

Geary, E., 2019. U.S. natural gas production hit a new record high in 2018. U.S. E.I.A. website. https://www.eia.gov/todayinenergy/detail.php?id=38692 (accessed Jan. 25, 2021).

Gregory, K., Mohan, A.M., 2015. Current perspective on produced water management challenges during hydraulic fracturing for oil and gas recovery. *Environ. Chemistry* 12 (3), 261-266.

Horseman, T., Yin, Y., Christie, K.S.S., Wang, Z., Tong, T., Lin, S., 2021. Wetting, scaling, and fouling in membrane distillation: State-of-the-art insights on fundamental mechanisms and mitigation strategies. *ACS EST Engg.* 1, 117-140.

Hincks, T., Aspinall, W., Cooke, R., Gernon, T., 2018. Oklahoma's induced seismicity strongly linked to wastewater injection depth. *Science* 359 (6381), 1251.

Jimenez, S., Mico, M.M., Arnaldos, M., Medina, F., Contreras, S., 2018. State of the art of produced water management. *Chemosphere* 192, 186-208.

Kahrilas, G.A., Blotevogel, J., Corrin, E.R., Borch, T., 2016. Downhole transformation of the hydraulic fracturing fluid biocide glutaraldehyde: Implications for flowback and produced water quality. *Environ. Sci. Technol.* 50 (20), 11414-11423.

Kondash, A., Lauer, N., Vengosh, A., 2018. The intensification of the water footprint of hydraulic fracturing. *Sci. Adv.* 4 (8), eaar5982.

Lai. X., Long, R., Liu, Z., Liu, W., 2018. A hybrid system using direct contact membrane distillation for water production to harvest waste heat from the proton exchange membrane fuel cell. *Energy* 147, 578-586.

Lawson, K.W., Lloyd, D.R., 1997. Membrane distillation. *J. Membr. Sci.* 124 (1), 1-25.

Lester, Y., Ferrer, I., Thurman, E. M., Sitterley, K. A., Korak, J. A., Aiken, G., Linden, K. G., 2015. Characterization of hydraulic fracturing flowback water in Colorado: Implications for water treatment. *Sci. Total Environ. 512-513*, 637-644.

Lokare, O. R., Tavakkoli, S., Wadekar, S., Khanna, V., Vidic, R. D., 2017. Fouling in direct contact membrane distillation of produced water from unconventional gas extraction. *J. Membr. Sci. 524*, 493-501.

Ma, G., Geza, M., Cath, T.Y., Drewes, J.E., Xu, P., 2018. iDST: An integrated decision support tool for treatment and beneficial use of non-traditional water supplies – Part II: Marcellus and Barnett Shale case studies. *J. Water Proc. Eng.* 25, 258-268.

Magill, B.. 2016. U.S. Has More Gas Flares than Any Country. *Scientific American* [Online], https://www.scientificamerican.com/article/u-s-has-more-gas-flares-than-any-country/ (accessed Jul. 5, 2019).

Rahm, B.G., Bates, J.T., Bertoia, L.R., Galford, A.E., Yoxtheimer, D.A., Riha, S.J., 2013. Wastewater management and Marcellus Shale gas development: Trends, drivers, and planning implications. *J. Environ. Manage.* 120, 105-113.

Rahm, B.G., Riha, S.J., 2014. Evolving shale gas management: Water resource risks, impacts, and lessons learned. *Environ. Sci. Proc. Impacts* 16 (6), 1400-1412.

Robbins, C.A., Grauberger, B.M., Garland, S.D., Carlson, K.H., Lin, S., Bandhauer, T.M., Tong, T., 2020. On-site treatment capacity of membrane distillation powered by waste heat or

natural gas for unconventional oil and gas wastewater in the Denver-Julesburg Basin. *Environ. Inter*. 145, 106142.

Robbins, C.A.; Carlson, K.H.; Garland, S.D.; Bandhauer, T.M.; Grauberger, B.M.; Tong, T., 2021. Spatial analysis of membrane distillation powered by waste heat from natural gas compressor stations for unconventional oil and gas wastewater treatment in Weld County, Colorado. *ACS Environ. Sci. Tech. Engg.* 1 (2), 192-203.

Scanlon, B.R., Weingarten, M.B., Murray, K.E., Reedy, R.C., 2018. Managing basin-scale fluid budgets to reduce injection-induced seismicity from the recent U.S. shale oil revolution. *Seis. Res. Let.* 90 (1), 171-182.

Schwantes, R., Chavan, K., Winter, D., Felsmann, C., Pfafferott, J., 2018. Techno-economic comparison of membrane distillation and MVC in a zero liquid discharge application. *Desalination 428*, 50-68.

Shaffer, D.L., Arias Chavez, L.H., Ben-Sasson, M., Romero-Vargas Castrillon, S., Yip., N.Y., Elimelech, M., 2013. Desalination and reuse of high-salinity shale gas produced water: Drivers, technologies, and future directions. *Environ. Sci. Technol.* 47 (17), 9569-9583.

Silva, T.L., Morales-Torres, S., Castro-Silva, S., Figueiredo, J.L., Silva, A.M., 2017. An overview on exploration and environmental impact of unconventional gas sources and treatment options for produced water. *Sep. Purification Tech.* 211, 310-321.

Sun, Y., Wang, D., Tsang, D.C., Wang, L., Ok, Y.S., Feng, Y., 2019. A critical review of risks, characteristics, and treatment strategies for potentially toxic elements in wastewater from shale gas extraction. *Environ. Int.* 125, 452.469.

Tavakkoli, S., Lokare, O. R., Vidic, R. D., Khanna, V., 2016. Systems-level analysis of waste heat recovery opportunities from natural gas compressor stations in the United States. *ACS Sustain. Chem. Eng. 4* (7), 3618-3626.

Tavakkoli, S., Lokare, O.R., Vidic, R.D., Khanna, V., 2017. A techno-economic assessment of membrane distillation for treatment of Marcellus shale produced water. *Desalination* 416, 24-34.

Tavakkoli, S., Lokare, O., Vidic, R., Khanna, V., 2020. Shale gas produced water management using membrane distillation: An optimization-based approach. *Resources, Conservation & Recycling* 158 (2020), 104803.

Thurman, E.M., Ferrer, I., Blotevogel, J., Borch, T., 2014. Analysis of hydraulic fracturing flowback and produced waters using accurate mass: Identification of ethoxylated surfactants. *Anal. Chem.* 86, 9653-9661.

Tong, T., Carlson, K.H., Robbins, C.A., Zhang, Z., Du, X., 2019. Membrane-based treatment of shale oil and gas wastewater: The current state of knowledge. *Front. Environ. Sci. Eng.* 13 (4): 63.

United States Environmental Protection Agency, 2018. Class II Oil and Gas Related Injection Wells. USEPA web site. https://www.epa.gov/uic/class-ii-oil-and-gas-related-injection-wells (accessed April 27, 2020).

United States Geological Survey, 2019. Induced Earthquakes. United States Geological Survey web site. https://www.usgs.gov/natural-hazards/earthquake-hazards/induced-earthquakes?qt-science_support_page_related_con=4#qt science_support_page_related_ con (accessed April 26, 2020).

Wang, Z., Lin, S., 2017. Membrane fouling and wetting in membrane distillation and their mitigation by novel membranes with special wettability. *Water Res.* 112, 38-47.

Whitfield, S., 2017. Permian, Bakken Operators Face Produced Water Challenges. Society of Petroleum Engineers web site. https://pubs.spe.org/en/jpt/jpt-article-detail/?art=2982 (accessed April 27, 2020).

Xu, P., Cath, T.Y., Robertson, A.P., Reinhard, M., Leckie, J.O., Drewes, J.E., 2013. Critical review of desalination concentrate management, treatment and beneficial use. *Environ. Eng. Sci.* 30 (8), 502-514.

Yuan, Z., Yu, Y., Wei, L., Sui, X., She, Q., Chen, Y., 2020. Pressure-retarded membrane distillation for simultaneous hypersaline brine desalination and low-grade heat harvesting. *J. Membr. Sci.* 597, 117765.

Zhang, Z.Y., Du, X.W., Carlson, K.H., Robbins, C.A., Tong, T.Z., 2019. Effective treatment of shale oil and gas produced water by membrane distillation coupled with precipitative softening and walnut shell filtration. *Desalination* 454, 82-90.

2.0 Literature Review[1]

2.1 UOG Wastewater Treatment Technologies

Numerous studies have focused on developing new technologies for the treatment of UOG wastewater. Thermal technologies, such as mechanical vapor compression (MVC), as well as membrane-based processes including reverse osmosis (RO) (Mondal and Wickramasinghe, 2008), forward osmosis (FO) (Bell et al., 2017; Chen et al., 2015; Coday et al., 2014; McGinnis et al., 2013), and membrane distillation (MD) (Lokare et al., 2017b; Singh and Sirkar, 2012) have been used to desalinate and treat UOG wastewater at laboratory or pilot scales. Shaffer et al. (Shaffer et al., 2013) published an excellent article that reviewed technologies that are suitable for desalination and reuse of UOG wastewater. However, full-scale implementation of wastewater treatment and external reuse has not been reported to any significant degree in the UOG industry. Therefore, a more in-depth understanding is needed based on a critical analysis of the benefits and limitations of existing treatment technologies tailored to UOG wastewater.

2.1.1 UOG Wastewater Volume and Composition

Understanding the volume and chemical composition of UOG wastewater is important to justify the necessity and to select appropriate treatment technologies. Typically, UOG wastewater generation is defined as two stages and varies with time: HF flowback and produced water (Bai et al., 2013; Bai et al., 2015). HF flowback water is referred to as the water returned to the earth's surface during the early stages of production lasting from several days to a few

[1] Section 2.1 has been published as part of a review article in *Frontiers of Environmental Science & Engineering*, in which I am among the primary authors, with the following citation:

Tong, T., Carlson, K.H., Robbins, C.A., Zhang, Z., Du, X., 2019. Membrane-based treatment of shale oil and gas wastewater: The current state of knowledge. *Front. Environ. Sci. Eng.* 13 (4), 63.

months (Bai et al., 2015). Produced water is the water returned to the earth's surface following the flowback stage for the remaining lifetime of the well. A third stage has also been defined in literature as the transition stage. The transition stage typically lasts for several months and bridges the gap between the high volume flowback stage and the more stable produced water stage (Bai et al., 2015) (Figure 2-1). In addition, a small fraction of wastewater generated from UOG production originates from the injected fracturing fluids, which return to the surface during the flowback stage (Kondash et al., 2017). The majority of the wastewater (>90%, particularly for produced water) is composed of formation brines that are native to the geologic formation. This difference results in varied chemical compositions of wastewater in different periods, which might require different treatment technologies. Overall, a significant volume (20-50%) of UOG wastewater is generated during the first 6 months of production (Kondash et al., 2017).

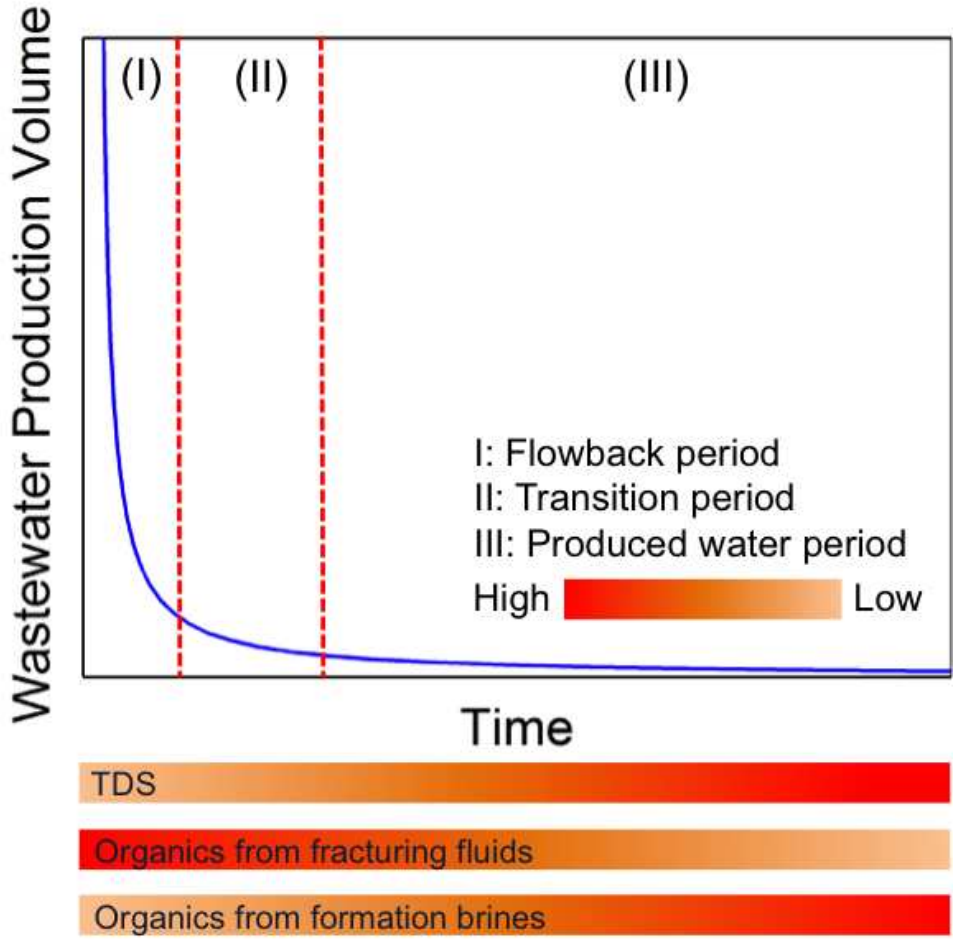

Figure 2-1. Three periods of wastewater production from UOG wells, as well as variation of total dissolved solids (TDS) and organics with time. The TDS and organics from formation brines typically increase with well age, whereas the organics associated with fracturing fluids decrease with time. The shape of wastewater production volume is adopted from Bai et al. (Bai et al., 2015; Tong et al., 2019)

From 2011 to 2016, the water use per production well increased by up to 770%, while the volume of flowback and produced water has hiked up to 1440% (Figure 2-2). For example, in the Niobrara shale play (which contains the Denver-Julesburg (DJ) Basin), water consumption increased from just over 8,997 m^3 per well to 22,296 m^3 per well from 2011 to 2016. Meanwhile, the wastewater generation during the first 12 months increased significantly from just over 8,000 m^3 per well to almost 30,000 m^3 per well over the same time period (Figure 2-2D) (Kondash et al., 2018; Tong et al., 2019). Similarly, a steady increase of wastewater production with time was

also observed in the Permian Basin (Texas and New Mexico), Eagle Ford Shale (Texas), and Marcellus Shale (Pennsylvania) (Figures 2-2A, B, and C).

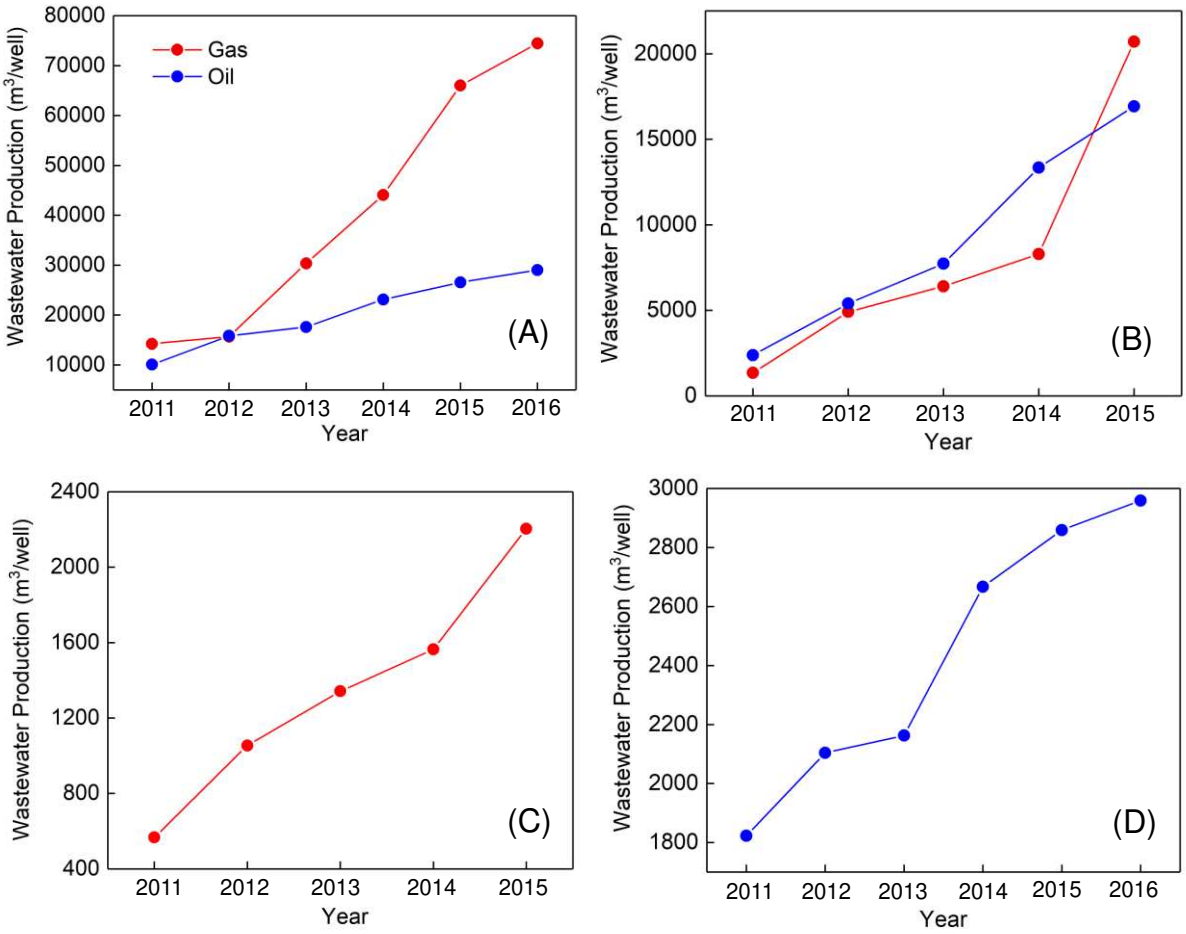

Figure 2-2. Wastewater production volume per well during the first 12 months after hydraulic fracturing from (A) Permian Basin, (B) Eagle Ford Shale, (C) Marcellus Shale, and (D) Niobrara Shale. The data marked in red indicate gas-producing regions while those marked in blue indicate oil-producing regions. The data used in this figure are extracted from Kondash et al. (Kondash et al., 2018; Tong et al., 2019)

The chemical composition of UOG wastewater directly determines its ecological and health risks, as well as the design of wastewater treatment systems. The components of wastewater generated from UOG production vary both spatially and temporally. One of the key components is salinity, which is typically indicated by total dissolved solids (TDS) and has a wide range from different shale plays in the United States. For example, the wastewater generated from the

Marcellus Shale has TDS values up to 390,000 mg/L (with a median TDS of 88,000 mg/L) (Shih et al., 2015), whereas the wastewater from the DJ Basin in Colorado displays a relatively low TDS in the range of 10,000 – 30,000 mg/L (Kim et al., 2016; Lester et al., 2015; Oetjen et al., 2018). Such difference has important implications in the selection of treatment technology because some technologies (e.g. pressure-driven membrane processes) are unable to cope with hypersaline wastewater (Shaffer et al., 2013). Further, the salinities of wastewater increase with time after HF in all the major shale plays in the U.S. (Kondash et al., 2017; Oetjen et al., 2018), due to the fact that the HF fluid contains much lower salinity than the saline formation brines and this water is present predominantly during the initial period of flowback. The high TDS of UOG wastewater disrupts the biological function of conventional wastewater treatment processes, increases the salt loading to the receiving waterway with significant ecological impacts, thereby prohibiting the discharge of such wastewater into publicly owned treatment works (POTWs) (Vidic et al., 2013). Desalination, therefore, is required to treat UOG wastewater for external discharge or reuse purposes.

Organic components are another important characteristic of UOG wastewater. The organic compounds associated with petroleum and HF fluids cause fouling during the wastewater treatment process and impose toxicity to ecosystems and human health. Butkovskyi et al. (Butkovskyi et al., 2017) presented a comprehensive review on the organic pollutants present in UOG flowback and produced waters, in which a diverse set of organic compounds, were identified. Several pollutants, such as polycyclic aromatic hydrocarbons (PAHs) and phthalate, were found at concentrations much higher than the predicted no effect concentration (PNEC), indicating their potential toxicity (Butkovskyi et al., 2017). Recently, He et al. (He et al., 2018) has showed that organic fractions isolated from HF flowback and produced water, including

PAHs and alkyl PAHs, imposed significant toxicity to the embryos of zebrafish. The development of analytical methods provides abundant information that decodes the complex composition of organic pollutants in UOG wastewater (Ferrer and Thurman, 2015). For example, Rosenblum et al. (Rosenblum et al., 2017) applied gas chromatography-mass spectrometry (GC-MS) and ultrahigh pressure liquid chromatography to quantify the organic chemicals presents in UOG wastewater during a 405-day period. The authors detected high levels of toxic volatile organic compounds (VOCs) such as benzene, toluene, ethylbenzene, and xylene (BTEX), as well as several non-volatile organic surfactants. The concentrations of BTEX in wastewater generated from various UOG production sites were reported to be in the mg/L levels (Shih et al., 2015; Rosenblum et al., 2017; Zhang et al., 2019), which far exceed the typical National Pollutant Discharge Elimination System (NPDES) discharge limits (<100 μg/L) regulated in various local permits (Arkansas Department of Environmental Quality, 2016; USEPA, 1995; USEPA, 2005). Also, signatures of petroleum-associated organic pollutants, including aliphatic hydrocarbons and aromatic compounds, have been commonly reported in foulant layers formed in the treatment of UOG wastewater (Bell et al., 2017; Du et al., 2018; Mondal and Wickramsinghe, 2008). In contrast to salinity, the contents of organic pollutants associated with HF generally reach their peak concentrations during the early stage of the wells and then decrease afterwards (Rosenblum et al., 2017). In a UOG production well in Colorado, for instance, the dissolved total organic carbon (TOC) decreased from ~1,500 mg/L to below 300 mg/L within ~400 days, during which the concentrations of surfactants were decreased by 40%-100% (Rosenblum et al., 2017).

Diverse inorganic components, which are responsible for mineral scaling in the wastewater treatment process, are also found in UOG wastewater (Kim et al., 2016; Oetjen et al., 2018). Alkalinity, dissolved barium (Ba), calcium (Ca), magnesium (Mg), strontium (Sr), silica, and

sulfate (SO_4^{2-}) are the major scale-forming species, which cause the formation of various mineral scales such as barite, calcite, gypsum, strontianite, and amorphous silica. In a recent study, the saturation indices (defined as the common logarithm ($\log_{10}$) of the ratio of ion activity product to solubility product) of calcite, silica, and strontianite were found to be 1.25, 0.37, and 0.62 in the produced water from the Wattenberg field of Colorado after 80% water recovery (Zhang et al., 2019), indicating their potential of precipitation during desalination processes. The contents and temporal variance of these inorganic constituents differ according to specific species and site location. For example, the total Ca concentrations in the wastewater from the Marcellus Shale have a median value of 6,200 mg/L and a maximum value of 40,000 mg/L (Shih et al., 2015), while that from the DJ Basin was reported in to be in the range of 100-900 mg/L (Kim et al., 2016; Oetjen et al., 2018; Zhang et al., 2019). Also, concentration range of Sr was 15.7-202 mg/L, 730-820 mg/L, and 0.011-16,141 mg/L for the Permian Basin, the DJ Basin, and the Marcellus shale play, respectively (Chang et al., 2019).

UOG wastewater is complex in nature as demonstrated by previous research. The variation of both wastewater quantity and quality imposes additional challenges to the treatment technologies. Appropriate technologies need to be adaptive to the dynamic treatment demands at the oil and gas field, while being resistant against potential fouling and scaling caused by diverse organic and inorganic components of the wastewater. Also, some components, such as salinity and toxic organic pollutants, need to be removed during wastewater treatment processes, due to their hazardous effects that constrain the external reuse or discharge of the wastewater. As a result, modular and on-site treatment technologies, which enable the production of high-quality water product, are ideally suited for the treatment of UOG wastewater.

2.1.2 Mechanical Vapor Compression

Mechanical vapor compression (MVC) is a thermal desalination technology that has been commercialized in the treatment of industrial wastewaters including those generated during UOG production (Tong and Elimelech, 2016). MVC utilizes electricity to power a compressor, which converts the evaporated water to a superheated steam. The condensation of the superheated steam provides the necessary thermal energy for the evaporation of high-salinity feedwaters (Shaffer et al., 2013). MVC is equipped with well-designed heat transfer and recovery systems. The feedwater of MVC is preheated by heat exchangers that utilize the sensible heat from the distillate and brine. Also, the feedwater flows to form a thin film on the internal surface of heat transfer tubes, which enhances the efficiency of heat transfer and reduces the required energy consumption (Figure 2-3).

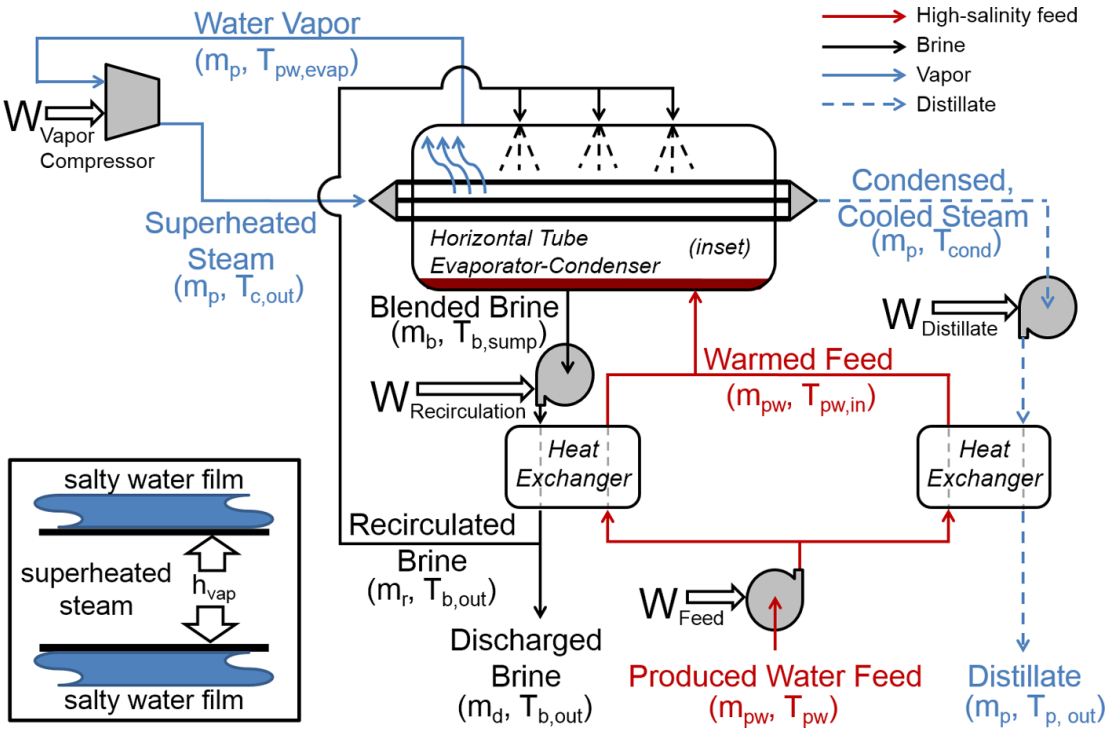

Figure 2-3. Schematic diagram of the mechanical vapor compression (MVC) process. The principal energy input into the system is in the form of electrical energy required to drive the vapor compressor, and the feed, distillate, and recirculation pumps (Shaffer et al., 2013).

MVC consumes substantial amounts of electrical energy (typically 20-25 kWh_e/m^3 of treated feedwater) due to its thermal nature (Tong and Elimelech, 2016). Higher values of 28-39 kWh_e/m^3 of treated feedwater have also been reported for MVC desalination of UOG wastewater (McGinnis et al., 2013). In thermal desalination processes like MVC, a large amount of energy is consumed by water evaporation, rather than separating water from salt molecules (Deshmukh et al., 2018). This undesirable feature renders MVC inherently energy consumptive. In addition, the reliance of MVC on high-grade electrical energy requires continuous electricity supply (i.e. from existing power grids), and thus MVC has a low potential to utilize low-grade thermal energy available at the oil and gas field.

MVC has been applied to seawater desalination (Aybar, 2002; Bahar et al., 2004) and the treatment of high-salinity wastewater at oil fields (Hayes et al., 2014; Koren and Nadav, 1994; Thiel et al., 2015). Several companies, including Veolia and Suez, are currently providing MVC-based treatment services targeting UOG wastewater. MVC is able to cope with feedwater containing high salinity (>200,000 mg/L of TDS), and meanwhile produce demineralized water product (e.g., TDS < 200 mg/L) (Burbano and Brankhuber, 2012; Eastern Municipal Water District, 2008; Hayes et al., 2014). Due to its technical maturity, MVC sets a benchmark for cost and energy comparison with other emerging treatment technologies. The major drawbacks of MVC are its high capital and maintenance costs due to its high operational temperature.

2.1.3 Membrane-based Treatment Technologies

Membrane-based technologies, including microfiltration (MF), ultrafiltration (UF), nanofiltration (NF), FO, RO, and MD, have been the focus of recent research efforts to develop new treatment approaches suitable for UOG wastewater. The modular configuration of these technologies renders them adaptive to the fluctuation of wastewater quality and quantity during

the treatment process. These technologies have different working principles, advantages, and limitations, particularly in terms of energy consumption, salinity limit, and water product quality.

Pressure-driven membrane Technologies

MF, UF, NF, and RO utilize an external hydraulic pressure to drive the transport of water molecules through a membrane substrate. MF and UF use porous membranes to remove suspended particles, pathogens, and macromolecules form the feedwater. These technologies, however, are not designed for desalination, and they are only used for applications that tolerate high salinity (e.g. internal reuse of wastewater for HF) or as pretreatment prior to the downstream desalination processes (He et al., 2014; Xiong et al., 2016). Several studies have reported the use of MF and UF to treat UOG wastewater generated from the Marcellus Shale (He et al., 2014; Jiang et al., 2013; Xiong et al., 2016), where internal reuse for HF is the primary wastewater management practice (Brantley et al., 2014). Colloidal fouling caused significant flux decline in all the studies and were identified as the major limiting factor that constrains the performance of MF/UF membranes (He et al., 2014; Jiang et al., 2013; Xiong et al., 2016). Therefore, removal of colloidal particles from raw UOG wastewater is necessary to improve the efficiencies of MF and UF for UOG wastewater treatment.

In contrast to MF and UF that utilize porous membranes, NF and RO use dense and "non-porous" membranes to achieve desalination and selective removal of contaminants. Thus, these two technologies are able to effectively reduce the TDS and other pollutants from UOG wastewater, producing higher quality water products that potentially meet the requirement for external reuse options such as direct discharge into surface waterways or agricultural irrigation. For example, Mondal and Wickramsinghe (Mondal and Wickramsinghe, 2008) compared the performance of two NF membranes (Dow NF90 and NF270) and one low-pressure RO

membrane (Dow BW30) for the treatment of oil and gas wastewater collected in Colorado. Their results demonstrated a wide range of salinity removal efficiencies (from 15%-50%) that depended on the membrane properties. Also, Miller et al. (Miller et al., 2013) combined UF with RO in a pilot-scale system, which was used to treat HF flowback generated from wells in Texas. The use of UF reduced the fouling potential of the feedwater prior to RO desalination, and an exceptional salt removal efficiency of >99% was achieved by the integrated UF-RO system.

Unlike thermal technologies, NF and RO do not require phase transition (from liquid to vapor) for water-salt separation. These processes avoid irreversible energy losses associated with evaporation and condensation in thermal processes making NF and RO more energy efficient than MVC. However, current RO and NF systems are unable to desalinate wastewater containing ultra-high salinity. The salinity limit of NF and RO (typically ~70,000 mg/L TDS (Shaffer et al., 2013)), which is imposed by the maximum tolerable hydraulic pressure of the membrane modules, imposes a ceiling on the salinity of wastewater that could be treated by these pressure-driven technologies. The salinity of UOG wastewater often exceeds this salinity limit, rendering NF and RO inappropriate technologies for hypersaline wastewater treatment. Therefore, NF and RO can be only applied to a small fraction of UOG wastewater. Figure 2-4A illustrates the comparison of energy consumption and salinity limit between RO and MVC, demonstrating the need of developing novel technologies that tolerate higher salinity than RO while consuming less energy and cost than MVC. Two technologies that meet this criterion, FO and MD, are depicted in Figures 2-4B and 2-4C.

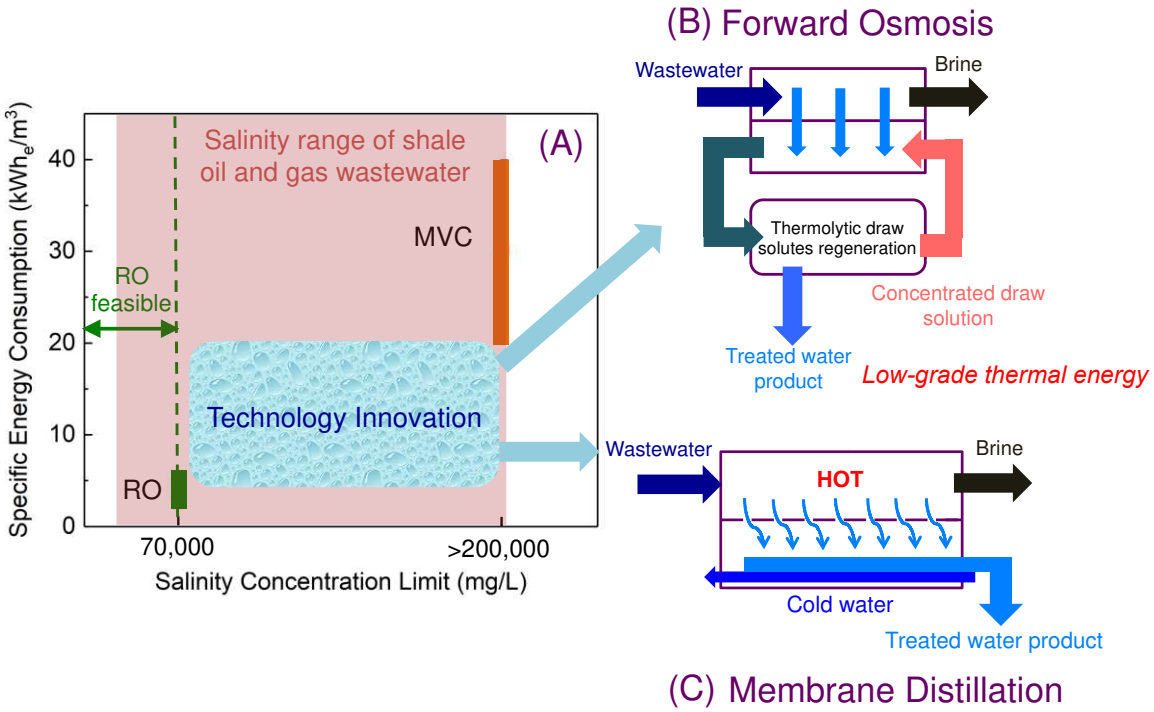

Figure 2-4. (A) The specific energy consumption of RO and MVC. Although RO is much more energy efficient than MVC, the salinity of UOG wastewater often exceeds the salinity limit of RO (typically 70,000 mg/L), constraining the use of RO in the treatment of UOG wastewater. This gap necessitates the development of technologies that tolerate higher salinity than RO and consume less energy than MVC. These technologies include (B) forward osmosis and (C) membrane distillation, both of which are able to utilize low-grade thermal energy and reduce the consumption of primary electric energy. The style of this figure is adopted from Tong and Elimelech. (Tong and Elimelech, 2016; Tong et al., 2019)

Forward Osmosis

FO is an engineered osmosis process that utilizes the osmotic pressure difference to power the water transport through a semipermeable membrane (Cath et al., 2006; Shaffer et al., 2015). In the FO process (Figure 2-4B), a draw solution containing higher salinity (i.e., higher osmotic pressure) than the feedwater is used to attract pure water transporting through the semipermeable membrane that behaves as a barrier to salt transport in order to achieve desalination. Since no external hydraulic pressure is applied in the FO process, FO tolerates high feedwater salinity (upper salinity > 200,000 mg/L TDS (Tong and Elimelech, 2016)) and requires almost no energy consumption for water transport through the membrane (except for the energy used for pumping

of feed and draw solutions). FO also has lower fouling propensity than pressure-driven RO because a loosely packed fouling layer is formed without hydraulic pressure (Shaffer et al., 2015). Therefore, FO was considered suitable for the treatment of hypersaline wastewater such as UOG wastewater (Shaffer et al., 2015), which has been conceptually proven at both laboratory and pilot scales (Coday and Cath, 2014; Coday et al., 2014; Coday et al., 2015).

However, it is misleading to consider FO as an energy-efficient desalination technology (Shaffer et al., 2015). At equilibrium, the diluted draw solution has higher salinity than the raw feedwater. This hypersaline solution cannot be discharged into either surface water or POTWs. As a result, water needs to be separated from the diluted draw solution, in order to produce high-quality water product and regenerate the concentrated draw solution. Due to the elevated salinity of the diluted draw solution compared to the raw UOG wastewater, this process cannot be achieved with pressure-driven technologies such as NF and RO, and requires a higher amount of energy input than direct desalination of UOG wastewater.

Thermolytic draw solutes, such as ammonia-carbon dioxide (NH_3-CO_2), generate high osmotic pressure and can be regenerated by moderate heating (at ~60°C) with low-temperature distillation (McCutcheon et al., 2005). The requirement of a relatively low temperature to regenerate the draw solution renders this technology suitable for the treatment of UOG wastewater, because of the abundant low-grade thermal energy (e.g., waste heat and geothermal energy) available at the oil and gas field. A pilot-scale system using thermolytic FO was established to treat UOG wastewater generated from the Marcellus Shale with an average salinity of 73,000 mg/L TDS, achieving a total water recovery of 64% and producing water product with only ~300 mg/L TDS (McGinnis et al., 2013). The authors reported that this pilot FO system consumed 275±12 kWh of thermal energy to obtain 1 m^3 of product water. If the regeneration of

draw solution is performed in a MVC configuration, this thermal energy consumption was equivalent to 21 kWh/m^3 of electricity, which is lower than that required by MVC desalination of comparable UOG wastewater (37 kWh/m^3 of electricity).

A drawback to FO for UOG wastewater treatment is the complexity of its configuration, which requires a draw solution recovery system that is independent from the main desalination units (i.e., the membrane modules). Also, the reverse flux of ammonia salts towards the feedwater consumes the NH_3-CO_2 draw solutes and increases the cost of the FO treatment system.

Membrane Distillation

MD is a hybrid thermal-membrane technology that has recently attracted tremendous interest in the treatment of complex and hypersaline industrial wastewater (Deshmukh et al., 2018). In MD, a partial vapor pressure difference generated between the heated feedwater and the cold permeate stream is used to drive the transport of water vapor across a microporous and hydrophobic membrane (Lawson and Lloyd, 1997). MD is typically operated at moderate temperatures (60°C-80°C), and thus it is also able to utilize the low-grade thermal energy described above. Due to its thermal nature, MD tolerates high salinity and enables the concentration of feedwater to a comparable extent to MVC. Along with its simpler configuration than thermolytic FO and lower capital costs than MVC, there has been a rise of research activities exploring the use of MD in the treatment of UOG wastewater.

Several studies have tested MD treatment of UOG wastewater at the laboratory scale, and the corresponding results are promising and demonstrate the feasibility of MD in producing high-quality distillate from wastewater collected from several oil and gas shale plays in the U.S. (Boo et al., 2016b; Du et al., 2018; Kim et al., 2016; Lokare et al. 2017b; Singh and Sirkar,

2012). Membrane fouling and scaling occurred in the MD treatment process, but MD generally has less fouling/scaling propensity than RO due to the lack of external pressure and the relatively large pores of MD membranes (i.e., micro-scale). However, significant water flux decline was typically observed at very high water recoveries (Kim et al., 2017; Kim et al., 2018), when the concentrations of scale-forming species exceed the solubility limits of sparingly soluble salts. Therefore, mitigation or prevention of membrane scaling, potentially by the use of anti-scalants (He et al., 2009), is still critical to enhance MD performance in the treatment of UOG wastewater. Further, MD is uniquely subjected to membrane wetting (Deshmukh et al., 2018), which is caused by low surface energy contaminants such as surfactants that are present in the UOG wastewater (Rosenblum et al., 2017). Various surfactants, which are used in HF fluids, lower the surface tension of the wastewater and induce the flooding of feedwater into the membrane pores and MD permeate (Boo et al., 2016b; Chew et al., 2017). Membrane wetting damages the water quality of MD product significantly and eventually causes process failure. Recently, membranes with improved wetting resistance (or so called omniphobic membranes) have been developed to mitigate membrane wetting in the MD process. Omniphobic membranes, which are fabricated by introducing both low surface energy materials (e.g., long-chain fluoroalkylsilane) and a re-entrant structure (Wang et al., 2016), have demonstrated stable desalination performance in MD treatment of hypersaline feedwater containing high concentrations of surfactants (Boo et al., 2016a, b; Huang et al., 2017; Lin et al., 2014). These membranes have the potential to play an important role in improving the robustness of MD in the treatment of UOG wastewater with high content of surfactants (e.g., HF flowback (Rosenblum et al., 2017)).

Technical maturity is a major factor that will determine whether MD-based wastewater treatment systems will be utilized in the future for large scale UOG wastewater treatment. MD treatment of industrial wastewater has mostly been performed at the laboratory scale (Deshmukh et al., 2018), and pilot-scale systems have rarely been reported in the literature. Duong et al. (Duong et al., 2015) reported a pilot-scale air gap MD system for the treatment of concentrated brine from RO desalination of coal seam gas (CSG) produced water. This system had a total membrane area of 7.2 m^2 and was able to recover 80% of freshwater with a TDS of 250 mg/L. However, the water flux of this system was quite low, although this undesired feature could be offset by an enhanced packing density of the spiral-wound membrane module. Due to the relative low salinity (i.e., ~14,000 mg/L (Duong et al., 2015)) and different chemical composition of RO brines from CSG produced water, it is still uncertain whether such pilot-scale systems are effective in the treatment of UOG wastewater. As a result, more efforts are needed in scaling up MD desalination for industrial wastewater treatment applications.

The above membrane technologies, along with MVC, perform as the main treatment step to remove both inorganic (e.g., TDS and heavy metals) and organic (e.g., petroleum-associated pollutants) components from UOG wastewater. Table 2-1 presents a qualitative comparison of those technologies on their advantages and limitations, which determine the feasibility of implementation in UOG wastewater treatment. At the current state, more research is required for membrane technologies to compete with MVC as cost- and energy-effective wastewater treatment options.

Table 2-1. Qualitative comparison of technologies used as main step for UOG wastewater treatment. A higher number of stars indicate more favorable features (Tong et al., 2019).

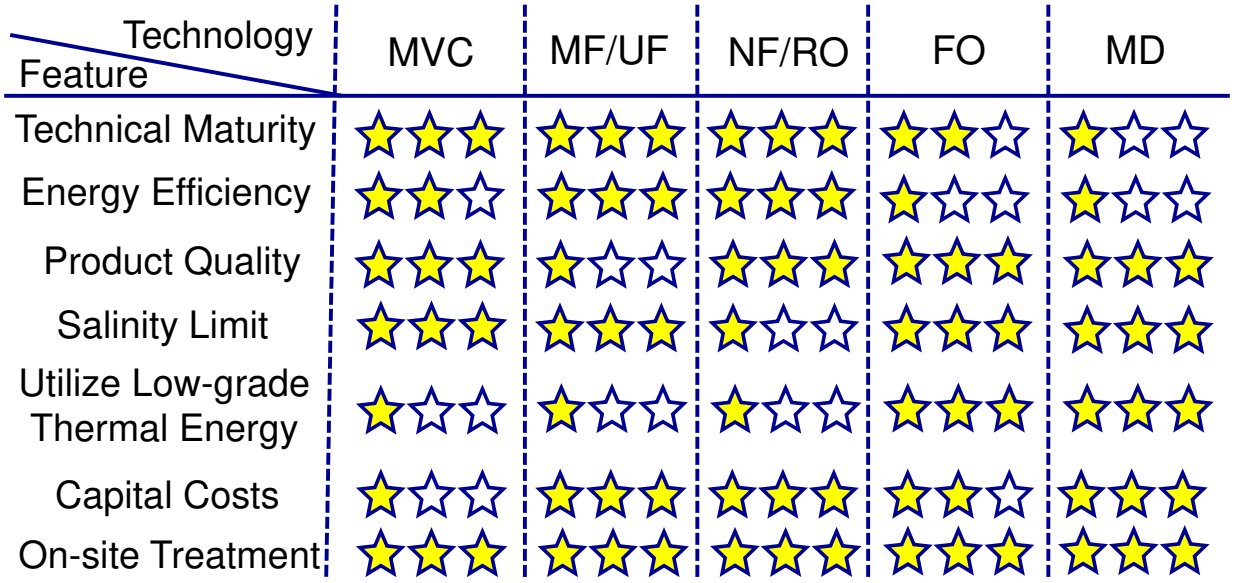

2.1.4 Pretreatment technologies for an integrated UOG wastewater treatment system

MVC and membrane technologies are constrained by fouling, scaling, wetting, and/or low removal of volatile contaminants

Pretreatment of UOG wastewater, which can be achieved by physicochemical and/or biological processes, are employed to reduce fouling, scaling, and membrane wetting and improve water product quality of the downstream main treatment step. Previous studies have demonstrated that the main treatment processes, in particular the membrane-based technologies, suffer from fouling, scaling, and wetting caused by the complex chemical compositions of UOG wastewater. For example, Xiong and coworkers (Xiong et al., 2016) reported that colloidal fouling caused significant flux decline during MF treatment of UOG wastewater from the Marcellus shale play. The authors attributed this degradation of membrane performance to the submicron particles present in the wastewater (Xiong et al., 2016). The same team recently reported that polyacrylamide (PAM), a polymer used as a friction reducer in the HF fluid, was also responsible for membrane fouling in MF treatment of flowback water (Xiong et al., 2018).

Similarly, drastic decrease of water flux has also been observed in NF/RO (Alazahrani et al., 2013), FO (Bell et al., 2017), and MD treatment processes (Zhang et al., 2019). The high organic content and scaling potential of UOG wastewater resulted in inevitable membrane fouling, scaling, and wetting, which reduces the water productivity as well as the membrane lifetime. Fourier-transform infrared spectroscopy (FTIR) revealed that aliphatic and aromatic hydrocarbons as well as carbonates were major organic foulants, all of which are associated with petroleum and/or HF fluids (Bell et al., 2017). Also, iron- and silica-related scales have been commonly found responsible for membrane scaling as revealed by elemental analysis of the fouling layers (Bell et al., 2017; Du et al., 2018). As a result, effective removal of organic foulants and inorganic scalants via appropriate pretreatment steps will be necessary to improve the performance of the main treatment processes.

Further, several contaminants present in UOG wastewater might escape from the main treatment processes, thereby constraining the applications of the treated water product. This issue is particularly problematic for the thermal-based technologies (e.g., MVC and MD), as VOCs are able to transport along with water vapor and enter the distillate. For example, Winglee et al. (Winglee et al., 2017) demonstrated that VOCs associated with oil production, including methyl-*tert*-butyl ether, acetone, pentanone, butanol, and hexanol, accumulated in the MD distillate at greater concentrations than the feedwater. This finding was consistent with the study performed by Yao et al. (Yao et al., 2018), who reported that the concentrations of VOCs in the MD distillate increased with water recovery. Recently, a study showed that volatile and toxic compounds such as BTEX were able to penetrate through MD membranes, resulting in high distillate concentrations well above the typical NPDES discharge limits (Zhang et al., 2019). The low removal efficiencies for VOCs should also apply to evaporation-based MVC. As a result,

pretreatment or post-treatment (e.g., air stripping) should be employed to remove such contaminants from the raw or treated UOG wastewater.

Physicochemical pretreatment processes

Physicochemical processes such as softening, coagulation, and adsorption have been used in the pretreatment of UOG wastewater (Ahmadun et al., 2009; Esmaeilirad et al., 2015; Lobo et al., 2016; Kong et al., 2017; Rosenblum et al., 2016; Zhai et al., 2017; Zhang et al., 2019). Softening and coagulation possess exceptional efficiency in removing colloidal and suspended particles as well as multivalent scaling-forming ions. For example, Esmaeilirad et al. (Esmaeilirad et al., 2015) reported that the combination of softening and electrocoagulation removed turbidity, hardness, and scale-forming cations such as Ba^{2+} and Sr^{2+} effectively. Also, Zhai et al. (Zhai et al., 2017) applied chemical coagulants (i.e., polyaluminum chloride and polyferric sulfate) to the pretreatment of wastewater from a natural gas drilling field in Chongqing City, China. After optimizing the coagulant doses and solution pH, coagulation was able to achieve substantial reduction (>85%) of organic contaminants, suspended solids, and color from the wastewater.

These physicochemical pretreatment processes have been employed in tandem with membrane technologies to form an integrated treatment train for UOG wastewater. In a study performed by Kong et al. (Kong et al., 2017), chemical coagulation using polyaluminum chloride greatly reduced membrane fouling of the subsequent UF process. Also, electrocoagulation was combined with MD to treat UOG wastewater in the Marcellus Shale (Sardari et al., 2018). The use of electrocoagulation mitigated membrane fouling caused by organic contaminants and suspended solids, and this integrated system was able to provide stable water flux for 434 hours continuously when concentrating the wastewater to an ultrahigh salinity of 265 g/L TDS (Sardari

et al., 2018). In a recent study (Zhang et al., 2019), precipitative softening and walnut shell filtration were coupled with MD to achieve an effective treatment train for UOG wastewater generated from the Wattenberg field in northeastern Colorado (Figure 2-5). Precipitative softening removed a variety of particulate, organic, and inorganic foulants, while walnut shell filtration displayed high efficiency (>95%) in eliminating VOCs (e.g., BTEX) from the wastewater. The subsequent MD exhibited stable and robust desalination performance, and meanwhile generated high-quality distillate containing minimal organic and inorganic contaminants (e.g., TDS, BTEX, and boron).

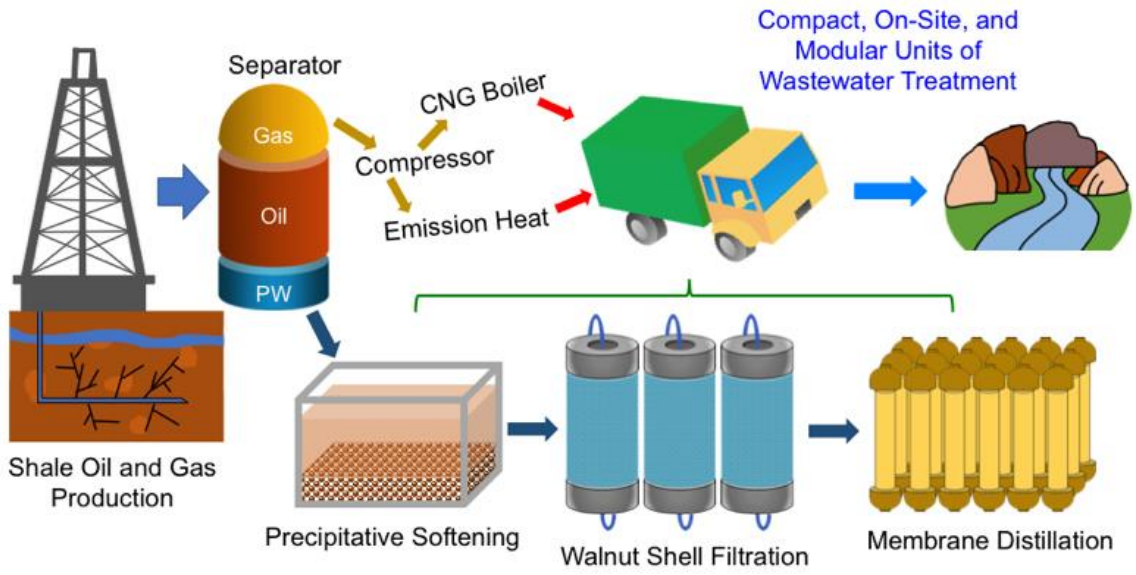

Figure 2-5. Schematic description of an on-site wastewater treatment train for UOG production, which utilizes precipitative softening and walnut shell filtration as the pretreatment steps, as well as membrane distillation as the main treatment step. CNG boiler stands for compressed natural gas boiler. This figure is adopted from Zhang et al. (Tong et al., 2019; Zhang et al., 2019)

Biological pretreatment processes

Biological pretreatment, such as biologically active filtration (BAF) (Freedman et al., 2017; Riley et al., 2016; Riley et al., 2018) and bioelectrochemical technology (Forrestal et al., 2015; Jain et al., 2017; Stoll et al., 2015), has been used to partially remove organic contaminants and foulants from UOG wastewater. For example, Riley et al. (Riley et al., 2016) developed a hybrid

treatment system consisting of BAF, UF, and NF for treating UOG wastewater from the Piceance and DJ Basins. BAF that contains microorganisms naturally present in the wastewater was found to biodegrade a majority (>70%) of organic matter, resulting in minimal fouling of the downstream UF and NF processes. This treatment train was successful in reducing >99% of organic constituents and >94% of TDS in total from the wastewater, and was adjustable to feedwaters with variable properties.

Further, microbial capacitive desalination cell (MCDC), a combined process of microbial fuel cell (MFC) and capacitive deionization (CDI), achieved simultaneous removal of organic matter and TDS from UOG wastewater while generating electricity (Forrestal et al., 2015; Stoll et al., 2015). However, MCDC is unable to produce low-salinity water product from hypersaline UOG wastewater, as a large salinity difference results in high electric resistance against salt migration. As a result, MCDC can be used as a pretreatment step prior to membrane desalination processes. The function of salt removal by MCDC could extend the applicability of RO and NF to the treatment of high-salinity wastewater. Such an integrated system, however, has not been reported in the literature. Compared to conventional CDI that is powered by an external electrical field, the relatively low kinetics of salt migration of MCDC might be the major barrier to its practical use.

2.2 Energy Sources for MD Treatment of UOG Wastewater

A key consideration for UOG wastewater treatment is the energy needed. A positive aspect of MD treatment of UOG wastewater is the ability to use low grade thermal energy to power treatment. Specifically, the integration of waste heat from various sources provides an opportunity to power MD treatment cost and energy efficiently. Other energy sources to be

considered to power MD treatment include solar energy, geothermal energy, and on-site natural gas.

2.2.1 Waste heat to power MD treatment

MD, which can harvest low-grade or waste heat to desalinate and treat high-salinity waters, is a potentially promising process to improve water sustainability at the water-energy nexus (Deshmukh et al., 2018). The integration of sufficient waste heat or other low-cost thermal energy sources in MD treatment of UOG wastewater is critical to its future viability. A techno-economic analysis (TEA) has been performed to assess the economic feasibility for the treatment of UOG wastewater from the Marcellus Shale (Tavakkoli et al., 2017). The results show that the total cost is \$5.70/m^3 of feedwater, with the cost of thermal energy being the primary fraction. The utilization of waste heat significantly reduced this cost to \$0.74/m^3 of feedwater, indicating the importance of integrating waste heat or other low-cost energy resources (e.g., geothermal energy and natural gas) into the MD treatment system. A study for a pilot scale trial of MD driven by low grade waste heat from a power plant showed the potential to treat saline industrial wastewater and produce a high volume of product water (8,000 m^3 per day) (Dow et al., 2016). However, for UOG wastewater treatment, it may be difficult to utilize power plant waste heat due to the remoteness of oil and gas fields. Within oil and gas fields, there exist other sources of waste heat that may be able to power MD treatment of UOG wastewater.

Waste heat from HF phase

During the HF phase, waste heat is generated from the coolant and exhaust systems of engines and pumps used in the HF process (Caterpillar, 2011; Encana, 2011b; Halliburton, 2012). The quantity of waste heat available from the HF phase and its ability to be integrated in MD treatment of UOG wastewater treatment has not been well studied in the literature. In order

to harness the waste heat from the HF phase, efficient thermal energy storage (TES) needs to be applied. Thermal desalination technologies may utilize TES to capture, store, and release to match the energy supply and demand trends (Figure 2-6) (Gude, 2015). TES technology requires a suitable medium for storage and circulation for heat transfer. The most commonly used sensible heat medium for TES is water and would be appropriate for TES associated with MD (Gude, 2015). TES systems can be placed on-site at a facility or transported by means of mobile TES systems to be used at the oil and gas well pad (Miro et al., 2016). The pairing of a TES system with waste heat generated from the HF phase may provide a viable energy source to power MD treatment of UOG wastewater during the initial months of production.

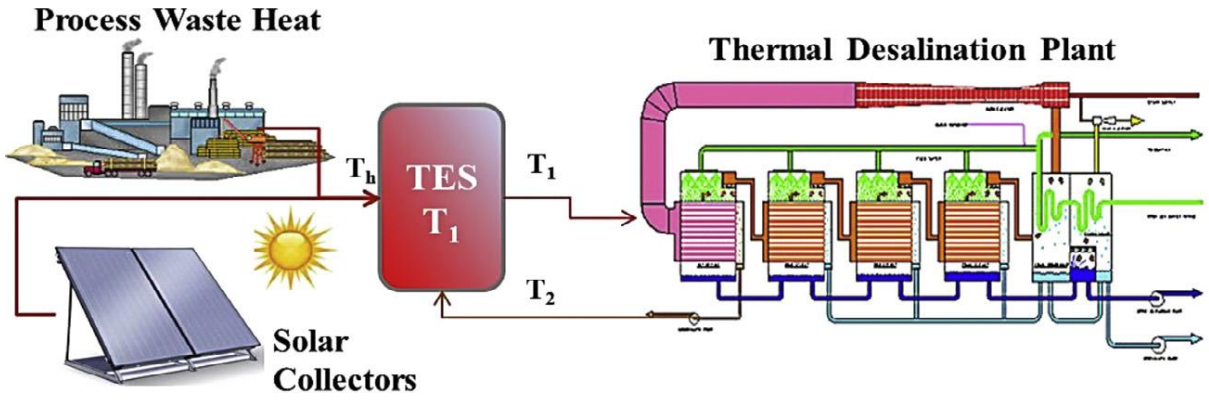

Figure 2-6. Thermal desalination system powered by solar collectors or waste heat sources augmented by TES (Gude, 2015).

Waste heat from the on-site electrical energy load

Waste heat is generated at the oil and gas pad by the engines meeting the full-time electrical energy load to operate well site components. An engine may power separation units, pumps, combustors, air compressors, and system controls at the well pad (Encana, 2011a). Estimates for the power load drawn by well-pad equipment are ~8 kW (Sevier, 2015; Wilcox, 2018). However, a thorough study of engines used at well-pads and waste heat available from their operation may indicate a larger amount of waste heat generated. Multiple studies have been conducted focusing

on the VOCs and hazardous air pollutants emitted from oil and gas well pads (Brantley et al., 2015; Khalaj and Sattler, 2018; Warneke et al., 2014), but the literature does not indicate research associated with the quantification of the waste heat generated at an oil and gas well pad. Due to monitoring of VOCs and hazardous air pollutants emissions at an oil and gas well pad, data on engines located on-site to meet the electrical energy load could be collected to better quantify the waste heat available.

Waste heat from natural gas compressor stations

A source of waste heat not generated at the well pad but located throughout the oil and gas footprint is from natural gas compressor stations (NGCSs). NGCSs are installed along natural gas transmission pipelines that connect gathering systems in producing areas, natural gas processing plants, other receipt points, and the main consumer service areas (U.S. EIA, 2020). Mobile wellhead compression, which is much smaller in size than NGCSs, may be installed on the well pad but not until the natural gas return pressure drops considerably (typically years after the initial HF of the well) (Siemens, 2012) and thus not suitable for MD treatment of UOG wastewater upon completion of the well.

Previous work (Tavakkoli et al., 2016) has quantified the amount of waste heat available at NGCSs in the U.S. through a systems-level analysis (Figure 2-7). The quantification of waste heat was accomplished using thermodynamic analysis, installed capacity of NGCS reported by the U.S. Energy Information Administration (EIA), and load factors (Tavakkoli et al., 2016). This analysis demonstrated the availability of a large quantity of available waste heat from NGCSs and the critical need for development of waste heat recovery technologies. Further research in the state of Pennsylvania determined with appropriate heat recovery systems that a sufficient amount of NGCS waste heat is available to treat all of the UOG wastewater generated

in that state by MD (Lokare et al., 2017a). Recent research integrated waste heat recovery at NGCSs at a county scale in Pennsylvania for MD treatment of UOG wastewater (Tavakkoli et al., 2020). This study focused on developing an optimization model for UOG wastewater management in the Marcellus shale region.

The transportation of UOG wastewater to the NGCS will be a major limiting factor, as the transportation cost would be significant or even prohibitive if the NGCS are not located in close proximity with the UOG production sites (Lokare et al., 2017a). This research highlights the promise in using NGCS waste heat for MD treatment but further analysis needs to be conducted at the regional and local scale to determine its feasibility.

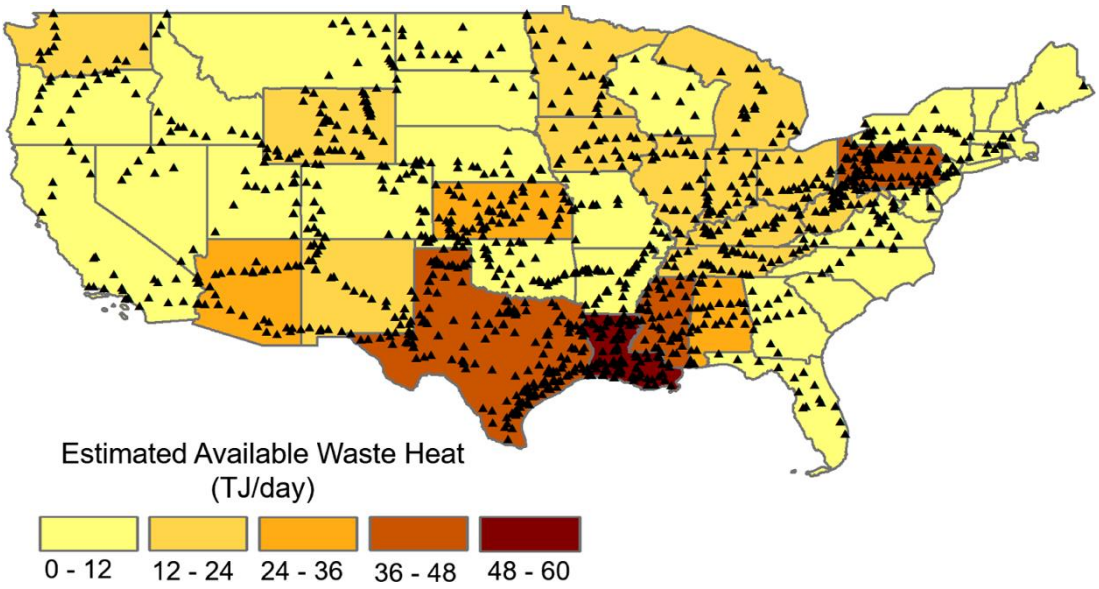

Figure 2-7. Spatial distribution of estimated waste heat at NGCS in the U.S. (TJ per day). Black triangles represent the actual location of NGCS obtained from the U.S. Energy Information Agency (Tavakkoli et al., 2016).

2.2.2 Solar energy to power MD treatment

Another option to power MD is through low grade solar energy (Deshmukh et al., 2018; Gonzalez et al., 2017; Ullah et al., 2018; Winter et al., 2011). Typically, the solar energy required to provide thermal energy to the MD system can be achieved using collector

technologies such as flat plate collectors (FPCs), evacuated tube collectors (ETCs), compound parabolic concentrators (CPCs), salt-gradient solar ponds (SGSPs) or solar stills (Gonzalez et al., 2017). Solar collectors can connect to MD modules either via a single-loop or two-loop system. In the single-loop system, the solar collector is directly connected to the membrane module. In the two-loop system, the solar collector and the MD module are connected by a heat exchanger, and also the system could have heat storage, which allows for the extending of operation beyond sunset (Figure 2-8) (Gonzalez et al., 2017).

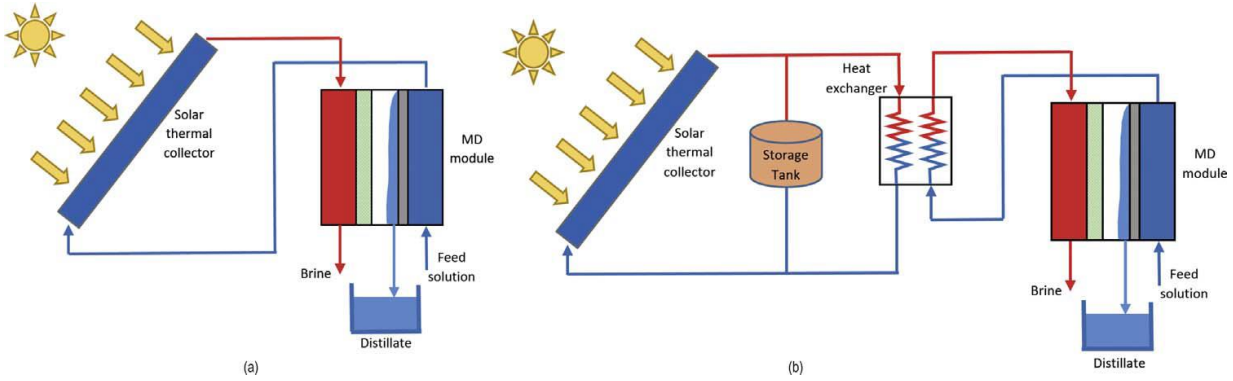

Figure 2-8. Schematic of a solar-powered MD system: (a) single-loop system; and (b) two-loop system (Gonzalez et al., 2017).

Previous studies have evaluated the performance of MD using solar thermal energy captured through solar collectors in desalination (Cipollina et al., 2012; Schwantes et al., 2013; Winter et al., 2011). The study conducted by Schwantes et al. (Schwantes et al., 2013) compared MD demonstration plants using either solar energy or waste heat. Waste heat from combustion engines proved to be a promising energy source, supplying a temperature level suitable for MD. Defective solar collectors and higher than expected heat losses in the solar collector array did not allow for operation to the complete potential of the desalination units. The authors recommended that if a constant waste heat source is available it is financially beneficial to save the investment costs of a solar thermal collector array (Schwantes et al., 2013).

A possible drawback identified by Ullah et al. (Ullah et al., 2018) is that the cost of solar powered MD systems remains higher than that of photovoltaic-powered RO. However, this drawback is mitigated somewhat due to the hypersalinity of UOG wastewater and the salinity limit of RO when comparing between the two technologies. The main cost in a solar powered MD system is the initial investment in the solar collector array (Qtaishat et al., 2013). Future research comparing costs of integrating waste heat or solar thermal energy in an MD system to treat UOG wastewater would help elucidate the more cost-effective energy source.

A further drawback is the mismatch between the source supply and demand and intermittent nature of solar energy (Gude, 2015). Solar thermal energy can only be provided during the daylight hours and the amount of solar energy varies by region (Ghaffour et al., 2014). TES, as previously discussed in regards to waste heat from the HF phase, is essential for reliable and continuous operation of a solar-powered MD system to treat UOG wastewater (Figure 2-8). This adds additional costs and complexity to the MD system and would need to be considered.

2.2.3 Geothermal energy to power MD treatment

Another option to power MD treatment of UOG wastewater with a low grade thermal source is geothermal energy. When compared to solar energy, it is expected that geothermal energy can reduce the cost of water production for desalination as geothermal systems do not need an energy converter (Gonzalez et al., 2017). Wet rock/water flow (WR), natural dry steam, and hot dry rock (HDR) are three types of geothermal energy systems (Ghaffour et al., 2014). Heat is extracted from either natural water flow from springs or from wells drilled into a hot-water aquifer for a wet rock system. This method mostly relies on heating from the groundwater system and operates similar to the heat-pump systems used in building heating and cooling systems (Ghaffour et al., 2014). Natural dry steam systems tend to occur near active volcanic activity

where groundwater comes in contact with naturally heated rock and produced superheated water under pressure in the subsurface (Ghaffour et al., 2014). This type of geothermal energy would be highly unlikely to be available near oil and gas fields. Heat is extracted in HDR geothermal systems by creating a man-made system of connected wells with artificial fractures used to collect an injected fluid from an injection well, through the fractures where heat is extracted, and ultimately to an extraction well where the superheated fluid is recovered (Figure 2-9) (Ghaffour et al., 2014). For MD, the most likely configuration would be to use dry steam production from wells or steam from an HDR collection system to heat the raw feedwater flowing in the system (Ghaffour et al., 2014).

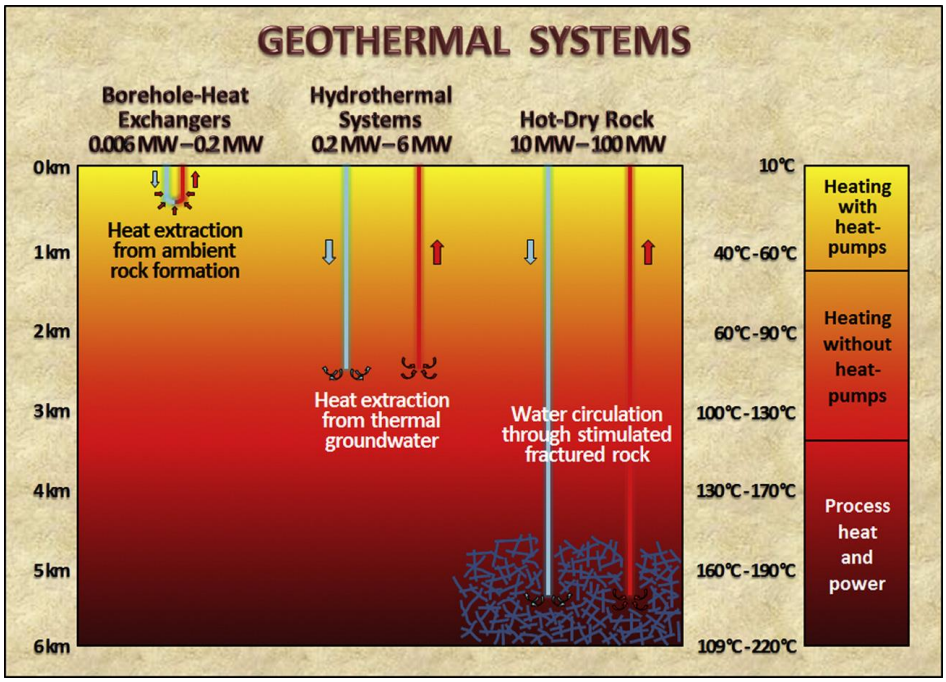

Figure 2-9. HDR geothermal collection systems can be engineered using hydraulic fracturing techniques to enhance fluid flow and allow better heat exchange (Ghaffour et al., 2014).

There are few studies of geothermal-powered MD in the literature (Gonzalez et al., 2017). Studies conducted by researchers in Malaysia (Jaafar et al., 2012; Sarbatly et al., 2012) explored powering MD desalination with geothermal water. The groundwater temperature in areas of

Malaysia is around 60°C thus offering the ability to desalinate with MD without the need for much additional energy for evaporation of the feedwater solution (Jaafar et al., 2012). It was reported that geothermal energy saved 95% on energy consumption costs for a vacuum MD system and achieved TDS levels below 500 ppm from a 900 ppm TDS feedwater (Sarbatly et al., 2012). This feedwater salinity is not representative of UOG wastewater and further examination is needed in demonstrating the reliability of MD powered by geothermal energy for UOG wastewater treatment. Further, some of the additional challenges that need to be addressed are the effect of the feed solution (e.g., hardness) on the systems performance, and the investigation of long-term, continuous operation (Gonzalez et al., 2017).

2.2.4 Well-pad natural gas to power MD treatment

Natural gas is readily available at the well-pad during UOG production. In 2018, the daily natural gas production in the U.S. hit a new record of 101.3 billion cubic feet (BCF) (Geary, 2019) and the price of natural gas has steadily dropped in the U.S. During the initial months of production, natural gas flaring is widely used by oil and gas producers to dispose of natural gas in places that lack sufficient infrastructure (Franklin et al., 2019). A study performed by NOAA (Magill, 2016) identified 6,292 flares in the U.S. in 2016, which burned off an estimated 1,376 BCF (10.65 billion cubic meters) of natural gas, with the majority of flare sites attributed to oil and gas production. Produced natural gas may be a viable energy source for MD treatment of UOG wastewater in lieu of flaring during the initial months of production or for the lifetime of a well depending on natural gas price compared to cost of deep-well injection.

A study evaluated seven shale regions in the U.S. from 2012 to 2014 to determine the technical potential for repurposing the energy from flared natural gas for treatment of HF wastewater (Table 2-2) (Glazer et al., 2017). The authors determined that from 2012 through

2014, the Bakken, Marcellus, Utica, and Niobrara shale plays flared between 2 and 48 times the amount of natural gas needed to provide energy for treatment of the wastewater produced from the oil and gas industry. The Permian Basin, Eagle Ford, and Haynesville shale plays did not have sufficient flared gas to treat the wastewater produced in each respective region (Glazer et al., 2017).

Table 2-2. Summary of the key characteristics for seven shale regions of interest (Glazer et al., 2017).

Shale Region	Predominantly Oil or Gas Play	PDSI Index Classification	Wastewater Volume	Average TDS* Concentration (mg/L)	Flared Gas Volumes	Sufficient Nearby Disposal
Bakken	Oil	Slightly Wet	Low	250,000	Very High	Yes
Marcellus/Utica	Gas	Near Normal-Slightly Wet	Very Low	130,000	Medium	No
Eagle Ford	Oil & Gas	Insipient Dry Spell	Medium	40,000	High	Yes
Niobrara	Oil & Gas	Mild to Moderate Drought	Very Low	25,000	Low	Yes
Haynesville	Gas	Near Normal	Low	120,000	Low	Yes
Permian Basin	Oil & Gas	Insipient Dry Spell	Very High	140,000	Medium	Yes

Red indicates the characteristic is unfavorable for potentially coupling wastewater treatment with flared gas energy. Conversely, green indicates that the characteristic is relatively favorable for implementing the strategy. The Palmer Drought Severity Index (PDSI) was used to describe the general water availability in a region and takes into consideration precipitation and temperature, among other factors.

Other studies have focused on using flared natural gas (termed as “waste” natural gas) to power water production through reverse osmosis, thermal desalination, and atmospheric water harvesting (Glazer et al., 2014; Kar and Bahadur, 2019; Kar and Bahadur, 2020). Glazer et al. (Glazer et al., 2014) reported that in Texas, thermal treatment technologies powered by flared natural gas could yield 180-540 million m^3 of product water that could be used to hydraulically fracture 9,400-28,000 wells. The authors recommend obtaining more granular information about the location and availability of the flared natural gas, regional wastewater flow rates, and wastewater quality to augment their framework for identifying suitable treatment options and

corresponding water recovery rates (Glazer et al., 2014). Kar and Bahadur (Kar and Bahadur, 2020) presented a TEA evaluating RO-based treatment of flowback water using excess flared natural gas. Their results indicate that this concept will significantly benefit the Eagle Ford and Niobrara shale plays by vastly reducing wastewater disposal by up to 60% with favorable payback periods as low as one year (Kar and Bahadur, 2020). The potential drawback of relying on flared natural gas is the intermittent nature of flaring due to oil and gas producers implementing Reduced Emissions Completion (REC) technology, otherwise known as "green completions," reducing the practice of flaring after completion (IPIECA, 2014). Additionally, on-site storage of natural gas for UOG wastewater treatment would be required to fully utilize flared natural gas and would only power treatment for the initial few months.

Another consideration in using natural gas intended for sale to power MD treatment would be the natural gas price. Fluctuations in natural gas prices occur often which may promote using well-pad natural gas to power UOG wastewater treatment as opposed to selling it for profit. This is evidenced in March 2019 when the natural gas price plunged into negative territory rendering operators to pay pipeline companies for the transport of produced natural gas (Crowley, 2019). Permian Basin, like the Niobrara shale play, focuses on crude oil production rather than natural gas. An economic analysis comparing the loss of profit in regards to natural gas used for UOG wastewater treatment versus the cost of deep-well injection (disposal fees and transportation costs) would be beneficial. Additionally, the capacity of well-pad natural gas for on-site MD treatment of UOG wastewater has not been quantified in the literature and would be worth examination.

2.3 Logistical Considerations for UOG Wastewater Management

Logistical considerations, specifically transportation, play an important role in UOG wastewater management. As previously discussed, the process of HF for recovery of oil and natural gas uses large amounts of fresh water and produces a comparable amount of wastewater, much of which is typically transported by truck (Duthu and Bradley, 2017). Truck transport of water is an expensive and energy-intensive process with significant external costs including road damages and pollution (Duthu and Bradley, 2017). Options to reduce or eliminate transportation of UOG wastewater needs further study.

2.3.1 Transportation costs for UOG wastewater

The most commonly reported range for transportation costs via trucks of UOG wastewater in the U.S. is $1-3 per barrel for a typical trip from a well site to a salt water disposal (SWD) well (Groundwater Protection Council, 2019). Transportation costs are typically reported by the metric of dollars per barrel as a barrel (0.16 m^3) is the most common water volume used by the oil and gas industry. The cost of constructing permanent pipelines currently averages about $1.45 million per mile depending on pipe size, terrain, right of way costs, and other factors (Groundwater Protection Council, 2019). The transportation cost of UOG wastewater for deep-well injection highly depends on the number of disposal wells active in a region and their proximity to producing wells. Reported trucking costs in Texas, with a plentiful number of active disposal wells, range from $0.50 to 1.00 per barrel. In Pennsylvania, where disposal wells are scarce, reported trucking costs ranges from $4-8 per barrel (McCurdy, 2011). Further analysis in regards to transportation costs for UOG wastewater need to be completed at the regional and local scale to inform the management decision making process.

In regards to beneficial reuse, remote UOG sites may require the use of modular treatment facilities where the logistics of transporting water to a centralized facility may be both difficult and cost prohibitive. In the 2019 Groundwater Protection Council Produced Water Report, in most of the regional discussions with stakeholders within the oil and gas industry conducted for the report, cost was the dominant driver for beneficial reuse (Groundwater Protection Council, 2019). Within the context of cost, transportation costs were a significant factor in beneficial reuse evaluations.

The transportation of UOG wastewater via trucks also has costs associated with road damage. A study to compare and quantify road damage and life-cycle greenhouse gas (GHG) emissions of trucking and pipeline water delivery systems for a generic oil and gas field sited in the DJ Basin of northern Colorado highlighted road damage costs (Duthu and Bradley, 2017). The authors determined that incorporating pipeline-based transport of water and wastewater with centralized wastewater treatment and high rates of wastewater recycling reduced GHG emissions and road damage by factors of as much as 6 and 7 respectively, when replacing freshwater transport and waste disposal routes by truck (Duthu and Bradley, 2017). A study in Pennsylvania (Patterson and Maloney, 2016) quantified UOG wastewater transportation costs associated with truck traffic and road damage in the range of $1.4-8.1 million over a 3 year period. These costs related to road damage and possible environmental impacts due to GHG emissions could also add to the overall transportation costs associated with UOG wastewater transportation.

2.3.2 Distance to transport UOG wastewater

In order to calculate transportation costs, accurate determination of route distances from UOG wells to disposal wells, centralized wastewater (CWT) facilities, or other alternatives is required. A recent study used data collected from 2011 to 2013 in Pennsylvania to quantify

transportation activities associated with high-volume HF operations in the Marcellus shale formation (Korfmacher et al., 2019). Focus was placed on analyzing environmental impacts of transporting sand and water to, and waste from these UOG wells. ArcGIS Network Analyst was used in the analysis to simulate the transportation network for HF operations and quantify number of one-way truck trips and total number of vehicle miles (Korfmacher et al., 2019). Another study used ArcGIS to quantify truck travel distances via both the preferred routes (minimum distance while also favoring higher-order roads) as well as, where available, the likely actual distances for freshwater and waste transport between pertinent locations (e.g., gas wells, treatment facilities, freshwater sources) (Figure 2-10) (Gilmore et al., 2014). A focus of this study was to achieve transport mileage reductions based on their analysis using preferred routes over likely transport routes. These studies demonstrate the value of using ArcGIS Network Analyst to simulate transportation networks in a UOG development region to determine wastewater transportation route distances. In turn, these realistic transportation distances paired with actual wastewater volume could produce valuable transportation cost data to compare options for UOG wastewater management in a region.

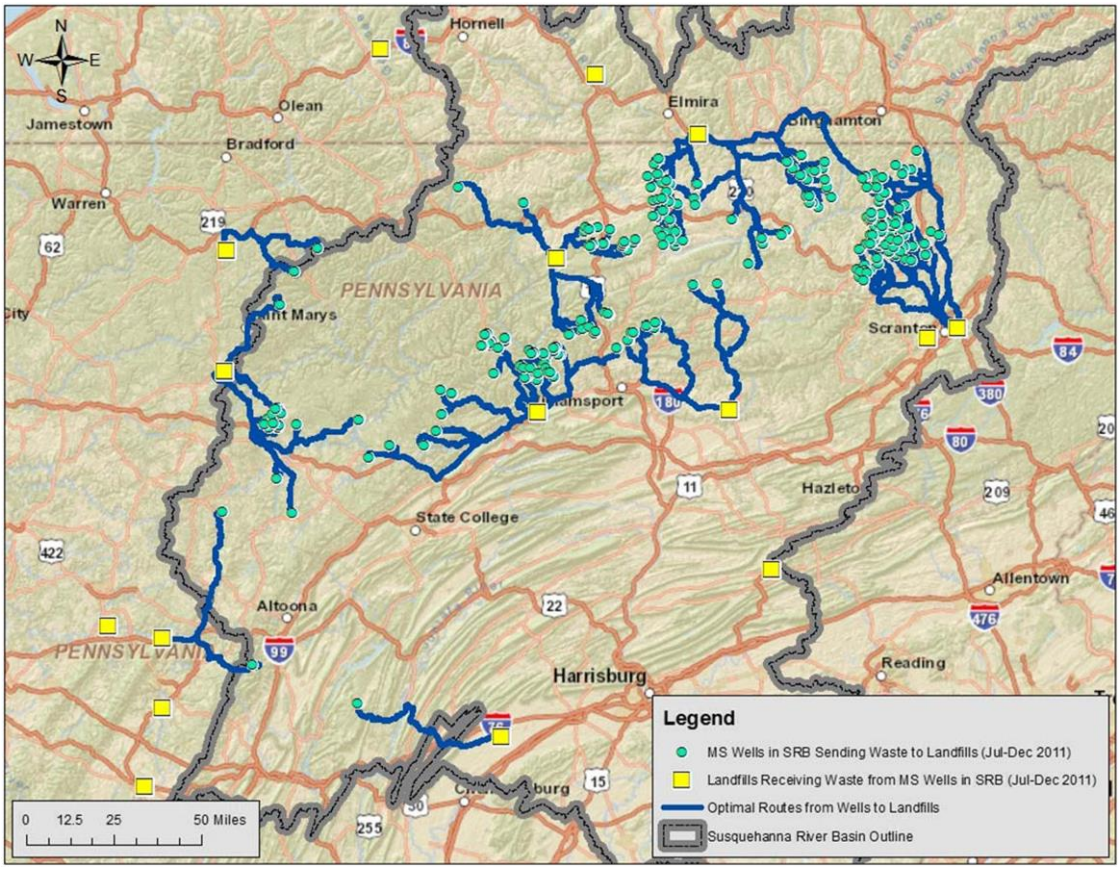

Figure 2-10. Example of network analysis results showing preferred routes of transport between gas wells (cyan circles) and landfills (yellow squares) in the Marcellus shale region. MS wells = Marcellus shale natural gas wells (Gilmore et al., 2014).

2.3.3 Incorporating UOG wastewater transportation into a systems-level analysis

To effectively evaluate UOG wastewater management strategies in a region, a systems-level analysis is needed. Within the framework of a systems-level analysis, cost of UOG wastewater transportation from UOG wells to treatment or disposal facilities is a vital component. A recent study for the Marcellus shale play in Pennsylvania emphasized a systems-level approach to optimizing UOG wastewater management with transportation being one of the critical factors in the approach (Tavakkoli et al., 2020). The analysis revealed that the result of their optimization model is most sensitive to variations in transportation cost with a 20% increase in transportation cost resulting in a 12% increase in total management cost (Tavakkoli et al., 2020). This underlies

the importance of factoring in accurate wastewater transportation distances and costs based on the region of interest in trying to determine the most feasible UOG wastewater management strategy. The authors of the study noted that transportation cost varies across states and counties and the results of their optimization model could be different across shale plays in the U.S. and should be assessed in the future (Tavakkoli et al., 2020). The importance of UOG wastewater transportation was clearly shown in this recent study and provides a strong impetus to evaluate its influence on selecting a UOG wastewater management strategy in other regions.

2.4 Regulatory Framework for UOG Wastewater Treatment

Another key component in the future of UOG wastewater treatment for beneficial reuse is the regulatory framework and outlook. In most states, the U.S. Environmental Protection Agency (USEPA) have delegated responsibility for regulating UOG wastewater beneficial reuse based on end use to state environmental agencies. However, in regards to discharge of UOG wastewater into publicly owned treatment works (POTWs), USEPA published a final rule in June 2016 that revised the Oil and Gas Extraction Effluent Guidelines and Standards requiring zero discharge of wastewater pollutants from UOG extraction facilities to POTWs (USEPA, 2016). This revised standard essentially eliminates the discharge of UOG wastewater to a POTW as an end use option. However, other beneficial reuse end-use options remain such as surface discharge to waterways and agricultural irrigation, although, regulatory requirements for these practices are not well-defined.

2.4.1 Current outlook on regulatory framework for UOG wastewater beneficial reuse

Presently, regulatory frameworks for overseeing beneficial reuse of UOG wastewater, particularly reuse outside the oil and gas industry (commonly referred to as external reuse), are not well-developed (Groundwater Protection Council, 2019). In order for UOG wastewater

treatment for beneficial reuse to be expanded in the future state-level regulatory agencies need solutions to several issues such as management of risk associated with commercial management of UOG wastewater from multiple sources at one CWT facility, ownership of UOG wastewater, and transfer of ownership (Groundwater Protection Council, 2019).

A recent study explored various disposal practices in five U.S. regions (Permian, Eagle Ford, Bakken, Marcellus, and Niobrara) and considered how the regulatory framework influenced those practices (Webb and Zodrow, 2019). The authors noted that within the six states with jurisdiction of the five regions studied, there existed remarkably different geology and therefore different quality of produced water. Additionally, these states possessed different levels of regulatory framework. The authors concluded in the absence of regulation, reuse of UOG wastewater is likely to remain limited, at least for the foreseeable future (Webb and Zodrow, 2019).

Within the current regulatory framework, it has been put forth that UOG wastewater beneficial reuse within the oil and gas industry (i.e., treatment for reuse as HF fluid) is more viable than beneficial reuse outside of this energy sector (Scanlon et al., 2020). Various beneficial end uses for UOG wastewater were examined both within the energy sector and outside the energy sector (Figure 2-11). The issue identified by the authors for beneficial end uses of UOG wastewater after treatment such as surface discharge and agricultural irrigation is that current regulations were not designed to address these practices (Scanlon et al., 2020). It was concluded that large uncertainties related to water quality issues currently preclude UOG wastewater reuse outside of the energy sector (Scanlon et al., 2020). This provides an impetus for state and federal regulatory agencies to promulgate updated regulations clearly focused on beneficial reuse outside of the oil and gas sector.

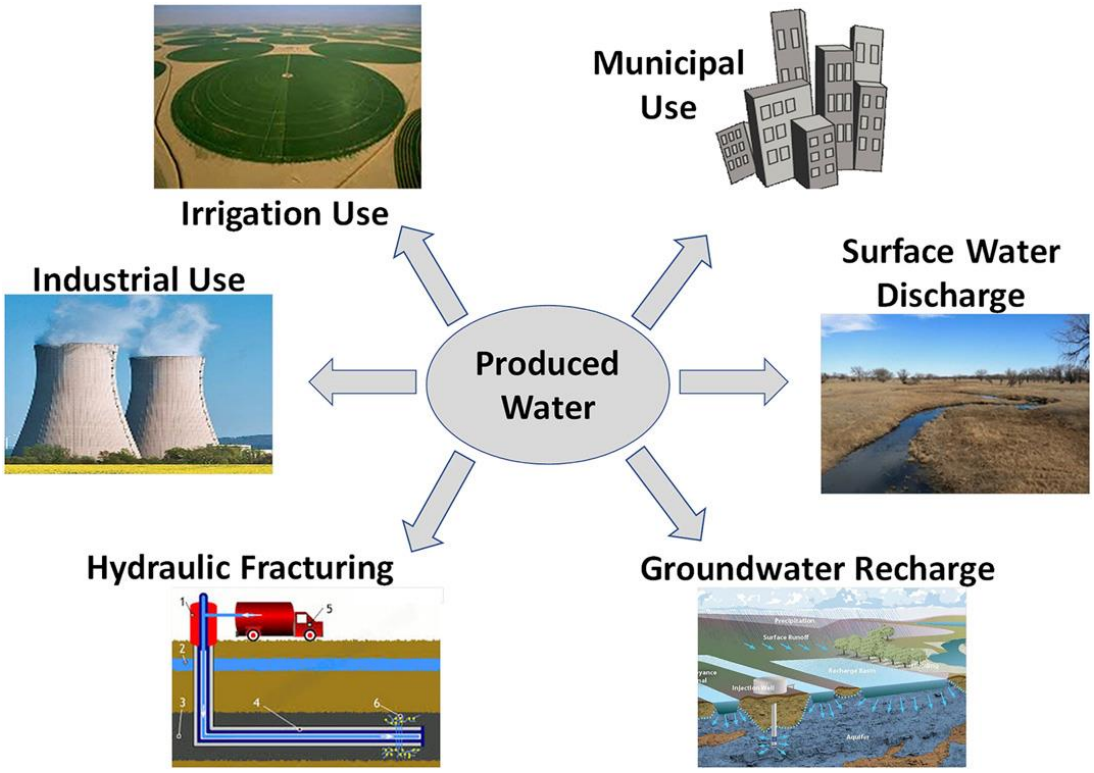

Figure 2-11. Beneficial use of UOG wastewater within the energy sector (hydraulic fracturing) and outside the energy sector (irrigation, municipal, industrial, and livestock), surface discharge (evaporation ponds, stream discharge) and groundwater recharge (Scanlon et al., 2020).

A recent study conducted in Wyoming provided a water quality assessment downstream of oil and gas produced water discharges for beneficial reuse (McLaughlin et al., 2020). The study area had discharge points upstream with approved surface discharge permits of oil and gas wastewater under the NPDES program. The study determined that concentrations of organic chemicals generally decreased downstream while concentrations of inorganic constituents increased downstream due to evaporation (McLaughlin et al., 2020). A recommendation was made that absent regulatory health thresholds for humans, livestock, and aquatic species for most chemical species at the discharge location and downstream, toxicity assays are necessary to determine impacts of oil and gas wastewater discharge. This research highlights the importance of establishing clear regulatory standards for UOG wastewater constituents to protect human and environmental health.

2.4.2 Regulatory management of UOG wastewater and proposed reuse evaluation framework

Adding to the complexity of management of UOG wastewater is that even within individual states, more than one agency may regulate its management. While underground injection control often falls under the jurisdiction of a state oil and gas agency, board, or commission, other management options such as NPDES discharge are typically regulated by either a state environmental quality agency, health agency, or the USEPA (Table 2-3) (Groundwater Protection Council, 2019). This greatly adds to the complexity for beneficial reuse and management of UOG wastewater as oil and gas producers must work with various states, or in some cases, federal agencies.

Table 2-3. Regulatory management of UOG wastewater by method and agency in six states (Groundwater Protection Council, 2019).

State	Underground Injection Control (Class II)	Land Application	Water Discharge via NPDES	Recycling
New Mexico	NMOCD	NMDOT[1]	USEPA[2]	NMOCD
North Dakota	NDIC	NDDoH[3]	NDDoH	NDSWC
Oklahoma	OCC	OCC/ ODEQ[4]	ODEQ	
Pennsylvania	USEPA		PADEP	
Texas	TRRC	TRRC	USEPA[5]	TRRC
Wyoming	WOGCC	WOGCC[6]	WDEQ	WDEQ

Agency Acronyms
NDDoH—North Dakota Department of Health
NDIC—North Dakota Industrial Commission
NDSWC—North Dakota State Water Commission
NMDOT—New Mexico Department of Transportation
NMED—New Mexico Environment Department
NMOCD—New Mexico Oil Conservation Division
OCC—Oklahoma Corporation Commission, Oil and Gas Division
ODEQ—Oklahoma Department of Environmental Quality
PADEP—Pennsylvania Department of Environmental Protection
TCEQ—Texas Commission on Environmental Quality
TRRC—Railroad Commission of Texas
USEPA—United States Environmental Protection Agency
WOGCC—Wyoming Oil and Gas Conservation Commission
WDEQ—Wyoming Department of Environmental Quality Agency Specific Provisions

1 The NMDOT may have jurisdiction over the use of produced water for road de-icing, http://www.emnrd.state.nm.us/OCD/education.html#OGProd4.
2 The NMED conducts compliance evaluation inspections on behalf of USEPA and reviews federal permits through certification.
3 The NDDoH has guidelines regarding use of certain produced water in dust and ice control. (NDDoH, supra Note 11)
4 The OCC regulates land application of produced water.
5 The TCEQ is not authorized to issue permits for activities associated with the exploration, development, or production of oil or gas or geothermal resources.
6 One-time land spreading on the well site is regulated by WOGCC. Other road spreading, land-spreading and land-farming operations are regulated by WDEQ and require a permit (Chapter 3 Permit Requirements for Treatment of CBM, Oil or Gas Produced Water, Wyoming Department of Environmental Quality, 7-8).

A pilot program for a comprehensive regulatory program to incentivize wastewater recycling from HF was put forth for the state of New Mexico (Small, 2015). Wastewater

recycling for future HF (otherwise known as internal reuse) requires less treatment than for beneficial reuse purposes. However, ideas brought forth in this pilot program could be utilized for a program focused on incentivizing beneficial reuse outside of the oil and gas field. Recommendations to best achieve both continuous technical improvement and provide cost effective alternatives to small businesses included governments implementing a hybrid system of marketable permits and underground injection taxes, employing taxes to provide research and development for new technological development, and loosening regulations to make recycling easier and support joint recycling initiatives (Small, 2015). It is possible that some of these recommended initiatives for UOG wastewater recycling applied for reuse could help spur increased beneficial reuse of UOG wastewater.

The Groundwater Protection Council in their 2019 report (Groundwater Protection Council, 2019) put forth a general framework for the evaluation of reuse options, focusing primarily on research needs (Figure 2-12). The framework was designed to assist decision-makers in working through analysis of a given beneficial reuse scenario. The framework consists of four key phases: preliminary review of the proposed program, identification of stressors of interest for treatment and risk analysis, risk assessment (applied to treated produced water), and risk management and decision making (Groundwater Protection Council, 2019). The aim of this framework is to serve as a useful guide in assessing a specific reuse scenario as opposed to prescribing a single set process for assessing individual reuse proposals. This effort is expected to encourage collaboration among various stakeholders, to include regulators, in regards to beneficial reuse. Existing data gaps in chemical and toxicological characterization of UOG wastewater limits implementation for specific reuse scenarios but future advancements with pairing characterization efforts with treatment studies or pilots could overcome this barrier

(Groundwater Protection Council, 2019). Within this proposed framework, there exist many regulatory questions that would need to be answered for reuse to occur. Research efforts should be focused at the state level to identify regulatory gaps and providing recommendations to enhance UOG wastewater treatment for beneficial reuse opportunities.

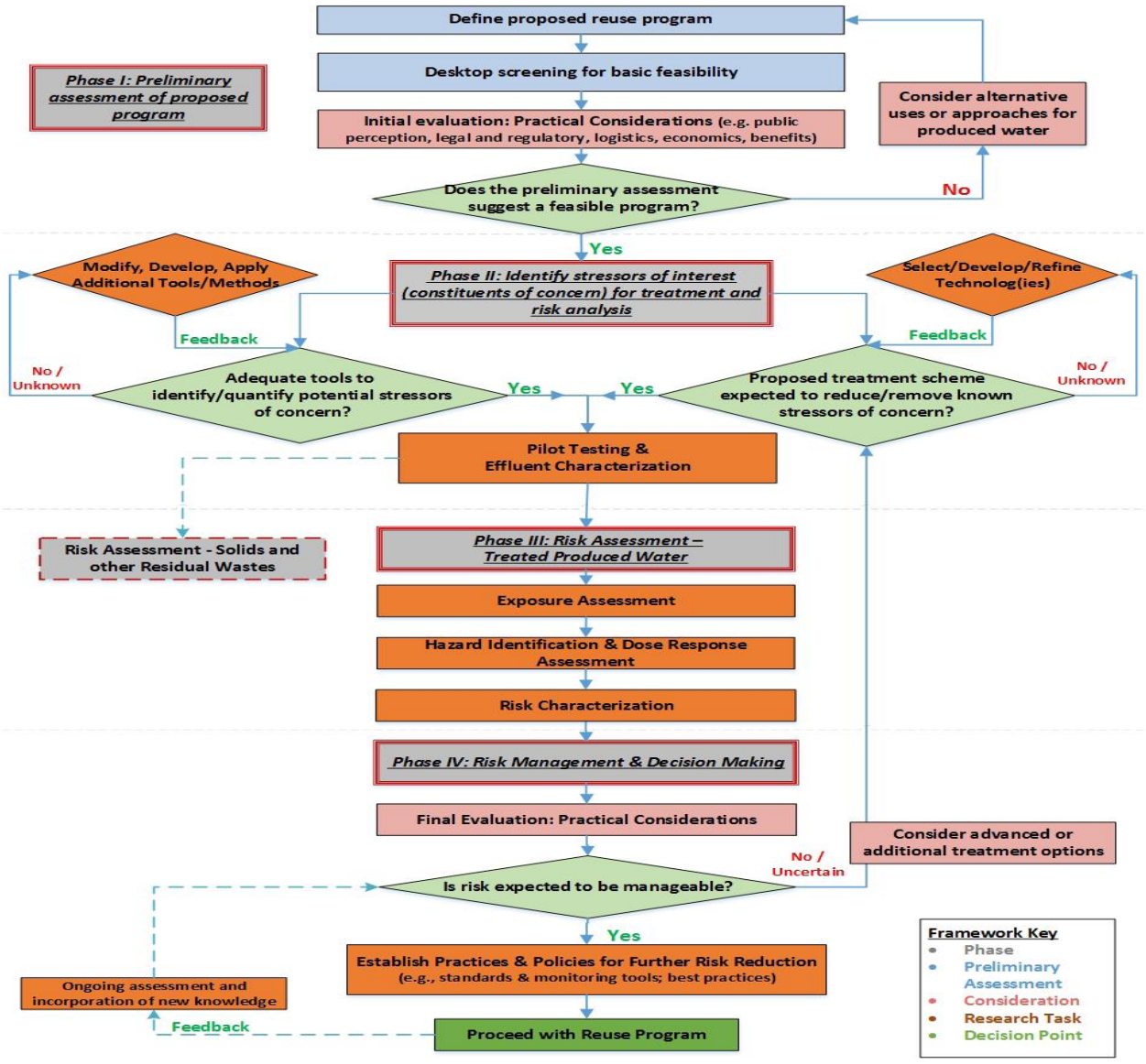

Figure 2-12. Framework for research, evaluation, and decision making for UOG wastewater reuse (Groundwater Protection Council, 2019).

References

Ahmadun, F.R., Pendashteh, A., Abdullah, L.C., Biak, D.R.A., Madaeni, S.S., Abidin, Z.Z., 2009. Review of technologies for oil and gas produced water treatment. *J. Haz. Mater.* 170 (2-3), 530-551.

Alzahrani, S., Mohammad, A.W., Hilal, N., Abdullah, P., Jaafar, O., 2013. Identification of foulants and fouling mechanisms and cleaning efficiency for NF and RO treatment of produced water. *Sep. Purification Technol.* 118, 324-341.

Arkansas Department of Environmental Quality, 2016. Fact Sheet and Supplementary Information for General Permit Discharges from Groundwater and Surface Water Clean Up Located within the State of Arkansas. ADEQ web site. https://www.adeq.state.ar.us/water/permits/npdes/nonstormwater/pdfs/arg790000/fact_sheet.pdf (accessed April 27, 2020).

Aybar, H.S., 2002. Analysis of a mechanical vapor compression desalination system. *Desalination* 142 (2), 181-186.

Bahar, R., Hawlader, M.N.A., Woei, L.S., 2004. Performance evaluation of a mechanical vapor compression desalination system. *Desalination* 166 (1-3), 123-127.

Bai, B., Carlson, K., Prior, A., Douglas, C., 2015. Sources of variability in flowback and produced water volumes from shale oil and gas wells. *J. Unconven. Oil Gas Resources* 12, 1-5.

Bai, B., Goodwin, S., Carlson, K., 2013. Modeling of frac flowback and produced water volume from Wattenberg oil and gas field. *J. Pet. Sci. Eng.* 108, 383-392.

Bell, E.A., Poynor, T.E., Newhart, K.B, Regnery, J., Coday, B.D., Cath, T.Y., 2017 Produced water treatment using forward osmosis membranes: Evaluation of extended-time performance and fouling. *J. Membr. Sci.* 525, 77-88.

Boo, C., Lee, J., Elimelech, M., 2016a. Engineering surface energy and nanostructure of microporous films for expanded membrane distillation applications. *Environ. Sci. Technol.* 50 (15), 8112-8119.

Boo, C., Lee, J., Elimelech, M., 2016b. Omniphobic polyvinylidene fluoride (PVDF) membrane for desalination of shale gas produced water by membrane distillation. *Environ. Sci. Technol.* 50 (22), 12275-12282.

Brantley, H.L., Thoma, E.D., Eisele, A.P., 2015. Assessment of volatile organic compound and hazardous air pollutant emissions from oil and natural gas well pads using mobile remote and on-site direct measurements. *J. Air Waste Manage. Assoc.* 65 (9), 1072-1082.

Brantley, S.L., Yoxtheimer, D., Arjmand, S., Grieve, P., Vidic, R., Pollak, J., Llewellyn, G.T., Abad, J., Simon, C., 2014. Water resource impacts during unconventional shale gas development: The Pennsylvania experience. *Int. J. Coal Geo.* 126, 140-156.

Butkovskyi, A., Bruning, H., Kools, S.A.E., Rijnaarts, H.H.M., Van Wezel, A.P., 2017. Organic pollutants in shale gas flowback and produced waters: Identification, potential ecological impact, and implications for treatment strategies. *Environ. Sci. Technol.* 51 (9), 4740-4754.

Caterpillar, 2011. 3512C HD Petroleum Engine. Caterpillar web site. https://s7d2.scene7.com/is/content/Caterpillar/LEHW0056-01 (accessed April 28, 2020).

Cath, T.Y., Childress, A.E., Elimelech, M., 2006. Forward osmosis: Principles, applications, and recent developments. *J. Membr. Sci.* 281 (1-2), 70-87.

Chang, H., Li., T., Liu, B., Vidic, R.D., Elimelech, M., Crittenden, J.C., 2019a. Potential and implemented membrane-based technologies for the treatment and reuse of flowback and produced water from shale gas and oil plays: A review. *Desalination* 455, 34-57.

Chen, G., Wang, Z.W., Ngehim, L.D., Li, X.M., Xie, M., Zhao, B.L., Zhang, M.X., Song, J.F., He, T., 2015. Treatment of shale gas drilling fluids (SGDFs) by forward osmosis: Membrane fouling and mitigation. *Desalination* 366, 113-120.

Chew, N.G.P., Zhao, S.S., Loh, C.H., Permogorov, N., Wang, R., 2017. Surfactant effects on water recovery from produced water via direct-contact membrane distillation. *J. Membr. Sci.* 528, 126-134.

Cippollina, A., Di Sparti, M.G., Tamburiini, A., Micale, G., 2012. Development of a membrane distillation module for solar energy seawater desalination. *Chem. Eng. Res. Design* 90 (12), 2101-2121.

Coday, B.D., Almaraz, N., Cath, T.Y., 2015. Forward osmosis desalination of oil and gas wastewater: Impacts of membrane selection and operating conditions on process performance. *J. Membr. Sci.* 488, 40-55.

Coday, B.D., Cath, T.Y., 2014. Forward osmosis: Novel desalination of produced water and fracturing flowback. *J. Amer. Water Works Assoc.* 106 (2), E55-E66.

Coday, B.D., Xu. P., Beaudry, E.G., Herron, J., Lampi, K., Hancock, N.T., Cath, T.Y., 2014. The sweet spot of forward osmosis: Treatment of produced water, drilling wastewater, and other complex and difficult liquid streams. *Desalination* 333 (1), 23-35.

Crowley, K., 2019. Gas Becomes Pricey Problem for Permian Basin Oil Drillers: Chart. *Bloomberg* [Online] https://www.bloomberg.com/news/articles/2019-04-03/gas-becomes-pricey-problem-for-permian-basin-oil-drillers-chart (accessed April 29, 2020).

Deshmukh, A., Boo, C., Karanikola, V., Lin, S.H., Straub, A.P., Tong, T.Z., Warsinger, D.M., Elimelech, M., 2018. Membrane distillation at the water-energy nexus: Limits, opportunities, and challenges. *Energy Environ. Sci.* 11, 1177-1196.

Dow, N., Gray, S., Jun-de, L., Zhang, J., Ostarcevic, E., Liubinas, A., Atherton, P., Roeszler, G., Gibbs, A., Duke, M., 2016. Pilot trial of membrane distillation driven by low grade waste heat: Membrane fouling and energy assessment. *Desalination* 391, 30-42.

Du, X.W., Zhang, Z.Y., Carlson, K.H., Lee, J., Tong, T.Z., 2018. Membrane fouling and reusability in membrane distillation of shale oil and gas produced water: Effects of membrane surface wettability. *J. Membr. Sci.* 567, 199-208.

Duong, H.C., Chivas, A.R., Nelemans, B., Duke, M., Gray, S., Cath, T.Y., Nghiem, L.D., 2015. Treatment of RO brine from CSG produced water by spiral-wound air gap membrane distillation – A pilot study. *Desalination* 366, 121-129.

Duthu, R.C., Bradley, T.H., 2017. A road damage and life-cycle greenhouse gas comparison of trucking and pipeline water delivery systems for hydraulically fractured oil and gas field development in Colorado. *PLoS One* 12 (7), e0180587.

Eastern Municipal Water District and Carollo Engineers, 2008. Evaluation and Selection of Available Processes for Zero-Liquid Discharge System for the Perris, California Ground Water Basin. Denver, CO: U.S. Department of the Interior, Bureau of Reclamation.

Encana, 2011a. Completed Well Pads and Equipment. Encana web site. https://www.encana.com/pdf/communities/usa/completedwellpadsandequipment(Piceance).pdf (accessed Apr. 28, 2020).

Encana, 2011b. DJ Basin, Colorado: Well completion and hydraulic fracturing. Encana web site. https://www.encana.com/pdf/communities/usa/wellcompletionandhydraulicfracturing(DJ).pdf (accessed Apr. 28, 2020).

Esmaeilirad, N., Carlson, K., Ozbek, P.O., 2015. Influence of softening sequencing on electrocoagulation treatment of produced water. *J. Haz. Mater.* 283, 721-729.

Ferrer, I., Thurman, E.M., 2015. Chemical constituents and analytical approaches for hydraulic fracturing waters. *Trends Environ. Anal. Chemistry* 5, 18-25.

Franklin, M., Chau, K., Cushing, L. J., Johnston, J. E., 2019. Characterizing flaring from unconventional oil and gas operations in South Texas using satellite observations. *Environ. Sci. Technol. 53* (4), 2220-2228.

Freedman, D.E., Riley, S.M., Jones, Z.L., Rosenblum, J.S., Sharp, J.O., Spear, J.R., Cath, T.Y., 2017. Biologically active filtration for fracturing flowback and produced water treatment. *J. Water Proc. Eng.* 18, 29-40.

Geary, E., 2019. U.S. natural gas production hit a new record high in 2018. U.S. E.I.A. website. https://www.eia.gov/todayinenergy/detail.php?id=38692 (accessed Apr. 29, 2020).

Ghaffour, N., Lattemann, S., Missimer, T., Ng, K.C., Sinha, S., Amy, G., 2014. Renewable energy-driven innovative energy-efficient desalination technologies. *Appl. Energy* 136, 1155-1165.

Gilmore, K.R., Hupp, R.L., Glathar, J., 2014. Transport of hydraulic fracturing water and wastes in the Susquehanna River Basin, Pennsylvania. *J. Environ. Eng.* 140 (5), B4013002.

Glazer, Y.R., Davidson, F.T., Lee, J.J., Webber, M.E., 2017. An inventory and engineering assessment of flared gas and liquid waste streams from hydraulic fracturing in the USA. *Curr. Sustain. Renew. Energy Rep.* 4, 219-231.

Glazer, Y.R., Kjellsson, J.B., Sanders, K.T., Webber, M.E., 2014. Potential for using energy from flared gas for on-site hydraulic fracturing wastewater treatment in Texas. *Environ. Sci. Technol. Lett.* 1, 300-304.

Gonzalez, D., Amigo, J., Suarez, F., 2017. Membrane distillation: Perspectives for sustainable and improved desalination. *Renew. Sustain. Energy Reviews* 80, 238-259.

Ground Water Protection Council, 2019. Produced Water Report: Regulations, Current Practices, and Research Needs. 310 p.

Gude, V. G., 2015. Energy storage for desalination processes powered by renewable energy and waste heat sources. *Appl. Energy 137*, 877-898.

Hayes, T.D., Halldorson, B., Horner, P., Ewing, J., Werline, J.R., Severin, B.F., 2014. Mechanical vapor recompression for the treatment of shale-gas flowback water. *Oil Gas Facil.* 3 (4), 54-62.

He, C., Wang, X.H., Liu, W.S., Barbot, E., Vidic, R.D., 2014. Microfiltration in recycling of Marcellus Shale flowback water: Solids removal and potential fouling of polymeric microfiltration membranes. *J. Membr. Sci.* 462, 88-95.

He, F., Sirkar, K.K., Gilron, J., 2009. Effects of antiscalants to mitigate membrane scaling by direct contact membrane distillation. *J. Membr. Sci.* 462, 88-95.

He, Y.H., Sun, C.X., Zhang, Y.F., Folkerts, E.J., Martin, J.W., Goss, G.G., 2018. Developmental toxicity of the organic fraction from hydraulic fracturing flowback and produced waters to early life stages of zebrafish (*Danio rerio*). *Environ. Sci. Technol.* 52 (6), 3820-3830.

Huang, Y.X., Wang, Z.X., Jin, J., Lin, S.H., 2017. Novel Janus membrane for membrane distillation with simultaneous fouling and wetting resistance. *Environ. Sci. Technol.* 51 (22), 13304-13310.

International Petroleum Industry Environmental Conservation Association, 2014. Green Completions. IPIECA web site. https://www.ipieca.org/resources/energy-efficiency-solutions/units-and-plants-practices/green-completions/ (accessed April 30, 2020).

Jaafar, S., Sarbatly, R., 2012. *Geothermal water desalination by using nanofiber membrane.* Proceedings of the International Conference of Chemical, Environmental and Biological Sciences. Penang, Malaysia.

Jain, P., Sharma, M., Dureja, P., Sarma, P.M., Lal, B., 2017. Bioelectrochemical approaches for removal of sulfate, hydrocarbon and salinity from produced water. *Chemosphere* 166, 96-108.

Jiang, Q.Y., Rentschler, J., Perrone, R., Liu, K.L., 2013. Application of ceramic membrane and ion-exchange for the treatment of the flowback water from Marcellus shale gas production. *J. Membr. Sci.* 431, 55-61.

Kar, A., Bahadur, V., 2019. *Comparing three methods for waste natural gas-based water production: Reverse osmosis, thermal desalination and atmospheric water harvesting*. Proceedings of the 4th Thermal and Fluids Engineering Conference, Las Vegas, NV, April 14-17, 2019.

Kar, A., Bahadur, V., 2020. Using excess natural gas for reverse osmosis-based flowback water treatment in US shale fields. *Energy* 196, 117145.

Khalaj, F., Sattler, M., 2019. Modeling of VOCs and criteria pollutants from multiple natural gas well pads in close proximity for different terrain conditions: A Barnett Shale case study. *Atmos. Poll. Res.* 10 (4), 1239-1249.

Kim, J., Kim, J., Hong, S., 2018. Recovery of water and minerals from shale gas produced water by membrane distillation crystallization. *Water Res.* 129, 447-459.

Kim, J., Kwon, H., Lee, S., Hong, S., 2017. Membrane distillation (MD) integrated with crystallization (MDC) for shale gas produced water (SGPW) treatment. *Desalination* 403, 172-178.

Kim, S.Y., Omur-Ozbek, P., Dhanasekar, A., Prior, A., Carlson, K., 2016. Temporal analysis of flowback and produced water composition from shale oil and gas operations: Impact of the frac fluid characteristics. *J. Pet. Sci. Eng.* 147, 202-210.

Kondash, A.J., Albright, E., Vengosh, A., 2017. Quantity of flowback and produced waters from unconventional oil and gas exploration. *Sci. Total Environ.* 574, 314-321.

Kondash, A., Lauer, N., Vengosh, A., 2018. The intensification of the water footprint of hydraulic fracturing. *Sci. Adv.* 4 (8), eaar5982.

Kong, F.X., Chen, J.F., Wang, H.M., Liu, X.N., Wang, X.M., Wen, X., Chen, C.M., Xie, Y.F.F., 2017. Application of coagulation-UF hybrid process for shale gas fracturing flowback water recycling: Performance and fouling analysis. *J. Membr. Sci.* 524, 460-469.

Koren, A., Nadav, N., 1994. Mechanical vapor compression to treat oil-field produced water. *Desalination* 98 (1-3), 41-48.

Korfmacher, K., Hawker, J.S., Winebrake, J., 2019. Transportation activities associated with high-volume hydraulic fracturing operations in the Marcellus shale formation: Analysis of environmental and infrastructure impacts. *Transport. Res. Rec.* 2503 (1), 70-80.

Lawson, K.W., Lloyd, D.R., 1997. Membrane distillation. *J. Membr. Sci.* 124 (1), 1-25.

Lester, Y., Ferrer, I., Thurman, E.M., Sitterley, K.A., Korak, J.A., Aiken, G., Linden, K.G., 2015. Characterization of hydraulic fracturing flowback water in Colorado: Implications for water treatment. *Sci. Total Environ.* 512, 637-644.

Lin, S.H., Nejati, S., Boo, C., Hu, Y.X., Osuji, C.O., Elimelech, M., 2014. Omniphobic membrane for robust membrane distillation. *Environ. Sci. Technol. Let.* 1 (11), 443-447.

Lobo, F.L., Wang, H.M., Huggins, T., Rosenblum, J., Linden, K.G., Ren, Z.J., 2016. Low-energy hydraulic fracturing wastewater treatment via AC powered electrocoagulation with biochar. *J. Haz. Mater.* 309, 180-184.

Lokare, O.R., Tavakkoli, S., Rodriguez, G., Khanna, V., Vidic, R.D., 2017a. Integrating membrane distillation with waste heat from natural gas compressor stations for produced water treatment in Pennsylvania. *Desalination* 413, 144-153.

Lokare, O.R., Tavakkoli, S., Wadekar, S., Khanna, V., Vidic, R.D., 2017b. Fouling in direct contact membrane distillation of produced water from unconventional gas extraction. *J. Membr. Sci.* 524, 493-501.

Magill, B.. 2016. U.S. Has More Gas Flares than Any Country. *Scientific American* [Online], https://www.scientificamerican.com/article/u-s-has-more-gas-flares-than-any-country/ (accessed Jul. 5, 2019).

McCurdy, R., 2011. Underground injection wells for produced water disposal U.S. Environmental Protection Agency (accessed Apr. 7, 2019).

McCutcheon, J.R., McGinnis, R.L., Elimelech, M., 2005. A novel ammonia-carbon dioxide forward (direct) osmosis desalination process. *Desalination* 171 (1), 1-11.

McGinnis, R.L., Hancock, N.T., Nowosielski-Slepowron, M.S., McGurgan, G.D., 2013. Pilot demonstration of the NH_3/CO_2 forward osmosis desalination process on high salinity brines. *Desalination* 312, 67-74.

McLaughlin, M.C., Borch, T., McDevitt, B., Warner, N.R., Blotevogel, J., 2020. Water quality assessment downstream of oil and gas produced water discharges intended for beneficial reuse in arid regions. *Sci. Total Environ.* 713, 136607.

Miller, D.J., Huang, X.F., Li, H., Kasemset, S., Lee, A., Agnihotri, D., Hayes, T., Paul, D.R., Freeman, B.D., 2013. Fouling-resistant membranes for the treatment of flowback water from hydraulic shale fracturing: A pilot study. *J. Membr. Sci.* 437, 265-275.

Miro, L., Gasia, J., Cabeza, L., 2016. Thermal energy storage (TES) for industrial waste heat (IWH) recovery: A review. *Appl. Energy* 179, 284-301.

Mondal, S., Wickramasinghe, S. R., 2008. Produced water treatment by nanofiltration and reverse osmosis membranes. *J. Membr. Sci.* 322 (1), 162-170.

Oetjen, K., Chan, K.E., Gulmark, K., Christensen, J.H., Blotevogel, J., Borch, T., Spear, J.R., Cath, T.Y., Higgins, C.P., 2018. Temporal characterization and statistical analysis of flowback and produced waters and their potential for reuse. *Sci. Total Environ.* 619, 654-664.

Patterson, L.A., Maloney, K.O., 2016. Transport of hydraulic fracturing waste from Pennsylvania wells: A county-level analysis of road use and associated road repair costs. *J. Environ. Manage.* 181, 353-362.

Qtaishat, M. R., Banat, F., 2013. Desalination by solar powered membrane distillation systems. *Desalination 308*, 186-197.

Riley, S.M., Ahoor, D.C., Oetjen, K., Cath, T.Y., 2018. Closed circuit desalination of O&G produced water: An evaluation of NF/RO performance and integrity. *Desalination* 442, 51-61.

Riley, S.M., Oliveira, J.M.S., Regnery, J., Cath, T.Y., 2016. Hybrid membrane bio-systems for sustainable treatment of oil and gas produced water and fracturing flowback water. *Sep. Purification Technol.* 171, 297-311.

Rosenblum, J.S., Sitterley, K.A., Thurman, E.M., Ferrer, I., Linden, K.G., 2016. Hydraulic fracturing wastewater treatment by coagulation-adsorption for removal of organic compounds and turbidity. *J. Environ. Chem. Eng.* 4, 1978-1984.

Rosenblum, J., Thurman, E.M., Ferrer, I., Aiken, G., Linden, K.G., 2017. Organic chemical characterization and mass balance of a hydraulically fractured well: From fractured fluid to produced water over 405 days. *Environ. Sci. Technol.* 51 (23), 14006-14015.

Sarbatly, R., Chiam, C-K., 2013. Evaluation of geothermal energy in desalination by vacuum membrane distillation. *Appl. Energy* 112, 737-746.

Sardari, K., Fyfe, P., Lincicome, D., Wickramsinghe, S.R., 2018. Combined electrocoagulation and membrane distillation for treating high salinity produced waters. *J. Membr. Sci.* 564, 82-96.

Scanlon, B.R., Reedy, R.C., Xu, P., Engle, M., Nicot, J.P., Yoxtheimer, D., Yang, Q., Ikonnikova, S. 2020. Can we beneficially reuse produced water from oil and gas extraction in the U.S.? *Sci. Total Environ.* 717, 137085.

Schwantes, R., Cipollina, A., Gross, F., Koschikowski, J., Pfeifle, D., Rolletschek, M., Subiela, V., 2013. Membrane distillation: Solar and waste heat driven demonstration plants for desalination. *Desalination* 323, 93-106.

Sevier, D. K., 2015. Oil & gas industry electric power for upstream operations. Advanced Research Projects Agency - Energy web site. https://arpa-e.energy.gov/sites/default/files/Sevier_SWN_GENSETS.pdf (accessed Apr. 28, 2020).

Shaffer, D.L., Arias Chavez, L.H., Ben-Sasson, M., Romero-Vargas Castrillon, S., Yip., N.Y., Elimelech, M., 2013. Desalination and reuse of high-salinity shale gas produced water: Drivers, technologies, and future directions. *Environ. Sci. Technol.* 47 (17), 9569-9583.

Shaffer, D.L., Werber, J.R., Jaramillo, H., Lin, S.H., Elimelech, M., 2015. Forward osmosis: Where are we now? *Desalination* 356, 271-284.

Shih, J.,S., Saiers, J.E., Anisfeld, S.C., Chu, Z.Y., Muehlenbachs, L.A., Olmstead, S.M.M., 2015. Characterization and analysis of liquid waste from Marcellus shale gas development. *Environ. Sci. Technol.* 49 (16), 9557-9565.

Siemens, 2012. Extending value through field redevelopment: Solutions that maximize the value of mature assets. Siemens web site. https://w3.siemens.com/markets/global/en/oil-gas/PublishingImages/applications/onshore-production/Extending_value.pdf (accessed Apr. 28, 2020).

Singh, D., Sirkar, K.K., 2012. Desalination of brine and produced water by direct contact membrane distillation at high temperatures and pressures. *J. Membr. Sci.* 389, 380-388.

Small, X.T., 2015. Water use and recycling in hydraulic fracturing: Creating a regulatory pilot for smarter water use in the West. *Nat. Resources J.* 55 (2), 409-440.

Stoll, Z.A., Forrestal, C., Ren, Z.J., Xu, P., 2015. Shale gas produced water treatment using innovative microbial capacitive desalination cell. *J. Haz. Mater.* 283, 847-855.

Tavakkoli, S., Lokare, O. R., Vidic, R. D., Khanna, V., 2016. Systems-level analysis of waste heat recovery opportunities from natural gas compressor stations in the United States. *ACS Sustain. Chem. Eng. 4* (7), 3618-3626.

Tavakkoli, S., Lokare, O.R., Vidic, R.D., Khanna, V., 2017. A techno-economic assessment of membrane distillation for treatment of Marcellus shale produced water. *Desalination* 416, 24-34.

Tavakkoli, S., Lokare, O., Vidic, R., Khanna, V., 2020. Shale gas produced water management using membrane distillation: An optimization-based approach. *Resourc. Conserv. Recycl.* 158, 104803.

Thiel, G.P., Tow, E.W., Banchik, L.D., Chung, H.W., Lienhard, J.H., 2015. Energy consumption in desalinating produced water from shale oil and gas extraction. *Desalination* 416, 24-34.

Tong, T., Carlson, K.H., Robbins, C.A., Zhang, Z., Du, X., 2019. Membrane-based treatment of shale oil and gas wastewater: The current state of knowledge. *Front. Environ. Sci. Eng.* 13 (4): 63.

Tong, T.Z., Elimelech, M., 2016. The global rise of zero liquid discharge for wastewater management: Drivers, technologies, and future direction. *Environ. Sci. Technol.* 50 (13), 6846-6855.

Ullah, R., Khraisheh, M., Esteves, R. J., McLeskey, J. T., AlGhouti, M., Gad-el-Hak, M., Vahedi Tafreshi, H., 2018. Energy efficiency of direct contact membrane distillation. *Desalination 433*, 56-67.

United States Energy Information Administration, 2020. Natural Gas Explained: Delivery and storage of natural gas. US E.I.A. web site. https://www.eia.gov/energyexplained/natural-gas/delivery-and-storage.php (accessed April 28, 2020).

United States Environmental Protection Agency, 2016. 40 CFR Part 435 Effluent Limitations Guidelines and Standards for the Oil and Gas Extraction Point Source Category. In Ed. Federal Register; Vol. 81 FR 67191, pp 41845 - 41857.

United States Environmental Protection Agency, 2005. 2005 Remediation General Permit Fact Sheet Excerpts. USEPA web site. https://www3.epa.gov/region1/npdes/remediation/RGP2010_FactSheet_AttachmentA.pdf (accessed April 27, 2020).

United States Environmental Protection Agency Region VIII, 1995. Technically-Based Local Limits Development Strategy. USEPA web site. https://www.epa.gov/sites/production/files/documents/LocalLimitsStrategy.pdf (accessed April 27, 2020).

Vidic, R.D., Brantley, S.L., Vandenbossche, J.M., Yoxtheimeer, D., Abad, J.D., 2013. Impact of shale gas development on regional water quality. *Science* 340 (6134), 1235009.

Warneke, C., Geiger, F., Edwards, P.M., Dube, W., Petron, G., Kofler, J., Zahn, A., Brown, S.S., Graus, M., Gilman, J.B., Lerner, B.M., Peischl, J., Ryerson, T.B., de Gouw, J.A., Roberts, J.M., 2014. Volatile organic compound emissions from the oil and natural gas industry in the Uintah Basin, Utah: Oil and gas well pad emissions compared to ambient air composition. *Atmos. Chem. Phys.* 14, 10977-10988.

Wang, Z.X., Elimelech, M., Lin, S.H., 2016. Environmental applications of interfacial materials with special wettability. *Environ. Sci. Technol.* 50 (5), 2132-2150.

Webb, R., Zodrow, K.R., 2019. *Disposal of Water for Hydraulic Fracturing: Case Study on the U.S.* In: Buono, R., Lopez Gunn, E., McKay, J., Staddon, C. (editors), Regulating Water Security in Unconventional Oil and Gas. Water Security in a New World. Springer, Cham.

Wilcox, A., 2018. *Determining Opportunities for Combined Heat and Power (CHP) in the Oilfield*, Proceedings of the 25th International Petroleum Environmental Conference, Denver, CO, October 30 - November 1, 2018.

Winglee, J.M., Bossa, N., Rosen, D., Vardneer, J.T., Wiesner, M.R., 2017. Modeling the concentration of volatile and semivolatile contaminants in direct contact membrane distillation (DCMD) product water. *Environ. Sci. Technol.* 51 (22), 13113-13121.

Winter, D., Koschikowski, J., Wieghaus, M., 2011. Desalination using membrane distillation: Experimental studies on full scale spiral wound modules. *J. Membr. Sci.* 375, 104-112.

Xiong, B.Y., Zydney, A.L., Kumar, M., 2016. Fouling of microfiltration membranes by flowback and produced waters from the Marcellus shale gas play. *Water Res.* 99, 162-170.

Yao, M.W., Woo, Y.C., Tijing, L.D., Choi, J.S., Shon, H.K., 2018. Effects of volatile organic compounds on water recovery from produced water via vacuum membrane distillation. *Desalination* 440, 146-155.

Zhai, J., Huang, Z.J., Rahaman, M.H., Li, Y., Mei, L.Y., Ma, H.P., Hu, X.B., Xiao, H.W., Luo, Z.Y., Wang, K.P., 2017. Comparison of coagulation pretreatment of produced water from natural gas well by polyaluminum chloride and polyferric sulphate coagulants. *Environ. Technol.* 38 (10), 1200-1210.

Zhang, Z.Y., Du, X.W., Carlson, K.H., Robbins, C.A., Tong, T.Z., 2019. Effective treatment of shale oil and gas produced water by membrane distillation coupled with precipitative softening and walnut shell filtration. *Desalination* 454, 82-90.

3.0 Research Objectives

After conducting a thorough literature review on various aspects of UOG wastewater management, knowledge gaps that my research intends to close are listed below:

- The availability and treatment capacity of waste heat at the well-pad to power on-site UOG wastewater treatment, as well as those at natural gas compressor stations to power centralized UOG wastewater treatment have not been quantified in literature.
- It is unclear how transportation distance might impact UOG wastewater management options in a region with readily available disposal wells.
- The current strategies that mitigate surfactant-induced wetting in MD treatment of UOG wastewater, including the use of pretreatment and omniphobic membrane, have not been compared in terms of their efficiency.
- The barriers to beneficial reuse in UOG wastewater management have not been fully revealed, especially those not related to technology development.

After reviewing the technological, economic, logistical, and regulatory aspects of UOG wastewater management, the following research questions for this study have been developed:

- What is the best source of energy for powering MD treatment of UOG wastewater in Weld County, CO?
- How much waste heat/natural gas is required and available for MD treatment of UOG wastewater?

- What is the impact of logistical considerations such as transportation distance on the UOG wastewater management paradigm in Weld County, CO?
- What are the options to mitigate surfactant-induced wetting in the MD treatment of DJ Basin UOG wastewater and which option is most effective?
- What are the barriers for beneficial reuse of UOG wastewater and what solutions are needed to enable increased beneficial reuse?

To attain a better understanding of these questions and determine answers, this study proposes the following research objectives:

- **Quantify on-site treatment capacity of MD powered by waste heat or natural gas in Weld County, CO**

On-site treatment eliminates the requirement for transportation of UOG wastewater greatly reducing a costly aspect of UOG wastewater management. However, using a thermal desalination technology such as MD requires a cost-effective energy source to be viable. Waste heat at the well-pad either, collected and stored from the hydraulic fracturing phase, or from the on-site electrical load may provide a low cost energy source. However, the quantity and availability of this waste heat source is not well-known. An additional thermal energy source is available from the well-pad natural gas that could be used to power on-site MD treatment of UOG wastewater. However, the quantity available and how much would be needed for treatment has not been well-studied.

A random sampling of wastewater and natural gas production data for UOG producing wells in Weld County, CO will be completed. This data will be used to inform a comparison between two sources of waste heat and natural gas to power MD treatment at the well-pad.

- **Determine transportation distance impact on deep-well injection and centralized wastewater treatment in Weld County, CO through spatial and cost analysis**

Logistical considerations such as transportation distance influences UOG wastewater management but its impact is not well known for an area (such as in northeast Colorado) where there are numerous active disposal wells. Centralized wastewater treatment is another option for UOG wastewater management but this strategy is also greatly affected by transportation of wastewater. Ultimately, the transportation costs associated with these two UOG wastewater management strategies may make one more favorable than the other.

ArcGIS software will be utilized to spatially analyze the one-way transportation distance required to move UOG wastewater from producing wells to the nearest disposal well for deep-well injection and moving the same volume to the nearest natural gas compressor station for centralized wastewater treatment. Natural gas compressor stations provide a source of waste heat that could power centralized MD treatment of UOG wastewater. These distances will be translated into a cost to allow for a comparison between the two management strategies.

- **Quantify waste heat available at natural gas compressor stations in Weld County, CO and determine how well correlated waste heat quantity is to UOG wastewater density**

The available amount of waste heat for NGCSs in Weld County, CO has not been quantified. For centralized MD treatment of UOG wastewater to be viable, a low cost energy source such as waste heat available at an NGCS is needed. Quantifying the amount of waste heat available at an NGCS and determining wastewater treatment demand from producing wells in close proximity to the NGCS will be completed. This analysis will inform a determination on the correlation of waste heat quantity and UOG wastewater density in Weld County, CO.

- **Compare pretreatment and an omniphobic membrane to mitigate surfactant-induced wetting from DJ Basin UOG wastewater during membrane distillation treatment**

For UOG wastewater treatment with MD, the detrimental effects of membrane wetting need to be mitigated. Specifically, surfactant-induced wetting is a major concern in MD treatment of UOG wastewater. Surfactants are low surface energy compounds commonly found in HF fluid and in turn commonly detected in UOG wastewater. Pretreatment or membranes with special wettability have been proposed as strategies to mitigate surfactant-induced wetting.

The performance of MD in treating DJ Basin UOG wastewater will be assessed at the laboratory scale. After evaluating the performance of MD in treating raw UOG wastewater, a pretreatment train and an omniphobic membrane will be evaluated on mitigating surfactant-induced wetting caused by UOG wastewater. A determination will be made on which option enables most effective treatment performance based on experimentation.

- **Understand and elucidate barriers to beneficial reuse of UOG wastewater and provide recommendations to overcome these barriers**

Barriers to beneficial reuse of UOG wastewater include technological, regulatory, economic, and social. To promulgate increased future beneficial reuse of UOG wastewater, these barriers need to be examined and clearly elucidated to attain a better understanding of the current UOG wastewater management paradigm. From this examination, possible solutions will be proposed to facilitate increased beneficial reuse of UOG wastewater in the future.

4.0 On-Site Treatment Capacity of Membrane Distillation Powered by Waste Heat or Natural Gas for Unconventional Oil and Gas Wastewater in the Denver-Julesburg Basin[2]

4.1 Introduction

In the past decade, the United States has witnessed a rapid growth of unconventional oil and gas (UOG) exploration and production. Meanwhile, the water use and wastewater production of hydraulic fracturing (HF) in major shale oil and gas regions have steadily increased (Kondash et al., 2018). During HF activities, large volumes of freshwater along with fracturing fluids and sand are injected under high pressure to fracture the underlying reservoir rock to stimulate hydrocarbon production (Barati and Liang, 2014), and subsequently produce substantial amounts of wastewater. For example, in the Niobrara shale formation situated in northeastern Colorado and parts of Wyoming, Nebraska, and Kansas, the volume of wastewater generated within the first 12 months of well completion increased from 1,823 m^3 (481,586 gallons)/well in 2011 to 2,959 m^3 (781,685 gallons)/well in 2016 (Kondash et al., 2018). In 2016 alone, ~12 billion gallons (300 million barrels) of wastewater were produced from oil and gas wells in Colorado (Dolan et al., 2018).

The current management practices for UOG wastewater rely heavily on injection into Class II Underground Injection Control (UIC) disposal wells (a practice referred to as deep-well injection). However, multiple concerns such as induced seismicity, potential groundwater contamination, and the lack of available reservoir capacity continue to plague deep-well

[2] This chapter has been published as a research article in *Environment International* with the following citation:

Robbins, C.A., Grauberger, B.M., Garland, S.D., Carlson, K.H., Lin, S., Bandhauer, T.M., Tong, T., 2020. On-site treatment capacity of membrane distillation powered by waste heat or natural gas for unconventional oil and gas wastewater in the Denver-Julesburg Basin. *Environ. Inter.* 145, 106142.

injection, leaving its future viability in doubt (Ellsworth, 2013; Shaffer et al., 2013; Gregory and Mohan, 2015; Tavakkoli et al., 2017; Hincks et al., 2018; Scanlon et al., 2018). In recent years, alternative approaches to manage UOG wastewater have gained increasing popularity, as highlighted by the extensive research activities associated with the treatment and beneficial reuse of such wastewater (e.g., discharge into surface waters and agricultural irrigation) (Rahm et al., 2013; Akob et al., 2016; Butkovskyi et al., 2017; Dolan et al., 2018; Jimenez et al., 2018; Ma et al., 2018; Chang et al., 2019a). UOG wastewater is characterized as having high salinity (often comparable or higher than seawater) along with various organic and inorganic contaminants such as petroleum-associated compounds, heavy metals, and radioactive materials (Kahrilas et al., 2016; Butkovskyi et al., 2017; Silva et al., 2017; Chang et al., 2019b; Sun et al., 2019). Therefore, effective treatment that removes those hazardous components is essential for the protection of environmental and human health if the UOG wastewater is to be beneficially reused.

Membrane distillation (MD) has emerged as a promising technology to treat hypersaline and complex wastewaters such as those produced during UOG exploitation (Boo et al., 2016; Lokare et al., 2017b; Tavakkoli et al., 2017; Tong et al., 2019; Wang et al., 2019; Zhang et al., 2019). MD is a hybrid thermal-membrane desalination process, in which a partial vapor pressure difference generated between the heated feedwater and the cold permeate stream drives the transport of water vapor across a microporous and hydrophobic membrane (Lawson and Lloyd, 1997; Deshmukh et al., 2018). MD requires moderate temperatures (60-80 °C) and thus has the potential to utilize low-grade thermal energy (e.g., waste heat, solar and geothermal energy) (Duong et al., 2015; Guillen-Burrieza et al., 2015; Deshmukh et al., 2018; Lu et al., 2019). Also, MD tolerates high salinity of the UOG wastewater, which cannot be treated by pressure-driven

processes such as reverse osmosis (RO) (Tong and Elimelech, 2016; Deshmukh et al., 2018). This favorable feature is of great importance to maximize the water recovery and minimize the brine volume in UOG wastewater treatment.

Previous work has proposed using waste heat to power MD for the treatment of UOG and other hypersaline wastewater, in order to reduce the economic cost and carbon footprint (Dow et al., 2016; Tavakkoli et al., 2016; Dow et al., 2017; Tavakkoli et al., 2017; Lai et al., 2018; Schwantes et al., 2018; Yuan et al., 2020). However, the availability of waste heat at individual oil and gas producing sites has not been rigorously investigated. At UOG well sites, there are typically small power loads limiting the amount of waste heat generated (Wilcox, 2018). It is still unknown whether waste heat provided on-site is able to meet the demand of UOG wastewater treatment. In a recent study, the viability of powering MD treatment by the exhaust stream from natural gas compression stations (NGCSs) was evaluated for the Marcellus Shale (Lokare et al., 2017a). Although waste heat from NGCSs was shown sufficient to treat all the UOG wastewater in the state of Pennsylvania, this study suggested that MD treatment facilities need to co-locate with the stations, with the economic cost of wastewater transportation potentially significant or prohibitive (Lokare et al., 2017a). Therefore, energy sources that avoid costly wastewater transport by enabling on-site treatment are highly desirable to promote the economic feasibility of UOG wastewater treatment by MD technology.

One such alternative energy source is natural gas that is readily available at the well pad during UOG production. In 2018, the daily natural gas production in the U.S. hit a new record of 101.3 billion cubic feet (BCF) (Geary, 2019) and the price of natural gas has steadily dropped in the U.S. In particular, it plunged into negative territory in March 2019 in the Permian Basin (Crowley, 2019), where the target hydrocarbon is crude oil rather than natural gas, rendering

operators to pay pipeline companies for the transport of produced natural gas. Therefore, utilizing natural gas to power the MD process might be an economically feasible alternative for UOG wastewater treatment. However, the capacity of well-pad natural gas for on-site MD treatment of UOG wastewater has not been quantified in the literature. In addition, the volume of wastewater production varies significantly during UOG production (Bai et al., 2015; Estrada and Bhamidimarri, 2016; Mohammad-Pajooh, 2018), and whether the energy supplies of waste heat and natural gas are compatible with the dynamic wastewater treatment demand at individual wells needs to be understood.

In this study, we investigate the viability of using waste heat and well-pad natural gas to power on-site MD treatment of UOG wastewater in the Denver-Julesburg (DJ) Basin of the Niobrara shale play in Colorado, a crude oil and gas liquids rich play located in Northeast Colorado and Southeast Wyoming (Higley and Cox, 2007; Natural Gas Intelligence, 2020). In contrast to the Marcellus shale play where dry natural gas is the main product, crude oil is the target hydrocarbon in the DJ Basin, with natural gas being a by-product of production. We first analyze the availability of waste heat at the UOG production sites and examine the feasibility of waste heat as a reliable and consistent energy source for UOG wastewater treatment at twenty randomly selected producing wells of the DJ Basin. Further, by integrating production data of natural gas and wastewater, we correlate the dynamic capacity of MD treatment powered by well-pad natural gas with the treatment demand of UOG wastewater. The thermal energy supplied by waste heat and natural gas was both quantified and compared with the energy requirement by MD treatment of UOG wastewater. Our results, for the first time, provide quantitative analyses that evaluate the potential and reliability of waste heat and well-pad natural

gas as alternative energy sources to electricity for on-site wastewater treatment in the UOG industry.

4.2 Material and Methods

4.2.1 Data collection

The data of natural gas and wastewater production were collected for hydraulically fractured producing wells in Weld County of northeastern Colorado from the Colorado Oil and Gas Information System (COGIS) database managed by the Colorado Oil and Gas Conservation Commission (COGCC) (COGCC, 2019). COGIS provides production data for oil and gas wells in Colorado on a monthly basis, including quantitative information of oil and gas production along with the volume of wastewater generation. A random sampling of 20 hydraulically fractured wells completed between June and September 2017 was performed (Figure A1, Appendix A), and the wastewater and natural gas production for these 20 wells are representative for the investigated region (Figure A2, Appendix A). Since the volume of wastewater production decreased with time and became relatively stable after 10 months (Figure A3, Appendix A), 12 months of data were obtained and used in the following analyses for each well.

4.2.2 DCMD model for evaluating energy consumption by MD treatment

In order to estimate the energy requirement by MD, a direct contact membrane distillation (DCMD) model was developed to simulate MD treatment of UOG wastewater from DJ Basin using Engineering Equation Solver (EES) software. EES is a general equation-solving program that can numerically solve multiple coupled non-linear algebraic and differential equations. A useful feature of EES is the high-accuracy thermodynamic and transport property database, which is provided for hundreds of substances in a manner that allows it to be used with the equation solving capability (F-Chart software, 2020).

The DCMD model created in EES is multi-pass with heat recovery, allowing for recirculation of brine fluid and latent heat recovery through a heat exchanger (Figure 4-1). Thus, the MD brine can be concentrated to a desired salinity to meet specific water recovery rate. The salinity of UOG wastewater in the DJ Basin is reported in the range of 20,000-40,000 mg L^{-1} of total dissolved solids (TDS) (Esmaeilirad et al., 2015; Lester et al., 2015; Rosenblum et al., 2016 Kim et al., 2016; Bell et al., 2017; Chang et al., 2019b; Zhang et al., 2019). A water recovery rate of 80-90% was used to achieve a brine salinity of 200,000 mg L^{-1}, depending on the feedwater salinity. Such brine salinity is achievable by MD and comparable to that of other thermal desalination technologies such as mechanical vapor compression (MVC) (Tong and Elimelech, 2016). However, at such high salinity, MD performance can be significantly affected by mineral scaling and temperature polarization. With an increased salinity concentration in the bulk feed solution due to high water recovery rates, the potential for mineral scaling increases. Additionally, temperature polarization could be enhanced due to an increase in viscosity and density of the bulk feedwater, which adversely affects the Reynolds number and heat transfer coefficient (Ali et al., 2013). However, we were not able to consider mineral scaling and the effect of salinity on temperature polarization in our DCMD model, and we suggest the readers consider these factors when applying the findings of our study to practical MD applications. The feed temperature was set in the range of 60°C to 90°C with the permeate temperature set at 20°C. The permeate stream temperature is lowered in a cooling system (e.g., air-cooled heat exchanger) to 20°C at node 13. A polyvinylidene fluoride (PVDF) membrane (HVHP, Durapore) with a nominal pore size of 0.45 μm, porosity of 75%, and an average thickness of 125 μm was used as representative membrane in the model. A membrane area of 5 m^2 per module was used with the module geometry consisting of a channel height of 0.7 m, channel length of 3.5 m, and channel

width of 1.42 m (Schwantes et al., 2018). Other important parameters for the model included the membrane permeability coefficient, *C*, which was experimentally measured in the laboratory (0.00038 kg m^{-2} s^{-1} Pa^{-1}), and the thermal conductivity of membrane (k_m) was 0.09004 W K^{-1} m^{-1} as calculated using Eq. 4-1:

$$k_m = (1 - \varepsilon) * k_{mm} + \varepsilon * k_g \qquad (4-1)$$

where ε is membrane porosity (%), k_{mm} and k_g are thermal conductivities of membrane material (PVDF polymer) and gas (air and water vapor) in the pores of the membrane, respectively (Olatunji and Camacho, 2018).

Also, 15 nodes were used in the model with each node having their own temperature, mass, volumetric and heat flow rates, salinity concentration, density, and specific heat capacity (Table A1, Appendix A). Additionally, the vapor pressure was calculated at nodes 3, 4, 9, and 10.

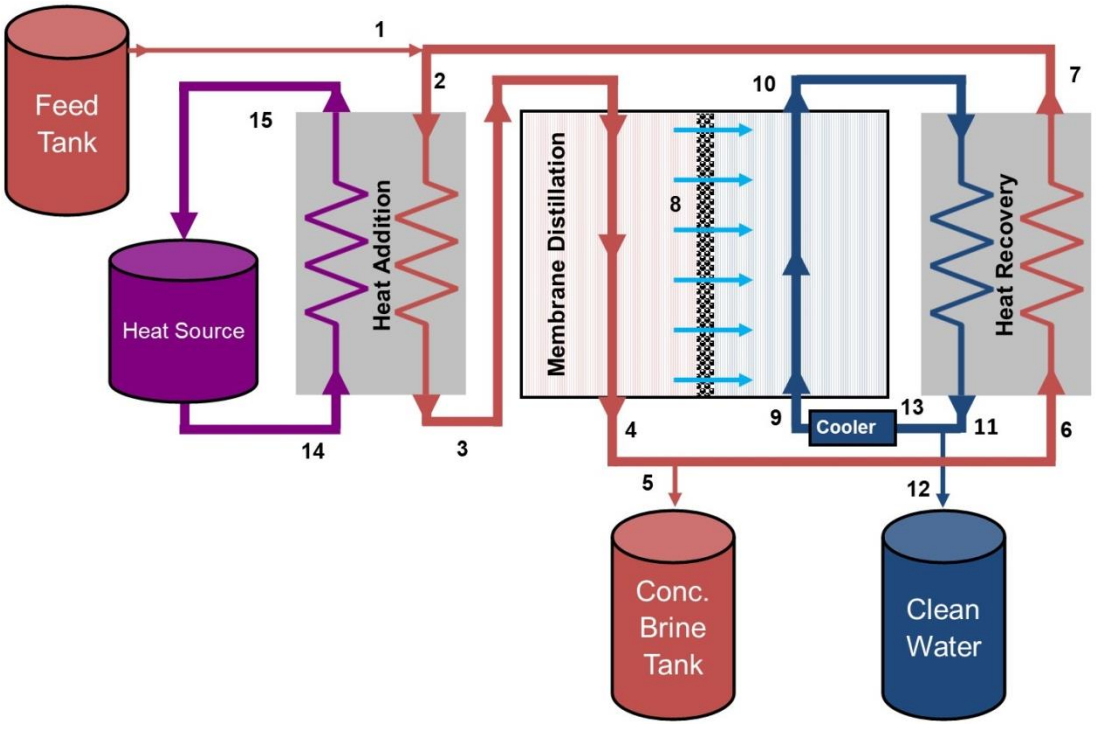

Figure 4-1. Schematic flow diagram of a DCMD system treating UOG wastewater in the modeling simulation

To determine the specific thermal energy consumption (STEC) and the gained output ratio (GOR) of MD, the heat needed to vaporize flow through the membrane, $\dot{Q}_{\text{vapor}}$ (kW), and heat added to the system, $\dot{Q}_{\text{addition}}$ (kW), were computed within the model using Eq. 4-2 through 4-4:

$$\dot{Q}_{\text{vapor}} = \dot{m}_8 * \bar{h}_v \qquad (4-2)$$

$$\dot{Q}_{\text{addition,max}} = C_{\min}(T_{14} - T_2) \qquad (4-3)$$

$$\dot{Q}_{\text{addition}} = \varepsilon_{\text{source}} * \dot{Q}_{\text{addition,max}} \qquad (4-4)$$

where $\bar{h}_v$ (kJ kg^{-1}) is the enthalpy vaporization of water determined based on the average of temperatures at nodes 3 and 9; T_2 and T_{14} (°C) are temperatures at nodes 2 and 14, respectively; $C_{\min}$ is the minimum heat capacity rate (kW C^{-1}) when comparing nodes 2 to 3 with nodes 14 to 15; and $\varepsilon_{\text{source}}$ is the heat exchanger (HX) effectiveness, equal to 0.8, which is calculated using the ε-NTU method for sizing heat exchangers (Swaminathan et al., 2018).

The STEC (β, kJ kg^{-1}) and GOR for the DCMD model were computed using Eq. 4-5 and 4-6:

$$\beta = \frac{\dot{Q}_{\text{addition}}}{\dot{m}_8} \qquad (4-5)$$

$$GOR = \frac{\dot{Q}_{\text{vapor}}}{\dot{Q}_{\text{addition}}} \qquad (4-6)$$

The STEC determined from the DCMD model was in the range of 910-2,035 kJ kg^{-1} permeate produced, corresponding to a GOR of ~1.1-2.5 (Figure A4, Appendix A). The STEC range determined from our DCMD model was consistent with multiple publications (Khayet and Matsuura, 2011; Thiel et al., 2015; Lokare et al., 2017; Tavakkoli et al., 2017). For further analysis, the STEC range was converted from kJ kg^{-1} permeate to kJ kg^{-1} feedwater by applying a water recovery rate of 80-90%. As a result, the STEC range used in our analysis was 750-1,815 kJ kg^{-1} feedwater.

The amount of energy required to treat the UOG wastewater (Q_{feed}) was calculated by multiplying the STEC required by MD treatment (β) with the amount of UOG wastewater (m_{feed}).

$$Q_{\text{feed}} = \beta * m_{\text{feed}} \qquad (4 - 7)$$

Integrating the COGIS data of wastewater generation for each well with the STEC range obtained by modeling simulation, the minimum and maximum energy requirements for MD were calculated and compared to the thermal energy provided by each energy source available at individual wells, which are described in the next section.

4.2.3 Waste heat and natural gas energy availability

There are a variety of potential energy sources available during and after HF of a well. The focus of this study is on-site wastewater treatment using MD, which requires a constant supply of thermal energy. Potential on-site energy sources include waste heat and well-pad natural gas (Wilcox, 2018). Three major sources of waste heat are identified during the lifetime of oil and gas production including the engines and pumps used for HF (pre-production phase), compressors for natural gas pipelines (post-production phase), and engines that provide the full-time electrical energy load required for well site equipment (production phase) (Figure A5, Appendix A). Alternatively, heat generated from direct burning of natural gas using a boiler paired with a heat exchanger to heat the feedwater could also provide the energy necessary for the MD process.

The first source of waste heat is from the coolant and exhaust systems of engines and pumps used in the HF process, which produce waste heat for 2-5 days (Caterpillar, 2011; Encana, 2011b; Halliburton, 2012). The amount of waste heat was quantitatively estimated at the well sites based on theoretical HF pressures, volumetric flow rate of water used for HF at each well,

and component efficiencies. The values of key parameters to calculate available waste heat are detailed in Table A2 of Appendix A.

The second source of waste heat is from NGCSs (Tavakkoli et al., 2016). While these stations produce a large amount of waste heat, they are not installed at the oil and gas producing sites but rather along the transmission pipelines. Mobile wellhead compression, which is much smaller in size than NGCSs, may be installed on the well pad but not until the natural gas return pressure drops considerably (typically years after the initial HF of the well) (Siemens, 2012). As a result, such waste heat is not appropriate for on-site wastewater treatment (in particular during the peak period of wastewater production) and is thus not evaluated further in our study.

The third source of waste heat energy comes from the full-time electrical energy load to operate well site components. In the state of Colorado, the typical configuration for a producing well pad includes wellheads, separation units, tanks, pumps, combustors, air compressors and a remote telemetry unit near the above-ground equipment (Encana, 2011a). The well pad equipment typically only draws a power load of ~8 kW (Sevier, 2015; Wilcox, 2018). Details for calculating the waste heat available from producing this amount of electricity with a natural gas or diesel engine is found in Tables A3 and A4 of Appendix A. The thermal energy available from waste heat generated (E_{waste}) due to the on-site electrical loads is a function of the waste heat rate available ($\dot{Q}_{\text{waste}}$) and total operating time (Δt).

$$E_{\text{waste}} = \dot{Q}_{\text{waste}} \Delta t \qquad (7)$$

Further, the energy obtained from burning natural gas (E_{gas}) is a function of the lower heating value (LHV) and the amount of natural gas flow (m_{gas}).

$$E_{gas} = LHV * m_{gas} \qquad (8)$$

The LHV of natural gas is based on its composition. The natural gas composition varies by region widely, so care was taken to select a representative composition for the DJ Basin. Based on the U.S. Geological Survey report on unconventional reservoirs in the DJ Basin (Higley and Cox, 2007), the composition of natural gas selected for this study was 82.6% methane, 10.1% ethane, 2.7% propane, 0.3% pentane and 2.6% carbon dioxide, with 1.7% of the composition not reported due to the low contents of the remaining compounds. As shown in Appendix A, the known parts were normalized to 100% to account for this unknown part of the natural gas composition. By weighting the LHV values of each component, an overall LHV was calculated, and the detailed calculation process is described in Tables A5 and A6 of Appendix A.

4.3 Results and Discussion

4.3.1 Production of UOG wastewater and natural gas from DJ Basin wells

Monthly production data of UOG wastewater and natural gas for the selected 20 wells are shown aggregated using a box-whisker plot in Figure 4-2 and individually in Figure A3 (Appendix A). The volume of UOG wastewater displayed a dramatic decline from Month 2 or Month 3 for the majority of the wells and continued to decrease afterwards (Figure A3A). UOG wastewater returns to the surface in two major stages, hydraulic fracturing flowback and produced water. The flowback stage occurs during the first few weeks after the well is hydraulically fractured followed by a transition within the next few months to the produced water stage (Bai et al., 2015). The flowback stage typically generates higher flow rates of wastewater than the produced water stage, contributing up to 10-40% of total UOG wastewater collected during the lifetime of a producing well (Estrada et al., 2016; Kondash et al., 2017; Mohammad-Pajooh et al., 2018).

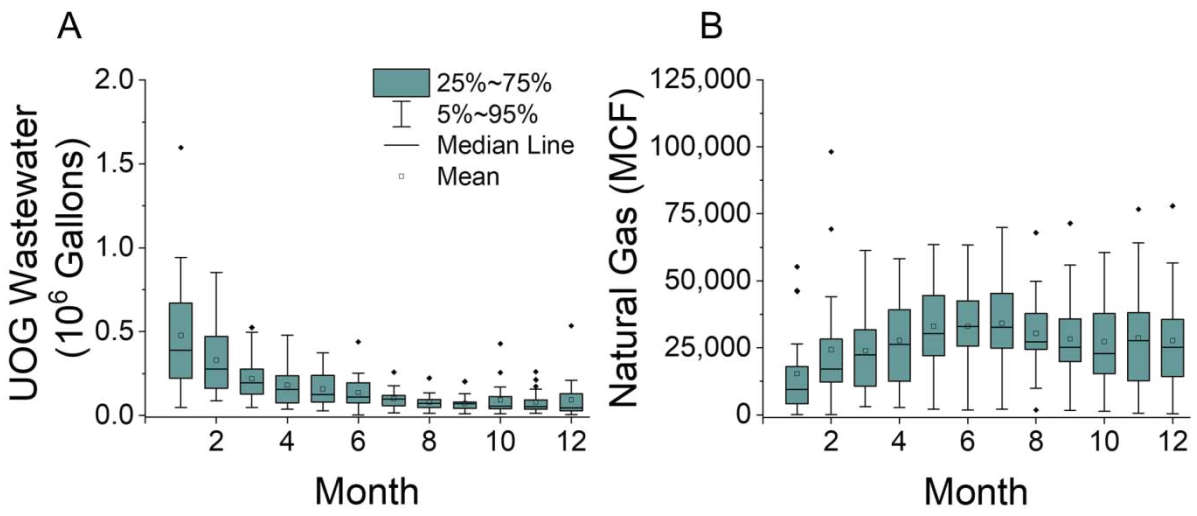

Figure 4-2. Statistical data for monthly (A) UOG wastewater and (B) natural gas production for 20 hydraulically fractured wells in Weld County, CO. Data were reported by Colorado Oil and Gas Conservation Commission (COGCC) through the Colorado Oil and Gas Information System (COGIS). Wells were completed between June 15, 2017 and September 14, 2017.

The average monthly UOG wastewater production was 403,696 gallons during the first two months for the 20 wells evaluated in this study, among which the JZM well generated the highest amount of 1,035,489 gallons per month. For the entire 12-month period, the average monthly UOG wastewater production was 168,544 gallons, with the final two months having an average production of only 87,010 gallons. It is demonstrated that wastewater generation decreases with time during the 12-month period. Hence, the most critical period for UOG wastewater treatment is within the first two months when the volume of wastewater is at its peak.

Compared to wastewater generation, the natural gas production during the same 12-month period showed greater variability among the selected wells (Figure 4-2B and Figure A3B). Natural gas production from UOG wells typically declines with time and reaches its peak production rate within the first year (Patzek et al., 2013; Male et al., 2015; Wang, 2017). In our study, five wells reached their peak production within the first three months and 19 of 20 wells reached peak production by the ninth month (Peterson well reached peak production in the 12th

month). For example, the TC Hiland well reached peak production in the second month with the highest monthly natural gas production of all the investigated wells (98,118 thousand cubic feet, MCF). In Month 9, the Wilson Ranch, Stromberger, and Wells Ranch wells reached peak production (55,836, 35,626, and 71,476 MCF respectively). The average monthly natural gas production rate within 12 months (27,820 MCF) was greater than the average production rate within the first two months (19,805 MCF) when the wastewater production rates were the highest. This indicates that more natural gas production typically occurred after the peak of UOG wastewater production. Wellbore clean-up operations including removing the debris and mud residues, which interfere with well efficiency, could affect early natural gas production and delay the peak production (Wang, 2017). With the offset by a few months between the peaks of wastewater and natural gas production, the dynamic correlation between treatment capacity of MD powered by natural gas and the treatment demand of UOG wastewater needs to be investigated.

4.3.2 Quantitative analysis of waste heat to power on-site MD treatment

The engines and pumps during the 2-5 day HF process generate waste heat at the UOG well sites. The availability of such heat source was estimated using an approach in which the efficiencies of engines and pumps are known (Tables A2, Appendix A). The waste heat ranged from $1.4 \times 10^9 - 7.9 \times 10^9$ kJ depending on the water usage to hydraulically fracture the well (Figure 4-3). Also, waste heat from the full-time electrical load at the well site typically generates a total of ~6×10^8 kJ of waste heat within 12 months (Table A3, Appendix A). In contrast to that generated in the short-term HF process, such waste heat persists during the well lifetime but with a much lower intensity.

Figure 4-3 compares the cumulative energy produced by waste heat from the HF phase, waste heat generated from full-time electrical load, and thermal energy required to treat wastewater with MD based on our modeling simulation (STEC of 750-1,815 kJ kg^{-1} of feedwater) for the 20 wells analyzed in this study. Using the Wilson Ranch well as an example (Figure 4-3, the first panel), the waste heat from the full-time electrical load fails to supply sufficient energy to treat all the wastewater, regardless of the applied STEC. Within the 12-month period, the thermal energy of waste heat from the full-time electrical load provided 3.5%–8.5% of needed energy for MD treatment at this well, depending on the STEC of MD. Similar to the Wilson Ranch well, the thermal energy of waste heat from the full-time electrical load only partially meets the energy demand of MD treatment when evaluating the other 19 wells (Figure 4-3). During the 12-month period, the thermal energy from this waste heat provided 5.4%–24.3% (median of 11.6%) with a STEC of 750 kJ kg^{-1} and 2.2%–10% (median of 4.8%) with a STEC of 1,815 kJ kg^{-1}. These findings demonstrate the insufficiency of waste heat from the full-time electrical load for MD treatment of all the UOG wastewater on-site.

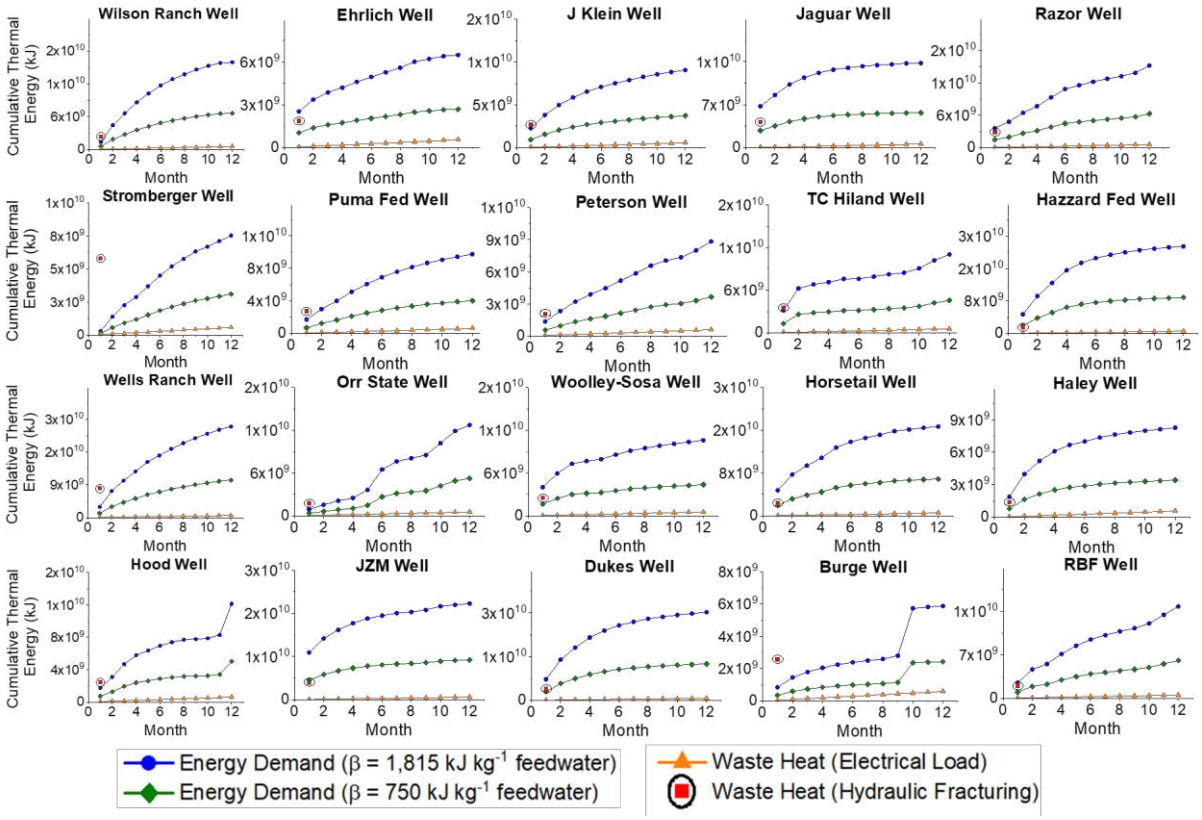

Figure 4-3. Cumulative thermal energy available from two sources of waste heat compared to cumulative energy demand of wastewater treatment at the 20 wells in Weld County, CO. The waste heat generated from hydraulic fracturing only persists for a short period of time, which is indicated by a circle marker. Our DCMD model range for STEC (750-1,815 kJ kg^{-1} feedwater) for thermal energy required to power MD technology was utilized.

For the waste heat generated from HF, we chose to investigate its potential to power MD treatment during the first two months (the peak period of wastewater production). Since the HF process finishes within a short timeframe, thermal energy storage is required for such waste heat source, rendering its usage for a short but intense period of wastewater treatment more practical. As shown in Figure 4-4, waste heat from the HF phase supplies 17%-415% (median of 54%) of thermal energy required by MD treatment during the first 2 months with a STEC of 1,815 kJ kg^{-1}, with such waste heat enabling full treatment capacity for four wells (Figure 4-4, highlighted with red asterisk). With a STEC of 750 kJ kg^{-1}, this percentage range increases to 40%–1,005%

(median of 136%), and waste heat from HF meets full treatment demand for an additional 11 well (Figure 4-4, highlighted with blue asterisk).

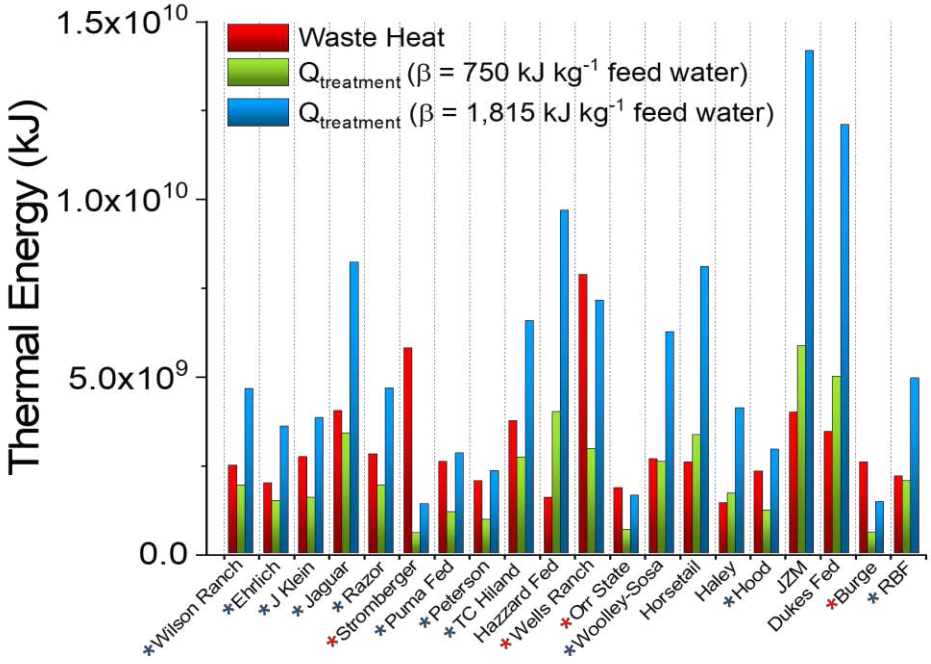

Figure 4-4. Thermal energy available from waste heat generated from HF along with energy demand for wastewater treatment by MD within the first two months after HF for the 20 wells in Weld County, CO. $Q_{treatment}$ represents the energy demand of treating all the wastewater by MD within the first two months for each well. STEC values from our DCMD model (750 and 1,815 kJ kg^{-1} feedwater) were utilized. The four wells in which waste heat meets the energy demand for treating all of the wastewater using a STEC of 1,815 kJ kg^{-1} feedwater are annotated with a red asterisk by the well name. The 11 additional wells in which waste heat meets the energy demand for treating all of the wastewater using a STEC of 750 kJ kg^{-1} feedwater are annotated with a blue asterisk.

We also calculated the critical GOR for each well, at which the waste heat generated from HF is equal to the energy demand by MD during the first two months (Figure 4-5, assuming an average feed salinity of 30,000 mg/L and corresponding water recovery of 85%). This dimensionless metric was used to further indicate the feasibility of MD powered by waste heat from HF to meet the treatment demand of UOG wastewater during the peak period of wastewater production. The critical GOR ranges from 0.25 to 6.44 (median of 1.89) for the 20 wells investigated in this study, among which 15 wells exhibit critical GOR values comparable or lower than the GOR range of 1.1-2.5 obtained by our modeling simulation (Figure 4-5).

Although higher energy efficiencies might be obtained than our modeling simulation (e.g., via decreasing feedwater temperature or applying multi-stage configuration) (Lee et al., 2011; Criscuoli, 2016; Ullah et al., 2018), significant improvement that enables MD powered by HF waste heat to meet UOG wastewater treatment demand for all the wells is extremely challenging if not infeasible. For example, a recent study by Christie et al. (2020) demonstrated that very small temperature differences in the MD system and heat exchanger are required to reach a GOR of ~4, resulting in low water flux and correspondingly high membrane and heat exchanger areas. Therefore, waste heat from HF has the potential to only power MD treatment of a proportion of UOG wastewater during the peak time of wastewater generation in the DJ basin, with such scenarios varying among different wells.

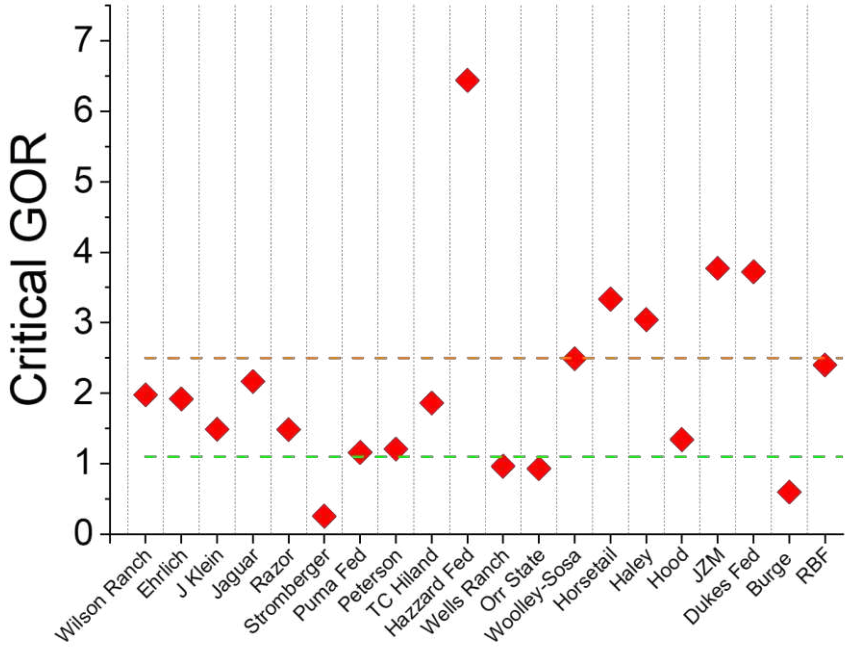

Figure 4-5. The critical GOR for MD treatment of all UOG wastewater produced using thermal energy provided by waste heat from HF at each of the 20 wells. The critical GOR ranges from 0.25 (Stromberger well) to 6.44 (Hazzard Fed well) with a median of 1.89 for all 20 wells reported. Orange and green dashed lines represent GOR values of 2.5 and 1.1, respectively, obtained from our DCMD model.

It should be noted that waste heat from the HF phase must be efficiently stored over time to treat UOG wastewater at individual wells. The aforementioned treatment capacities assume

perfect thermal efficiency (i.e., no loss of energy) during storage. The efficiency for thermal energy storage has been reported in the range of 90%–98% associated with MD and other low temperature desalination processes (i.e. humidification-dehumidification and solar still) (Gude, 2015). Thermal energy storage technologies require a suitable medium for storage and circulation for heat transfer. Examples of potentially suitable media include molten salt, concrete, phase change materials, and various other solid state and liquid/molten heat mediums (Gude et al., 2015). Also, the complexity and cost of integrating both waste heat capture and an energy storage system into the well site infrastructure needs to be considered. The prospect of utilizing waste heat from the HF phase is improved when attempting to use it for a relatively short duration (e.g., within the first two months of production as discussed previously). However, the UOG wells do not always begin producing immediately after HF. Wells can be "shut-in" for a period of time post-HF (typically 10–30 days), primarily to accommodate the laying of gas pipelines (Liu et al., 2015). This would require longer waste heat storage that inevitably results in some loss of energy. Another possibility is to coordinate such waste energy to treat stored wastewater from nearby completed wells (ideally on the same pad). The feasibility of this strategy is uncertain and highly dependent on the relative locations and wastewater volumes of UOG wells. Therefore, the above analyses collectively indicate that although waste heat could be used to treat UOG wastewater during the first few months of production, practical utilization of such an energy source needs to be further investigated by considering the temporal variation and the requirement of energy storage.

4.3.3 Dynamic correlation of MD treatment capacity powered by well-pad natural gas with treatment demand of UOG wastewater

The energy available by burning natural gas is calculated and compared with the energy requirements of MD treatment for all the 20 wells during a 12-month period (Figure 4-6). In 15

of the 20 wells, the thermal energy available in the natural gas outpaces the energy required by MD treatment of all the UOG wastewater along the 12 months, regardless of the applied STEC value. At the 5 wells where the initial natural gas productions are low (i.e., the Razor, Hazzard Fed, Horsetail, JZM, and Dukes wells), energy available from natural gas production starts to exceed the energy requirement of MD treatment by Month 2 or 3.

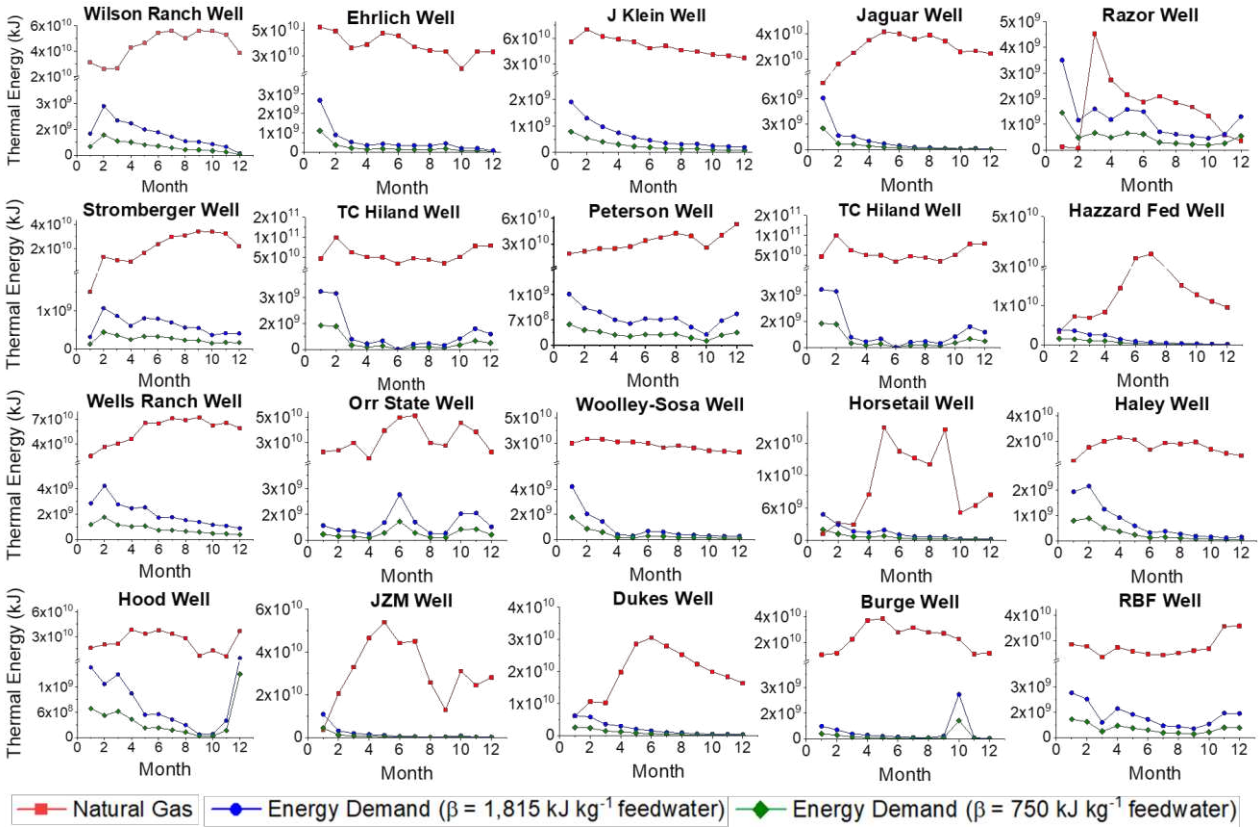

Figure 4-6. Monthly thermal energy available from natural gas compared to monthly thermal energy required for MD treatment of wastewater during 12 months for 20 wells in Weld County, CO. For each month, when the thermal energy of natural gas is greater than that required by MD treatment, all the wastewater produced at the well is fully treated and potentially reused. STEC values from our DCMD model (750 and 1,815 kJ kg^{-1} feedwater) were used.

Figure 4-7 compares the total thermal energy requirement for MD treatment with the total thermal energy available from burning natural gas within the first two months of production. The available energy contained in natural gas significantly surpasses the energy demand of MD treatment of all the wastewater by one or two orders of magnitude in a majority (18 out of 20) of

the wells. For example, during the first two months, the Wilson Ranch well produced 339,507 gallons of wastewater and 15,566 MCF of natural gas per month. At this well, the thermal energy needed for MD treatment is in the range of 1.9×10^9 to 4.7×10^9 kJ, depending on the STEC of MD, while well-pad natural gas is able to supply 3.1×10^{10} kJ of thermal energy that exceeds the treatment demand remarkably. When examining the other 17 wells where the thermal energy available in natural gas is sufficient for MD treatment of all the wastewater, wastewater treatment by MD consumes a range of 3%–72% (median of 11%) of natural gas during the first two months, when a STEC of 1,815 kJ kg^{-1} was used. For the Razor well and Horsetail well, however, the thermal energy provided by natural gas is able to treat only 4.1% and 57% of the generated wastewater during the first two months of production with a STEC of 1,815 kJ kg^{-1} (the treatment percentage increases to 10% and 137% when using a STEC of 750 kJ kg^{-1}). The low natural gas production during the first two months for these two wells might be due to the formation characteristics and/or post-completion practices of the operator (i.e. wellbore cleanup operations that could affect early natural gas production). Therefore, although natural gas is an abundant energy source for on-site UOG wastewater treatment, its availability during the peak period of UOG wastewater production needs to be considered with caution.

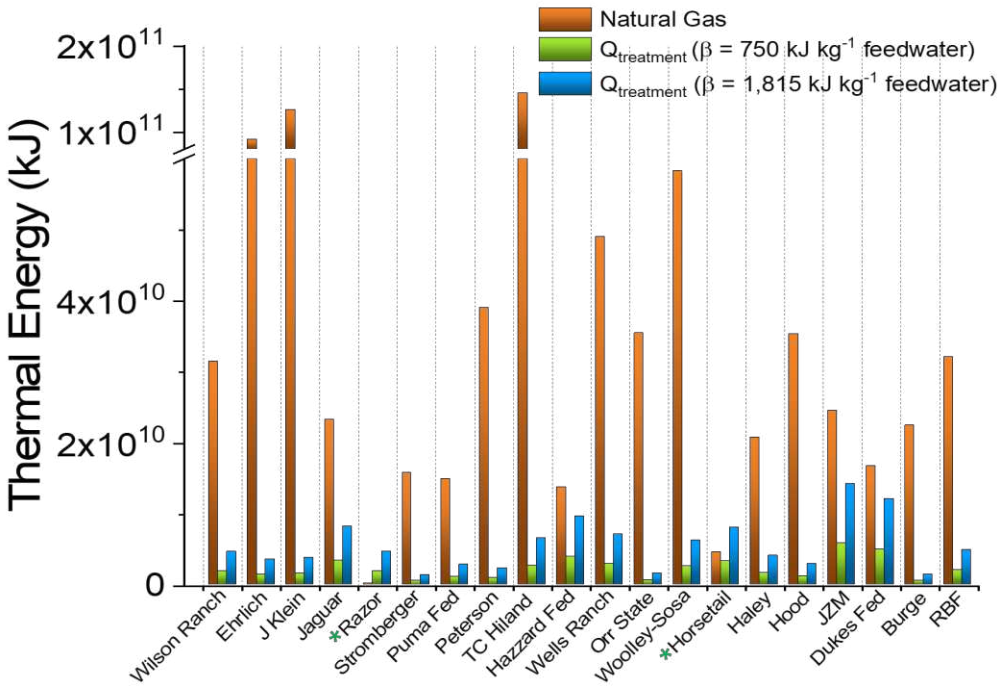

Figure 4-7. Thermal energy available from natural gas compared to thermal energy required by MD treatment of wastewater produced within the first two months after hydraulic fracturing for 20 wells located in Weld County, CO. $Q_{treatment}$ represents the amount of thermal energy required to treat all the wastewater within the first two months for each well. STEC values obtained from our DCMD model (750 and 1,815 kJ kg^{-1} feedwater) were used. The two wells in which the thermal energy from natural gas does not meet the high energy requirement of MD treatment are annotated with a green asterisk.

We also calculated the ratio of the energy required for MD treatment to the energy available from burning natural gas on-site (q_{ww}/q_{ng}) (Figure A6, Appendix A). This ratio provides a snapshot of the sufficiency of natural gas as an energy source for on-site MD treatment on a month-to-month basis. When this ratio is above 1, the thermal energy from natural gas is insufficient to power real-time MD treatment, and thus storage of wastewater is needed. The storage of wastewater is feasible at the well sites but requires a logistical cost of wastewater storage tanks. As an alternative to wastewater storage, UOG wastewater could be transported to nearby wells with higher natural gas production for on-site treatment. However, the economics of this strategy may not be favorable depending on transportation costs in the region. The q_{ww}/q_{ng} ratio is far below 1 along the 12-month period at 16 of the 20 selected wells, indicating that no

storage of wastewater is needed for a majority of the wells. When excluding the Razor well with relatively low natural gas production along 12 months and using a STEC of 1,815 kJ kg^{-1} feedwater, a range of 1.4-52% (median of 5.2%) of natural gas is consumed for wastewater treatment within the first 12 months. When using a STEC of 750 kJ kg^{-1} feedwater, this range decreases to 0.6-21% (median of 2.1%). As natural gas in the DJ Basin is a byproduct of crude oil production, using natural gas to power on-site MD treatment of UOG wastewater will be likely to not affect the economic prospect of the UOG industry in the region significantly.

4.4 Implications

In the current study, the treatment capacity of MD powered by waste heat or natural gas was quantified for the treatment of UOG wastewater in the DJ Basin. The intensity of waste heat produced from the on-site electrical load is insufficient for MD treatment of all the wastewater generated during UOG production. Waste heat from HF meets all or a good proportion of thermal energy required by MD treatment during the first two months of production. It is noteworthy to mention that these findings only apply to basins with similar characteristics, while the protocol is still applicable to other regions. Additionally, energy storage is needed to utilize such waste heat with potential energy losses occurring during long-term storage. This energy source, therefore, should be utilized for UOG wastewater treatment within a short timeframe or coordinated to treat stored wastewater from adjacent wells.

Well-pad natural gas provides a more consistent supply of thermal energy than waste heat generated from the on-site electrical load or the HF phase. Natural gas derived from the well pad is sufficient to treat all the wastewater generated from all 20 wells investigated in this study, although short-term wastewater storage is needed for 4 wells. Compared to the waste heat from NGCSs, on-site MD treatment directly powered by well-pad natural gas avoids the cost of

wastewater transport. This strategy, therefore, is not constrained by the relative location of drilling wells to NGCSs.

One possibility is to combine waste heat and natural gas as the energy sources for MD treatment. In such a hybrid configuration, waste heat would be stored for UOG wastewater treatment during the first months after HF. When the stored waste heat is depleted, the system can switch to natural gas for continuing wastewater treatment. Although this practice would result in energy savings by utilizing waste heat, the economic and spatial requirements could be high (U.S. Department of Energy, 2008; Jouhara et al., 2018). Waste heat recovery systems often require large heat exchangers due to the low temperature difference between the heat stream and process fluid (i.e. MD feedwater in this study). Also, the storage of waste heat from HF requires highly insulated storage tanks with high areal footprint. Therefore, although HF waste heat has the potential to reduce the energy cost of UOG wastewater treatment, a techno-economic analysis (TEA) needs to be performed to understand whether such cost savings could compensate for the capital, operational, and maintenance costs associated with the additional waste heat recovery and storage system.

Considering the Citygate natural gas price of $2.39 per MCF in Colorado as reported by the U.S. Energy Information Administration (EIA, data for February 2020) (U.S. EIA, 2019b), the energy cost of MD treatment is in the range of $0.28-0.68 per barrel of treated wastewater using a STEC of 750-1,815 kJ kg^{-1} feedwater. It should be noted that EIA does not report wellhead price of natural gas and the Citygate price includes the transportation and storage costs associated with getting natural gas from the wellhead to the gas distributing utility via pipeline. Thus, it can be safely assumed that the actual price of natural gas used on-site would be less than the Citygate price. To compare, EIA reported electricity costs in Colorado for industrial and

commercial users as 6.94 cents and 9.62 cents per kWh respectively (data for February 2020) (U.S. EIA, 2020a). In literature, the energy consumption for MVC to treat UOG wastewater ranges from 30-40 kWh/m^3. (McGinnis et al., 2013; Hayes et al., 2014). Using an energy consumption value of 35 kWh/m^3, the energy cost is $0.39 and $0.54 per barrel of treated wastewater depending on the user classification of UOG producers in Colorado. Considering the high capital cost of MVC due to the use of expensive materials (e.g., stainless steel or titanium) (Tong and Elimelech, 2016), using natural gas to power on-site MD treatment of UOG wastewater could be economically comparable or beneficial. In addition, applying a hybrid energy system that uses both waste heat and natural gas as discussed above (MVC is unable to utilize waste heat and powered only by electricity) would further lower the energy cost of on-site MD treatment.

Another consideration that favors the use of natural gas to power MD treatment of UOG wastewater is the practice of natural gas flaring. Flaring is widely used by oil and gas producers to dispose of natural gas in places that lack sufficient infrastructure (Franklin et al., 2019), primarily during the early stages of well production. A study performed by NOAA (Magill, 2016) identified 6,292 flares in the U.S. in 2016, which burned off an estimated 1,376 BCF (10.65 billion cubic meters) of natural gas, with the majority of flare sites attributed to oil and gas production. However, natural gas flaring is not consistent among regions and more granular information is needed in regard to its location and availability (Glazer et al., 2014). For the 20 wells investigated in this study, only 7 had reports of natural gas flaring after completion of the wells (COGIS, 2019). Based on the data in the production reports of these wells, a wide variability exists for the volume (0.1-73% of monthly gas production) and timeframe (1 to 6 months) of flared natural gas. By pairing areas where natural gas flaring is prevalent with on-site

UOG wastewater MD treatment, the economic feasibility would be greatly enhanced. By doing so, an otherwise wasted energy resource would be instead used to reduce the volume of UOG wastewater and greenhouse gas emissions, as well as producing valuable product water for beneficial reuse.

A promising strategy to enhance the feasibility of waste heat for powering on-site MD treatment of UOG wastewater is to employ reverse osmosis (RO) treatment prior to MD. RO is the most energy efficient desalination technology, which requires much less energy than MD (Tong et al., 2019). However, the salinity limit of RO is only ~70,000 mg/L, which is constrained by the limited hydraulic pressure that RO systems could tolerate (Shaffer et al., 2013; Tong and Elimelech, 2016; Tong et al., 2019). For DJ Basin UOG wastewater with typical salinities of 20,000-40,000 mg/L, RO could potentially reduce the volume of UOG wastewater for MD treatment by 40-70%, thereby significantly improving the possibility of waste heat in meeting wastewater treatment demand within the first two months. However, a hybrid RO-MD system increases system complexity. More intensive pretreatment needs to be employed due to the high fouling and scaling potential of RO, and a hybrid energy resource that combines waste heat and electricity is needed (RO is only powered by electricity). Therefore, a hybrid RO-MD system could be beneficial in UOG wastewater treatment in the DJ Basin, but its practical feasibility requires further investigation.

Furthermore, powering MD using waste heat and/or natural gas on-site is competitive with deep-well injection, the business-as-usual practice of UOG wastewater management in Colorado. The typical cost of wastewater transportation from well pad to a SWD well ranges from $1 to $3 per barrel, depending on the availability of SWD wells within the region (McCurdy, 2011; Ground Water Protection Council, 2019), and this cost is likely to increase due to the

progressively limited capacity of disposal wells. On-site wastewater treatment avoids transportation costs as well as environmental risks induced by deep-well injection (e.g., increased frequency of seismicity and water contamination), thereby improving the wastewater management paradigm for the UOG industry. Additionally, on-site wastewater treatment avoids capital costs associated with constructing a large centralized wastewater treatment plant which is another alternative to deep-well injection. The selection of best energy source or combination for MD technology, which considers the dynamic energy availability, capital cost, and the MD energy efficiency synergistically, will facilitate the practical implementation of on-site UOG wastewater treatment, thereby promoting water sustainability in the context of rising UOG production.

4.5 Conclusions

Using well-pad waste heat and natural gas as alternative energy sources for on-site wastewater treatment of UOG wastewater has the potential to minimize the transportation costs and primary energy consumption associated with UOG wastewater management practices. In this work, their feasibility of powering MD treatment of UOG wastewater is evaluated for 20 randomly selected wells located in the DJ Basin. The main conclusions drawn from this study are summarized as follows:

- Waste heat from HF activity, which persists only for a short timeframe, is a valuable energy source for on-site MD treatment during the initial few months (i.e., the peak period) of wastewater production. When evaluating the first 2 months of wastewater production, such waste heat meets 17-415% and 40-1,005% of thermal energy demand for the treatment of all UOG wastewater using STEC values of 1,815 kJ kg^{-1} feedwater and 750 kJ kg^{-1} feedwater by MD, which were obtained by modeling simulation,

respectively. The feasibility of waste heat from HF as an alternative energy source for on-site MD treatment varies among well sites and is dependent on the efficiencies of MD and thermal energy storage.

- Waste heat produced from on-site electrical loads is insufficient for MD treatment of UOG wastewater. Along with the short-term availability of waste heat from HF, waste heat generated during UOG production is unlikely to supply sufficient thermal energy required by MD for long-term wastewater treatment in the DJ Basin.
- Well-pad natural gas provides a more consistent supply of thermal energy than waste heat. By the third month of production, the thermal energy from well-pad natural gas meets the thermal energy demand for MD treatment of all UOG wastewater in all 20 wells.
- A combination of both well-pad natural gas and waste heat from HF is an intriguing option of energy source for on-site MD treatment of UOG wastewater. Such a hybrid configuration would take advantage of available waste heat while also utilizing abundant well-pad natural gas to ensure the treatment of all UOG wastewater. However, the complexity and economic cost of a hybrid energy system might hinder its practical implementation.
- For future work, a comparison of on-site MD treatment with other treatment technologies (such as MVC) and management options (i.e. deep-well injection) for UOG wastewater needs to consider capital, operating and maintenance, and transportation costs, which should be performed in a thorough TEA to determine their economic prospect and viability in the region of interest.

References

Akob, D. M., Mumford, A. C., Orem, W., Engle, M. A., Klinges, J. G., Kent, D. B., Cozzarelli, I. M., 2016. Wastewater disposal from unconventional oil and gas development degrades stream quality at a West Virginia injection facility. *Environ. Sci. Technol. 50* (11), 5517-5525.

Ali, A., Macedonio, F., Drioli, E., Aljli, S., Alharbi, O.A., 2013. Experimental and theoretical evaluation of temperature polarization phenomenon in direct contact membrane distillation. *Chem. Eng. Res. Design* 91, 1966-1977.

Bai, B., Carlson, K., Prior, A., Douglas, C., 2015. Sources of variability in flowback and produced water volumes from shale oil and gas wells. *J. Uncon. Oil Gas Resources 12*, 1-5.

Barati, R., Liang, J.-T., 2014. A review of fracturing fluid systems used for hydraulic fracturing of oil and gas wells. *J. Appl. Polym. Sci. 131* (16), 40735.

Bell, E. A., Poynor, T. E., Newhart, K. B., Regnery, J., Coday, B. D., Cath, T. Y., 2017. Produced water treatment using forward osmosis membranes: Evaluation of extended-time performance and fouling. *J. Membr. Sci. 525*, 77-88.

Boo, C., Lee, J., Elimelech, M., 2016. Omniphobic polyvinylidene fluoride (PVDF) membrane for desalination of shale gas produced water by membrane distillation. *Environ. Sci. Technol. 50* (22), 12275-12282.

Butkovskyi, A., Bruning, H., Kools, S. A. E., Rijnaarts, H. H. M., Van Wezel, A. P., 2017. Organic pollutants in shale gas flowback and produced waters: Identification, potential ecological impact, and implications for treatment strategies. *Environ. Sci. Technol. 51* (9), 4740-4754.

Caterpillar, 2011. 3512C HD Petroleum Engine. Caterpillar web site. https://s7d2.scene7.com/is/content/Caterpillar/LEHW0056-01 (accessed May 13, 2019).

Chang, H.; Li, T.; Liu, B.; Chen, C.; He, Q.; Crittenden, J.C., 2019a. Smart ultrafiltration membrane fouling control as desalination pretreatment of shale gas fracturing wastewater: The effects of backwash water. *Environment International 130* (2019), 104869.

Chang, H.; Li, T.; Liu, B.; Vidic, R. D.; Elimelech, M.; Crittenden, J. C., 2019b. Potential and implemented membrane-based technologies for the treatment and reuse of flowback and produced water from shale gas and oil plays: A review. *Desalination 455*, 34-57.

Colorado Oil and Gas Conservation Commission, 2019. Colorado Oil and Gas Information System Home Page., https://cogcc.state.co.us/data.html#/cogis (accessed May 4, 2019).

Christie, K.S., Horseman, T., Lin, S., 2020. Energy efficiency of membrane distillation: Simplified analysis, heat recovery, and the use of waste-heat. *Environ. Inter.* 138 (2020), 105588.

Criscuoli, A., 2016. Improvement of the membrane distillation performance through the integration of different configurations. *Chem. Eng. Res. Design* III, 316-322.

Crowley, K., 2019. Gas Becomes Pricey Problem for Permian Basin Oil Drillers: Chart. *Bloomberg* [Online] https://www.bloomberg.com/news/articles/2019-04-03/gas-becomes-pricey-problem-for-permian-basin-oil-drillers-chart (accessed May 20, 2019).

Deshmukh, A., Boo, C., Karanikola, V., Lin, S., Straub, A. P., Tong, T., Warsinger, D. M., Elimelech, M., 2018. Membrane distillation at the water-energy nexus: Limits, opportunities, and challenges. *Energ. Environ. Sci. 11* (5), 1177-1196.

Dolan, F. C., Cath, T. Y., Hogue, T. S., 2018. Assessing the feasibility of using produced water for irrigation in Colorado. *Sci. Total Environ. 640-641*, 619-628.

Dow, N., Gray, S., Jun-de, L., Zhang, J., Ostarcevic, E., Liubinas, A., Atherton, P., Roeszler, G., Gibbs, A., Duke, M., 2016. Pilot trial of membrane distillation driven by low grade waste heat: Membrane fouling and energy assessment. *Desalination* 391, 30-42.

Dow, N ., Villalobos Garcia, J., Niadoo, L., Milne, N., Zhang, J., Gray, S., Duke, M., 2017. Demonstration of membrane distillation on textile waste water: Assessment of long term performance, membrane cleaning and waste heat integration. *Environ. Sci.: Water Res. Technol.* 3, 433-449.

Duong, H.C., Chivas, A.R., Nelemans, B., Duke, M., Gray, S., Cath, T.Y., Nghiem, L.D., 2015. Treatment of RO brine from CSG produced water by spiral-wound air gap membrane distillation – A pilot study. *Desalination* 366, 121-129.

Ellsworth, W. L., 2013. Injection-induced earthquakes. *Science 341* (6142), 1225942.

Encana, 2011a. Completed Well Pads and Equipment. Encana web site. https://www.encana.com/pdf/communities/usa/completedwellpadsandequipment(Piceance).pdf (accessed Apr. 20, 2019).

Encana, 2011b. DJ Basin, Colorado: Well completion and hydraulic fracturing. Encana web site. https://www.encana.com/pdf/communities/usa/wellcompletionandhydraulicfracturing(DJ).pdf (accessed Apr. 20, 2019).

Esmaeilirad, N., Carlson, K., Omur Ozbek, P., 2015. Influence of softening sequencing on electrocoagulation treatment of produced water. *J. Hazard. Mater. 283*, 721-729.

Estrada, J. M., Bhamidimarri, R., 2016. A review of the issues and treatment options for wastewater from shale gas extraction by hydraulic fracturing. *Fuel 182*, 292-303.

F-Chart Software, 2020. Engineering Equation Solver Overview. F-Chart Software web site. http://www.fchartsoftware.com/ees/ (accessed May 4, 2020).

Franklin, M., Chau, K., Cushing, L. J., Johnston, J. E., 2019. Characterizing flaring from unconventional oil and gas operations in South Texas using satellite observations. *Environ. Sci. Technol. 53* (4), 2220-2228.

Geary, E., 2019. U.S. natural gas production hit a new record high in 2018. U.S. E.I.A. website. https://www.eia.gov/todayinenergy/detail.php?id=38692 (accessed Apr. 25, 2019).

Glazer, Y.R., Kjellsson, J.B., Sanders, K.T., Webber, M.E., 2014. Potential for using energy from flared gas for on-site hydraulic fracturing wastewater treatment in Texas. *Environ. Sci. Technol. Lett.* 1, 300-304.

Gregory, K., Mohan, A. M., 2015. Current perspective on produced water management challenges during hydraulic fracturing for oil and gas recovery. *Environ. Chem. 12* (3), 261-266.

Ground Water Protection Council, 2019. Produced Water Report: Regulations, Current Practices, and Research Needs. 310 p.

Gude, V. G., 2015. Energy storage for desalination processes powered by renewable energy and waste heat sources. *Appl. Energy 137*, 877-898.

Guillen-Burrieza, E., Alarcon-Padilla, D.C., Palenzuela, P., Zaragoza, G., 2015. Techno-economic assessment of a pilot-scale plant for solar desalination based on existing plate and frame MD technology. *Desalination* 374, 70-80.

Halliburton, 2012. HT-2000 Pump Trailer (FPR-I). Halliburton web site. https://www.halliburton.com/content/dam/ps/public/pe/contents/Data_Sheets/web/H/H09147-HT-2000-Pump-Trailer-SDS.pdf (accessed Apr. 7, 2019).

Hayes, T. D., Halldorson, B., Horner, P., Ewing, J., Werline, J., Severin, B. F., 2014. Mechanical vapor recompression for the treatment of shale-gas flowback water. *Oil Gas Facil.* 3 (4), 54-62.

Higley, D. K.; Cox, D. O., 2007. *Oil and gas exploration and development along the front range in the Denver Basin of Colorado, Nebraska, and Wyoming*, in Highley, D.K., compiler, Petroleum systems and assessment of undiscovered oil and gas in the Denver Basin Province, Colorado, Kansas, Nebraska, South Dakota, and Wyoming - USGS Province 39: U.S. Geological Survey Digital Data Series DDS-69-P, ch. 2, 41 p.

Hincks, T., Aspinall, W., Cooke, R., Gernon, T., 2018. Oklahoma's induced seismicity strongly linked to wastewater injection depth. *Science 359* (6381), 1251.

Jimenez, S., Mico, M. M., Arnaldos, M., Medina, F., Contreras, S., 2018. State of the art of produced water treatment. *Chemosphere 192*, 186-208.

Jouhara, H., Khordehgah, N., Almahmoud, S., Delpech, B., Chauhan, A., Tassou, S. A., 2018. Waste heat recovery technologies and applications. *Therm. Sci. Eng. Progress 6,* 268-289.

Kahrilas, G. A., Blotevogel, J., Corrin, E. R., Borch, T., 2016. Downhole transformation of the hydraulic fracturing fluid biocide glutaraldehyde: Implications for flowback and produced water quality. *Environ. Sci. Technol. 50* (20), 11414-11423.

Khayet, M. S., Matsuura, T., 2011. *Membrane Distillation: Principles and Applications*. Elsevier: Amsterdam.

Kim, S., Omur-Ozbek, P., Dhanasekar, A., Prior, A., Carlson, K., 2016. Temporal analysis of flowback and produced water composition from shale oil and gas operations: Impact of frac fluid characteristics. *J. Petrol. Sci. Eng. 147*, 202-210.

Kondash, A., Lauer, N., Vengosh, A., 2018. The intensification of the water footprint of hydraulic fracturing. *Sci. Adv. 4*: eaar5982.

Lai. X., Long, R., Liu, Z., Liu, W., 2018. A hybrid system using direct contact membrane distillation for water production to harvest waste heat from the proton exchange membrane fuel cell. *Energy* 147, 578-586.

Lawson, K. W., Lloyd, D. R., 1997. Membrane Distillation. *J. Membr. Sci. 124* (1), 1-25.

Lee, H., He, F., Song, L., Gilron, J., Sirkar, K.K., 2011. Desalination with a cascade of cross-flow hollow fiber membrane distillation devices integrated with a heat exchanger. *AIChE Journal* 57 (7), 1780-1795.

Lester, Y., Ferrer, I., Thurman, E. M., Sitterley, K. A., Korak, J. A., Aiken, G., Linden, K. G., 2015. Characterization of hydraulic fracturing flowback water in Colorado: Implications for water treatment. *Sci. Total Environ. 512-513*, 637-644.

Liu, N., Liu, M., Zhang, S., 2015. Flowback patterns of fractured shale gas wells. *Natural Gas Industry B 2* (2-3), 247-251.

Lokare, O. R., Tavakkoli, S., Rodriguez, G., Khanna, V., Vidic, R. D., 2017a. Integrating membrane distillation with waste heat from natural gas compressor stations for produced water treatment in Pennsylvania. *Desalination 413*, 144-153.

Lokare, O. R., Tavakkoli, S., Wadekar, S., Khanna, V., Vidic, R. D., 2017b. Fouling in direct contact membrane distillation of produced water from unconventional gas extraction. *J. Membr. Sci. 524*, 493-501.

Lu, K.J., Cheng, Z.L., Chang, J., Luo, L., Chung, T.S. 2019. Design of zero liquid discharge desalination (ZLDD) systems consisting of freeze desalination, membrane distillation, and crystallization powered by green energies. *Desalination* 458, 66-75.

Ma, G., Geza, M., Cath, T. Y., Drewes, J. E., Xu, P., 2018. iDST: An integrated decision support tool for treatment and beneficial use of non-traditional water supplies – Part II. Marcellus and Barnett Shale case studies. *J. Water Process Eng. 25*, 258-268.

Magill, B.. 2016. U.S. Has More Gas Flares than Any Country. *Scientific American* [Online], https://www.scientificamerican.com/article/u-s-has-more-gas-flares-than-any-country/ (accessed Jul. 5, 2019).

Male, F., Islam, A. W., Patzek, T. W., Ikonnikova, S., Browning, J., Marder, M. P., 2015. Analysis of gas production from hydraulically fractured wells in the Haynesville Shale using scaling methods. *J. Uncon. Oil Gas Resources 10*, 11-17.

McCurdy, R., 2011. Underground injection wells for produced water disposal U.S. Environmental Protection Agency (accessed Apr. 7, 2019).

McGinnis, R. L., Hancock, N. T., Nowosielski-Slepowron, M. S., McGurgan, G. D., 2013. Pilot demonstration of the NH_3/CO_2 forward osmosis desalination process on high salinity brines. *Desalination 312*, 67-74.

Mohammad-Pajooh, E., Weichgrebe, D., Cuff, G., Tosarkani, B. M., Rosenwinkel, K. H., 2018. On-site treatment of flowback and produced water from shale gas hydraulic fracturing: A review and economic evaluation. *Chemosphere 212*, 898-914.

Natural Gas Intelligence, 2020. Information on the Niobrara-DJ Basin. Natural Gas Intelligence web site. https://www.naturalgasintel.com/niobraradjinfo (accessed May 16, 2020).

Olatunji, S.O., Camacho, L.M., 2018. Heat and mass transport in modeling membrane distillation configurations: A review. *Front. Energy Res.* 6, 130.

Patzek, T. W., Male, F., Marder, M., 2013. Gas production in the Barnett Shale obeys a simple scaling theory. *Proc. Natl. Acad. Sci. U.S.A. 110*, (49), 19731-19736.

Rahm, B. G., Bates, J. T., Bertoia, L. R., Galford, A. E., Yoxtheimer, D. A., Riha, S. J., 2013. Wastewater management and Marcellus Shale gas development: Trends, drivers, and planning implications. *J. Environ. Manage. 120*, 105-13.

Rosenblum, J. S., Sitterley, K. A., Thurman, E. M., Ferrer, I., Linden, K. G., 2016. Hydraulic fracturing wastewater treatment by coagulation-adsorption for removal of organic compounds and turbidity. *J.Environ.Chem. Eng. 4* (2), 1978-1984.

Scanlon, B. R., Weingarten, M. B., Murray, K. E., Reedy, R. C., 2018. Managing basin ‐ scale fluid budgets to reduce injection ‐ Induced seismicity from the recent U.S. shale oil revolution. *Seismol. Res. Let. 90* (1), 171-182.

Schwantes, R., Chavan, K., Winter, D., Felsmann, C., Pfafferott, J., 2018. Techno-economic comparison of membrane distillation and MVC in a zero liquid discharge application. *Desalination 428*, 50-68.

Sevier, D. K., 2015. Oil & gas industry electric power for upstream operations. Advanced Research Projects Agency - Energy web site. https://arpa-e.energy.gov/sites/default/files/Sevier_SWN_GENSETS.pdf (accessed Apr. 25, 2019).

Shaffer, D. L., Arias Chavez, L. H., Ben-Sasson, M., Romero-Vargas Castrillon, S., Yip, N. Y., Elimelech, M, 2013. Desalination and reuse of high-salinity shale gas produced water: Drivers, technologies, and future directions. *Environ. Sci. Technol. 47* (17), 9569-9583.

Siemens, 2012. Extending value through field redevelopment: Solutions that maximize the value of mature assets. Siemens web site. https://w3.siemens.com/markets/global/en/oil-gas/PublishingImages/applications/onshore-production/Extending_value.pdf (accessed Apr. 17, 2019).

Silva, T. L. S., Morales-Torres, S., Castro-Silva, S., Figueiredo, J. L., Silva, A. M. T., 2017. An overview on exploration and environmental impact of unconventional gas sources and treatment options for produced water. *J. Environ. Manage. 200*, 511-529.

Sun, Y., Wang, D., Tsang, D.C.W., Wang, L., Ok, Y.S., Feng, Y. 2019. A critical review of risks, characteristics, and treatment strategies for potentially toxic elements in wastewater from shale gas extraction. *Environment International 125* (2019), 452-469.

Swaminathan, J., Chung, H.W., Warsinger, D.W., Lienhard, J.H., 2018. Energy efficiency of membrane distillation up to high salinity: Evaluating critical system size and optimal membrane thickness. *Appl. Energy* 211, 715-734.

Tavakkoli, S., Lokare, O. R., Vidic, R. D., Khanna, V., 2016. Systems-level analysis of waste heat recovery opportunities from natural gas compressor stations in the United States. *ACS Sustain. Chem. Eng. 4* (7), 3618-3626.

Tavakkoli, S., Lokare, O. R., Vidic, R. D., Khanna, V., 2017. A techno-economic assessment of membrane distillation for treatment of Marcellus shale produced water. *Desalination 416*, 24-34.

Thiel, G., Tow, E., Banchik, L., Chung, H. W., Leinhard, J., 2015. Energy consumption in desalinating produced water from shale oil and gas extraction. *Desalination 366*, 94-112.

Tong, T., Elimelech, M., 2016. The global rise of zero liquid discharge for wastewater management: Drivers, technologies, and future directions. *Environ. Sci. Technol. 50* (13), 6846-6855.

Ullah, R., Khraisheh, M., Esteves, R. J., McLeskey, J. T., AlGhouti, M., Gad-el-Hak, M., Vahedi Tafreshi, H., 2018. Energy efficiency of direct contact membrane distillation. *Desalination 433*, 56-67.

U.S. Department of Energy. 2008. Waste Heat Recovery: Technology and opportunities in U.S. industry. 112 p..

U.S. Energy Information Administration, 2019a. Electric Power Monthly. U.S. EIA web site. https://www.eia.gov/electricity/monthly/epm_table_grapher.php?t=epmt_5_6_a (accessed Jul. 23, 2019).

U.S. Energy Information Administration, 2019b. Natural Gas Prices. U.S. EIA web site. https://www.eia.gov/dnav/ng/ng_pri_sum_dcu_nus_m.htm (accessed Jul. 23, 2019).

Wang, H., 2017. What factors control shale-gas production and production-decline trend in fractured systems: A comprehensive analysis and investigation. *SPE Journal 22* (02), 562-581.

Wang, W., Du, X. W., Vahabi, H., Zhao, S., Yin, Y. M., Kota, A. K., Tong, T. Z., 2019. Trade-off in membrane distillation with monolithic omniphobic membranes. *Nat. Commun. 10*, 3220.

Wilcox, A., 2018. *Determining Opportunities for Combined Heat and Power (CHP) in the Oilfield*, Proceedings of the 25th International Petroleum Environmental Conference, Denver, CO, October 30 - November 1, 2018.

Yuan, Z., Yu, Y., Wei, L., Sui, X., She, Q., Chen, Y., 2020. Pressure-retarded membrane distillation for simultaneous hypersaline brine desalination and low-grade heat harvesting. *J. Membr. Sci.* 597, 117765.

Zhang, Z., Du, X., Carlson, K., Robbins, C., Tong, T., 2019. Effective treatment of shale oil and gas produced water by membrane distillation coupled with precipitative softening and walnut shell filtration. *Desalination 454*, 82-90.

5.0 Spatial Analysis of Membrane Distillation Powered by Waste Heat from Natural Gas Compressor Stations for Unconventional Oil and Gas Wastewater Treatment in Weld County, Colorado[3]

5.1 Introduction

With the continuing rise of water footprint in unconventional oil and gas (UOG) development in the United States, managing the high volume of wastewater (includes flowback and produced water) generated from UOG activities has become of paramount importance (Kondash et al., 2018). Injecting wastewater into Class II Underground Injection Control (UIC) disposal wells (i.e., deep-well injection, DWI) remains the most common management approach for the UOG industry. However, concerns regarding induced seismicity and regional water scarcity render this practice unsustainable (Ellsworth, 2013; Weingarten et al., 2015; Scanlon et al., 2017; Kondash et al., 2018; Scanlon et al., 2018). Many ongoing efforts to reduce the dependence of UOG wastewater management on DWI have focused on wastewater treatment for beneficial reuse, with a primary emphasis on developing technologies to remove various pollutants effectively (Rodriguez et al., 2015; Liden et al., 2017; Chang et al., 2019). The economic cost of these technologies needs to be competitive compared to DWI to shift the paradigm of UOG wastewater management toward treatment and reuse (Tavakkoli et al., 2017; Dolan et al., 2018; Mohammad-Pajooh et al., 2018; Wenzlick et al., 2020). While more research is still needed to further improve the energy- and cost-efficiency of UOG wastewater treatment,

[3] This chapter has been published as a research article in *ACS ES&T Engineering* with the following citation:

Robbins, C.A., Carlson, K.H., Garland, S.D., Bandhauer, T.M., Grauberger, B.M., Tong, T., 2021. Spatial analysis for membrane distillation powered by waste heat from natural gas compressor stations for unconventional oil and gas wastewater treatment in Weld County, Colorado. *ACS EST Engg.* 1 (2), 192-203.

logistical considerations such as transportation distance and costs have been rarely discussed in the literature (Tavakkoli et al., 2020). Compared to the treatment cost, these often neglected aspects could play an equally important role in determining the economic feasibility of UOG wastewater treatment, requiring further investigations to promulgate changes of the current wastewater management paradigm.

The transportation costs of moving wastewater to a disposal well in the U.S. are typically in the range of $1-3 per barrel of wastewater (Ground Water Protection Council, 2019). This cost range is highly dependent on the regional availability of disposal wells. For example, due to the scarcity of disposal wells in Pennsylvania (only 16 wells reported in 2018) (U.S. Environmental Protection Agency, 2019), the cost of UOG wastewater transportation for DWI has been reported in a range of $4-8 per barrel in that state (McCurdy, 2011). This much higher than the national average transportation cost renders logistics an important factor to determine UOG wastewater management practices in Pennsylvania, leading to more favorable economics for wastewater treatment (Tavakkoli et al., 2017; Tavakkoli et al., 2020). However, in other states with a higher density of active disposal wells (e.g., Colorado), the effect of wastewater transportation on the selection of the best UOG wastewater management practice could be different and needs more investigation.

As an alternative management strategy to DWI, centralized wastewater treatment (CWT) has garnered increasing interest by researchers and governmental regulators. CWT facilities accept and treat UOG wastewater for disposal, discharge, reuse, recycling, or material recovery (U.S. Environmental Protection Agency, 2016). As compared to decentralized, on-site wastewater treatment, CWT facilities have better economics of scale and encounter less regulatory barriers (Ren et al., 2019), because a high wastewater volume is treated and only a

single water quality standard needs to be complied for the entire facility. Like DWI, however, the UOG wastewater needs to be transported to the CWT facility, resulting in transportation costs that render the feasibility of centralized UOG wastewater treatment questionable.

Recently, membrane distillation (MD) has emerged as a promising technology for UOG wastewater treatment due to its capability of dealing with hypersaline wastewater and leveraging low-grade waste heat (Lokare et al, 2017; Deshmukh et al., 2018; Tong et al., 2019). In MD, a partial vapor pressure difference between the hotter feedwater and the colder permeate stream creates the driving force for water vapor to transport across a hydrophobic and microporous membrane (Lawson and Lloyd, 1997; Deshmukh et al., 2018). Due to its moderate feedwater temperatures (60-80°C), MD has the potential to utilize low-grade waste heat as the energy source (Deshmukh et al., 2018). However, a large amount of energy is consumed in MD due to phase transition (i.e., from liquid to vapor), leading to lower energy efficiency of MD than pressure-driven treatment technologies such as reverse osmosis (RO). Therefore, the use of waste heat is vital to improve the economic feasibility of MD technology while reducing the carbon footprint of UOG wastewater treatment (Dow et al., 2016; Gonzalez et al., 2017; Schwantes et al., 2018; Tavakkoli et al., 2017; Deshmukh et al., 2018).

Natural gas compressor stations (NGCSs) are potential sources of waste heat that could be used to power MD treatment at CWT facilities (Lokare et al., 2017). Previous work by Lokare et al. quantified the amount of waste heat at NGCSs in the state of Pennsylvania, in which waste heat was shown to meet the thermal energy requirement for MD treatment of all UOG wastewater statewide (Lokare et al., 2017). However, a more refined analysis at a smaller scale needs to be conducted to determine whether waste heat availability matches wastewater treatment demand at each NGCS. Further, for each individual UOG well, the wastewater

transportation cost associated with CWT at an NGCS needs to be compared with DWI. The resultant cost difference is a key factor that determines the viability of co-locating CWT facilities with NGCSs. Such comparison can be only performed at a local or regional scale, at which the transportation of UOG wastewater occurs.

In this study, we performed a comparative investigation on the feasibility of CWT facilities co-located with NGCSs and DWI for UOG wastewater management in Weld County of Colorado, a major UOG-producing state in the U.S. Weld County falls within the Denver-Julesburg Basin of the Niobrara shale play. In 2018, the Denver-Julesburg Basin ranked 5th in crude oil production in the U.S (U.S. Energy Information Administration, 2019) and the Wattenberg Field (located in southwest Weld County) ranked 4th in the U.S. Energy Information Administration's 2013 list of top 100 oil-producing fields in the U.S (U.S. Energy Information Administration, 2015). Weld County also produced the most crude oil in Colorado, generating more than 154 million barrels of oil in 2018 (when the second-ranked county in Colorado generated under 4 million barrels) (Colorado Oil and Gas Conservation Commission, 2020). By analyzing 7,583 active UOG production wells with available data for 2018, we compared the distance and corresponding cost of transporting wastewater to NGCSs or disposal wells to determine the well site-specific management strategy that minimizes the transportation cost. We also estimated the treatment capacity of MD powered by waste heat available at each NGCS in Weld County, and investigated the feasibility of centralized MD treatment to meet local wastewater treatment demand. Our results demonstrate that wastewater transportation plays an important role in the selection of wastewater management practice for UOG production, highlighting the need of integrating spatial analysis (in particular at the local scale) with

treatment technologies when designing and selecting feasible strategies of UOG wastewater management.

5.2 Materials and Methods

5.2.1 Data sources

The data associated with UOG wastewater were obtained from the Colorado Oil and Gas Information System (COGIS) database managed by the Colorado Oil and Gas Conservation Commission (COGCC) (COGCC, 2020). For this study, the UOG producing wells that generated greater than 100 barrels of wastewater in 2018 were analyzed. These wells accounted for approximately 95% of the wastewater generated within the entire county.

The number and locations of active disposal wells and NGCSs in Weld County were also obtained via the COGIS database using the facility inquiry function. The daily compression capacity of each NGCS was found on the COGCC Form 12 (Gas Facility Registration/Change of Operator) submitted by the operator to the COGIS database.

5.2.2 Spatial distribution of UOG wastewater production density

Geographic Information System (GIS) software (ArcGIS 10.6, ESRI) was utilized to provide spatial distribution of UOG wastewater production density in Weld County. The wastewater volume for each producing well was represented as point data, and Weld County was divided into 100 m × 100 m rasters to create a wastewater production density map. The wastewater production density of each raster was calculated as wastewater production volume per 10,000 m^2 and grouped into nine categories (Figure 5-1).

5.2.3 The calculation of transportation distance from UOG wells to disposal wells and NGCSs

The nearest disposal well and NGCS to each UOG producing well was determined using the "Near" analysis tool in ArcGIS 10.6. This analysis tool calculates the distance between the input

features and the closest features in another layer or feature class (ESRI, 2018). The locations of UOG producing wells were loaded as input features while those of disposal wells or NGCSs were loaded as the closest features. Such analysis identified the nearest disposal well and NGCS for each producing well.

The distance of each producing well to the nearest disposal well or NGCS was calculated by using the Network Analyst toolbox of ArcGIS 10.6. This toolbox allows the creation of a network dataset that models a transportation network in Weld County in order to perform a closest facility analysis (ESRI, 2018). The closest facility analysis was conducted to determine the route distance between each producing well and the nearest disposal well or NGCS. The route depicts the actual transportation distance of wastewater using the available roads of the county. A TIGER/Line shapefile that depicts the road infrastructure in Weld County was input into ArcGIS 10.6 to accurately calculate the route distance (U.S. Census Bureau, 2019).

To the best of our knowledge, trucking is the major approach of UOG wastewater transportation in Colorado, with piping primarily used in freshwater transportation for hydraulic fracturing. The use of a pipeline to transport wastewater in oil and gas fields is another viable option. However, further information related to developing theoretical pipeline infrastructures (such as the effect of geological features in the area, relevant capital costs, and regulatory aspects) is not available and beyond the scope of this study. In Weld County, a typical truck that hauls wastewater from the UOG producing well to a disposal well typically possesses a capacity of 120 barrels (19 m^3) (Neal, 2019). A truck capacity of 120 barrels is typical in the U.S. but there may be other truck capacities used in other regions (Ground Water Protection Council, 2019). By integrating this truck capacity with the route distance and wastewater volume of each well, we calculated the total one-way transportation distance to move all the wastewater

generated from each UOG producing well to the nearest disposal well or NGCS via trucking using Eq. 5-1.

$$D = \frac{r_{\mathrm{d}} * V}{c_{\mathrm{truck}}} \qquad (5-1)$$

where D is the total one-way travel distance in miles, r_{d} is route distance in miles, V is UOG wastewater volume in barrels, and c_{truck} is truck capacity of transporting wastewater.

It should be noted that transportation providers may charge for the full round-trip to transport wastewater (i.e. from the time a truck leaves the transportation hub until its return). However, the transportation hub locations are not known, and thus only the one-way transportation distance and cost could be estimated in the analysis of this study.

A common metric to compare the economic cost in the oil and gas industry for wastewater management is the cost per barrel of wastewater. As a result, although we mainly use m^3 as the unit of wastewater volume in this study, U.S. dollar per barrel is used as the unit for the cost of wastewater transportation. To calculate the cost of one-way wastewater transportation, a median value of $105 per hour (cost range in Weld County is $90-120 per hour) and an average speed of 45 miles per hour were used for truck transportation in Weld County (Neal, 2019). These values are reasonable estimates for Weld County and may vary in other regions. For Weld County, the speed limit is typically 55 miles per hour on all county roads except within business districts and residential areas (Weld County Public Works, 2020). To account for the reduction in speed due to traveling on unpaved roads and also the time for a truck to accelerate to 55 miles per hour (and also decelerate when arriving at destination), 45 miles per hour provides a reasonable trip travel speed. Additionally, the typical time to load and unload wastewater from the truck (15 minutes for each, which could vary due to actual operating conditions) was added to the overall cost (Neal, 2019). Eq. 5-2 was used to calculate the wastewater transportation cost,

$$C = \left(\frac{D}{s} + \frac{V}{c_{\text{truck}}} * t_{\text{l/u}}\right) * c \qquad (5-2)$$

where C is equal to the total wastewater transportation cost in U.S. dollars, c is travel time cost ($105 per hour), s is travel speed (45 miles per hour), and $t_{\text{l/u}}$ is time to load and unload wastewater (0.5 hours).

For this study, we assume that no systematic differences exist for conditions of transportation to either a disposal well or CWT facility (e.g., a disposal well and CWT facility have similar conditions of paved and unpaved roads to get to their location) and that operating conditions are similar at each (e.g., it consistently takes 15 minutes to unload wastewater at either disposal well or CWT facility). To validate this assumption, a thorough analysis of actual conditions at each disposal well and proposed CWT facility would be required, which is outside the scope of this study. But we suggest the readers consider the relevant uncertainty when applying the findings of our study.

5.2.4 Quantitative estimation of waste heat availability at NGCSs

We quantified the waste heat availability at 35 NGCSs in Weld County, Colorado. The daily compression capacities of NGCSs along with the number of compressors were reported in the COGIS database (COGCC, 2020). Additionally, for each NGCS, the number and type of engines on-site were reported in documents in the Colorado Department of Public Health and Environment (CDPHE) air quality control database (CDPHE, 2020).

In order to quantitatively estimate the waste heat available at each NGCS, technical data were collected for the engines used for natural gas compression on-site at the 35 Weld County NGCSs (Table B1, Appendix B). Waste thermal energy can be recovered from the engine exhaust, cooling water, and lubricating oil (U.S. Department of Energy, 2016), and then used to heat the UOG wastewater for MD treatment. The technical data sheets provide a heat balance

that was used to determine waste heat available from the coolant (cooling water and lubricating oil) and exhaust. The heat rejection to jacket water/aftercooler (coolant waste heat) and exhaust were typically provided at 100% and 75% load in kW, respectively.

Another major source of waste heat at the NGCSs is thermodynamic heating of the natural gas when it is compressed to higher pressures. Depending on the desired outlet pressure, compressor efficiency, and number of compression stages, the temperature of the compressed gas can reach temperatures as high as 200°C (Gas Processors Suppliers Association, 2004). Typical industry practice is to remove this heat with air or liquid coupled intercooler heat exchangers connected to the engine coolant system (Jouhara et al., 2018). However, this heat represents a viable source for low grade heat capture that can be used for MD treatment. To quantify the amount of such waste heat, a multistage compression model was developed in Engineering Equation Solver based on fundamental conservation of energy equations and property relationships. The engine brake horsepower ($\dot{W}_{\mathrm{engine}}$) from each NGCS was input with a shaft efficiency of 90% (η_{shaft}) to calculate the compressor work (Eq. 5-3):

$$\dot{W}_{\mathrm{comp}} = \dot{W}_{\mathrm{engine}}\eta_{\mathrm{shaft}} \qquad (5-3)$$

The compressor work was input into a one or two stage compressor model with the NGCS mass flow rate of gas ($\dot{m}_{\mathrm{gas}}$), an assumed outlet pressure of 1000 psig (P_{out}), inlet gas temperature of 50°C, and storage temperature of 90°C (T_{s}) (Gas Processors Suppliers Association, 2004; Borgnakke and Sonntag, 2013). By setting the efficiency of each compressor stage at 85%, assuming a heat exchanger effectiveness of 80% (ε_{s}), and utilizing the equations below, the state points (temperature, pressure, entropy, and enthalpy) were determined for the entire system (Eq. 5-4 and 5-5):

$$r = \left(\frac{P_{\text{out}}}{P_{\text{in}}}\right)^{(1/N)} \qquad (5-4)$$

$$\dot{Q}_{\text{IC}} = \varepsilon_{\text{s}} \dot{m}_{\text{gas}} C_{\text{p}} \left(T_{\text{c,out}} - T_{\text{s}}\right) \qquad (5-5)$$

where r is the compression ratio per stage, N is the number of stages, P_{in} is the inlet pressure, C_{p} is the specific heat capacity, and $\dot{Q}_{\text{IC}}$ is the intercooler heat duty. The sum of the intercooler heat duties (if multiple stages used) and the waste thermal energy from engine exhaust, cooling water, and lubricating oil yields the total available heat duty for each NGCS.

5.2.5 Estimation of treatment capacity and required thermal efficiency for MD powered by waste heat generated from NGCSs

To evaluate the feasibility of using waste heat available at NGCSs to power MD treatment of UOG wastewater, we estimated the MD treatment capability at each assumed CWT facility co-located with a NGCS. The MD treatment capability quantifies the amount of UOG wastewater that could be treated via MD powered by waste heat at each NGCS.

To determine the MD treatment capacity at each NGCS, we estimated the specific thermal energy consumption (STEC) using a DCMD model simulation from our previous study (Figure B1, Appendix B) (Robbins et al., 2020). The model simulated DCMD treatment of UOG wastewater with a salinity range of 20,000-40,000 mg/L, which is typical for the DJ Basin (Esmaeilirad et al., 2015; Lester et al., 2015; Kim et al., 2016; Rosenblum et al., 2016; Bell et al, 2017; Chang et al., 2019; Zhang et al., 2019), and a MD brine salinity of 200,000 mg/L (corresponding to recovery rate varied between 80-90%). The STEC range of MD from the model was ~910-2,035 kJ kg^{-1} permeate (750-1,815 kJ kg^{-1} feedwater), depending on the salinity and operational temperature of the feedwater. The STEC range obtained from our DCMD model was in accordance with several STEC values in the literature (Khayet and Matsuura, 2011; Thiel et al., 2015; Lokare et al, 2017; Tavakkoli et al., 2017). Since the energy efficiency of MD

depends on the MD type and operating conditions, we also performed a thorough literature review to obtain reported values for STEC (Table B2, Appendix B). This would render our analysis more accurate regardless of any potential limitation of our model. In literature, gained output ratio (GOR) is typically reported along with STEC. GOR is defined as the vaporization enthalpy of distilled water produced by MD divided by the heat input into the MD system (Deshmukh et al., 2018; Christie et al., 2020), which is a useful metric to quantify the energy efficiency of the MD process (Thiel et al., 2015). A STEC range of 300-2,260 kJ kg^{-1} permeate (or a GOR range of 1-7.5) is reported for different MD configurations and operating conditions (Khayet and Matsuura, 2011; Swaminathan et al., 2011; Summers et al., 2012; Qtaishat and Banat, 2013; Thiel et al., 2015; Lokare et al., 2017; Tavakkoli et al., 2017; Deshmukh et al., 2018; Kim et al., 2018; Schwantes et al., 2018; Ullah et al., 2018). In terms of the upper limit of GOR, it is practically difficult to achieve an energy efficiency of MD greater than a GOR of 5 (Christie et al., 2020). To exceed such high energy efficiency, the temperature differences of both MD (i.e., between feedwater and permeate) and heat exchanger must be very small, which makes the vapor flux of MD and the heat flux of heat exchanger impractically low (Christie et al., 2020). Further discussion of the DCMD model can be found in Appendix B (Figure B1, Appendix B).

We also estimated the critical GOR required at each NGCS. The critical GOR refers to the GOR value at which the available waste heat at each NGCS is equal to the thermal energy required by MD treatment of all the UOG wastewater received by this NGCS. To determine critical GOR, we assume that the UOG wastewater is delivered to the closest available NGCS, and the waste heat available at each NGCS is correlated to the UOG wastewater treatment demand to calculate the critical GOR. A higher critical GOR suggests that the MD system needs

to have higher energy efficiency. Thus, the value of GOR indicates the practicality of using MD powered exclusively by waste heat to meet the wastewater treatment demand of each NGCS.

5.3 Results and Discussion

5.3.1 Spatial distribution of UOG wastewater production density

In 2018, 11.96 million m^3 (75.2 million barrels) of wastewater was generated from UOG producing wells in Weld County (COGCC, 2020). Meanwhile, there were 7,583 producing wells that generated at least 100 barrels of wastewater per well, and they contributed to approximately 95% of wastewater generated in the county. In this study, we focused on those wells and compared DWI and CWT co-located with NGCSs as potential wastewater management strategies. There are 47 active disposal wells in Weld County, which receive wastewater for injection. Also, there are 35 NGCSs with a compression capacity of at least 7.5 million standard cubic feet per day (MMSCFD) in Weld County (COGCC, 2020). Among those NGCSs, the maximum, median, and minimum compression capacities are 170 MMSCFD, 60 MMSCFD, and 7.5 MMSCFD, respectively, with 10 NGCSs possessing a capacity higher than 100 MMSCFD. Accordingly, we created a density map of annual wastewater production, which overlaps with the spatial distribution of active disposal wells and NGCSs in Weld County (Figure 5-1).

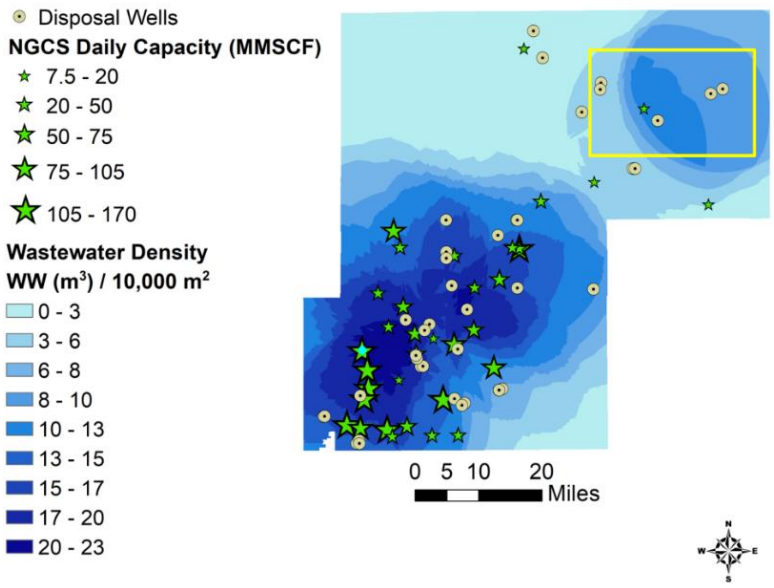

Figure 5-1. Wastewater density (in m^3 per 10,000 m^2) for Weld County in 2018. The spatial distribution of NGCSs and disposal wells are also shown in the map. The yellow square indicates an area in northeast Weld County where the number of disposal wells is much higher than that of NGCSs.

The highest density of annual wastewater generation from UOG production is shown to be in central and southwest Weld County, with a peak density ranging from 20 to 23 m^3 (126 to 145 barrels) of wastewater per 10,000 m^2 in 2018. Another notable area is northeast Weld County, which has a peak density in the range from 13 to 15 m^3 (82 to 94 barrels) per 10,000 m^2. The wastewater density is important as it depicts the areas where wastewater management is essential due to high wastewater generation. The spatial distribution of NGCSs shows a dearth of NGCSs in northeast Weld County, whereas a higher number of NGCSs, in particular those with relatively high daily compression capacities, are located in southwest Weld County. The disposal wells appear to cover areas with high densities of UOG wastewater generation (i.e., the northeast, central, and southwest Weld County). To better understand the spatial relationship of UOG production wells with NGCSs and disposal wells, the associated transportation distances were calculated and analyzed further.

5.3.2 Total transportation distance from UOG wells to disposal wells or NGCSs

In order to understand how logistics may affect wastewater management strategies, an analysis of transportation distance from individual UOG wells to the nearest disposal well or NGCS was performed in Weld County using ArcGIS software. We assume that CWT facilities applying MD treatment are powered by waste heat co-located at NGCSs. Such practice has been demonstrated potentially feasible in Pennsylvania where the waste heat available at NGCSs is sufficient to drive MD treatment of all the produced water of the state (Lokare et al., 2017). In addition to UOG wastewater transportation to the CWT facility, there is additional transportation distance to haul MD brines from a CWT facility to the nearest disposal well, if zero liquid discharge (ZLD) is not achieved. In this section, we will focus only on the transportation distance of the raw UOG wastewater to simplify the analysis. The transportation of MD brines will be considered in the local scale analysis later in this study. The transportation distance will largely determine whether wastewater treatment at CWT facilities is competitive compared to DWI. When evaluating the entire Weld County, the total transportation distance for moving all wastewater generated from the 7,583 UOG wells to their nearest disposal wells was 4.23 million miles, using ground transportation with 120-barrel capacity trucks. For comparison, moving such a quantity of wastewater to the nearest NGCSs resulted in a total transportation distance of 5.64 million miles (Figure 5-2A). Therefore, the total transportation distance of UOG wastewater was ~25% less for DWI than CWT facilities co-located with NGCSs. Statistically, the median distances to transport all UOG wastewater of an individual producing well generated in 2018 via 120-barrel capacity trucks to either a disposal well (80 miles) or a NGCS (79 miles) were similar, while the mean distance was greater for transportation to an NGCS (743 miles) as compared to a disposal well (557 miles) (Figure 5-2B).

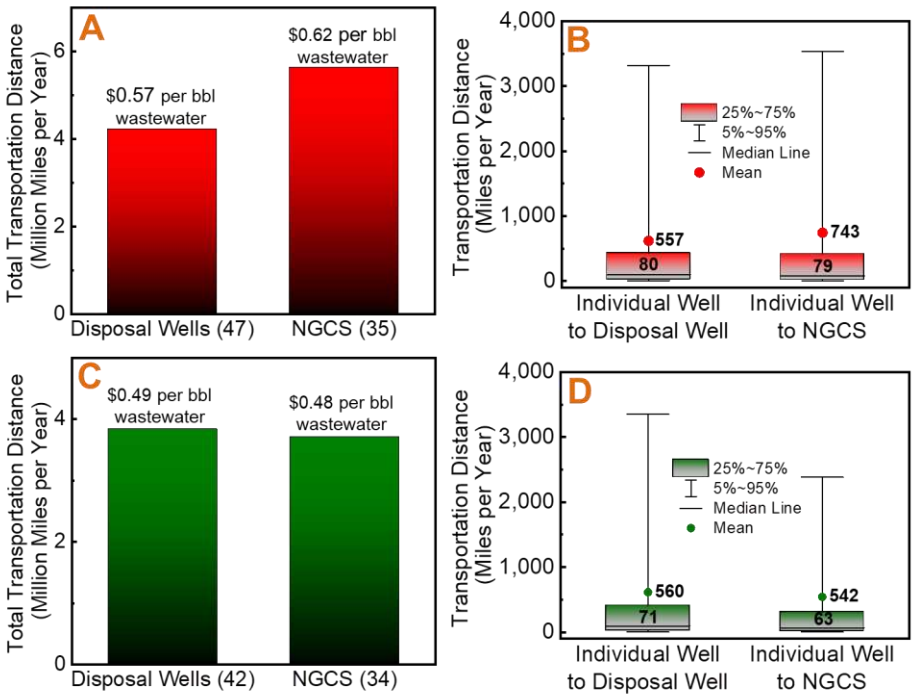

Figure 5-2. (A and C) Total and (B and D) individual transport distance required to move all wastewater generated in 2018 in Weld County to the nearest disposal wells or NGCSs. Compared to Figures 5-2A and 5-2B, Figures 5-2C and 5-2D exclude northeast Weld County (including 1 NGCS and 5 disposal wells, highlighted in Figure 5-1) due to the extremely low number of NGCSs in this region. The numbers in the parenthesis indicate the number of NGCSs and disposal wells included in the analysis.

Using the total transportation distances to calculate transportation costs, DWI and CWT co-located with NGCSs requires $0.57 and $0.62 per barrel for wastewater transportation, respectively. This makes DWI more economically favorable at the county scale.

However, we noticed that in northeast Weld County, a limited number of NGCSs are located within a relatively dense wastewater production area. For example, only one NGCS is located within the area highlighted in Figure 5-1, whereas there are at least five disposal wells located in close proximity. In our calculation, this one NGCS accounts for 34% of the total transportation distance from individual wells to the nearest NGCSs in Weld County, while the five disposal wells only account for 9% of total transportation distance for DWI. Therefore, we removed this area (including 1 NGCS, 5 disposal wells, and 12.2 million barrels of wastewater) from the

analysis to better compare DWI and CWT facilities co-located with NGCSs. When excluding this region, wastewater transportation to the nearest NGCSs and disposal wells requires 3.71 million and 3.84 million miles (Figure 5-2C), corresponding to $0.48 and $0.49 per barrel for wastewater transportation, respectively. The median and mean distances to transport all UOG wastewater generated from an individual well in 2018 (with 120-barrel capacity trucks) to NGCSs are 63 and 542 miles, respectively, slightly lower than 71 and 560 miles for wastewater transportation to disposal wells (Figure 5-2D). The 75^{th} and 95^{th} quantiles of transportation distance to the nearest NGCS are also lower than those to the nearest disposal well. These results highlight the importance of refining the scale of analysis for the selection of UOG wastewater management strategy. In the following sections, we will further refine the analysis to the local scale for specific producing wells and NGCSs, which will reveal a clearer comparison between different management strategies in regard to logistical considerations.

5.3.3 Comparison of deep-well injection and centralized wastewater treatment co-located with NGCSs for individual producing wells

In order to better illustrate where a CWT facility co-located with an NGCS would be more viable based on wastewater transportation distance, we compared the distances to the nearest disposal well and NGCS for each individual UOG well in Weld County, labeling the wells with different colors that indicate the transportation preference (i.e., purple for less distance to a NGCS and orange for less distance to a disposal well, Figure 5-3A). It should be noted that transportation distance of UOG wastewater is not the only criteria for selecting a UOG wastewater management practice. In this study, however, we focus on the transportation distance to demonstrate its importance in the economic feasibility of UOG wastewater treatment.

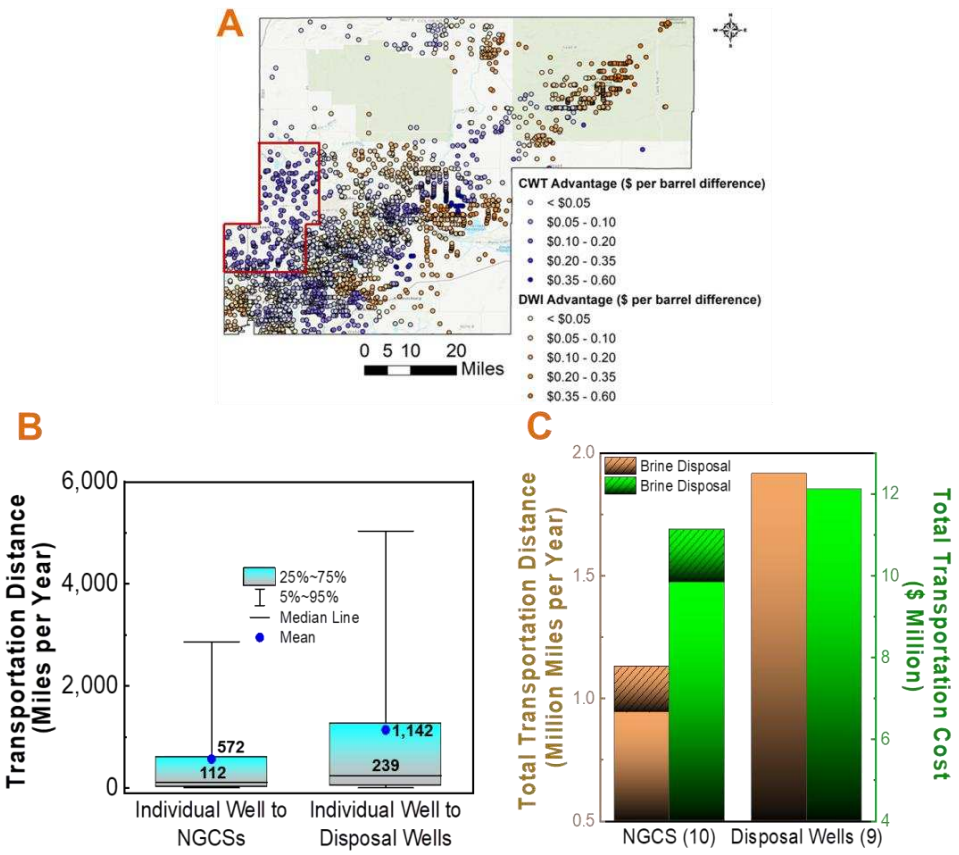

Figure 5-3. (A) Comparison of the transportation cost difference from UOG producing wells to the nearest NGCS (CWT) and disposal well (DWI). The wells labeled in purple are producing wells closer to a NGCS than a disposal well. The wells labeled in orange are producing wells closer to a disposal well than an NGCS. Wells with greater cost difference between CWT and DWI are indicated with darker hues of purple or orange. The area highlighted within the red square in western Weld County identifies a cluster of producing wells with less distance to NGCSs than disposal wells, which is used as an example study area. (B) Analysis of the transportation distance of 1,679 wells to either one of the 10 NGCSs or 9 disposal wells in our example study area. (C) The total transportation distance and cost for DWI and CWT co-located NGCSs within our example study area. The transportation distance and cost of CWT includes those associated with moving both raw wastewater and MD brines.

Within the 7,583 individual producing wells analyzed in this study, slightly more than half of the wells are located closer to an NGCS (3,942 wells with 34.4 million barrels of wastewater generated) than a disposal well (3,641 wells with 36.6 million barrels of wastewater generated). As shown in Figure 5-3A, there are clusters of producing wells that are closer to NGCSs in southwest Weld County, whereas a cluster of producing wells is found closer to disposal wells in

northeast Weld County. This is consistent with our above discussion that emphasizes the importance of analysis scale for wastewater transportation.

An area in western Weld County is highlighted in Figure 5-3A for further analysis due to the favorability towards transportation to NGCSs versus disposal wells. This area, which possesses 10 NGCSs and 9 disposal wells, includes 1,679 producing wells generating 2.78 million m^3 (17.5 million barrels) of wastewater in 2018. This represents 23.2% of wastewater generated from producing wells in Weld County. The mean and median transportation distance to move all UOG wastewater generated from an individual producing well to the nearest NGCS was 572 and 112 miles per year, respectively (Figure 5-3B). In comparison, the mean and median transportation distance to move all UOG wastewater to the nearest disposal well in this area was 1,142 and 239 miles per year, respectively. The total transportation distance to move the 2.78 million m^3 of wastewater to the nearest disposal wells is 1.92 million miles, which is twice the distance needed to transport to the nearest NGCSs (945,000 miles) (Figure 5-3C).

However, the transportation of MD brines to the nearest disposal well needs to also be considered into the overall transportation distance for a CWT facility located at an NGCS in this area. The TDS of UOG wastewater in the DJ basin is typically 20,000-40,000 mg/L (Esmaeilirad et al., 2015; Lester et al., 2015; Kim et al., 2016; Rosenblum et al., 2016; Bell et al., 2017; Chang et al., 2019; Zhang et al., 2019). For this study, a recovery rate of 85% was used to represent a feed TDS of 30,000 mg/L and a brine TDS at 200,000 mg/L. Such high water recovery and brine salinity could be achieved by MD and comparable to those of other thermal desalination technologies (Tong and Elimelech, 2016), which is important to minimize the volumes of UOG brine for disposal. Using this assumption, MD treatment of wastewater sent to the presumptive CWT facilities at the 10 NGCSs in this area resulted in 417,000 m^3 (2.62 million barrels) of

brines requiring transportation to the nearest disposal wells. This added 186,177 miles of transportation distance to CWT, increasing the total transportation distance to 1.13 million miles. When converting such a distance into the transportation cost (note that the transportation cost is not a linear function of transportation distance, due to the consideration of the time to load and unload wastewater), CWT facilities co-located with an NGCS provided a cost savings of ~$1 million when compared to DWI ($11.1 million for CWT versus $12.1 million for DWI) (Figure 5-3C). This equates to a transportation cost of $0.64 per barrel of wastewater for CWT and $0.69 per barrel of wastewater for DWI. Therefore, due to the increase of transportation cost for the disposal of MD brine, the advantage for transporting UOG wastewater to a NGCS as opposed to the nearest disposal well is reduced, rendering CWT co-located with NGCS only slightly favorable in regard to the logistical cost. A summary table (Table B3, Appendix B) is provided that displays transportation distance and cost at the various scales used in this study.

The above analysis demonstrates that analyses of transportation distance performed at the local scale could result in conclusions that differ from those made at other larger scales. When evaluating Weld County as a whole, DWI was shown to be more favorable than centralized wastewater treatment based on transportation distance and economics. By removing a portion of northeast Weld County from the analysis (Figure 5-1), the two management strategies became comparable for transportation. When further reducing the analysis to a localized scale, CWT becomes favorable when compared to DWI, even considering the transportation of MD brines for disposal. Therefore, the scale of analysis is essential for decision making when CWT is compared with DWI, and analysis at the local scale could correct information that is biased for large-scale analysis.

5.3.4 Waste heat availability at NGCSs to power UOG wastewater treatment by MD

Another important factor for evaluating the feasibility of CWT co-located with NGCSs is the waste heat availability that corresponds to wastewater treatment capacity. An estimation for the waste heat generated from engines and compressors was made at all the NGCSs investigated in this study (Figure 5-4A). The wastewater generated from each individual UOG well is assigned to the specific NGCS if it results in the shortest transportation distance among all the NGCSs and disposal wells, and the volumes of wastewater assigned to each NGCS are summed. Using a GOR range of ~1-2.5 (STEC range of ~910-2,035 kJ kg^{-1} permeate) from our DCMD model and a high-end GOR of 5 for MD treatment according to the literature, the range of MD treatment capacity was calculated at each NGCS. This allows for the comparison of wastewater treatment demand with the treatment capacity of MD powered by waste heat available at the NGCSs (Figure 5-4B).

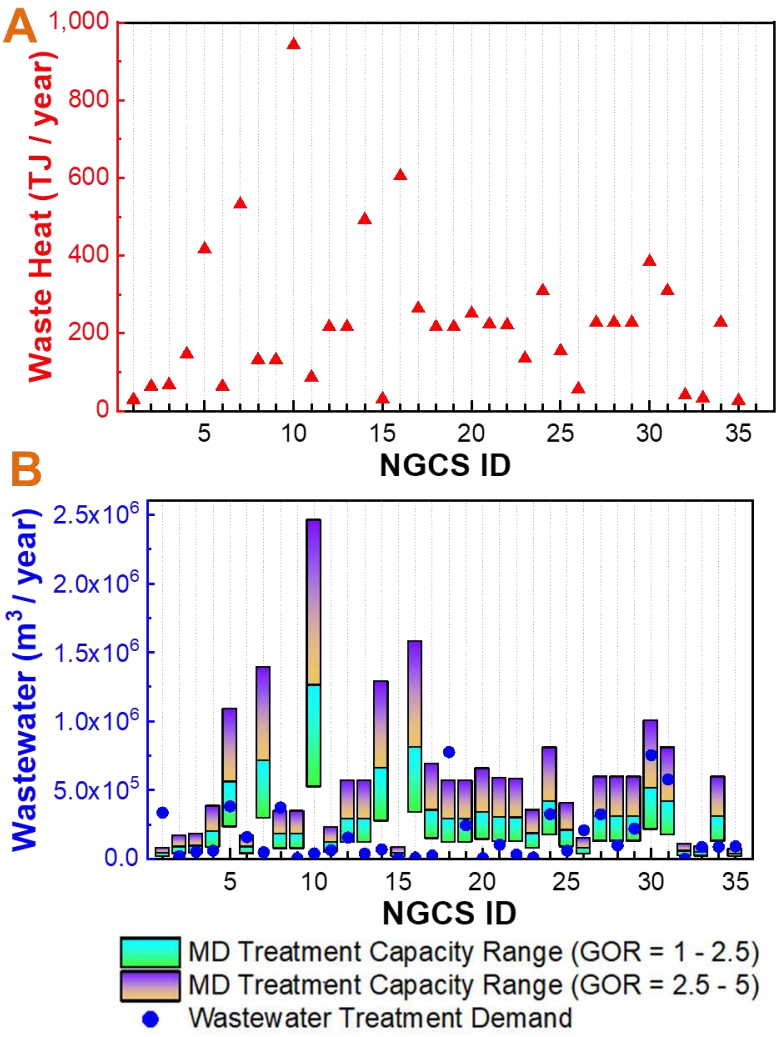

Figure 5-4. (A) Waste heat available to power MD treatment at a CWT facility co-located at each NGCS. (B) Annual UOG wastewater volume potentially transported to an NGCS and MD treatment capacity based on a GOR range of ~1-2.5 attained from our DCMD model and a high-end GOR of 5 according to the literature. Only producing wells with UOG wastewater transportation distances to NGCSs smaller than those to disposal wells were used for calculating wastewater volume.

The estimated waste heat available at the 35 NGCSs investigated in the current study ranged from 29.2-942 TJ per year with a median of 216 TJ per year and a mean of 226 TJ per year. These NGCSs generate available waste heat of 7,921 TJ per year in total. Among all the NGCSs, the Hudson NGCS (ID # 10, located in south Weld County, with 170 MMSCFD compression capacity) provides the highest amount of thermal energy (942 TJ per year) available from waste heat. There are also four NGCSs (ID # 5, 7, 14, and 16) that provide relatively abundant waste

heat of greater than 400 TJ per year. Three out of these four NGCSs (except for NGCS ID # 5) are located in southwest Weld County, which correlate well with the area possessing the highest density of UOG wastewater production.

To better understand the feasibility of utilizing such waste heat for UOG wastewater treatment, the potential treatment demand at each NGCS was estimated. Since this study focuses on wastewater transportation, we used the transportation distance as the criteria for assigning wastewater to NGCSs or disposal wells in our analysis. At the Hudson NGCS with the most quantity of waste heat (corresponding to 520,000-1.26 million m^3 wastewater treatment capacity by MD using our modeling estimation and up to 2.46 million m^3 capacity at the high-end of the feasible GOR range), only 85 producing wells had their optimal transportation distance (i.e. the shortest distance to any NGCS or disposal well) with this NGCS, generating 40,500 m^3 (254,800 barrels) of wastewater in 2018. Thus the availability of waste heat exceeds the UOG wastewater treatment demand at this NGCS significantly. In contrast, the St. Vrain NGCS (ID # 18) potentially received wastewater from 483 producing wells with optimal transportation distance, resulting in the highest wastewater treatment demand of 776,000 m^3 per year. Although the St. Vrain NGCS has a relatively large compression capacity (120 MMSCFD) and a high amount of available waste heat (216 TJ per year), the MD treatment capacity at this NGCS (120,000 to 289,000 m^3 of wastewater per year using our DCMD model and up to 565,000 m^3 using the high-end of the feasible GOR range) is insufficient compared to the wastewater treatment demand. There are additional NGCSs that potentially receive a high volume of wastewater but possess low waste heat availability. For example, the Angus NGCS (ID # 1), which is the northernmost NGCS in Weld County, could potentially receive 461,800 m^3 (2.9 million barrels) of UOG wastewater but this NGCS only generates 29.2 TJ/year of waste heat that corresponds to

16,100-76,200 m^3 MD treatment capacity (based on GOR of 1-5). Another example is the Kersey NGCS (ID # 26) located in central Weld County, which could receive 208,938 m^3 (1.31 million barrels) of wastewater, but only has 31,200-147,600 m^3 MD treatment capacity (based on GOR of 1-5). There are also several NGCSs (for example, ID # 3, 5, 11, 19, 24, 27, and 29) that have UOG wastewater treatment demand aligned well with their MD treatment capacity powered by waste heat based on our DCMD model (Figure 5-4B). Therefore, the waste heat availability at NGCSs does not always match the potential UOG wastewater treatment demand, rendering it necessary to further investigate the feasibility of MD treatment powered by waste heat.

Using the waste heat availability and the volume of wastewater potentially received by each NGCS, we also estimated the critical GOR that reflects the required energy efficiency of MD treatment to meet the wastewater treatment demand at the NGCSs (Figure 5-5 and Figure B2, Appendix B). Different from the above analyses based on MD treatment capacity and STEC, critical GOR is independent of our DCMD modeling, and thus provides additional insight on the feasibility of using waste heat as the energy source for MD treatment of UOG wastewater. The critical GOR values for the 35 NGCS in this study varied from 0.1 to 22.1 with a mean of 2.47 and a median of 0.88. There are 25 NGCSs (~71%) with a critical GOR less than 2.5, which is at the high-end of our DCMD modeling estimation (GOR of 1-2.5) and others (Khayet and Matsuura, 2011; Thiel et al., 2015; Lokare et al., 2017; Tavakkoli et al., 2017). At those NGCSs, the generated waste heat is likely to meet the wastewater treatment capacity even if a relatively conservative estimation of MD energy efficiency is used. Also, there are 5 NGCSs with a critical GOR between 2.5 and 5, indicating that MD treatment of all the received UOG wastewater is feasible at those NGCSs if high energy efficiency of MD is achieved. Finally, there are 5 NGCSs

with a critical GOR higher than 5. Therefore, the waste heat generated at those NGCSs is unlikely to be sufficient for the treatment of all the received UOG wastewater by MD.

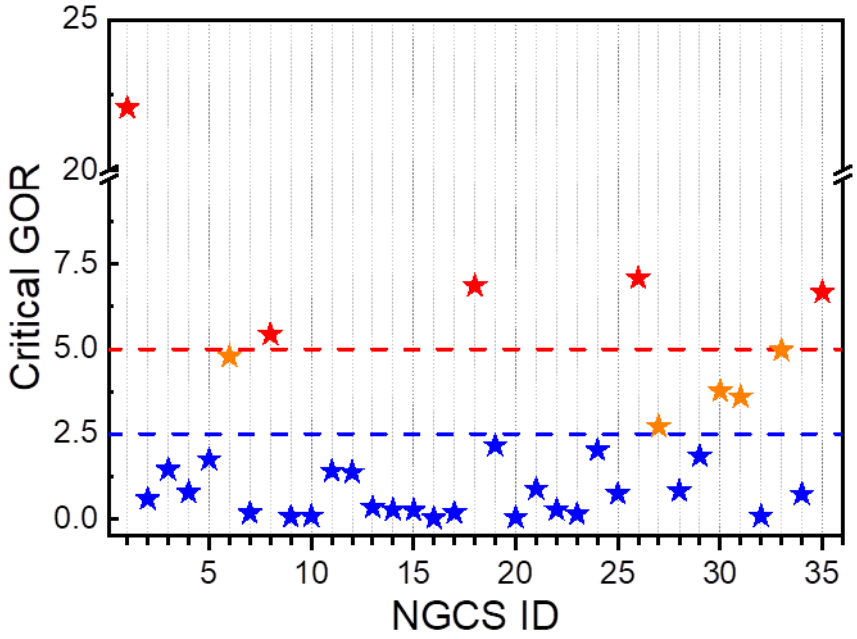

Figure 5-5. Critical GOR values for CWTs co-located with the 35 NGCSs in Weld County, CO. The critical GOR represents the GOR required for MD treatment to treat all wastewater sent to each NGCS location. Lines at a critical GOR of 5 and 2.5 are depicted which represents feasible high-end values for GOR practical for MD treatment with latent heat recovery from literature and our DCMD model, respectively. NGCSs with a critical GOR greater than 5 are represented with red stars, NGCSs with a critical GOR between 2.5 and 5 are represented with orange stars, and NGCSs with a critical GOR below 2.5 are represented with blue stars.

Ideally, the volumes of wastewater received by CWT facilities co-located with NGCSs should be aligned well with the available waste heat. However, as discussed above, such ideal scenarios are not achieved by only considering transportation distances of UOG wastewater. Therefore, in addition to the total amount of available waste heat, matching wastewater treatment demand and the treatment capacity of waste heat should be considered in evaluating the feasibility of CWT co-located at NGCSs. For our analysis, CWT facilities located at 30 NGCSs could feasibly treat all the UOG wastewater from producing wells that are located closest using the available waste heat (i.e., critical GOR <5). CWT at these 30 NGCSs provided a ~$2.9 million annual transportation cost savings compared to DWI, when the cost of brine

transportation was not considered ($12.6 million and $0.52 per barrel for CWT as compared to $15.5 million and $0.64 per barrel for DWI) (Figure B3, Appendix B). When factoring in brine transportation to the nearest disposal well for CWT, the transportation cost savings between CWT and DWI is reduced to ~$700,000 annually for the associated wells. For the 5 NGCSs with insufficient waste heat to treat all UOG wastewater, they potentially receive 11.2 million barrels of wastewater based on transportation distance (as compared to 25.5 million barrels received by the other 30 NGCSs). Using a GOR of 5 for MD treatment, 6.4 million barrels of UOG wastewater could be treated with the available waste heat at these 5 NGCSs (57.2% of treatment demand). Therefore, 4.8 million barrels of UOG wastewater would need to be diverted. Further optimization should be performed to divert wastewater from the NGCSs receiving excess wastewater to those with excess waste heat, while such a practice further increases the distance and cost of wastewater transportation. The excess wastewater could also be diverted to the nearest disposal well, and thus the potential of waste heat to power MD treatment would not be fully realized. This systems-level optimization requires more complex computational approaches that are beyond the scope of this work.

5.4 Implications

Our study demonstrates the importance of logistical considerations in the decision making for UOG wastewater management. We show that the transportation costs associated with CWT co-located with NGCSs are higher or comparable to those associated with DWI in Weld County, Colorado, and such costs could be significant in deciding the feasibility of UOG wastewater treatment. Taking the highlighted area in Figure 5-3A as an example, the transportation cost for CWT co-located at NGCSs is ~$0.64 when considering the transportation of both raw UOG wastewater and MD brine. Such a cost is slightly lower than that for wastewater transportation to

disposal wells (~$0.69). In comparison, wastewater treatment costs for MD technology are in the range of $0.12-1.08 per barrel in the literature (Tavakkoli et al., 2017; Schwantes et al., 2018). In the recent Chevron Tech Challenge organized by Chevron Corporation in collaboration with the U.S. Department of Energy, the suggested treatment cost for produced water treatment is $0.40-0.75 per barrel (Chevron Technology Ventures, 2018). Therefore, the cost associated with transporting wastewater for CWT co-located at NGCSs is comparable to that of wastewater treatment itself, indicating that optimization of the transportation cost is equally important to reducing the wastewater treatment cost via technological innovation. In addition, considering the comparable transportation costs between CWT and DWI in this study, the treatment cost of MD technology needs to be competitive compared to DWI. The cost of MD depends on its energy efficiency and the availability of alternative energy sources (e.g., waste heat). In Colorado for non-state owned fluids, the standard injection cost rate for wastewater produced from wells is $0.65 per barrel (Colorado State Land Board, 2020) which falls towards the low-end of the reported national range of $0.50-2.50 per barrel for injection (McCurdy, 2011). Therefore, the treatment cost of MD *per se* needs to be comparable or lower than $0.65 per barrel for industry adoption in Colorado, and this treatment cost is consistent with the goal set by the Chevron Tech Challenge (Chevron Technology Ventures, 2018).

It should be noted that there may be an additional transportation cost post-treatment to move treated water product from the CWT facility to its desired end uses (i.e. surface water discharge or possibly agricultural irrigation). However, such end uses depend on both water demand and regulations, which are still not clear for wastewater reuse in the UOG industry. This knowledge gap prevents us from considering these associated costs in the current study. The end uses of treated water product are ideally located within close proximity to the CWT facility, and the

spatial analysis used in this study could help minimize post-treatment transportation. For example, the St. Vrain NGCS is located less than 1 mile from a large surface water body (South Platte River), making it practical to move water for discharge at this location if regulatory requirements are met. Also, the monetary value of the treated water, if carefully considered, could offset a portion of the transportation and treatment costs. In northern Colorado, water rights were sold in excess of $20,000 per acre-foot (1,233 m^3 or 7,758 barrels) in 2018 (Runyon, 2018; Smith, 2019), demonstrating that water could be a valuable commodity in water scarce regions. Wastewater treatment would also allow for valuable water to remain in the hydrologic cycle and be available for use at the surface, rather than becoming inaccessible within geologic formations via DWI.

Furthermore, the scale of analysis plays an important role in determining the viability of UOG wastewater treatment. As demonstrated in this study, the transportation cost of DWI is less than that of CWT co-located with NGCSs at the county scale. However, the transportation costs for both management strategies become almost equal by eliminating a small geographic area with unbalanced number of NGCSs relative to disposal wells (Figures 5-1 and 5-2). When we further refine the analysis to a local scale (highlighted in Figure 5-3A), the comparison of transportation economics is reversed to be in slight favor of CWT compared to DWI. Therefore, considering the important role of logistics, the best management strategy for UOG wastewater varies case by case at the local scale, at least in terms of economic feasibility. A detailed analysis at the local level, rather than at the county or state level, needs to be completed for decision makers to make well-informed decisions on the implementation of UOG wastewater management strategy.

We notice that the transportation cost for DWI estimated in this study is lower than the reported national average of $1-3 per barrel of wastewater. This is due to the relatively abundant availability of disposal wells in Colorado (47 wells in Weld County as compared to only 16 wells in the entire state of Pennsylvania). Hence, in other regions with a lower density of disposal wells, transportation cost would be more advantageous towards centralized treatment as compared to DWI, as recently demonstrated for Pennsylvania (Tavakkoli et al., 2020). Even with such a low transportation cost of DWI, centralized UOG wastewater treatment could be viable and beneficial. For example, truck transportation of UOG wastewater has additional costs such as road damage and pollution (e.g., pollutants from vehicle emissions and greenhouse gas emissions) that increases the need to minimize transportation (Duthu and Bradley, 2017). As shown in this study, transportation distances could be reduced by up to 50% in certain areas of Weld County when selecting CWT at NGCSs over DWI, thereby greatly reducing these additional costs. Further, an additional benefit of replacing DWI with CWT is the demonstration to the local communities for water stewardship through wastewater treatment and beneficial reuse. However, it is worth mentioning that the liability associated with UOG wastewater treatment needs to be considered because any potential incidents might result in significant liability costs. Such costs could outweigh the cost savings and discourage UOG operators from adopting wastewater treatment.

Another viable strategy for UOG wastewater management is decentralized, on-site treatment, which eliminates the transportation cost of UOG wastewater and is thus an intriguing solution. Compared to on-site treatment, CWT provides a better opportunity to treat higher volumes of wastewater, providing better “economics of scale” (Ren et al., 2019). CWT facilities receive wastewater from many UOG wells, reducing the dramatic fluctuation of wastewater

quantity and quality that typically occurs at individual wells (Bai et al., 2015; Kondash et al., 2017). Another consideration when selecting between on-site and CWT is the regulatory burden associated with each strategy. With centralized UOG wastewater treatment, a single permit is likely required by a CWT facility for water quality control (e.g., the National Pollutant Discharge Elimination System permit for discharge of the treated wastewater). In contrast, permits need to be acquired at each well site for on-site treatment, thereby increasing the regulatory burden on the wastewater service providers.

Additionally, the reservoir capacity of disposal wells needs to be considered. COGCC manages cumulative injection volume in permitting disposal wells by applying a maximum injection volume based on the thickness and porosity of geological reservoirs. This restriction is intended to constrain the total volume of injected fluids during the lifetime of the injection well (COGCC, 2015). Reducing the regional cumulative injection volume has been put forth as a solution to minimize induced seismicity (Scanlon et al., 2018). Alternatives to DWI such as CWT could play an important role in reducing the regional cumulative injection volume and thus preventing induced seismicity. Using data from the COGIS database, the wastewater volumes sent for DWI in 2018 based on the optimization of UOG wastewater transportation account for ~0.01%-34.4% of the maximum injection capacity of the 47 disposal wells, with mean and median values of 6.2% and 2.3%, respectively. These results indicate sufficient reservoir capacity of DWI in Weld County based on our analysis. However, the available reservoir capacity could be a limiting factor for DWI in the future. For example, one disposal well had 27% of its maximum injection capacity occupied by 2019, while the UOG wastewater sent to this disposal well potentially accounts for 34.4% of its capacity. Therefore, this disposal well would reach its maximum capacity in the near future and become unavailable unless there is an

amendment that increases its maximum injection volume. Considering that the availability of disposal well capacity becomes progressively constrained due to the increasing wastewater volumes generated from UOG production (Kondash et al., 2018), the resultant increase of transportation distance and cost associated with DWI will provide additional incentives for UOG wastewater treatment.

In addition, further work should focus on performing a techno-economic assessment (TEA) that compare the economic prospects among CWT facilities co-located with NGCSs, on-site treatment, and DWI in UOG-producing regions such as Weld County. Such an analysis should consider the treatment cost, logistics cost, and the effect of treatment capacity comprehensively. In contrast to previous TEA studies that were mainly based on one assumed treatment facility (Tavakkoli et al., 2017; Schwantes et al., 2018), a systems engineering approach should be applied to consider optimization at the regional or local scale. This approach is an essential component that is complementary with the current efforts of developing technologies for UOG wastewater treatment.

5.5 Conclusions

In this study, we developed a spatial analysis framework to understand the feasibility of UOG wastewater treatment by MD powered by waste heat available at NGCSs in Weld County, Colorado. An emphasis was placed on logistics, particularly wastewater transportation, to compare CWT facilities co-located at NGCSs with DWI.

Our results show that the cost of transporting raw UOG wastewater and MD brines for CWT at NGCSs is higher or comparable to that of wastewater transportation for DWI in Weld County, and that the comparison between these two wastewater management strategies is dependent on the scale of analysis. These findings indicate the importance of considering the transportation

cost and carefully selecting the scale of interest when determining the best management strategy for UOG wastewater. Furthermore, we correlated the waste heat availability at each NGCS with the potential wastewater treatment demand based on the optimization of UOG wastewater transportation. We found that the waste heat availability at NGCSs does not always match the potential wastewater treatment demand, resulting in diverting of UOG wastewater that further increases the transportation cost. Therefore, regional optimization considering the treatment capacities of CWT facilities co-located at NGCSs needs to be performed to fully utilize the potential of waste heat to power UOG wastewater treatment. Our study suggests that a detailed and comparative TEA analysis should be performed to compare the economic feasibility of different UOG wastewater management strategies. The combination of TEA with the spatial analysis framework shown in this study will help better inform future decision making of UOG wastewater management and identify viable locations to facilitate the wide adoption of wastewater treatment in the UOG industry.

References

Bai, B., Carlson, K., Prior, A., Douglas, C., 2015. Sources of variability in flowback and produced water volumes from shale oil and gas wells. *J. Unconven. Oil Gas Resources* 12 (2015), 1-5.

Bell, E. A., Poynor, T. E., Newhart, K. B., Regnery, J., Coday, B. D., Cath, T. Y., 2017. Produced water treatment using forward osmosis membranes: Evaluation of extended-time performance and fouling. *J. Membr. Sci. 525*, 77-88.

Borgnakke, C., Sonntag, R.E., 2013. *Fundamentals of Thermodynamics*. 8th ed., New Jersey: John Wiley & Sons.

Chang, H.; Li, T.; Liu, B.; Vidic, R. D.; Elimelech, M.; Crittenden, J. C., 2019. Potential and implemented membrane-based technologies for the treatment and reuse of flowback and produced water from shale gas and oil plays: A review. *Desalination* 455, 34-57.

Chevron Technology Ventures, 2018. Chevron tech challenge: In search of a step change in technology. https://www.chevron.com/stories/chevron-tech-challenge (accessed April 10, 2020).

Christie, K.S., Horseman, T., Lin, S., 2020. Energy efficiency of membrane distillation: Simplified analysis, heat recovery, and the use of waste-heat. *Environ. Inter.* 138, 105588.

Colorado Department of Public Health and Environment, 2020. Colorado Environmental Records. https://environmentalrecords.colorado.gov/HPRMWebDrawer/Search (accessed May 20, 2020).

Colorado Oil and Gas Conservation Commission, 2015. Governor's Task Force on State & Local Regulation of Oil & Gas Operation: Engineering Unit Class II UIC Wells https://cogcc.state.co.us/documents/about/TF_Summaries/GovTaskForceSummary_Engineering%20UIC%20Wells.pdf (accessed April, 11, 2020).

Colorado Oil and Gas Conservation Commission, 2020. Colorado Oil and Gas Information System Home Page. https://cogcc.state.co.us/data.html#/cogis (accessed Feb. 23, 2020).

Colorado State Land Board, 2020. State Land Board Disposal Rates. https://www.colorado.gov/pacific/statelandboard/disposal-wells (accessed April 14, 2020).

Deshmukh, A., Boo, C., Karanikola, V., Lin, S., Straub, A. P., Tong, T., Warsinger, D. M., Elimelech, M., 2018. Membrane distillation at the water-energy nexus: Limits, opportunities, and challenges. *Energ. Environ. Sci.* 11 (5), 1177-1196.

Dolan, F. C., Cath, T. Y., Hogue, T. S., 2018. Assessing the feasibility of using produced water for irrigation in Colorado. *Sci. Total Environ. 640-641*, 619-628.

Dow, N., Gray, S., Jun-de, L., Zhang, J., Ostarcevic, E., Liubinas, A., Atherton, P., Roeszler, G., Gibbs, A., Duke, M., 2016. Pilot trial of membrane distillation driven by low grade waste heat: Membrane fouling and energy assessment. *Desalination* 391, 30-42.

Duthu, R.C., Bradley, T.H., 2017. A road damage and life-cycle greenhouse gas comparison of trucking and pipeline water delivery systems for hydraulically fractured oil and gas field development in Colorado. *PLoS One* 12 (7), e0180587.

Ellsworth, W. L., 2013. Injection-induced earthquakes. *Science* 341 (6142), 1225942.

Esmaeilirad, N., Carlson, K., Omur Ozbek, P., 2015. Influence of softening sequencing on electrocoagulation treatment of produced water. *J. Hazard. Mater. 283*, 721-729.

ESRI. ArcGIS Desktop: Release 10.6. Environmental Systems Research Institute. 2018, Redlands, CA.

Gas Processors Suppliers Association. *Engineering Data Book, Twelfth Edition.* 2004, Tulsa, OK.

Gonzalez, D., Amigo, J., Suarez, F., 2017. Membrane distillation: Perspectives for sustainable and improved desalination. *Renew. Sustain. Energy Rev.* 80, 238-259.

Ground Water Protection Council. Produced Water Report: Regulations, Current Practices, and Research Needs. 2019, 310 p.

Jouhara, H., Khordehgah, N., Almahmoud, S., Delpech, B., Chauhan, A., Tassou, S. A., 2018. Waste heat recovery technologies and applications. *Therm. Sci. Eng. Progress 6,* 268-289.

Khayet, M. S., Matsuura, T., 2011. *Membrane Distillation: Principles and Applications*. Elsevier: Amsterdam.

Kim, J., Kim, J., Hong S., 2018. Recovery of water and minerals from shale gas produced water by membrane distillation crystallization. *Water Res.* 129, 447-459.

Kim, S., Omur-Ozbek, P., Dhanasekar, A., Prior, A., Carlson, K., 2016. Temporal analysis of flowback and produced water composition from shale oil and gas operations: Impact of frac fluid characteristics. *J. Petrol. Sci. Eng. 147*, 202-210.

Kondash, A., Albright, E., Vengosh, A., 2017. Quantity of flowback and produced waters from unconventional oil and gas exploration. *Sci. Total Environ.* 574 (2017), 314-321.

Kondash, A., Lauer, N., Vengosh, A., 2018. The intensification of the water footprint of hydraulic fracturing. *Sci. Adv.* 4: eaar5982.

Lawson, K. W., Lloyd, D. R., 1997. Membrane Distillation. *J. Membr. Sci. 124* (1), 1-25.

Lester, Y., Ferrer, I., Thurman, E. M., Sitterley, K. A., Korak, J. A., Aiken, G., Linden, K. G., 2015. Characterization of hydraulic fracturing flowback water in Colorado: Implications for water treatment. *Sci. Total Environ. 512-513*, 637-644.

Liden, T., Clark, B.G., Hildenbrand, Z.L., Schug, K.A. 2017. *Environmental Issues Concerning Hydraulic Fracturing, Volume 1.* Elsevier: Amsterdam.

Lokare, O. R., Tavakkoli, S., Rodriguez, G., Khanna, V., Vidic, R. D., 2017. Integrating membrane distillation with waste heat from natural gas compressor stations for produced water treatment in Pennsylvania. *Desalination* 413, 144-153.

McCurdy, R., 2011. Underground injection wells for produced water disposal. U.S. Environmental Protection Agency. https://www.epa.gov/sites/production/files/documents/21_McCurdy_-_UIC_Disposal_508.pdf (accessed Apr. 7, 2019).

Mohammad-Pajooh, E., Weichgrebe, D., Cuff, G., Tosarkani, B. M., Rosenwinkel, K. H., 2018. On-site treatment of flowback and produced water from shale gas hydraulic fracturing: A review and economic evaluation. *Chemosphere* 212, 898-914.

Neal, Z. personal communication, Expedition Water Services, December 4, 2019.

Qtaishat, M.R., Banat, F., 2013. Desalination by solar powered membrane distillation systems. *Desalination* 308, 186-197.

Ren, K., Tang, X., Jin, Y., Wang, J., Feng, C., Hook, M., 2019. Bi-objective optimization of water management in shale gas exploration with uncertainity: A case study from Sichuan, China. *Res. Conserv. Recycl.* 143 (2019), 226-235.

Robbins, C.A., Grauberger, B.M., Garland, S.D., Carlson, K.H., Lin, S., Bandhauer, T.M., Tong, T., 2020. On-site treatment capacity of membrane distillation powered by waste heat or natural gas for unconventional oil and gas wastewater in the Denver-Julesburg Basin. *Environ. Inter*. 145, 106142.

Rodriguez, R.S., Soeder, D.J., 2015. Evolving water management practices in shale oil & gas development. *J. Uncon. Oil Gas Resources* 10, 18-24.

Rosenblum, J. S., Sitterley, K. A., Thurman, E. M., Ferrer, I., Linden, K. G., 2016. Hydraulic fracturing wastewater treatment by coagulation-adsorption for removal of organic compounds and turbidity. *J.Environ.Chem. Eng. 4* (2), 1978-1984.

Runyon, L., 2018. Prices of key northern Colorado water supply reaches new peak. https://www.kunc.org/post/price-key-northern-colorado-water-supply-reaches-newpeak#stream/0 (accessed June 19, 2020).

Scanlon, B. R., Reedy, R.C., Male, F., Walsh, M., 2017. Water issues related to transitioning from conventional to unconventional oil production in the Permian Basin. *Environ. Sci. Technol.* 51, 10903-10912.

Scanlon, B. R., Weingarten, M. B., Murray, K. E., Reedy, R. C., 2018. Managing basin-scale fluid budgets to reduce injection - Induced seismicity from the recent U.S. shale oil revolution. *Seismol. Res. Let.* 90 (1), 171-182.

Schwantes, R., Chavan, K., Winter, D., Felsmann, C., Pfafferott, J., 2018. Techno-economic comparison of membrane distillation and MVC in a zero liquid discharge application. *Desalination* 428, 50-68.

Smith, J., 2019. Front range housing boom sends water prices soaring. https://www.watereducationcolorado.org/fresh-water-news/front-range-housing-boom-sends-water-prices-soaring/ (accessed June 19, 2020).

Summers, E.K., Arafat, H.A., Lienhard, J.H., 2012. Energy efficiency comparison of single-stage membrane distillation (MD) desalination cycles in different configurations. *Desalination* 290, 54-66.

Swaminathan, J., Chung, H.W., Warsinger, D.M., Al-Marzooqi, F.A., Arafat, H.A., Lienhard, J.H., 2011. Energy efficiency of permeate gap and novel conductive gap membrane distillation. *J. Membr. Sci.* 375 (1-2), 104-112.

Tavakkoli, S., Lokare, O. R., Vidic, R. D., Khanna, V., 2017. A techno-economic assessment of membrane distillation for treatment of Marcellus shale produced water. *Desalination* 416, 24-34.

Tavakkoli, S., Lokare, O., Vidic, R., Khanna, V., 2020. Shale gas produced water management using membrane distillation: An optimization-based approach. *Resources, Conservation & Recycling* 158 (2020), 104803.

Thiel, G., Tow, E., Banchik, L., Chung, H.W., Leinhard, J., 2015. Energy consumption in desalinating produced water from shale oil and gas extraction. *Desalination* 366, 94-112.

Tong, T., Carlson, K.H., Robbins, C.A., Zhang, Z., Du, X., 2019. Membrane-based treatment of shale oil and gas wastewater: The current state of knowledge. *Front. Environ. Sci. Eng.* 13 (4): 63.

Tong, T., Elimelech, M., 2016. The global rise of zero liquid discharge for wastewater management: Drivers, technologies, and future directions. *Environ. Sci. Technol. 50* (13), 6846-6855.

Ullah, R., Khraisheh, M., Esteves, R.J., McLeskey, J.T., Al-Ghouti, M., Gad-el-Hak, M., Vahedi Tafreshi, H., 2018. Energy efficiency of direct contact membrane distillation. *Desalination* 433, 56-67.

U.S. Census Bureau, 2019. 2018 Weld County, CO TIGER/Line Shapefile (All Roads). Data.gov web site.

U.S. Department of Energy, 2016. Combined Heat and Power Technology Fact Sheet Series. https://www.energy.gov/eere/amo/combined-heat-and-power-basics (accessed April 12, 2020).

U.S. Energy Information Administration. Top 100 U.S. Oil and Gas Fields. U.S. Department of Energy. 2015, Washington, D.C.

U.S. Energy Information Administration, 2019. U.S. Crude Oil and Natural Gas Proved Resources, Year-end 2018. https://www.eia.gov/naturalgas/crudeoilreserves/ (accessed August 25, 2020).

U.S. Environmental Protection Agency. Technical Development Document for the Effluent Limitations Guidelines and Standards for the Oil and Gas Extraction Point Source Category. 2016, Washington, D.C.: 182 p.

U.S. Environmental Protection Agency, 2019. UIC Injection Well Inventory. U.S. EPA web site. https://www.epa.gov/uic/uic-injection-well-inventory (accessed Feb. 23, 2020).

Weingarten, M., Ge, S., Godt, J.W., Bekins, B.A., Rubinstein, J.L., 2015. High-rate injection is associated with the increase in U.S. mid-continent seismicity. *Science* 3486 (6241), 1336-1340.

Weld County Public Works. https://www.weldgov.com/departments/public_works/traffic_signing. (accessed 4/15/2020).

Wenzlick, M., Siefert, N., 2020. Techno-economic analysis of converting oil & gas produced water into valuable resources. *Desalination* 481 (2020), 114381.

Zhang, Z., Du, X., Carlson, K., Robbins, C. Tong, T., 2019. Effective treatment of shale oil and gas produced water by membrane distillation coupled with precipitative softening and walnut shell filtration. *Desalination* 454, 82-90.

6.0 Comparison of Pretreatment and Membrane Modification to Mitigate Membrane Wetting in Unconventional Oil and Gas Wastewater Treatment via Membrane Distillation[4]

6.1 Introduction

With the recent rise in unconventional oil and gas (UOG) exploration in the U.S., wastewater management has become an important challenge due to the vast quantities of wastewater generated after hydraulic fracturing (HF) (Kondash et al., 2018; Scanlon et al., 2020a). Effective treatment of UOG wastewater for beneficial reuse has been proposed as an alternative to deep-well injection (DWI), the primary wastewater management approach in the UOG industry (Butkovskyi et al., 2017; Dolan et al., 2018; Jimenez et al., 2018; Ma et al., 2018; Chang et al., 2019a; Robbins et al., 2020; Scanlon et al., 2020b). Due to the complex composition of UOG wastewater that typically contains a high salinity along with various organic and inorganic contaminants (Kahrilas et al., 2016; Butkovskyi et al., 2017; Silva et al., 2017; Chang et al., 2019b; Sun et al., 2019), advanced treatment technologies are necessary for rendering beneficial reuse a viable option for UOG wastewater management.

Membrane distillation (MD), a hybrid thermal-membrane desalination process, has emerged as a suitable technology to treat complex and hypersaline wastewater such as UOG wastewater (Boo et al., 2016; Lokare et al., 2017; Tavakkoli et al., 2017; Tong et al., 2019a; Zhang et al., 2019; Robbins et al., 2020, Robbins et al., 2021). MD is driven by a vapor pressure difference generated between the warmer feedwater and cooler permeate stream (Lawson and Lloyd, 1997). MD tolerates the high salinity of UOG wastewater, which ranges between ~10,000-360,000 mg

[4] This chapter will be submitted for publication as a research article in *Journal of Membrane Science.*

L^{-1} total dissolved solids (TDS) (Chang et al., 2019b), thereby improving the viability of hypersaline UOG wastewater treatment (Shaffer et al., 2013; Xu et al., 2013). Also, the feedwater only needs to be heated to a moderate temperature (60-80°C), and thus MD has the potential to utilize low-grade thermal energy (e.g., waste heat) as an energy source to improve the economic viability of UOG wastewater treatment (Deshmukh et al., 2018; Robbins et al., 2020).

However, MD treatment of UOG wastewater is constrained by membrane pore wetting. Surfactant-induced wetting is a major concern in MD desalination (Wang and Lin, 2017; Horseman et al., 2021). Wetting caused by surfactants, which are typically low surface-tension amphiphilic molecules, occurs gradually due to the limited capability of the membrane pore surface for surfactant adsorption (Wang et al., 2018). When the pore surface is saturated, surfactant adsorption stops followed by an increase in surfactant concentration at the wetting frontier. The elevated concentration of surfactants lowers the surface tension of the feedwater and the liquid entry pressure (LEP) of membrane pores, resulting in membrane pore wetting (Wang et al., 2018; Horseman et al., 2021). In UOG wastewater, high levels of surfactants along with other low surface tension contaminants such as oil, grease, and organic solvents have been reported (Lester et al., 2015; Thurman et al., 2015; Boo et al., 2016; Butkovskyi et al., 2017). Surfactants are typical components of HF fluids to facilitate the recovery of shale oil and gas (Butkovskyi et al., 2017). Other factors that could constrain MD treatment of UOG wastewater include organic fouling and mineral scaling. Organic fouling occurs due to fouling agents (such as oil and hydrophobic organics commonly found in UOG wastewater) attaching to the membrane surface, blocking membrane pores, and subsequently causing a significant decrease in water vapor flux (Tijing et al., 2015; Warsinger et al., 2015; Wang and Lin, 2017; Horseman et

al., 2021). Mineral scaling, which takes place when barely soluble salts precipitate on the membrane surface (Tong et al., 2019b), is also problematic in MD due to the typically high salinity and scaling potential of MD feedwater (Warsinger et al., 2015; Horseman et al., 2019; Xiao et al., 2019; Yin et al., 2019).

Potential solutions to mitigate the effect of membrane fouling and wetting in MD treatment include effective pretreatment of the feedwater and the development of MD membranes with special wetting properties (Wang and Lin, 2017; Zhang et al., 2019; Horseman et al., 2020; Zhu et al., 2020). Common pretreatment methods in desalination processes include oxidation, filtration, flocculation, coagulation, and adsorption (Tijing et al., 2015; Warsinger et al., 2015; Rosenblum et al., 2016; Cho et al., 2018). Pretreatment in UOG wastewater treatment has primarily focused on the removal of organic contaminants and inorganic scalants commonly found in UOG wastewater (Cho et al., 2018; Sardari et al., 2018; Tong et al., 2019a; Zhang et al., 2019). By removing such contaminants known to induce deleterious effects on MD performance, effective treatment of UOG wastewater is feasible. On the other hand, omniphobic membranes resisting wetting to liquids of a wide range of surface tensions have been developed (Boo et al., 2016; Lee et al., 2016; Wang and Lin, 2017; Woo et al., 2017; Lu et al., 2018; Zheng et al., 2018; Deng et al., 2019; Li et al., 2019; Lu et al., 2019; Zhu et al., 2020). These membranes, which are achieved by creating a rough surface of reentrant structure and low solid surface energy (Boo et al., 2016; Wang and Lin, 2017; Horseman et al., 2021), are resistant to wetting by low surface tension feedwater, possessing the capability of preventing feed solutions containing surfactants (e.g., UOG wastewater) from penetrating into membrane pores

In the literature, synthetic feedwaters containing specific surfactants such as sodium dodecyl sulfate (SDS) have been primarily used to investigate membrane wetting in MD (Lee et al.,

2016; Chew et al., 2017; Eykens et al, 2017; Chen et al., 2018; Deng et al., 2018; Lu et al., 2018; Zheng et al., 2018). However, actual surfactant-laden UOG wastewater has been rarely tested in MD experiments. For a few studies that investigated UOG wastewater, the wastewater had been typically pre-filtered prior to MD treatment, likely reducing the wetting potential of the feedwater (Boo et al., 2016; Lokare et al., 2017; Kamaz et al., 2019). Although pretreatment is likely installed prior to UOG wastewater treatment in industrial applications, the use of raw UOG wastewater is valuable to understanding the wetting potential of UOG wastewater and selecting appropriate strategies for wetting mitigation. Further, a comparison between different wetting mitigation strategies such as pretreatment and altering membrane wettability has not been explored in the literature. Such a comparison will reveal the advantages and limitations of each strategy, providing insights for rational selection of wetting mitigation strategy for MD treatment of UOG wastewater in practice.

In this study, we compare the use of pretreatment and omniphobic membrane to mitigate membrane wetting in MD treatment of UOG wastewater collected from the Denver-Julesburg (DJ) Basin located in Colorado, U.S. A pretreatment train consisting of chemical coagulation and walnut shell filtration (WSF) was applied to primarily remove constituents such as surfactants that hinder MD performance for UOG wastewater treatment. Pretreatment was compared to the replacement of a commercial hydrophobic PVDF membrane with an omniphobic membrane. We performed direct contact MD (DCMD) experiments to evaluate the effectiveness of these two strategies in improving the resiliency and efficiency of MD treatment. To better understand the roles of pretreatment in mitigating membrane wetting, we applied ultrahigh pressure liquid chromatography (UHPLC) coupled with quadrupole time-of-flight mass spectrometry (LC/QToF/MS) to identify and semi-quantify surfactants present in the UOG wastewater before

and after pretreatment. In addition, the surfaces of membranes after MD treatment were characterized using scanning electron microscopy (SEM), energy-dispersive X-ray (EDX) spectroscopy, and attenuated total reflectance-Fourier transform infrared (ATR-FTIR) spectroscopy to provide additional insight on membrane fouling and scaling. Our results indicate that the pretreatment train was more effective in improving MD efficiency than using an omniphobic membrane, with the corresponding implications for wetting mitigation in practical industrial applications of MD (e.g., UOG wastewater treatment) discussed.

6.2 Materials and Methods

6.2.1 Materials, chemicals, and UOG wastewater

Microporous and hydrophobic flat sheet polyvinylidene fluoride (PVDF) membranes (HVHP, Durapore) with a nominal pore size of 0.22 μm (Millipore Sigma) were used in our DCMD experiments. The PVDF membranes were modified using the procedures employed by Yin et al. to fabricate an omniphobic membrane (Yin et al., 2020). Materials used for omniphobic membrane fabrication included (3-aminopropyl)triethoxysilane (APTES, ≥98%, Sigma-Aldrich), LUDOX HS-30 colloidal silica (15 nm, 30% suspension in water, Sigma-Aldrich), silica nanospheres (120 nm, NanoComposix), (Heptadecafluoro-1,1,2,2-tetrahydrodecyl)-triethoxysilane (17-FAS, Gelest Inc.), sodium hydroxide (NaOH, Fisher Chemical), and pure anhydrous ethanol (200 proof, Decon Laboratories). Incorporating materials with ultra-low surface energy (17-FAS) and a hierarchical texture provided by grafting two layers of silica nanoparticles into the membrane surface created an omniphobic membrane (referred to as PVDF-SiNP-FAS membrane) in this study (Yin et al., 2020). Further, ferric chloride ($FeCl_3$) was purchased from VWR BDH Chemicals and hydrochloric acid (HCl) was

supplied by Fisher Chemical. Eastwood Company provided the blast media walnut shells with an average grain size of 1.6 mm.

UOG wastewater was provided from a 500-gallon sample obtained from a 10-well unconventional pad from the Niobrara formation of the DJ Basin in Weld County, Colorado, which has been used in previous studies (Miller et al., 2019; Sedlacko et al., 2019; Miller et al., 2020). The well pad was in operation for more than three years. The wastewater samples were sent to an independent, certified laboratory (Technology Laboratory, Inc., Fort Collins, CO) to characterize key water quality parameters. The concentration of total dissolved solids (TDS) for the UOG wastewater was 34,358 mg L^{-1}, consistent with other studies using UOG wastewater from the DJ Basin (Esmaeiliard et al., 2015; Lester et al., 2015; Kim et al., 2016; Rosenblum et al. 2016; Bell et al., 2017; Zhang et al., 2019). Other water quality parameters measured included total volatile petroleum hydrocarbons (0.78 mg L^{-1}), oil and grease (37.6 mg L^{-1}), and total organic carbon (390 mg L^{-1}). The UOG wastewater was stored at 4°C at our laboratory located on the campus of Colorado State University in Fort Collins, Colorado until its use.

6.2.2 Coagulation and walnut shell filtration

The coagulant dose was optimized using a series of jar tests with doses from 25-150 mg L^{-1} of $FeCl_3$. The coagulation-flocculation experiments followed the procedures outlined by Rosenblum et al. (2016), using a six-paddle jar tester (Model 7700, Phipps & Bird, Richmond, VA). The jars were filled with 1 L of raw UOG wastewater at room temperature (22°C ± 2°C). After rapid mixing at 300 RPM for 1 minute, a three-stage tapered flocculation period was performed (55 RPM for 10 minutes, 35 RPM for 10 minutes, and 15 RPM for 10 minutes). After settling, the supernatants were immediately collected (two inches below the water surface) for turbidity analysis using a turbidimeter (Model 2100N, Hach, Loveland, CO). Turbidity removal

percentage ranged from ~90% (for 25 mg L^{-1} $FeCl_3$) to 98% (for 100 mg L^{-1} $FeCl_3$) (Table C1, Appendix C). Although higher $FeCl_3$ doses could achieve higher turbidity removal, a coagulant dose of 25 mg L^{-1} $FeCl_3$ was selected due to its satisfying turbidity removal percentage and to minimize the dose and corresponding cost of coagulant needed for coagulation.

A cylindrical filter column packed with walnut shells was used to treat the UOG wastewater after coagulation. The filter column (10.4 cm in diameter and 103.5 cm in height) was prepared in accordance with the procedures outlined in our previous study (Zhang et al., 2019). The filter column was cleaned with ~19 L of DI water before the start of any experiment. UOG wastewater pretreated with coagulation was filtered through one column at a constant flow rate of 4.5 L/min and filtered UOG wastewater was collected and stored at 4°C for the following DCMD experiments.

6.2.3 DCMD treatment of UOG wastewater

The UOG wastewater with and without pretreatment was treated in a laboratory-scale, DCMD unit equipped with an acrylic flow cell (effective membrane area of 20.02 cm^2). When the hydrophobic PVDF membrane was used, three different MD feedwaters were used: raw UOG wastewater without pretreatment, UOG wastewater pretreated by only coagulation, and UOG wastewater pretreated by coagulation and WSF. For comparison, the raw UOG wastewater without pretreatment was also treated in the same DCMD unit using the fabricated PVDF-SiNP-FAS membrane. The feed solution reservoir contained 1.5 L of wastewater, while deionized water (0.6 L) was added into the permeate reservoir. The temperatures of the feed solution and permeate were maintained at 60 °C and 20 °C, respectively. Two variable gear pumps (Cole-Parmer) were used to circulate the hot feed and cold permeate streams. Crossflow velocities of the feed and permeate streams were set at 9.6 cm s^{-1} (0.45 L min^{-1}) and 7.4 cm s^{-1} (0.35 L min^{-1}).

Continuous monitoring of the mass and conductivity of the permeate reservoir was performed to calculate the water vapor flux and assess membrane wetting. The DCMD experiments were terminated after at least 0.4 L of permeate was collected or membrane fouling caused significant water flux decline (flux reduction of at least 50%). The salt rejection rate was computed using Eq. 6-1 (Bush et al., 2016):

$$Salt\ rejection\ (\%) = \left(1 - \frac{V_{p2}\sigma_{p2} - V_{p1}\sigma_{p1}}{(V_{p2} - V_{p1})\sigma_f}\right) \times\ 100 \qquad (6-1)$$

where σ_f and σ_p are the conductivities of the feed and permeate solutions, and V_{d1} and V_{d2} represent the total volume of the permeate system at times 1 and 2 across a time interval. The membranes were collected and air dried after the DCMD experiments for future analyses.

6.2.4 Surfactant analysis in raw and pretreated UOG wastewater

The surfactants present in the raw and pretreated UOG wastewater were characterized in order to understand the mechanisms of pretreatment in mitigating membrane wetting in DCMD treatment. Prior to instrumental analysis, all samples were processed through a solid phase extraction (SPE) procedure to concentrate organics and remove salts. Samples (~50 mL) were first vacuum-filtered through 0.2 μm glass fiber filters, after which the pH of the samples was adjusted to 3 with HCl. For SPE, Supel Select HLB cartridges (200 mg / 6 mL, Supelco, Bellefonte, PA) were first conditioned with 10 mL each of methanol (Thermo Fisher Scientific), double-deionized water, and double-deionized water with pH of 3 in sequence. Samples were extracted under vacuum, after which the SPE columns were rinsed with 5% methanol before being dried for 15 min. The cartridges were eluted with 10 mL of methanol and immediately stored at -20 °C until analysis. Ultrahigh pressure liquid chromatography (UHPLC) with quadrupole time-of-flight mass spectrometry (LC/QToF/MS; Agilent 1100 series LC and Agilent G3250AA QToF) was used following previous methods (Thurman et al., 2014; McLaughlin et

al., 2016). The Agilent MassHunter Qualitative Analysis 10.0 software was used for LC/QToF/MS data analysis; molecular features were extracted from the mass spectra using an abundance cutoff of 10× the noise level. The samples were clearly dominated by surfactant series, and as such we focused solely on the identification of these species. For the identification of surfactant species using the accurate masses from the LC/QToF/MS analysis, we followed the procedures outlined by Thurman et al. (Thurman et al., 2014). We created an in-house database of known polyethoxylated surfactants, including polyethylene glycols (PEGs), alkyl ethoxylates (AEOs), and nonylphenol polyethoxylates (NPEOs), in addition to polypropylene glycols (PPGs) that have been previously reported for UOG wastewaters (Thurman et al., 2014; McLaughlin et al., 2016; Hanson et al., 2019). We added to this database surfactant series identified in the samples (the most predominant series present in the samples) for which chemical formulas were assigned based on accurate masses. For positive surfactant identification, species had to be visibly within a series in the chromatogram following the correct elution order, have the same computed Kendrick mass defect (KMD) for a given surfactant series, and have a mass error of less than 5 ppm compared to our surfactant database. To evaluate the relative changes in the abundance of surfactant species across samples, the peak areas of the treated samples were normalized to the peak areas of the untreated water. A cutoff of 95% was set for A/A_0 (peak area of surfactant after full pretreatment / peak area of surfactant in raw UOG wastewater) and surfactant species that fell below the cutoff were included in the surfactant species decreased by full pretreatment.

6.2.5 Membrane characterization

The surface morphologies of the membranes after DCMD experiments were observed by SEM (JEOL JSL-6500F). The membranes were dried and coated with a thin layer of gold using a

sputter coater prior to imaging (Denton Desk IV, Denton Vacuum). In addition to SEM, EDX (JEOL JSM-6500F) and ATR-FTIR (Nicolet iS-50, Thermo Fisher Scientific) spectroscopy were performed to further investigate the chemical compositions and functionality of the foulant layers formed on the membrane surfaces.

6.3. Results and Discussion

6.3.1 Membrane distillation performance in the treatment of UOG wastewater

The UOG wastewater from DJ Basin was first treated by DCMD with and without pretreatment using a commercial available PVDF membrane. Significant membrane wetting was observed when no pretreatment of UOG wastewater was performed (Figure 6-1A). The permeate conductivity rapidly increased from ~20 μS cm^{-1} to more than 7,000 μS cm^{-1}, accompanied by an increase of water vapor flux by 75%. The permeate conductivity slowly increased by ~1-2 μS cm^{-1} per minute until ~100 mL of permeate was collected (~3.5 hours of desalination), and then began steadily increasing at a rate of greater than 5 μS cm^{-1} per minute afterwards. Correspondingly, the salt rejection rate of MD desalination remained above 95% for the first 100 mL of permeate, and then steadily declined to 55% at the conclusion of the experiments (with cumulative permeate of ~400 mL). This is consistent with dynamic surfactant-induced wetting as described by Wang et al. (Wang et al., 2018), in which wetting did not occur instantaneously. The wetting kinetics is controlled by the rate at which the membrane pore surface is saturated by the adsorbed surfactants, which is regulated by the rate of surfactant transport to the wetting frontier via convection (Wang et al., 2018).

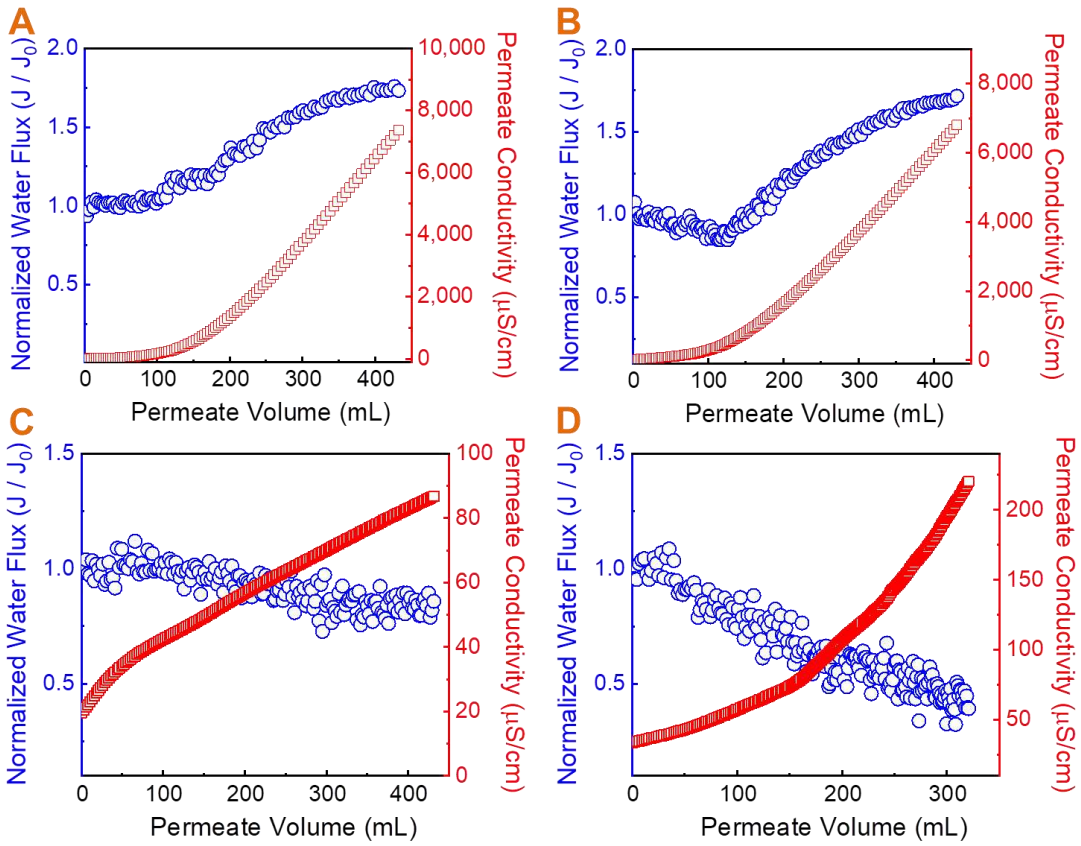

Figure 6-1. MD performance for the treatment of UOG wastewater from DJ Basin using (A) PVDF membrane without any pretreatment, (B) PVDF membrane with coagulation as pretreatment, (C) PVDF membrane with coagulation and walnut shell filtration as pretreatment, and (D) PVDF-SiNP-FAS membrane without any pretreatment. The temperatures of the feed and permeate solutions were maintained at 60°C and 20°C, respectively. The crossflow velocities of feed and permeate solutions were 9.6 and 7.4 cm s^{-1}, respectively. The initial water vapor fluxes of Figures 1A-D were 18.9 L m^{-2} h^{-1}, 18.8 L m^{-2} h^{-1}, 18.6 L m^{-2} h^{-1}, and 15.0 L m^{-2} h^{-1}, respectively. These flux values are used to normalize the fluxes in all figures.

Pretreatment via coagulation with 25 mg L^{-1} of $FeCl_3$ was applied to investigate whether coagulation only could mitigate membrane wetting in MD treatment of UOG wastewater. Coagulation or electrocoagulation processes have been used to remove both organic and inorganic constituents from UOG wastewater (Esmaeilirad et al., 2015; Lobo et al., 2016; Rosenblum et al., 2016; Zhai et al., 2017; Kong et al., 2017; Sardari et al., 2018; Kamaz et al., 2019). However, significant membrane wetting occurred with pretreatment of UOG wastewater via coagulation, resulting in a remarkable increase of permeate conductivity to 6,800 μS cm^{-1}

when 400 mL of permeate was collected (12 hours of MD desalination, Figure 6-1B). Correspondingly, the salt rejection rate decreased to 59% and the normalized water flux increased to ~1.7 at the conclusion of the MD desalination, indicating that saline UOG water had permeated through the hydrophobic membrane and contaminated the product water. Compared to MD treatment without any pretreatment, negligible improvement was observed when coagulation was applied as the standalone pretreatment approach.

We further combined coagulation and walnut shell filtration (WSF) as pretreatment. Adsorption processes have been previously proposed as pretreatment methods for UOG wastewater (Rosenblum et al., 2016; Zhang et al., 2019), but they have not been investigated in regards to their effects in controlling membrane wetting in MD desalination. As shown in Figure 6-1C, MD performance was greatly improved with pretreatment via coagulation and WSF, after which the permeate conductivity increased to only ~85 μS cm^{-1} when a comparable amount of permeate was collected (16 hours of MD desalination). Also, the salt rejection rate was maintained at above 99.5% during the experiment. Therefore, the combination of coagulation and WSF successfully mitigated membrane wetting during MD treatment of UOG wastewater. The water vapor flux of MD decreased by ~20% at the conclusion of the experiments, probably caused by membrane fouling and scaling due to the complex composition of UOG wastewater.

In addition to testing the efficiencies of pretreatment in reducing membrane wetting using hydrophobic membranes, we also investigated the performance of an omniphobic membrane in MD treatment of UOG wastewater. Due to its low surface energy and a robust reentrant structure created by the grafting of nanoparticles to the membrane surface, omniphobic membranes have shown high repellency to both high and low surface tension liquids, providing the ability to mitigate surfactant-induced wetting (Lee et al., 2016; Deng et al., 2018; Lu et al., 2018; Zheng et

al., 2018; Li et al., 2019; Lu et al., 2019). The omniphobicity of the PVDF-SiNP-FAS membrane used in this study is shown in Figure C1 of Appendix C. Compared to the hydrophobic membrane, PVDF-SiNP-FAS membrane resulted in improved desalination performance when no pretreatment was applied (Figures 6-1A and 6-1D). The permeate conductivity increased to ~250 μS cm^{-1} for 18 hours, when ~300 mL of permeate was collected. The salt rejection rate stayed above 98.6% during the experiment. Therefore, the use of an omniphobic membrane significantly reduced membrane wetting despite the high wetting potential of raw UOG wastewater. However, its efficiency in wetting mitigation was lower compared to pretreatment using coagulation coupled with WSF. Further, the water vapor flux of MD decreased by more than 50% at the conclusion of the experiments, indicating that significant membrane fouling/scaling occurred. As a result, only 300 mL of permeate was collected from MD treatment, which was less and took a longer time (~18 hours) than that with a hydrophobic PVDF membrane and full pretreatment (~400 mL for ~16 hours). The fouling behavior observed for the PVDF-SiNP-FAS membrane was likely attributable to the enhanced hydrophobic-hydrophobic interaction between membrane surface and foulants, due to its low surface energy (Wang and Lin, 2017; Boo et al., 2018). We also noticed that the PVDF-SiNP-FAS membrane was not fully able to resist membrane wetting, despite its anticipated wetting resistance to prevent saline feedwater from contaminating the permeate stream. The increase of permeate conductivity observed in Figure 6-1D could be due to intrinsic membrane defects (Boo et al., 2016; Du et al., 2018).

6.3.2 Surfactant analysis in raw and pretreated UOG wastewater

The most likely cause of membrane wetting observed during MD treatment of UOG wastewater was surfactants. UOG wastewater is well-known to contain surfactants (Thurman et

al., 2014; Lester et al., 2015; Chai et al., 2019), which are typical wetting agents for MD desalination (Chew et al., 2017; Eykens et al., 2017; Rezaei et al., 2018). Thus, LC/QToF/MS was applied to identify surfactant species in our various types of feedwater (i.e., raw UOG wastewater, UOG wastewater pretreated with coagulation, and UOG wastewater pretreated with coagulation and WSF) and quantify their relative abundance. In the raw UOG wastewater, 192 surfactants were identified with unique putative formulas (Tables C2-C9, Appendix C). The total ion chromatogram (TIC, Figure 6-2A) shows the chromatographic resolution of the three types of feedwater analyzed wherein four classes of surfactant species commonly found in UOG wastewater were identified: polyethylene glycols (PEGs), polypropylene glycols (PPGs), alkyl ethoxylates (AEOs), and nonylphenol ethoxylates (NPEOs). As shown in Figure 6-2A, general retention time ranges for each surfactant class is provided where the majority of surfactants of each class fall. It should be noted that some surfactants from each class may have a retention time that is outside the general ranges provided.

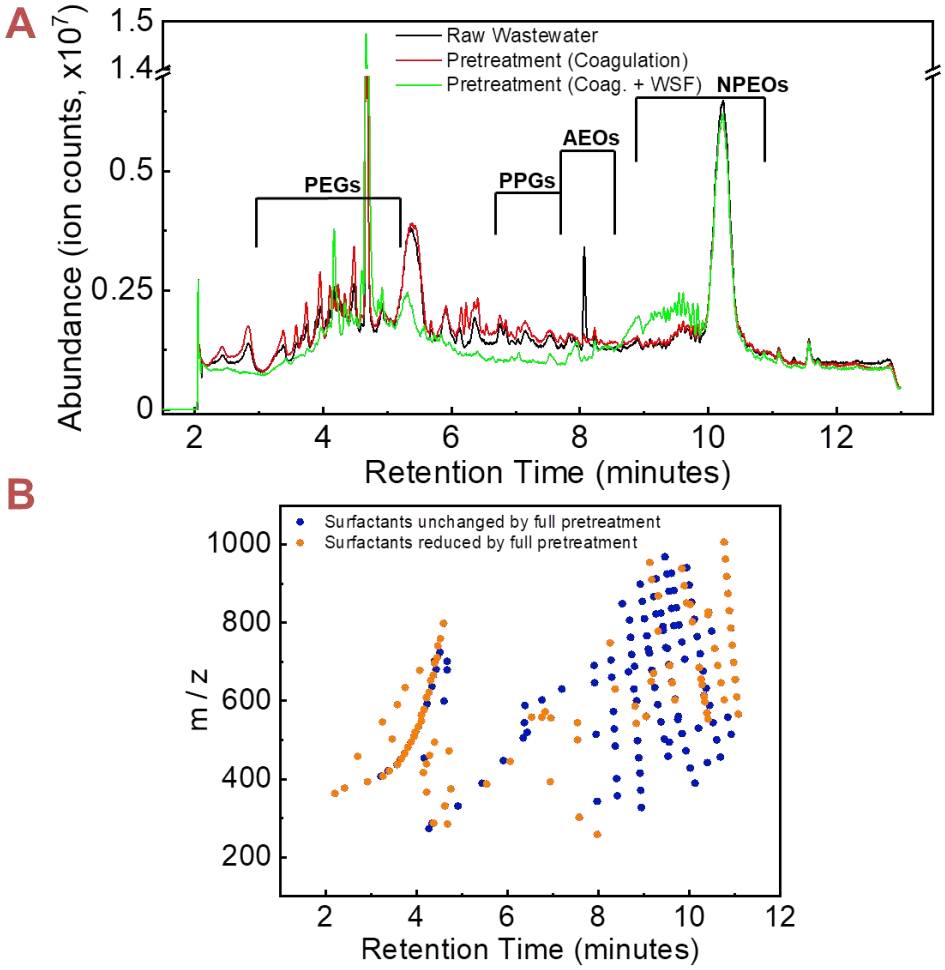

Figure 6-2. (A) Total ion chromatogram (TIC) for raw UOG wastewater, UOG wastewater pretreated with coagulation, and UOG wastewater pretreated with coagulation and WSF. The relative abundance of positively identified polyethoxylated surfactants, including polyethylene glycols (PEGs), alkyl ethoxylates (AEOs), and nonylphenol polyethoxylates (NPEOs, and polypropylene glycols (PPGs), are shown. (B) Identification of surfactant species unchanged by full pretreatment (coagulation and WSF) and surfactant species decreased due to full pretreatment. The surfactant species are identified by their mass to charge ratio (m / z).

For the PEG (retention time of ~3 to 5 minutes) and PPG (retention time of ~6.7 to 7.5 minutes) classes, the relative abundance of surfactant species generally decreased with pretreatment via coagulation and WSF (Figure 6-2A). Along with the efficiency of coagulation combined with WSF in mitigating membrane wetting (Figure 6-1C), this result suggests that these surfactants might contribute to membrane wetting that occurred in MD treatment of UOG wastewater. For the AEO range (retention time of ~7.5 to 8.3 minutes), the relative abundance

seems to have a slight decrease (Figure 6-2A). For the NPEO range (retention time of ~8.9 to 11 minutes), the relative abundance of some identified species appeared to increase with full pretreatment using coagulation and WSF (Figure 6-2A). Additionally, we identified a compound within the PEG range based on accurate mass, namely, $C_{23}H_{48}O_8$ (retention time of 4.76 minutes) that also appeared to increase in relative abundance (Figure 6-2A). A possible explanation is the leaching of organic matter from the walnut shell media that could occur after initially starting the column operation (Rodriguez et al., 2020). The molecular structure of the organic matter could result in the same behaviors in LC/QToF/MS analysis to those of the molecules identified in our study. While some surfactant species appeared to be enriched in the fully pretreated sample, we note that the pretreatment contributed to an overall reduction in surfactants, resulting in a less complex matrix for the treated samples with respect to LC/QToF/MS analysis. Consequently, the ionization efficiencies for individual surfactant species may have been affected, thus any apparent enrichment in individual species may be artefactual. Nevertheless, the abundance increase of some surfactants after full pretreatment did not inhibit wetting mitigation, indicating that these species were unlikely to cause pore wetting in MD treatment.

In order to better understand the effect of pretreatment on wetting potential of UOG wastewater, a more detailed comparison was made between the abundance of surfactant species with and without full pretreatment (i.e., coagulation and WSF) (Figure 6-2B). For the surfactant species whose abundance is reduced, their peak areas after pretreatment need to be 95% or less than their corresponding peak areas for the raw UOG wastewater. The majority of surfactants within the PEG range or identified as PEGs (37 out of 45) were reduced after full pretreatment (Figure 6-2C; Tables C2 and C3, Appendix C). Such surfactants are considered more hydrophilic than the other surfactant classes, and they are removed most effectively by the pretreatment. For

surfactants identified within the general PPG range or identified as PPGs, 8 out of 19 were reduced by pretreatment (Figure 6-2C; Tables C4 and C5, Appendix C). The majority of surfactants within the general AEO range or identified as AEOs (17 out of 22) were unchanged or enriched by pretreatment (Figure 6-2C; Tables C6 and C7, Appendix C). PPGs and AEOs were the two smallest classes by number. Surfactants within the NPEO range or identified as NPEOs were the most abundant by number of species (106) with 41 surfactants being reduced by pretreatment (Figure 6-2C; Tables C8 and C9, Appendix C). These surfactants are considered more hydrophobic than the other surfactant classes. We cannot accurately pinpoint the relative contributions of specific surfactant species to the mitigation of membrane wetting from full pretreatment in this study. However, surfactants whose abundance was reduced were mainly identified within the PEG and NPEO classes, and thus their reduction by pretreatment might contribute greatly to wetting mitigation, although the contribution of the PPG and AEO classes could not be excluded. Future research is warranted to fully reveal the contributions of specific surfactants identified in our study to membrane wetting during MD treatment.

6.3.3 Membrane characterization after MD treatment of UOG wastewater

To investigate membrane fouling and scaling during MD treatment of UOG wastewater, we characterized the membrane surface under different scenarios (hydrophobic PVDF membrane and PVDF-SiNP-FAS membrane with raw UOG wastewater; PVDF membrane with fully pretreated UOG wastewater) using SEM, EDX, and ATR-FTIR. As shown in Figure 6-3A, a thick foulant layer was observed to fully cover the PVDF membrane surface after MD treatment of raw UOG wastewater. However, despite the formation of this foulant layer, the water vapor flux increased with time due to membrane wetting (Figure 6-1A). The permeation of feedwater into membrane pores outweighed the resistance of water transport due to the presence of foulant

layers. Also, the PVDF-SiNP-FAS membrane after treatment of UOG wastewater appears to have particles with sizes in the range of 50-300 nm deposited on the membrane surface (Figure 6-3B). For the PVDF membrane after MD treatment of fully pretreated UOG wastewater, no obvious foulant layers or particles were observed on the membrane surface (Figure 6-3C).

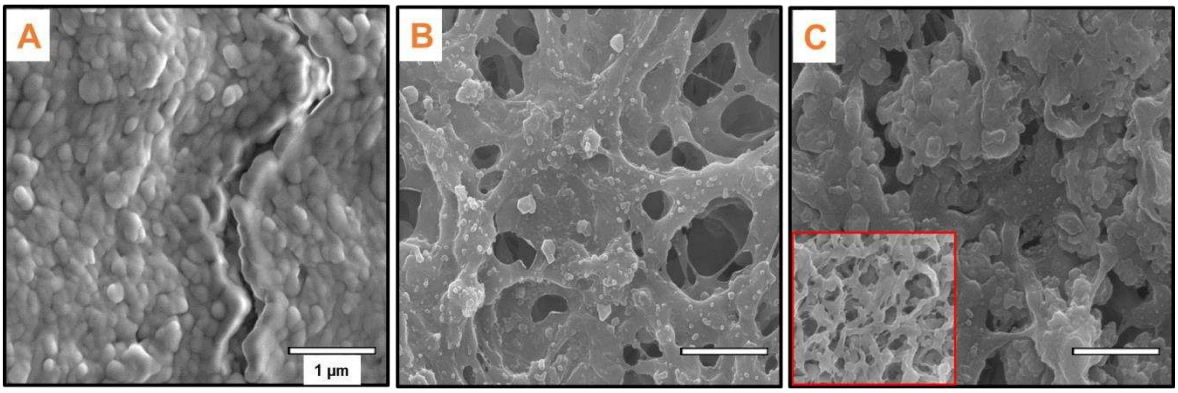

Figure 6-3. Top view SEM micrographs (with magnification of 10,000X) of a (A) PVDF membrane after MD treatment of raw wastewater, (B) PVDF-SiNP-FAS membrane after MD treatment of raw UOG wastewater, and (C) PVDF membrane after MD treatment of UOG wastewater pretreated by coagulation and walnut shell filtration. The inset of (C) shows a SEM micrograph of a pristine PVDF membrane for reference.

SEM-EDX spectroscopy was utilized to analyze the chemical compositions of foulant layers. The EDX spectra and elemental analysis for the PVDF membrane treating raw UOG wastewater confirms the presence of elements C, Si, and O (Figures 6-4A and B). PVDF has theoretically 38% of C and 59% of F according to its molecular structure. The much higher percentage of C (89.2%) on the PVDF membrane treating raw UOG wastewater probably originated from a layer of organic foulants. It is worth mentioning that element F was not detected, indicating that the thickness of foulant layer was higher than the penetration depth of the evanescent wave in FTIR (typically in the magnitude of 100 nm) (Tang et al., 2009). Also, the presence of Si and O suggests that silica scaling occurred during MD treatment, consistent with our previous study of UOG wastewater treatment (Du et al., 2018). Similarly, the elements C, Si, and O were detected for the PVDF-SiNP-FAS membrane treating raw UOG wastewater,

despite their lower relative abundance compared to PVDF membrane treating the same feedwater (Figures 6-4C and D). Along with the result that element F was detected on this membrane, the foulant and scalant layer covered the membrane surface to a less extent, which was reflected by Figures 6-3A and 6-3B. For the PVDF membrane treating fully pretreated UOG wastewater (Figures 6-4E and 6-4F), the element weights of C and F reached 52.8% and 35.8%, respectively, both of which were highest among the investigated membranes. Meanwhile, no Si element was detected on the membrane surface. Thus, organic fouling and silica scaling were significantly mitigated on this membrane, despite the formation of some NaCl and KCl scales. Therefore, both pretreatment and the use of omniphobic membrane were able to mitigate organic fouling and silica scaling, but pretreatment exhibited a better efficiency of fouling and scaling mitigation. This result was consistent with the MD performance as shown in Figure 6-1.

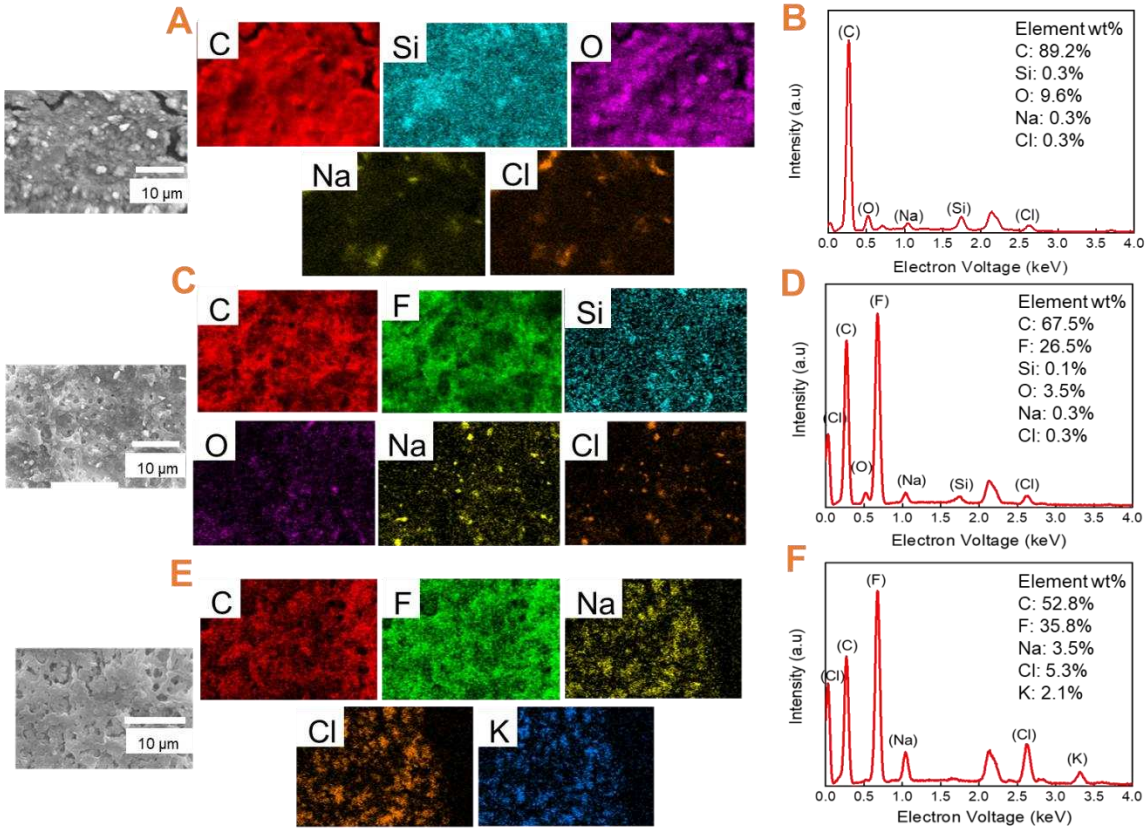

Figure 6-4. (A-B) SEM-EDX elemental analysis and EDX spectra for PVDF membrane after DCMD treatment of raw wastewater, (C-D) PVDF-SiNP-FAS membrane after DCMD treatment of raw UOG wastewater, and (E-F) PVDF membrane after DCMD treatment of UOG wastewater pretreated by coagulation and walnut shell filtration.

ATR-FTIR was used to characterize the functionality of organic foulants on the membrane surfaces (Figure 6-5). Using a pristine PVDF membrane as reference, three foulant peaks were identified on the PVDF membrane that treated raw UOG wastewater (Figure 6-5A). These peaks were located at 1538 cm^{-1}, 1645 cm^{-1}, and 3175-3500 cm^{-1}. The peak at 1538 cm^{-1} was attributed to amide II bands (Belfer et al., 2000) and representative of proteins (Zularisam et al., 2006). The peak at 1645 cm^{-1} was attributed to amide I bands (Belfer et al., 2000) and representative of humic substances (Zularisam et al., 2006). The peak between 3175 and 3500 cm^{-1} is attributed to the stretching vibration of O-H (Li et al., 2010; Lu et al., 2017) and also representative of humic

substances (Zularisam et al., 2006). Proteins and humic substances are commonly found in UOG wastewater (Alzahrani et al., 2013; Hickenbottom et al., 2013; Bell et al., 2017; Du et al., 2018).

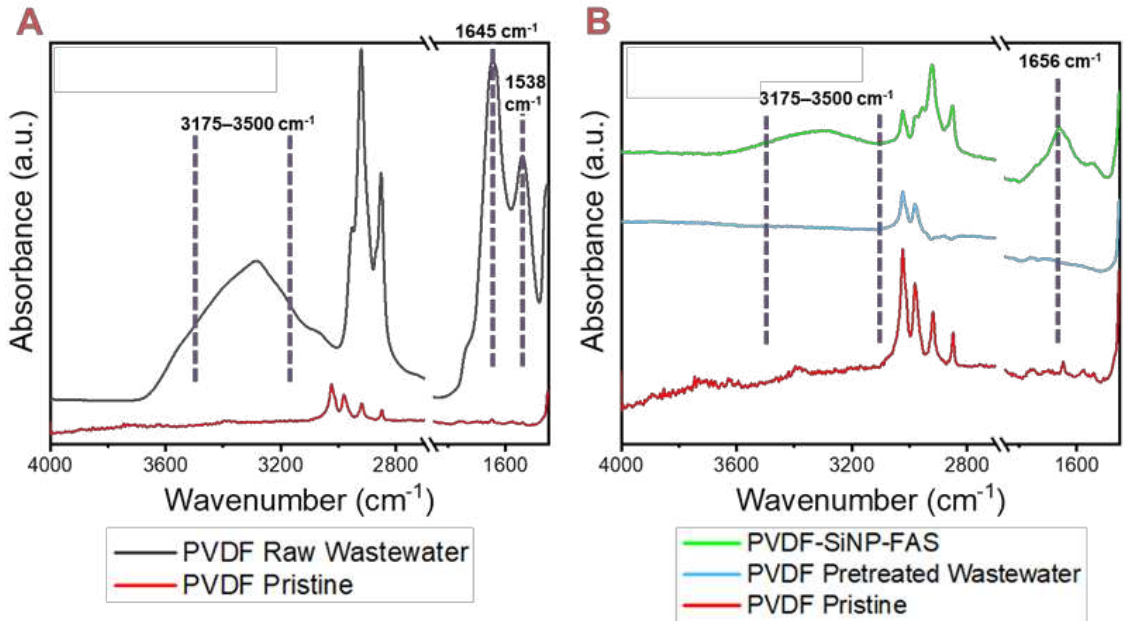

Figure 6-5. (A) ATR-FTIR spectra for pristine PVDF membrane and PVDF membrane treating raw wastewater and (B) for pristine PVDF membrane, PVDF membrane treating fully pretreated UOG wastewater, and PVDF-SiNP-FAS membrane treating raw UOG wastewater. Peaks due to organic fouling are labeled.

The ATR-FTIR spectra of PVDF-SiNP-FAS membrane and the PVDF membrane that treated fully pretreated wastewater were also compared to that of the pristine PVDF membrane (Figure 6-5B). Two foulant peaks were identified for the PVDF-SiNP-FAS membrane that treated raw UOG wastewater. These peaks were located at 1656 cm^{-1} and 3175-3500 cm^{-1}, which were attributed to amide I bands and the stretching vibration of O-H, respectively (Belfer et al., 2000; Li et al., 2010; Lu et al., 2017). The foulants represented by these peaks were representative of humic substances (Zularisam et al., 2006). For the ATR-FTIR spectrum of PVDF membrane after treating fully pretreated UOG wastewater, the peaks discussed above were much smaller or negligible compared to those of the same membrane after treating raw

UOG wastewater, indicating that fewer organic foulants were present on the PVDF membrane surface.

6.4 Implications for UOG Wastewater Treatment

Our study shows that both pretreatment with coagulation and WSF and the use of an omniphobic membrane were able to mitigate membrane wetting during MD treatment of UOG wastewater. However, the overall MD treatment performance with an omniphobic membrane was hindered by significant flux decline due to membrane fouling and scaling. Therefore, at least in our study, pretreatment seemed to outperform omniphobic membrane for the treatment of UOG wastewater with high wetting and fouling/scaling potential. In practical MD applications, both strategies can be considered to improve MD performance. In this section, we discuss the benefits and limitations of each strategy in order to inspire future studies for achieving resilient and cost-effective MD system for UOG wastewater treatment.

When evaluating the pretreatment mitigation strategy of coagulation and adsorption, a wealth of information and data exist from their previous usage in water and wastewater treatment. A chemical coagulation method, such as using $FeCl_3$ as a coagulant, is very common in classical wastewater and industrial treatment processes and consistent in reducing suspended solids and colloidal particles (Alexander et al., 2012; Bratby, 2016). Coagulation is recognized as one of the effective and low-cost pretreatment methods for membrane separation processes (Tijing et al., 2015). The costs associated with coagulation are primarily chemical and sludge disposal costs. For sludge disposal, a determination will need to be made on whether the sludge is a hazardous solid waste which increases its cost. Also, dewatering and transportation to the appropriate landfill incurs additional costs. Adsorption processes, such as activated carbon or WSF, are also commonly used in the treatment of municipal and industrial wastewater due to the

inherent ability of the processes to adsorb a vast array of organic contaminants (Srinivasan and Viraraghavan, 2008; Zhang et al., 2013). An advantage of using walnut shell media is its cost-effectiveness and outstanding durability (Jahanban-Esfahlan et al., 2020). Walnut shell media is considered an agricultural waste material with no commercial value, thus, making it economically advantageous (Jahanban-Esfahlan et al., 2020). Cost is dependent on the frequency of media replacement and would need to be further quantified for its use in UOG wastewater pretreatment. Due to their common use in wastewater treatment, coagulation-adsorption processes pose a low risk to the environment and human health. Precautions need to be taken in the handling of chemical coagulants such as $FeCl_3$ due to its corrosive nature. The risk of coagulation-adsorption in UOG wastewater pretreatment needs to be characterized. Also, coagulation-adsorption pretreatment needs to be incorporated into a thorough techno-economic analysis to fully quantify its costs.

For the fabrication of omniphobic membranes, long-chain per- and polyfluoroalkyl substance (PFASs) are typically used to lower the membrane surface energy (Boo et al., 2016; Lee et al., 2016; Wang and Lin, 2017; Chen et al., 2018; Deng et al., 2018; Du et al., 2018; Lu et al., 2018; Zheng et al., 2018; Li et al., 2019; Yin et al., 2020). PFASs are costly to produce (e.g., fluorosurfactants are 100-1,000 times more expensive than conventional hydrocarbon surfactants per unit volume) (Thomas, 2006; Gluge et al., 2020). For omniphobic membranes to be applied on a large industrial scale, such as for MD treatment of UOG wastewater, cost-effective fabrication strategies need to be developed (Lu et al., 2019).

Further, PFASs are very persistent in the environment due to their C-F bonds. The perfluorocarbon components in PFASs are both hydrophobic and oleophobic, making them surface protectors (Buck et al., 2012; Gluge et al., 2020). This feature makes PFASs very

attractive in the development of omniphobic membranes to resist wetting in MD. However, evidence that exposure to PFASs can lead to adverse human health effects have been reported (USEPA, 2021). The United States Environmental Protection Agency (USEPA) instituted an action plan in addressing challenges with PFASs with a goal being to minimize their use when possible. Further, some fabrication strategies require harsh reaction conditions and hazardous reagents such as concentrated alkaline solutions at high temperatures (Lu et al., 2019). At the manufacturing scale, the risk associated with the fabrication approach will be magnified. If fabricating omniphobic membranes for large scale applications, a thorough human health risk assessment needs to be completed to mitigate risk to humans. The drawbacks associated with using PFASs and harsh conditions for omniphobic membrane fabrication need to be considered when selecting a wetting mitigation strategy and could hinder the future viability of omniphobic membrane manufacturing for MD treatment.

6.5 Conclusions

In this study, two strategies to mitigate surfactant-induced wetting (i.e., pretreatment with coagulation and WSF and the use of an omniphobic membrane) in MD treatment of UOG wastewater were compared. Both strategies were able to mitigate membrane wetting, but fouling and scaling caused more flux decline in MD treatment with an omniphobic membrane. LC/QToF/MS analysis identified 192 surfactants in the raw UOG wastewater, which belong to four known classes (PEGs, PPGs, AEOs, and NPEOs). Pretreatment was shown to be effective in reducing PEGs (37 of 45 PEGs reduced) and NPEOs (41 of 106 NPEOs reduced). Further, SEM-EDX and ATR-FTIR analyses showed reduced foulant and scalant layers on the PVDF membrane after full pretreatment or the omniphobic membrane, compared to those on the PVDF membrane after the treatment of raw UOG wastewater. However, a higher extent of fouling and

scaling was found on the omniphobic membrane. Our study provides a comparative evaluation of strategies that could be applied to wetting mitigation, and identified surfactants present in UOG wastewater as potential wetting agents that linked to MD performance. The findings of this study provide valuable insights that have the potential to guide future research on better understanding membrane wetting in practical MD applications to industrial wastewater treatment and creating more effective strategies of wetting mitigation.

References

Alexander, J.T., Hai, F.I., Al-Aboud, T.M., 2012. Chemical coagulation-based processes for trace organic contaminant removal: Current state and future potential. *J. Environ. Manage.* 111, 195-207.

Alzahrani, S., Mohammad, A.W., Hilal, N., Abdullah, P., Jaafar, O., 2013. Identification of foulants, fouling mechanisms and cleaning efficiency for NF and RO treatment of produced water. *Sep. Purif. Technol.* 118, 324-341.

Bai, B., Carlson, K., Prior, A., Douglas, C., 2015. Sources of variability in flowback and produced water volumes from shale oil and gas wells. *J. Uncon. Oil Gas Resources 12*, 1-5.

Belfer, S., Fainchtain, R., Purinson, Y., Kedem, O., 2000. Surface characterization by FTIR-ATR spectroscopy of polyethersulfone membranes-unmodified, modified and protein fouled. *J. Membr. Sci.* 172, 113-124.

Bell, E. A., Poynor, T. E., Newhart, K. B., Regnery, J., Coday, B. D., Cath, T. Y., 2017. Produced water treatment using forward osmosis membranes: Evaluation of extended-time performance and fouling. *J. Membr. Sci. 525*, 77-88.

Boo, C., Lee, J., Elimelech, M., 2016. Omniphobic polyvinylidene fluoride (PVDF) membrane for desalination of shale gas produced water by membrane distillation. *Environ. Sci. Technol.* 50 (22), 12275-12282.

Boo, C., Hong, S., Elimelech, M., 2018. Relating organic fouling in membrane distillation to intermolecular adhesion forces and interfacial surface energies. *Environ. Sci. Technol.* 52 (24), 14198-14207.

Bratby, J., 2016. *Coagulation and Flocculation in Water and Wastewater Treatment*. Third Edition, IWA Publishing: London.

Buck, R.C., Franklin, J., Berger, U., Conder, J.M., Cousins, I.T., Voogt, P.D.J., Allan, A.K., Kurunthachalam, M., van Leeuwen, S.A., Stefan, P.J.J., 2011. Perfluoroalkyl and polyfluoroalkyl substances in the environment: Terminology, classification, and origins. *Integr. Environ. Assess. Manage.* 7, 513-541.

Bush, J.A., Vanneste, J., Cath, T.Y., 2016. Membrane distillation for concentration of hypersaline brines from the Great Salt Lake: Effects of scaling and fouling on performance, efficiency, and salt rejection. *Sep. Purif. Technol.* 170, 78-91.

Butkovskyi, A., Bruning, H., Kools, S.A.E., Rijnaarts, H.H.M., Van Wezel, A.P., 2017. Organic pollutants in shale gas flowback and produced waters: Identification, potential ecological impact, and implications for treatment strategies. *Environ. Sci. Technol.* 51 (9), 4740-4754.

Chai, Y., Li, X., Jing, D., 2019. Application of surfactants in hydraulic fracturing for enhanced oil-gas recovery. *J. Oil Res.* 5 (1), 161.

Chang, H., Liu, B., Yang, B., Yang, X., Guo, C., He, Q., Liang, S., Chen, S., Yang, P., 2019a. An integrated coagulation-ultrafiltration-nanofiltration process for internal reuse of shale gas flowback and produced water. *Sep. Purification Tech.* 211, 310-321.

Chang, H., Li., T., Liu, B., Vidic, R.D., Elimelech, M., Crittenden, J.C., 2019b. Potential and implemented membrane-based technologies for the treatment and reuse of flowback and produced water from shale gas and oil plays: A review. *Desalination* 455, 34-57.

Chen, L.H., Huang, A., Chen, Y.R., Chen, C.H., Hsu, C.C., Tsai, F.Y., Tung, K.L., 2018. Omniphobic membrane for direct contact membrane distillation: Effective deposition of zinc oxide nanoparticles. *Desalination* 428, 255-263.

Chew, N.G.P., Zhao, S., Loh, C.H., Permogorov, N., Wang, R., 2017. Surfactant effects on water recovery from produced water via direct-contact membrane distillation. *J. Membr. Sci.* 528, 126-134.

Cho, H., Choi, Y., Lee. S., 2018. Effect of pretreatment and operating conditions of membrane distillation for the treatment of shale gas wastewater. *Desalination* 437, 195-209.

Deng, L., Ye, H., Li, X., Li, P., Zhang, J., Wang, X., Zhu, M., Hsiao, B.S., 2019, Self-roughened omniphobic coatings on nanofibrous membrane for membrane distillation. *Sep. Purif. Technol.* 206, 14-25.

Deshmukh, A., Boo, C., Karanikola, V., Lin, S.H., Straub, A.P., Tong, T.Z., Warsinger, D.M., Elimelech, M., 2018. Membrane distillation at the water-energy nexus: Limits, opportunities, and challenges. *Energy Environ. Sci.* 11, 1177-1196.

Dolan, F.C., Cath, T.Y., Hogue, T.S., 2018. Assessing the feasibility of using produced water for irrigation in Colorado. *Sci. Total Environ.* 640-641, 619-628.

Du, X.W., Zhang, Z.Y., Carlson, K.H., Lee, J., Tong, T.Z., 2018. Membrane fouling and reusability in membrane distillation of shale oil and gas produced water: Effects of membrane surface wettability. *J Membr. Sci.* 567, 199-208.

Esmaeilirad, N., Carlson, K., Omur Ozbek, P., 2015. Influence of softening sequencing on electrocoagulation treatment of produced water. *J. Hazard. Mater. 283*, 721-729.

Eykens, L., De Sitter, K., Dotremont, C., De Schepper W., Pinoy, L., Van Der Bruggen, B., 2017. Wetting resistance of commercial membrane distillation membranes in waste streams containing surfactants and oil. *Appl. Sci.* 7, 118.

Gluge, J., Scheringer, M., Cousins, I.T., DeWitt, J.C., Goldenman, G., Herzke, D., Lohmann, R., Ng, C.A., Trier, Z., Wang, Z., 2020. An overview of the uses of per- and polyfluoroalkyl substances (PFAS). *Environ. Sci.: Processes Impacts* 22, 2345-2373.

Hanson, A.J., Luek, J.L., Tummings, S.S., McLaughlin, M.C., Blotevogel, J., Mouser, P.J., 2019. High total dissolved solids in shale gas wastewater inhibit biodegradation of alkyl and nonylphenol ethoxylate surfactants. *Sci. Total Environ.* 668, 1094-1103.

Hickenbottom, K.L., Hancock, N.T., Hutchings, N.R., Appleton, E.W., Beaudry, E.G., Xu, P., Cath, T.Y., 2013. Forward osmosis treatment of drilling mud and fracturing wastewater from oil and gas operations. *Desalination* 312, 60-66.

Horseman, T., Su, C., Christie, K.S.S., Lin, S., 2019 Highly effective scaling mitigation in membrane distillation using a superhydrophobic membrane with gas purging. *Environ. Sci. Technol. Let.*6, 423-429.

Horseman, T., Yin, Y., Christie, K.S.S., Wang, Z., Tong, T., Lin, S., 2021. Wetting, scaling, and fouling in membrane distillation: State-of-the-art insights on fundamental mechanisms and mitigation strategies. *ACS EST Engg.* 1, 117-140.

Jahanban-Esfahlan, A., Jahanban-Esfahlan, R., Tabibiazar, M., Roufegarinejad, L., Amarowicz, R., 2020. Recent advances in the use of walnut (*Juglans regia L.*) shell as a valuable plant-based bio-sorbent for the removal of hazardous materials.

Jimenez, S., Mico, M.M., Arnaldos, M., Medina, F., Contreras, S., 2018. State of the art of produced water management. *Chemosphere* 192, 186-208. *RSC Adv.* 10, 7026-7047.

Kahrilas, G.A., Blotevogel, J., Corrin, E.R., Borch, T., 2016. Downhole transformation of the hydraulic fracturing fluid biocide glutaraldehyde: Implications for flowback and produced water quality. *Environ. Sci. Technol.* 50 (20), 11414-11423.

Kamaz, M., Sengupta, A., Gutierrez, A., Chiao, Y.H., Wickramasinghe, R., 2019. Surface modification of PVDF membranes for treating produced water by direct contact membrane distillation. *Int. J. Environ. Res. Public Health* 16, 685.

Kim, S., Omur-Ozbek, P., Dhanasekar, A., Prior, A., Carlson, K., 2016. Temporal analysis of flowback and produced water composition from shale oil and gas operations: Impact of frac fluid characteristics. *J. Petrol. Sci. Eng. 147*, 202-210.

Kondash, A., Lauer, N., Vengosh, A., 2018. The intensification of the water footprint of hydraulic fracturing. *Sci. Adv.* 4, eaar5982.

Kong, F.X., Chen, J.F., Wang, H.M., Liu, X.N., Wang, X.M., Wen, X., Chen, C.M., Xie, Y.F.F., 2017. Application of coagulation-UF hybrid process for shale gas produced water treatment. *J. Membr. Sci.* 524, 460-469.

Lawson, K.W., Lloyd, D.R., 1997. Membrane distillation. *J. Membr. Sci.* 124 (1), 1-25.

Lee, J., Boo, C., Ryu, W.H., Taylor, A.D., Elimelech, M., 2016. Development of omniphobic desalination membranes using a charged electrospun nanofiber scaffold. *ACS Appl. Mater. Interfaces* 8, 11154-11161.

Lester, Y., Ferrer, I., Thurman, E. M., Sitterley, K. A., Korak, J. A., Aiken, G., Linden, K. G., 2015. Characterization of hydraulic fracturing flowback water in Colorado: Implications for water treatment. *Sci. Total Environ. 512-513*, 637-644.

Li, J., Guo, S., Xu, Z., Li, J., Pan, Z., Du, Z., Cheng, F., 2019. Preparation of omniphobic PVDF membranes with silica nanoparticles for treating coking wastewater using direct contact membrane distillation: Electrostatic adsorption vs. chemical bonding. *J. Membr. Sci.* 574, 349-357.

Lin, P.J., Yang, M.C., Li, Y.L., Chen, J.H., 2015. Prevention of surfactant wetting with agarose hydrogel layer for direct contact membrane distillation used in dyeing wastewater treatment. *J. Membr. Sci.* 475, 511-520.

Lobo, F.L., Wang, H.M., Huggins, T., Rosenblum, J., Linden, K.G., Ren, Z.J., 2016. Low-energy hydraulic fracturing wastewater treatment via AC powered electrocoagulation with biochar. *J. Hazard. Mater.* 309, 180-184.

Lokare, O.R., Tavakkoli, S., Wadekar, S., Khanna, V., Vidic, R.D., 2017. Fouling in direct contact membrane distillation of produced water from unconventional gas extraction. *J. Membr. Sci.* 524, 493-501.

Lu., C., Su, C., Cao, H., Ma, X., Duan, F., Chang, J., Li, Y., 2018. F-POSS based omniphobic membrane for robust membrane distillation. *Mater. Lett.* 228, 85-88.

Lu, K.J., Chen, Y., Chung, T.S., 2019. Design of omniphobic interfaces for membrane distillation – A review. *Water Res.* 162, 64-77.

Lu, X.M., Peng, Y.L., Qiu, H.R., Liu, X.R., Ge. L., 2017. Anti-fouling membranes by manipulating surface wettability and their anti-fouling mechanism. *Desalination* 413, 127-135.

Ma, G., Geza, M., Cath, T.Y., Drewes, J.E., Xu, P., 2018. iDST: An integrated decision support tool for treatment and beneficial use of non-traditional water supplies – Part II: Marcellus and Barnett Shale case studies. *J. Water Proc. Eng.* 25, 258-268.

McLaughlin, M.C., Borch, T., Blotevogel, J., 2016. Spill of hydraulic fracturing chemicals on agricultural topsoil: Biodegradation, sorption, and co-contaminant interactions. *Environ. Sci. Technol.* 50, 6071-6078.

Miller H., Trivedi, P., Qiu, Y., Sedlacko, E.M., Higgins, C.P., Borch, T., 2019. Food crop irrigation with oilfield-produced water suppresses plant immune response. *Environ. Sci. Technol. Lett.* 6, 656-661.

Miller, H., Dias, K., Hare, H., Borton, M.A., Blotevogel, J., Danforth, C., Wrighton, K.C., Ippolito, J.A., Borch, T., 2020. Reusing oil and gas produced water for agricultural irrigation: Effects on soil health and the soil microbiome. *Sci. Total Environ.* 722, 137888.

Rezaei, M., Warsinger, D.M., Lienhard, J.H., Duke, M.C., Matsuura, T., Samhaber, W.M., 2018. Wetting phenomena in membrane distillation: Mechanisms, reversal, and prevention. *Water Res.* 139, 329-352.

Robbins, C.A., Grauberger, B.M., Garland, S.D., Carlson, K.H., Lin, S., Bandhauer, T.M., Tong, T., 2020. On-site treatment capacity of membrane distillation powered by waste heat or natural gas for unconventional oil and gas wastewater in the Denver-Julesburg Basin. *Environ. Inter*. 145, 106142.

Robbins, C.A.; Carlson, K.H.; Garland, S.D.; Bandhauer, T.M.; Grauberger, B.M.; Tong, T., 2021. Spatial analysis of membrane distillation powered by waste heat from natural gas compressor stations for unconventional oil and gas wastewater treatment in Weld County, Colorado. *ACS Environ. Sci. Tech. Engg.* 1 (2), 192-203.

Rodriguez, A.Z., Wang, H., Hu, L., Zhang, Y., Xu, P., 2020. Treatment of produced water in the Permian Basin for hydraulic fracturing: Comparison of different coagulation processes and innovative filter media. *Water* 12 (3), 770.

Rosenblum, J.S., Sitterley, K.A., Thurman, E.M., Ferrer, I., Linden, K.G., 2016. Hydraulic fracturing wastewater treatment by coagulation-adsorption for removal of organic compounds and turbidity. *J. Environ. Chem. Eng.* 4, 1978-1984.

Sardari, K., Fyfe, P., Lincicome, D., Wickramsinghe, S.R., 2018. Combined electrocoagulation and membrane distillation for treating high salinity produced waters. *J. Membr. Sci.* 564, 82-96.

Scanlon, B.R., Ikonnikova, S., Yang, Q., Reedy, R.C., 2020a. Will water issues constrain oil and gas production in the United States? *Environ. Sci. Technol.* 54, 3510-3519.

Scanlon, B.R., Reedy, R.C., Xu, P., Engle, M., Nicot, J.P., Yoxtheimer, D., Yang, Q., Ikonnikova, S., 2020b. Can we beneficially reuse produced water from oil and gas extraction in the U.S.? *Sci. Total Environ.* 717, 137085.

Sedlacko, E.M., Jahn, C.E., Heuberger, A.L., Sindt, N.M., Miller, H.M., Borch, T., Blaine, A.C., Cath, T.Y., Higgins, C.P., 2019. Potential for beneficial reuse of oil and gas-derived produced water in agriculture: Physiological and morphological responses in spring wheat (*triticum aestivum*). *Environ. Toxicol. Chem.* 38 (8), 1756-1769.

Shaffer, D. L., Arias Chavez, L. H., Ben-Sasson, M., Romero-Vargas Castrillon, S., Yip, N. Y., Elimelech, M, 2013. Desalination and reuse of high-salinity shale gas produced water: Drivers, technologies, and future directions. *Environ. Sci. Technol. 47* (17), 9569-9583.

Silva, T.L., Morales-Torres, S., Castro-Silva, S., Figueiredo, J.L., Silva, A.M., 2017. An overview on exploration and environmental impact of unconventional gas sources and treatment options for produced water. *Sep. Purification Tech.* 211, 310-321.

Srinivasan, A., Viraraghavan, T., 2008. Removal of oil by walnut shell media. *Bioresour. Technol.* 99 (17), 8217-8220.

Sun, Y., Wang, D., Tsang, D.C., Wang, L., Ok, Y.S., Feng, Y., 2019. A critical review of risks, characteristics, and treatment strategies for potentially toxic elements in wastewater from shale gas extraction. *Environ. Int.* 125, 452.469.

Tang, C.Y., Kwon, Y.N., Leckie, J.O., 2009. Effect of membrane chemistry and coating layer on physiochemical properties of thin film composite polyamide RO and NF membranes - I. FTIR and XPS characterization of polyamide and coating layer chemistry. *Desalination* 242, 149-167.

Tavakkoli, S., Lokare, O.R., Vidic, R.D., Khanna, V., 2017. A techno-economic assessment of membrane distillation for treatment of Marcellus shale produced water. *Desalination* 416, 24-34.

Thomas, R.R., 2006. Fluorinated Surfactants. *Chemistry and Technology of Surfactants*. Wiley-Blackwell Publishing: Hoboken, NJ.

Thurman, E.M., Ferrer, I., Blotevogel, J., Borch, T., 2014. Analysis of hydraulic fracturing flowback and produced waters using accurate mass: Identification of ethoxylated surfactants. *Anal. Chem.* 86, 9653-9661.

Tijing, L.D., Woo, Y.C., Choi, J.S., Lee, S., Kim, S.H., Shon, H.K., 2015. Fouling and its control in membrane distillation – A review. *J. Membr. Sci.* 475, 215-244.

Tong, T., Carlson, K.H., Robbins, C.A., Zhang, Z., Du, X., 2019a. Membrane-based treatment of shale oil and gas wastewater: The current state of knowledge. *Front. Environ. Sci. Eng.* 13 (4): 63.

Tong, T., Wallace, A.F., Zhao, S., Wang, Z., 2019b. Mineral scaling in membrane distillation: Mechanisms, mitigation strategies, and feasibility of scaling-resistant membranes. *J. Membr. Sci.* 579, 52-69.

U.S. Environmental Protection Agency, 2021. Per- and Polyfluoroalkyl Substances (PFAS). USEPA web site. https://www.epa.gov/pfas (accessed Feb. 8, 2021).

Wang, W., Du, X. W., Vahabi, H., Zhao, S., Yin, Y. M., Kota, A. K., Tong, T. Z., 2019. Trade-off in membrane distillation with monolithic omniphobic membranes. *Nat. Commun. 10*, 3220.

Wang, Z., Chen, Y., Sun, X., Duddu, R., Lin, S., 2018. Mechanism of pore wetting in membrane distillation with alcohol vs. surfactant. *J. Membr. Sci.* 559, 183-195.

Wang, Z., Lin, S., 2017. Membrane fouling and wetting in membrane distillation and their mitigation by novel membranes with special wettability. *Water Res.* 112, 38-47.

Warsinger, D.M., Swaminathan, J., Guillen-Burrieza, E., Arafat, H.A., Lienhard, J.H., 2015. Scaling and fouling in membrane distillation for desalination applications: A review. *Desalination* 356, 294-313.

Woo, Y.C., Chen, Y., Tijing, L.D., Phuntsho, S., He, T., Choi, J.S., Kim, S.H., Shon, H. K., 2017. CF_4 plasma-modified omniphobic electrospun nanofiber membrane for produced water brine treatment by membrane distillation. *J. Membr. Sci.* 529, 234-242.

Xiao, Z., Li, Z., Guo, H., Liu, Y., Wang, Y., Yin, H., Li, X., Song, J., Nghiem, L.D., He, T., 2019. Scaling mitigation in membrane distillation: From superhydrophobic to slippery. *Desalination* 466, 36-43.

Xu, P., Cath, T.Y., Robertson, A.P., Reinhard, M., Leckie, J.O., Drewes, J.E., 2013. Critical review of desalination concentrate management, treatment and beneficial use. *Environ. Eng. Sci.* 30 (8), 502-514.

Yin, Y., Jeong, N., Tong, T., 2020. The effects of membrane surface wettability on pore wetting and scaling reversibility associated with mineral scaling in membrane distillation. *J. Membr. Sci.* 614, 118503.

Yin, Y., Wang, W., Kota, A.K., Zhao, S., Tong, T., 2019. Elucidating mechanisms of silica scaling in membrane distillation: Effects of membrane surface wettability. *Environ. Sci.: Water Res.* 5, 2004-2014.

Zhai, J., Huang, Z.J., Rahaman, M.H., Li, Y., Mei, L.Y., Ma, H.P., Hu, X.B., Xiao, H.W., Luo, Z.Y., Wang, K.P., 2017. Comparison of coagulation pretreatment of produced water from natural gas well by polyaluminum chloride and polyferric sulphate coagulants. *Environ. Technol.* 38, 1200-1210.

Zhang, W., Yang, X., Wang, D., 2013. Complete removal of organic contaminants from hypersaline wastewater by the integrated process of powdered activated carbon adsorption and thermal fenton oxidation. *Ind. Eng. Chem. Res.* 52, 5765-5771.

Zhang, Z.Y., Du, X.W., Carlson, K.H., Robbins, C.A., Tong, T.Z., 2019. Effective treatment of shale oil and gas produced water by membrane distillation coupled with precipitative softening and walnut shell filtration. *Desalination* 454, 82-90.

Zheng, R., Chen, Y., Wang, J., Song, J., Li, X.M., He, T., 2018. Preparation of omniphobic PVDF membrane with hierarchical structure for treating saline oily wastewater using direct contact membrane distillation. *J. Membr. Sci.* 555, 197-205.

Zhu, Z., Zhong, L., Horseman, T., Liu, Z., Zeng, G., Li, Z., Lin, S., Wang, W., 2020. Superhydrophobic-omniphobic membrane with anti-deformable pores for membrane distillation with excellent resistance. *J. Membr. Sci.* 118768.

Zularisam, A.W., Ismail, A.F., Salim, R., 2006. Behaviours of natural organic matter in membrane filtration for surface water treatment – A review. *Desalination* 194, 211-231.

7.0 Beyond Treatment Technology: Understanding Motivations and Barriers for Wastewater Treatment and Reuse in Unconventional Energy Production[5]

7.1 Introduction

Wastewater management represents a major challenge to the unconventional oil and gas (UOG) industry (Shaffer et al., 2013; Vengosh et al., 2014; Kondash et al., 2017; Chang et al., 2019) as hydraulic fracturing (HF) consumes a vast quantity of freshwater while generating substantial volumes of wastewater (Kondash et al., 2015). A steady increase in water footprint has been reported in the major UOG producing regions across the U.S (Scanlon et al., 2016; Kondash et al., 2017). This ever-growing problem is exemplified by the Permian Basin in the states of Texas and New Mexico, where spending on wastewater management is projected to double in the next five years. This increase is expected to add $6/barrel cost to the basin breakeven price by 2025 strictly due to wastewater management costs (Matthews, 2020; Wethe and Crowley, 2020). Water scarcity, which is intensified by a changing climate and growing freshwater demand, imposes increasingly adverse effects on local water resources. Many of the western shale plays in the U.S. are located in water-scarce areas (Vengosh et al., 2014), with 38% of shale resources worldwide situated within regions under water stress (Reig et al., 2013). Considering the hazardous nature of UOG wastewater (Shaffer et al., 2013; Butkovskyi et al., 2017), a dual challenge of water shortage and pollution is created by UOG production at the water-energy nexus. Strategies that economically treat UOG wastewater into a valuable asset has

[5] This chapter will be submitted for publication as a perspective article.

the potential to positively impact not only oil and gas operations but the communities in which they are being developed.

The current management of UOG wastewater is relying on injecting wastewater into deep and isolated subterranean formations (a practice referred to as deep-well injection) (Rahm et al., 2014; Vengosh et al., 2014). This strategy is plagued with concerns related to induced seismicity, groundwater contamination, and the removal of significant amounts of water from the hydrologic cycle (Ellsworth, 2013; Gregory and Mohan, 2015; Scanlon et al., 2019). These issues highlight the necessity of pursuing alternative paradigms such as beneficial reuse and reclamation after appropriate wastewater treatment. To date, numerous studies have investigated technologies and materials for such purposes (Shaffer et al., 2013; Chang et al., 2019; Tong et al., 2019), leading to a versatile technological portfolio for advanced treatment of UOG wastewater.

However, wastewater treatment and reuse (except for internal reuse for HF activities) has not been widely adopted by the UOG industry. Current research efforts remain focused on improving the performance and energy efficiency of treatment technologies, but treatment technology is *not* the only barrier to shift the UOG wastewater management paradigm towards treatment and reuse. Other aspects beyond treatment technology, including regulation and policy, economics, system logistics, as well as social acceptance, play equally or more important roles collectively in the selection and deployment of UOG wastewater management practices. These aspects are analogous to what are considered for municipal wastewater reuse (National Research Council, 2012), an application that can inform future adoption of wastewater treatment and reuse by the UOG industry. Such non-treatment aspects, which have not received sufficient attention in the literature for UOG wastewater reuse, have created significant barriers that prohibit practical implementation of any newly-developed wastewater treatment technology. An in-depth

understanding of those barriers, therefore, is an urgent need to guide future research to facilitate UOG wastewater treatment and reuse.

In this feature article, we begin with a critical analysis of motivations that drive oil and gas producers and policy makers towards treating and reusing UOG wastewater in the U.S. We then examine four main barriers against wide adoption of wastewater treatment and reuse in the UOG industry, pertaining to not only treatment technology but also regulatory compliance, economic feasibility, and social acceptance. We highlight that overcoming those barriers requires a system-level approach to integrate knowledge and collaborative efforts from engineers, regulators, policy makers, economists, and social scientists. Accordingly, future research work should be directed at domains well beyond treatment technology, and a broader collaboration across multiple disciplines is needed to translate technology innovation into solutions that truly improve water sustainability in the context of rising UOG production in areas of water stress.

7.2 Motivations of Wastewater Treatment and Reuse in UOG Production

The vast majority of the wastewater generated during UOG development is currently disposed via deep-well injection. The United States Environmental Protection Agency (USEPA) estimates that more than 2 billion gallons of fluid associated with oil and natural gas production are being injected into Class II injection wells in the U.S. every day (USEPA, 2020a). Deep-well injection is considered technically mature and favored by oil and gas producers due to its predictable cost, well-established business relationships, and explicit liability. This practice does have issues with social acceptance but this has not been limiting in terms of adoption.

One of the primary limitations of deep-well injection is induced seismicity. Multiple studies have showed a strong connection between increased frequency of seismic activities and deep-well disposal of wastewater in major UOG producing regions of the U.S (Ellsworth, 2013;

Keranen et al., 2014; Weingarten et al., 2015; Hincks et al., 2018). Numerous lawsuits have been filed and litigated regarding seismicity events induced by deep-well injection of UOG wastewater (Supreme Court of Oklahoma, 2015; Shaffer et al., 2017; Deshmukh et al., 2018; USEPA, 2020b). As a result, several U.S. states have issued directives, executive orders, or other regulatory actions to limit UOG wastewater disposal via deep-well injection. This includes a well volume reduction plan and the closure of multiple disposal wells in Oklahoma (Skinner, 2015), as well as new permitting requirements that include information on seismic activity in Texas, Arkansas, and Ohio (Kasich, 2012; Self, 2014).

The cost of deep-well injection is highly dependent on the distance required for wastewater transportation. Once the capacities of disposal wells are saturated near UOG producing sites, longer distances are needed to transport wastewater to the closest available wells, which increases the cost of wastewater disposal. Taking Texas and Colorado as examples, the number of horizontal production wells significantly increased in the period of 2002−2018, accompanied by a substantial increase of both freshwater consumption and wastewater generation (Figures 7-1a and 7-1b). In contrast, the number of Class II disposal wells stayed nearly constant during the same period. As a result, the availability of disposal wells is becoming progressively limited, which translates to higher costs of deep-well injection. It is reported that the capacity of disposal wells is heavily constrained in the Permian Basin, with multiple counties experiencing high (60%-80%) to complete (>80%) levels of utilization (Whitfield, 2017). This situation, along with the increasingly stringent regulations on deep-well injection, has resulted in growing concerns among oil and gas producers and has attracted increasing investments in wastewater treatment and reuse (Matthews, 2020; Wethe and Crowley, 2020).

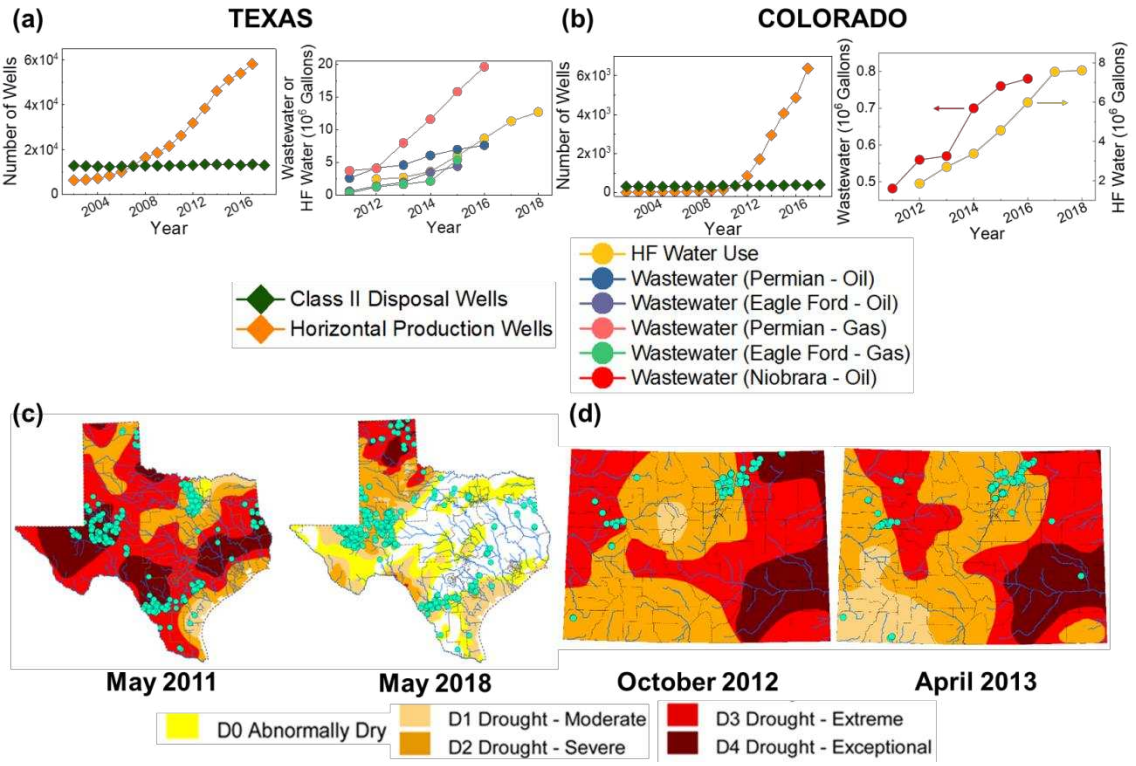

Figure 7-1. The changes of Class II disposal wells, horizontal production wells, hydraulic fracturing (HF) water use, and UOG wastewater production with time in the states of (a) Texas and (b) Colorado. The data are adopted from the USEPA UIC injection well inventory, Colorado Oil and Gas Information System (COGIS) database, and Kondash et al. (Kondash et al., 2018). Maps of newly drilled UOG wells (indicated by the light blue dots) with different drought categories are shown for (c) Texas and (d) Colorado. The drought maps are generated via data from U.S. drought monitor (National Drought Mitigation Center, 2020). The data of well locations are from the FracFocus registry (Groundwater Protection Council and Interstate Oil and Gas Conservation Commission, 2020). Note that one light blue dot might represent multiple wells due to their close locations.

Furthermore, many western U.S. shale plays are within areas suffering high to severe water stress, where freshwater withdrawals exceed 40% of water availability (Vengosh et al., 2014). As shown in Figures 7-1c and 7-1d, many UOG wells were drilled and completed in the presence of extensive drought climate. The intense HF freshwater consumption during relatively short time periods competes with other water-demanding sectors such as agricultural irrigation and municipal water use. The constrained water resource availability during drought conditions poses threats on local water sustainability, provokes stronger public resistance against UOG activities, and increases the difficulty and expense of water acquisition by UOG producers.

It should be noted that UOG wastewater reuse does not always require advanced wastewater treatment. Internal wastewater reuse for HF of new wells has gained popularity (Estrada and Bhamidimarri, 2016; Scanlon et al., 2020b). As recorded by the Pennsylvania Department of Environmental Protection (Brantley et al., 2014), 87% of the flowback water from HF was recycled in the Marcellus Shale for internal reuse. Owing to the blending with a larger quantity of freshwater (Mantell, 2011; Shaffer et al., 2013), internal reuse of UOG wastewater tolerates high salinity and hardness (Table D1, Appendix D), rendering conventional inexpensive treatment processes such as filtration, sedimentation, and disinfection sufficient for such applications. However, internal reuse is economically feasible only when new wells are drilled in close proximity to the existing wells due to water transport costs, and the production volumes of UOG wastewater do not always match the water demand of HF activities. For instance, wastewater generation was reported to outpace HF freshwater consumption in the Bakken shale play (located in North Dakota), Eagle Ford shale play (located in Texas) and Permian Basin, as well as in the state of Oklahoma (Scanlon et al., 2019; Scanlon et al. 2020a). As a result, there remains UOG wastewater that cannot be assimilated into regional oil and gas activities, leaving the option of advanced treatment and external reuse of the excess wastewater necessary to minimize deep-well injection. In this article, the term “wastewater treatment and reuse” is hereafter referring to activities involving advanced treatment technologies and external reuse off the well sites. This is for the ease of writing, but the authors suggest the readers not underestimate the role of internal reuse in UOG wastewater management.

7.3 Understanding the Barriers to UOG Wastewater Treatment and Reuse

As discussed above, the constraints associated with deep-well injection and intensified freshwater scarcity are the primary incentives that motivate the UOG industry towards

wastewater treatment and reuse. However, this alternative strategy of wastewater management needs to be economically favorable compared to deep-well injection and be applied only to wastewater that cannot be internally used for new HF activities (Estrada and Bhamidimarri, 2016). Further, the reuse applications of treated wastewater, which direct the selection of appropriate treatment technologies, should be carefully considered to meet regulatory requirements while minimizing the economic cost. Additionally, social acceptance is critical to the viability of UOG wastewater reuse. Therefore, UOG wastewater management exists within a multi-objective decision-making framework (Figure 7-2), in which UOG wastewater treatment and reuse is much more complicated than simply developing effective treatment technologies. Instead, a systems approach needs to be employed to integrate technology development within the broader lifecycle of UOG wastewater, and to integrate interdisciplinary factors such as regulation, policy, economics, and social acceptance. Herein, we perform a comprehensive examination of barriers associated with technological, regulatory, economic, and social aspects. By doing so, we identify research needs both upon and beyond treatment technology, in order to catalyze the transition of the UOG wastewater management paradigm away from deep-well injection and towards treatment and reuse.

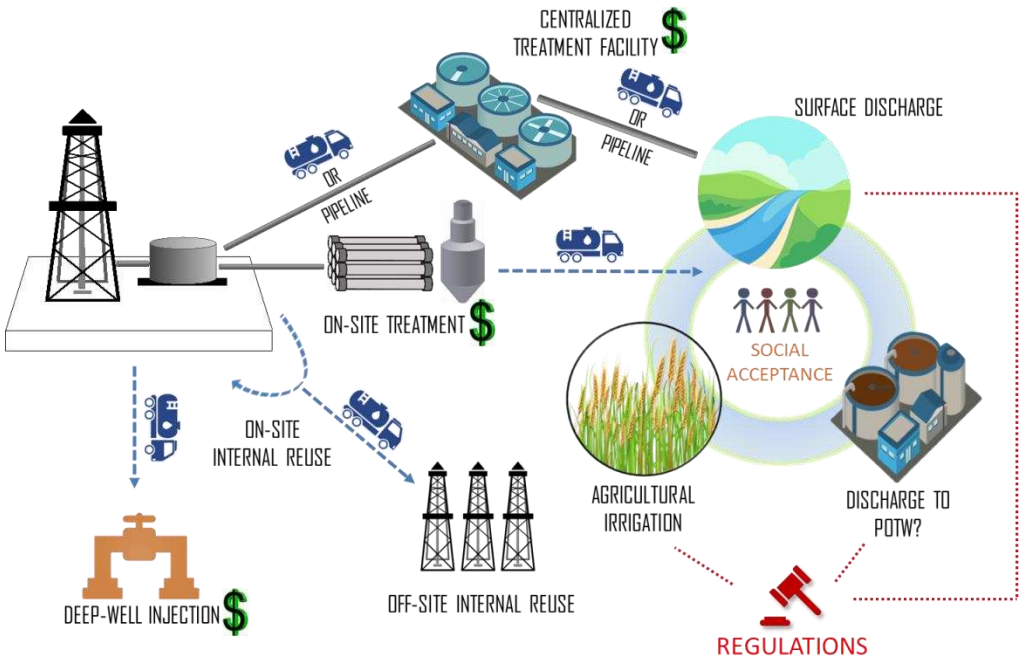

Figure 7-2. Schematic of UOG wastewater management system. The implementation of wastewater treatment and reuse needs to be favored in a multi-objective framework involving treatment technology, regulation, economics, as well as social acceptance (POTW: publicly owned treatment works). It should be noted that water/wastewater transportation using truck or pipeline can represent an economic barrier.

7.3.1 The barrier of treatment technology

Extensive research efforts have been invested in developing treatment technologies for UOG wastewater, which are generally grouped into two categories – thermal and membrane technologies. Compared to thermal technologies, membrane technologies including nanofiltration (NF) and reverse osmosis (RO) have superior energy efficiency because no phase transition (from liquid to vapor) is required for water purification. However, NF and RO are constrained by their salinity limit (typically ~70,000 mg/L of total dissolved solids, TDS) imposed by the maximum pressure tolerated by existing membranes and auxiliaries (Scanlon et al., 2020a). Thermal technologies such as mechanical vapor compression (MVC) need to be employed to treat UOG wastewater with ultra-high salinity (up to >200,000 mg/L of TDS) (Chang et al., 2019). MVC is much more energy consumptive and costly than NF and RO, due to the energy penalty for water evaporation and condensation as well as the use of expensive

corrosion-resistant materials (e.g., titanium) (Tong and Elimelech, 2016). This renders high cost and energy consumption a primary technical barrier to UOG wastewater treatment.

Recently, hybrid thermal-membrane technologies such as thermolytic forward osmosis (FO) and membrane distillation (MD) have been considered as alternatives for the treatment of UOG wastewater (Shaffer et al., 2013; Chang et al., 2019; Tong et al., 2019). These technologies, although still energy intensive due to their thermal nature, are able to leverage low-grade thermal energy such as solar energy, geothermal energy, and waste heat. This feature has the potential to reduce the cost and carbon footprint associated with electrical energy consumption. However, the viability of UOG wastewater treatment powered by those alternative energy sources needs to be further evaluated, because their availability and actual expenses have not been thoroughly investigated. For example, although waste heat generated from natural gas compressor stations (NGCSs) was found sufficient for MD treatment of all UOG wastewater in Pennsylvania, the cost of wastewater transport could be significant or even prohibitive if the wells are not located in close proximity with the NGCSs (Lokare et al., 2017). The utilization of waste heat and geothermal energy generated at well pads would avoid the need for wastewater transportation. But the availability and corresponding treatment capacity have been rarely quantified (Robbins et al., 2020), with the cost and efficiency of recovering such energy sources still unknown. Encouraging progress in high-efficiency photothermal materials have recently made solar-driven, off-grid wastewater treatment a promising solution (Dongare et al., 2017; Wang et al., 2019). Their performance and economics, however, need to be assessed and compared to MVC powered by electricity generated from photovoltaic panels (Wang et al., 2019). Therefore, the use of low-grade thermal energy to reduce the energy and cost consumption of UOG wastewater treatment is encouraging but not simple. The translation of this idea to full-scale applications at

the oil and gas fields still requires intensive efforts of technological research, techno-economic assessment, and systems integration demonstration.

However, even achieving high performance and acceptable cost, practical implementation of UOG wastewater treatment is still hindered by the lack of explicit treatment goals. The selection of suitable treatment technologies should be tailored to specific wastewater reuse applications and regulatory requirements, which are typically unclear in the literature. The disconnect of treatment technology development from reuse applications prevents rational design of "fit-for-purpose" technologies for UOG wastewater treatment (Groundwater Protection Council, 2019). Furthermore, a reasonable regulatory framework, which defines water quality standards for UOG wastewater reuse applications, has yet to be established, imposing an additional barrier to wide adoption of wastewater treatment and reuse in the UOG industry.

7.3.2 The barrier of regulatory compliance

Potential reuse options for treated UOG wastewater include discharging into surface water or publicly owned treatment works (POTWs), as well as direct use for agricultural irrigation. Other reuse applications such as industrial usage (e.g., as water supply for power plants (Scanlon et al., 2020a)) are possible and likely to face different regulatory challenges. However, the options discussed in this section represent more common strategies, which have been either applied in practice or proposed frequently in the literature.

In regard to discharging into POTWs, the USEPA has promulgated the Oil and Gas Extraction Effluent Guidelines and Standards to regulate such practice from oil and gas exploration activities (USEPA, 2016). In the final rule published in June 2016, the revised standards require zero discharge of wastewater pollutants from UOG extraction facilities to POTWs. Because no treatment technologies guarantee complete removal of all the pollutants,

this regulation essentially prohibits the discharge of treated UOG wastewater into POTWs. Before this rule was enacted, discharging UOG wastewater into POTWs had been implemented in the Marcellus Shale from 2008 to 2009 (Vidic et al., 2013). Such a practice led to an increase of salt loading to local rivers, because the POTWs were not designed to remove TDS. This problem, which resulted in the elimination of the practice (Vidic et al., 2013), supported the explanation provided by the USEPA on the final rule that UOG wastewater is not a typical influent of POTWs.

The concerns for high salinity of UOG wastewater can be addressed by currently available technologies, which enable the removal of most salts from wastewater. The salt rejection of RO is typically higher than 90% (Yang et al., 2019), and thermal-based technologies including MVC and MD have the potential to remove all the non-volatile components including TDS. The salinity of treated UOG wastewater, therefore, is unlikely to compromise POTW operation. However, the EPA regulation does not distinguish raw from treated UOG wastewater, rendering discharging into POTWs infeasible under the current regulatory framework. Also, the effects of treated UOG wastewater on municipal wastewater treatment (e.g., organics and nutrient removal, the structure and activity of microbial communities in the activated sludge) have not been fully researched. Future investigations that elucidate those effects are needed to provide regulators with necessary information to reconsider the feasibility of discharging treated UOG wastewater into POTWs. It should be noted that this practice partially transfers the liability associated with UOG wastewater from oil and gas producers to the POTWs. The involvement of POTWs as an important stakeholder in the UOG production system is necessary but could complicate the formulation of relevant regulations.

Surface discharge into a nearby receiving waterway, which could potentially be in exchange for downstream water rights, is a promising option for regulatory compliant reuse of UOG wastewater. Since 1979, direct discharge of wastewater from onshore oil and gas extraction has been regulated under Part 435 of the Code of Federal Regulations (USEPA, 2020). A National Pollutant Discharge Elimination System (NPDES) permit (or its counterpart at the state level) needs to be issued before any surface discharge activities occur in the U.S, providing detailed standards that regulate the maximum concentrations of specific pollutants allowed in the discharged wastewater. While a permit is required there is a large variability in the maximum concentrations of pollutants geographically.

Table D2 (Appendix D) summarizes twelve NPDES permits associated with UOG wastewater in the states of Colorado, Pennsylvania, and Texas. These permits include marked variation in water quality standards. Among the seven NPDES permits of Colorado, for example, only one permit specifies the discharge limit for TDS (3,500 mg/L for 30-day average), while chloride concentration is regulated in only three permits (250 mg/L for 30-day average). Texas has loose regulations on the allowable salinity in the discharged wastewater, as TDS and chloride are not regulated in all three permits. In contrast, both NPDES permits of Pennsylvania exhibit stringent regulation on TDS (500 mg/L for 30-day average).

Similar variation is seen in the regulation of organic contaminants. For example, benzene, a toxic volatile organic compound commonly found in UOG wastewater, is regulated in all the Colorado NPDES permits with a daily maximum concentration of 5,300 μg/L (Table D2, Appendix D), which is comparable to the benzene concentration reported in some raw UOG wastewaters (Butkovskyi et al., 2017; Chang et al., 2019). However, much lower concentrations of benzene are allowed for long-term discharge in some of these permits (2.2 μg/L for 30-day

average, and 0.33-795 μg/L for 2-year average). Such regulation provides a potential challenge to thermal technologies such as MVC and MD, because volatile pollutants are able to transport along with water vapor into the treated product water (Winglee et al., 2017; Zhang et al., 2019). Pre- or post-treatment steps (e.g., adsorption and air-stripping) are thus needed to meet such NPDES standards if high benzene concentrations are present in the UOG wastewater. Since benzene is not regulated in the NPDES permits of Pennsylvania and Texas, its removal is not considered in practical selection of treatment technologies. Additionally, more than ten organic compounds of concern are regulated in the NPDES permits of Pennsylvania, but they are not specified in those of Colorado or Texas. These inconsistencies shown in NPDES permits are most likely attributable to varied characteristics of the receiving water body (e.g., its water quality and usage, volume) and the UOG wastewater (e.g., its chemical composition and discharge flow rate). The lack of consistent regulation represents a challenge for the development and deployment of UOG treatment systems that results in surface discharge.

As a comparison, the water quality requirements for municipal wastewater reuse also vary state by state (National Research Council, 2012). However, municipal wastewater is less hazardous than UOG wastewater (resulting in simpler and more explicit water quality criteria) and its treatment technologies are more established (National Research Council, 2012). As a result, the variation in regulation brings more uncertainties to the selection of treatment technology for UOG wastewater. For example, the oil and gas producers are resistant to employ expensive desalination technologies unless salinity is clearly regulated. Due to the varied water quality standards, researchers cannot know whether a technology under development for UOG wastewater treatment is sufficient or necessary, unless the regulatory requirements to be met are specified. Therefore, aligning treatment technologies with water quality targets as regulated in

the NPDES permits is essential to translate the technologies developed in the laboratory to practical field applications. Environmental regulatory constraints have been shown to drive innovation (Ford et al., 2014) and the establishment of a more explicit regulatory framework is needed to direct technology innovation for surface discharge (and other reuse applications) of treated UOG wastewater.

A primary concern of wastewater reuse is the unknown chemical contaminants in which discrete chemical monitoring for a pre-identified suite of contaminants will not be sufficient to address the large number of potential contaminants (National Research Council, 2012). Due to the complex nature of UOG wastewater and its regional variations, it is infeasible to sample and regulate the plethora of possible contaminants. Regulating contaminants by groups, which has been employed by USEPA in the original trihalomethane regulation and the subsequent disinfection by-products (DBPs) regulations (National Research Council, 2012), could be a solution. The strategy of identifying key indicator species, analogous to monitoring fecal indicator as the representative of bacterial pathogens in treated wastewater effluent (USEPA, 2003; Sanders et al., 2013), could be valuable. To further protect human health and the environment, it is also beneficial to perform toxicity testing, which is well suited for complex waste streams including treated UOG wastewater for beneficial reuse (McLaughlin et al., 2020).

Another reuse application of treated UOG wastewater is agricultural irrigation, which has attracted great interest to mitigate freshwater scarcity in arid areas (Dolan et al., 2018; Echchelh et al., 2018). Since irrigation is directly related to public and environmental health, UOG wastewater must be treated to a sufficient level that protects humans and ecosystems. Kern County in the Central Valley of California has been reusing produced water from *conventional* oil and gas production to irrigate food crops for decades (Enviro-Tox Services, 2016; Kondash et

al., 2020). The resulting food products have been sold throughout the U.S. However, due to the complex composition of HF fluids and formation brines, such a practice has not been allowed for UOG wastewater. The irrigation of non-edible crops (e.g., cotton and bioenergy crops) is more practical with better public acceptance and less health risks. Similar to surface discharge, however, there is a lack of explicit regulations tailored to the reuse of treated UOG wastewater for crop irrigation. For example, reclaimed water allowed for irrigation in Colorado, as regulated by the Colorado Department of Public Health and Environment (CDPHE), is defined as domestic wastewater that has received secondary treatment from municipal wastewater treatment works (CDPHE, 2018). Considering the distinct physicochemical characteristics between UOG and domestic wastewaters, the legitimacy of UOG wastewater reuse for agricultural irrigation remains in question. In addition, the potential effects of irrigation with treated UOG wastewater on crop health and safety have not been thoroughly evaluated. Existing studies have shown that untreated UOG wastewater, even diluted, reduces plant growth, yield, and even disease resistance (Pica et al., 2017; Miller et al., 2019; Sedlacko et al., 2019). It is unknown whether wastewater treatment would avoid such adverse effects. The knowledge gaps at the interface of food, human health, and wastewater hinder the development of appropriate guidelines for the reuse of UOG wastewater in agricultural irrigation.

7.3.3 The barrier of economic feasibility

The economic cost is the ultimate determining factor for the feasibility of UOG wastewater treatment and reuse. If the economic prospect of wastewater treatment and reuse is uncertain or potentially unfavorable, the UOG industry will not shift the wastewater management paradigm away from deep-well injection voluntarily, unless pushed by regulatory or policy incentives or resource limitations. The total cost of UOG wastewater treatment and reuse needs to include the

expenses of both wastewater treatment (capital, operational, and maintenance cost) and logistics (for transportation and storage of raw and treated wastewater). Energy consumption accounts for a large proportion of the treatment cost (Deshmukh et al., 2018), and technologies that can leverage inexpensive energy sources such as low-grade thermal energy have the potential to improve the economic viability of UOG wastewater treatment. For example, the use of waste heat was estimated to decrease the cost of MD treatment dramatically from \$5.70/m^3_{feed} to \$0.74/m^3_{feed} (Tavakkoli et al., 2017). As discussed above, the feasibility of utilizing low-grade thermal energy have not been well understood for UOG wastewater treatment (Robbins et al., 2020). The cost associated with additional facilities or materials required for harvesting low-grade thermal energy (such as equipment and material for waste heat capture and storage, solar panels or photothermal materials for the use of solar energy) needs to be considered and compared with the benefit of energy savings. These issues, if not adequately addressed, will prevent practical usage of low-grade thermal energy as a feasible energy resource for UOG wastewater treatment.

Furthermore, the logistics cost for water transportation and storage plays an important but often neglected role in the economic prospect of UOG wastewater treatment (Robbins et al., 2021). UOG wastewater could be treated either by on-site individual facilities or off-site at a centralized wastewater treatment plant. The latter requires the transport of wastewater to the plant via either trucks or pipelines, with distance dictating the economic viability (Duthu and Bradley, 2017). Conversely, on-site treatment avoids wastewater transportation costs, while in this distributed treatment scenario economy of scale is sacrificed. A high number of small-scale treatment facilities have to be deployed to the well sites that require permitting, encountering more regulatory burdens. While deployment of small-scale systems represents challenges,

advantages include the opportunity to tailor the treatment capacity to wastewater flow rates. The economic cost of UOG wastewater treatment is influenced by the utilization of treatment capacity, which is determined by the flexibility to adjust assets (i.e., treatment equipment) based on the treatment demand. Thus, modular treatment systems (such as membrane-based technologies) could improve the viability of UOG wastewater treatment by being adaptable to the variation of wastewater volume. Furthermore, the treated product water needs to be distributed to the end-use locations, resulting in an additional cost that is not needed by deep-well injection. Logistics cost, which could outweigh the treatment cost itself, need to be considered when comparing with deep-well injection.

Additionally, the above discussions do not include the benefits of water conservation because of UOG wastewater treatment and reuse. When the value of water is estimated in the context of use, its value varies greatly (Colby, 1989; Ward et al., 1996). Thus, the value of UOG wastewater treatment is intertwined with the valuation of water across its reuse applications. So far, the broader economic and social values of the treated wastewater have not been adequately quantified. Compared to deep-well injection, UOG wastewater reuse conserves significant amounts of water within the hydrologic cycle, thereby improving the inter- and intra-generation equity associated with water supply. A comprehensive quantification of such benefits would present a fuller decision environment and result in policy incentives that promote the feasibility of UOG wastewater treatment and reuse. Triple bottom line reporting, which includes economics, social and environmental considerations, and full cost accounting are required, broadening economic accounting frameworks by including internal and external costs as well as benefits across the social and environmental considerations of wastewater treatment and reuse (Antheaume, 2004; Kenway et al., 2007). Accounting for the value of the water that UOG

wastewater treatment supplants would provide context for determining the feasibility of treatment projects as well as aid in resolving conflicts between UOG production and the public.

7.3.4 The barrier of social acceptance

The wide adoption of UOG wastewater treatment for beneficial reuse requires overcoming the issue of social acceptance. Although the social aspect has been rarely discussed for UOG wastewater treatment and reuse, it has been reported that municipal wastewater reuse projects have encountered skepticism and negative perceptions from the public, resulting in various project failures (Harris-Lovett et al., 2015). These negative perceptions are grounded in cognitive bias and failures in risk communication in which water managers routinely label such water as treated wastewater instead of recycled water, two terms that functionally describe identical processes but result in vastly different views of social acceptance (Menegaki et al., 2009; Mukheibir and Mitchell, 2018).

Establishing the legitimacy of beneficial wastewater reuse, as attempted with municipal wastewater reuse for potable purposes (Harris-Lovett et al., 2015), is an essential step to attaining social acceptance. Reframing public communication (e.g., branding the water product as recycled water) and promoting wastewater reuse through demonstration projects accessible to the public can encourage broader social acceptance. Similarly, beneficial reuse of UOG wastewater needs to mesh with the values and social beliefs of the communities where legitimacy needs to be gained (Harris-Lovett et al., 2015). A better understanding of the social context within the communities is needed to evaluate the viability of UOG wastewater reuse in a specific area. Furthermore, a reasonable and explicit regulatory framework, which is based on solid and transparent scientific evidence, is crucial to obtain legitimacy and public acceptance.

Furthermore, UOG wastewater reuse faces a greater challenge in gaining social acceptance compared to municipal wastewater reuse, due to the controversial nature of the UOG industry. Negative connotations plague UOG production regarding environmental and public health consequences, socio-economic impacts, and environmental justice (Clarke et al., 2016; Macnaghten, 2017; Cotton and Charnley-Parry, 2018; Kroepsch et al., 2019). Communicating the magnitude of potential impacts associated with UOG wastewater management to the public in transparent and logical manners is challenging but vital (Mukheibir and Mitchell, 2018). Narrative-based risk communication has been proposed as an option that helps the public think in a more concrete manner on community impacts, providing a potential avenue to greater public acceptance of UOG activities and its beneficial wastewater reuse (Clarke et al., 2016). However, accounting for nuanced geographic, cultural, and social variations across UOG production regions is imperative to achieve any success in communicating risk to facilitate informed decisions on UOG wastewater treatment and reuse (Clarke et al., 2016).

7.4 A Systems Approach is Needed for Wide Implementation of UOG Wastewater Treatment and Reuse

In this article, we analyzed four major barriers (i.e., technology, regulation, economics, and social acceptance) to wide implementation of wastewater treatment and reuse in the UOG industry (Figure 7-3). We emphasize that overcoming these barriers cannot rely strictly on technology development but require system-level innovations that take the entire system of UOG wastewater treatment and reuse into comprehensive consideration. The development of treatment technologies should be tailored to specific reuse applications and the corresponding regulations. Meanwhile, the establishment of reasonable water quality standards for UOG wastewater reuse is built upon the best available technologies as well as an in-depth understanding of the ecological and health risks of the treated wastewater. The logistics cost due to the transportation of both raw

and treated UOG wastewater need to be included in the economics analysis, and such a cost is dependent on the available reuse options that need to comply with the regulatory framework. Further, a reasonable regulatory framework and a better understanding of the social, economic, and environmental benefits by converting UOG wastewater to a valuable water resource are the prerequisites in gaining public acceptance. As a result, an integrated and interactive treatment system needs to be established based on a combination of technology innovation, regulatory compliance, cost minimization, and public communication. Such a system is essential to render UOG wastewater treatment and reuse a feasible and advantageous practice compared to deep-well injection.

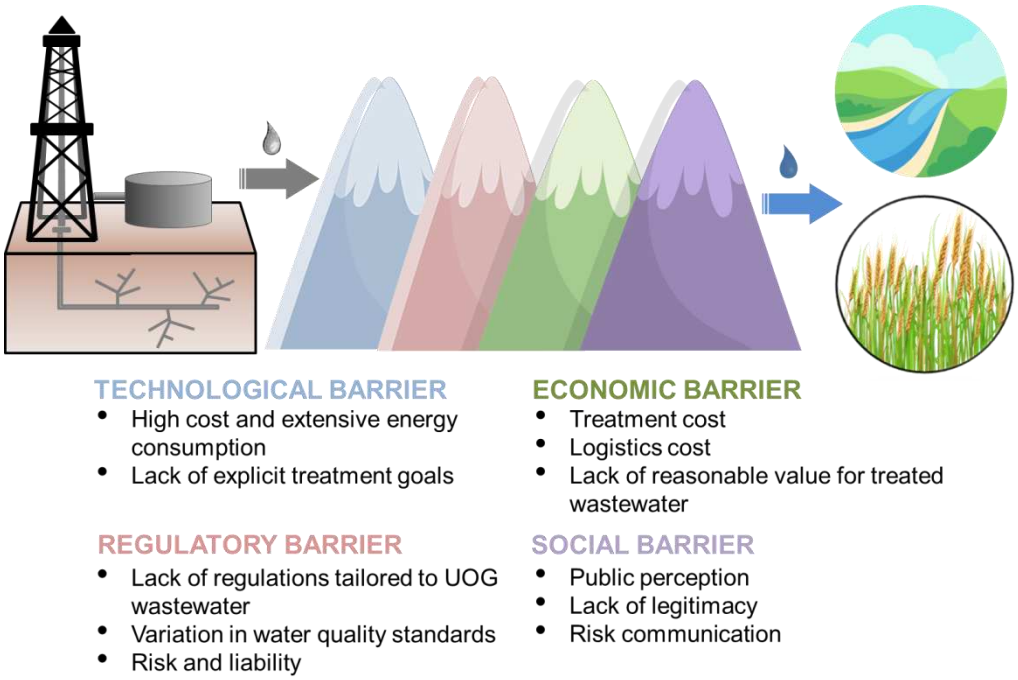

Figure 7-3. A summary of four main barriers against the wide implementation of UOG wastewater treatment and reuse. Addressing those barriers require a systems approach beyond technology development.

Achieving such a system requires broad collaborations across multiple disciplines pertaining to technology, policy, legislation, economics, and social science. More interactions and communications between academia, industry, and regulators are crucial to identify cross-cutting

research needs to shift UOG wastewater management towards treatment and reuse. The involvement of economists will help engineers and policy makers to better understand the value of water recovered from UOG wastewater reuse, creating necessary incentives that motivate UOG producers to employ wastewater treatment for external reuse. Social scientists will also be pivotal in elucidating sociological factors that could hinder or enhance the viability of UOG wastewater reuse in various communities. Furthermore, the rise of the big-data era provides more avenues to build a more efficient, agile, and smarter system for UOG wastewater treatment and reuse. Joint efforts of computer scientists, data scientists, and environmental engineers will greatly enhance our capability to engage with the complexity of this integrated system. For example, by leveraging an increasing number of publicly accessible databases, we are able to better understand and predict both spatial and temporal variations in the demands of UOG wastewater treatment and reuse, thereby minimizing the system cost and fragility through data-driven optimization. It should be emphasized that the perspectives we convey in this article do not underappreciate the value of technology development, which has significantly promoted the efficacy, versatility, and energy efficiency of UOG wastewater treatment. Instead, we are encouraging researchers to apply a systems approach to guide more appropriate and tailored technology innovation, thereby transforming treatment technologies invented in the laboratory into true environmental solutions that improve environmental sustainability in the context of rising UOG production.

References

Antheaume, N., Valuing external costs – from theory to practice: Implications for full cost environmental accounting. *European Accounting Review* **2004**, 13 (3), 443-464.

Brantley, S. L.; Yoxtheimer, D.; Arjmand, S.; Grieve, P.; Vidic, R.; Pollak, J.; Llewellyn, G. T.; Abad, J.; Simon, C. Water resource impacts during unconventional shale gas development: The Pennsylvania experience. *Int. J. Coal Geol.* **2014,** *126*, 140-156.

Butkovskyi, A.; Bruning, H.; Kools, S. A. E.; Rijnaarts, H. H. M.; Van Wezel, A. P. Organic Pollutants in Shale Gas Flowback and Produced Waters: Identification, Potential Ecological Impact, and Implications for Treatment Strategies. *Environ. Sci. Technol.* **2017,** *51* (9), 4740-4754.

Chang, H.; Li, T.; Liu, B.; Vidic, R.; Elimelech, M.; Crittenden, J. C. Potential and implemented membrane-based technologies for the treatment and reuse of flowback and produced water from shale gas and oil plays: A review. *Desalination* **2019,** *455*, 34-57.

Clarke, C.E.; Bugden, D.; Hart, P.S.; Stedman, R.C.; Jacquet, J.B.; Evensen, D.T.N.; Boudet, H.S. How geographic distance and political ideology interact to influence public perception of unconventional oil/natural gas development. *Energy Policy.* **2016**, 97, 301-309.

Colby, B.G. Estimating the value of water in alternative uses. *Nat. Resour. J.* **1989**, 29 (2), 511-527.

Colorado Department of Public Health and Environment. Reclaimed water control regulation. *5 CCR 1002-84*, Denver, CO, 2018.

Cotton, M.; Charnley-Parry, I. Beyond opposition and acceptance: Examining public perceptions of the environmental and health impacts of unconventional oil and gas extraction. *Curr. Opinion Environ. Sci. Health.* **2018**, 3, 8-13.

Deshmukh, A.; Boo, C.; Karanikola, V.; Lin, S. H.; Straub, A. P.; Tong, T. Z.; Warsinger, D. M.; Elimelech, M. Membrane distillation at the water-energy nexus: limits, opportunities, and challenges. *Energy Environ. Sci.* **2018,** *11*, 1177-1196.

Dolan, F. C.; Cath, T. Y.; Hogue, T. S. Assessing the feasibility of using produced water for irrigation in Colorado. *Sci. Total Environ.* **2018,** *640*, 619-628.

Dongare, P. D.; Alabastri, A.; Pedersen, S.; Zodrow, K. R.; Hogan, N. J.; Neumann, O.; Wu, J. J.; Wang, T. X.; Deshmukh, A.; Elimelech, M.; Li, Q. L.; Nordlander, P.; Halas, N. J. Nanophotonics-enabled solar membrane distillation for off-grid water purification. *P. Natl. Acad. Sci. USA* **2017,** *114* (27), 6936-6941.

Duthu, R.C.; Bradley, T.H. A road damage and life-cycle greenhouse gas comparison of trucking and pipeline water delivery systems for hydraulically fractured oil and gas field development in Colorado. *PLoS One* **2017**, 12 (7), e0180587.

Echchelh, A.; Hess, T.; Sakrabani, R. Reusing oil and gas produced water for irrigation of food crops in drylands. *Agr. Water Manage.* **2018,** *206*, 124-134.

Ellsworth, W. L. Injection-induced earthquakes. *Science* **2013,** *341* (6142), 1225942.

Enviro-Tox Services. *Irrigation Water Quality Evaluation Cawelo Water District Bakersfield, California*; Irvine, CA: 2016, p. 484.

Estrada, J. M.; Bhamidimarri, R. A review of the issues and treatment options for wastewater from shale gas extraction by hydraulic fracturing. *Fuel* **2016,** *182*, 292-303.

Ford, J.A.; Steen, J.; Verreynne, M-L. How environmental regulations affect innovation in the Australian oil and gas industry: Going beyond the Porter Hypothesis. *J. Clean. Prod.* **2014**, 84, 204-213.

Gregory, K.; Mohan, A. M. Current perspective on produced water management challenges during hydraulic fracturing for oil and gas recovery. *Environ. Chem.* **2015,** *12* (3), 261-266.

Groundwater Protection Council. *Produced Water Report: Regulations, Current Practices, and Research Needs*; Oklahoma City, OK, 2019, p. 310.

Groundwater Protection Council and Interstate Oil and Gas Compact Commission. FracFocus Data Download. https:/fracfocus.org/data-download (accessed June 18, 2020).

Harris-Lovett, S.R.; Binz, C.; Sedlak, D.L.; Kiparsky, M.; Truffer, B. Beyond user accetpance: A legitimacy framework for potable water reuse in California. *Environ. Sci. Technol.* **2015**, 49, 7552-7561.

Hincks, T.; Aspinall, W.; Cooke, R.; Gernon, T. Oklahoma's induced seismicity strongly linked to wastewater injection depth. *Science* **2018,** *359* (6381), 1251.

Lokare, O. R.; Tavakkoli, S.; Rodriguez, G.; Khanna, V.; Vidic, R. D. Integrating membrane distillation with waste heat from natural gas compressor stations for produced water treatment in Pennsylvania. *Desalination* **2017,** *413*, 144-153.

Kasich, J. Executive Order 2012-09K: The Emergency Amendment of Rules 1501:9-3-06 and 1501:9-3-07 of the Ohio Administrative Code by the Ohio Department of Natural Resources, Division of Oil and Gas Resources Management. Office of Ohio Governor: Columbus, OH, 2012.

Kenway, S.J.; Howe, C.; Maheepala, S. *Triple Bottom Line Reporting of Sustainable Water Utility Performance*. American Water Works Association Research Foundation: Denver, Colorado, 2007, p. 147.

Keranen, K. M.; Weingarten, M.; Abers, G. A.; Bekins, B. A.; Ge, S. Sharp increase in central Oklahoma seismicity since 2008 induced by massive wastewater injection. *Science* **2014,** *345* (6195), 448-451.

Kondash, A. J.; Albright, E.; Vengosh, A. Quantity of flowback and produced waters from unconventional oil and gas exploration. *Sci. Total Environ.* **2017,** *574*, 314-321.

Kondash, A.; Lauer, N.; Vengosh, A. The intensification of the water footprint of hydraulic fracturing. *Sci. Advances* **2018,** *4*, eaar5982.

Kondash, A.J.; Redmon, J.H.; Lambertini, E.; Feinstein, L.; Weinthal, E.; Cabrales, L.; Vengosh, A. The impact of using low-saline oilfield produced water for irrigation on water and soil quality in California. *Sci. Total Environ.* **2020**, 733, 139392.

Kondash, A.; Vengosh, A., Water footprint of hydraulic fracturing. *Environ. Sci. Technol. Let.* **2015,** *2* (10), 276-280.

Kroepsch, A.C.; Maniloff, P.T.; Adgate, J.L.; McKenzie, L.M.; Dickinson, K.L. Environmental justice in unconventional oil and natural gas drilling and production: A critical review and research agenda. *Environ. Sci. Technol.* **2019**, 53, 6601-6615.

Macnaghten, P. Distrust for fracking. *Nature Energy.* **2017**, 2, 17059.

Mantell, M. E. Produced Water Reuse and Recycling Challenges and Opportunities Across Major Shale Plays. *USEPA Technical Workshops for the Hydraulic Fracturing Study: Water Resources Management*, USEPA Office of Research and Development: Arlington, VA, 2011.

Matthews, C. The Next Big Bet in Fracking: Water. *Wall Street Journal (online)*, https://www.wsj.com/articles/the-next-big-bet-in-fracking-water-1534930200 (accessed May 10, 2020).

McLaughlin, M. C.; Borch, T.; McDevitt, B.; Warner, N. R.; Blotevogel, J. Water quality assessment downstream of oil and gas produced water discharges intended for beneficial reuse in arid regions. *Sci. Total Environ.* **2020,** *713*, 136607.

Menegaki, A.N.; Mellon, R.C.; Vrentzou, A.; Koumakis, G.; Tsagarakis, K.P. What's in a name: Framing treated wastewater as recycled water increases willingness to use and willingness to pay. *J. Econ. Psychol.* **2009**, 30 (3), 285-292.

Miller, H.; Trivedi, P.; Qiu, Y. H.; Sedlacko, E. M.; Higgins, C. P.; Borch, T. Food crop irrigation with oilfield-produced water suppresses plant immune response. *Environ. Sci. Tech. Let.* **2019,** *6* (11), 656-661.

Mukheibir, P.; Mitchell, C. The influence of context and perception when designing out risks associated with non-potable urban water reuse. *Urban Water J.* **2018**, 15 (5), 461-468.

National Drought Mitigation Center. U.S. Drought Monitor. https://droughtmonitor.unl.edu (accessed June 20, 2020).

National Research Council. *Water Reuse: Potential for Expanding the Nation's Water Supply Through Reuse of Municipal Wastewater*; The National Academies Press: Washington DC, 2012, p. 276.

Pica, N. E.; Carlson, K.; Steiner, J. J.; Waskom, R. Produced water reuse for irrigation of non-food biofuel crops: Effects on switchgrass and rapeseed germination, physiology and biomass yield. *Ind. Crop Prod.* **2017,** *100*, 65-76.

Rahm, B. G.; Riha, S. J. Evolving shale gas management: water resource risks, impacts, and lessons learned. *Environ. Sci. Process Impacts* **2014,** *16* (6), 1400-12.

Reig, P.; Luo, T.; Proctor, J. N. *Global Shale Gas Development: Water Availability and Business Risks*; World Resources Institute: January 2013, p. 66.

Robbins, C.A.; Grauberger, B.M.; Garland, S.D.; Carlson, K.H.; Lin, S.; Bandhauer, T.M.; Tong, T. On-site treatment capacity of membrane distillation powered by waste heat or natural gas for unconventional oil and gas wastewater in the Denver-Julesburg Basin. *Environ. Inter.* **2020**, 145, 106142.

Robbins, C.A.; Carlson, K.H.; Garland, S.D.; Bandhauer, T.M.; Grauberger, B.M.; Tong, T. Spatial analysis of membrane distillation powered by waste heat from natural gas

compressor stations for unconventional oil and gas wastewater treatment in Weld County, Colorado. *ACS Environ. Sci. Tech. Engg.* **2021**, 1 (2), 192-203.

Sanders, E.; Yuan, Y.; Pitchford, A. Fecal coliform and E. coli concentrations in effluent-dominated streams of the upper Santa Cruz watershed. *Water* **2013,** *5* (1), 243-261.

Sandra Ladra v. New Dominion, LLC. Supreme Court of Oklahoma (February 10, 2015).

Scanlon, B. R.; Ikonnikova, S.; Yang, Q.; Reedy, R. C. Will Water Issues Constrain Oil and Gas Production in the United States? *Environ. Sci. Technol.* **2020a,** *54* (6), 3510-3519.

Scanlon, B. R.; Reedy, R. C.; Male, F.; Hove, M. Managing the Increasing Water Footprint of Hydraulic Fracturing in the Bakken Play, United States. *Environ. Sci. Technol.* **2016,** *50* (18), 10273-10281.

Scanlon, B. R.; Reedy, R. C.; Xu, P.; Engle, M.; Nicot, J. P.; Yoxtheimer, D.; Yang, Q.; Ikonnikova, S. Can we beneficially reuse produced water from oil and gas extraction in the U.S.? *Sci. Total Environ.* **2020b,** *717*, 137085.

Scanlon, B. R.; Weingarten, M. B.; Murray, K. E.; Reedy, R. C. Managing Basin‐Scale Fluid Budgets to Reduce Injection‐Induced Seismicity from the Recent U.S. Shale Oil Revolution. *Seis. Res. Let.* **2019**, 90 (1), 171-182.

Sedlacko, E. M.; Jahn, C. E.; Heuberger, A. L.; Sindt, N. M.; Miller, H. M.; Borch, T.; Blaine, A. C.; Cath, T. Y.; Higgins, C. P. Potential for beneficial reuse of oil and gas-derived produced water in agriculture: Physiological and morphological responses in spring wheat (Triticum aestivum). *Environ. Toxicol. Chem.* **2019,** *38* (8), 1756-1769.

Self, C. Adoption of Amendments to 16 Tex. Admin. code 3.9, relating to disposal wells, and 3.46, relating to fluid injection into productive reservoirs; oil and gas docket No. 20-0290951. Texas Railroad Commission: Austin, TX, 2014.

Shaffer, D. L.; Arias Chavez, L. H.; Ben-Sasson, M.; Romero-Vargas Castrillon, S.; Yip, N. Y.; Elimelech, M. Desalination and reuse of high-salinity shale gas produced water: drivers, technologies, and future directions. *Environ. Sci. Technol.* **2013,** *47* (17), 9569-83.

Shaffer, D. L.; Tousley, M. E.; Elimelech, M. Influence of polyamide membrane surface chemistry on gypsum scaling behavior. *J. Membr. Sci.* **2017,** *525*, 249-256.

Skinner, M. Oil and Gas Disposal Well Volume Reduction Plan. Oklahoma Oil & Gas Conservation Division: Oklahoma City, OK, 2015.

Tavakkoli, S.; Lokare, O. R.; Vidic, R. D.; Khanna, V. A techno-economic assessment of membrane distillation for treatment of Marcellus shale produced water. *Desalination* **2017,** *416*, 24-34.

Tong, T. Z.; Carlson, K. H.; Robbins, C. A.; Zhang, Z. Y.; Du, X. W. Membrane-based teatment of shale oil and gas wastewater: The current state of knowledge. *Front. Environ. Sci. Eng.* **2019,** *13*, 63.

Tong, T. Z.; Elimelech, M. The global rise of zero liquid discharge for wastewater management: Drivers, technologies, and future directions. *Environ. Sci. Technol.* **2016,** *50* (13), 6846-6855.

USEPA. 40 CFR Part 435 Effluent Limitations Guidelines and Standards for the Oil and Gas Extraction Point Source Category. Federal Register, 2016; Vol. 81 FR 67191, pp 41845 - 41857.

USEPA. *Bacterial Water Quality Standards for Recreational Waters*; Washington, D.C., 2003.

USEPA. Class II Oil and Gas Related Injection Wells. https://www.epa.gov/uic/class-ii-oil-and-gas-related-injection-wells (accessed April 24, 2020a).

USEPA. Unconventional Oil and Gas Extraction Effluent Guidelines. https://www.epa.gov/eg/unconventional-oil-and-gas-extraction-effluent-guidelines (accessed April 24, 2020b).

Vengosh, A.; Jackson, R. B.; Warner, N.; Darrah, T. H.; Kondash, A. A critical review of the risks to water resources from unconventional shale gas development and hydraulic fracturing in the United States. *Environ. Sci. Technol.* **2014,** *48* (15), 8334-48.

Vidic, R. D.; Brantley, S. L.; Vandenbossche, J. M.; Yoxtheimer, D.; Abad, J. D. Impact of shale gas development on regional water quality. *Science* **2013,** *340* (6134), 1235009.

Ward, F.A.; Roach, B.A.; Henderson, J.E. The economic value of water in recreation: Evidence from the California drought. *Water Resour. Res.* **1996**, 32 (4), 1075-1081.

Wang, Z. X.; Horseman, T.; Straub, A. P.; Yip, N. Y.; Li, D. Y.; Elimelech, M.; Lin, S. H. Pathways and challenges for efficient solar-thermal desalination. *Sci. Advances* **2019,** *5* (7).

Weingarten, M.; Ge, S.; Godt, J. W.; Bekins, B. A.; Rubinstein, J. L. High-rate injection is associated with the increase in U.S. mid-continent seismicity. *Science* **2015,** *348* (6241), 1336-1340.

Wethe, D.; Crowley, K. Drowning in dirty water, Permian seeks $22 billion lifeline. *Bloomberg News (online)*, https://www.bloomberg.com/news/articles/2018-08-29/drowning-in-dirty-water-permian-seeks-a-22-billion-lifeline (accessed May 11, 2020).

Whitfield, S. Permian, Bakken Operators Face Produced Water Challenges. *J. Petrol. Technol.* **2017,** *69* (6). https://doi.org/10.2118/0617-0048-JPT.

Winglee, J. M.; Bossa, N.; Rosen, D.; Vardner, J. T.; Wiesner, M. R. Modeling the concentration of volatile and semivolatile contaminants in direct contact membrane distillation (DCMD) product water. *Environ. Sci. Technol.* **2017,** *51* (22), 13113-13121.

Yang, Z.; Guo, H.; Tang, C. Y. The upper bound of thin-film composite (TFC) polyamide membranes for desalination. *J. Membr. Sci.* **2019,** 590, 117297.

Zhang, Z. Y.; Du, X. W.; Carlson, K. H.; Robbins, C. A.; Tong, T. Z. Effective treatment of shale oil and gas produced water by membrane distillation coupled with precipitative softening and walnut shell filtration. *Desalination* **2019,** 454, 82-90.

8.0 CONCLUSIONS AND RECOMMENDATIONS

8.1 Conclusions

Beneficial reuse in unconventional oil and gas (UOG) wastewater management is an emerging alternative to deep-well injection (DWI) to handle the ever-increasing wastewater volumes from unconventional energy production. In water stressed regions, beneficial reuse of UOG wastewater could help alleviate water sourcing issues within various sectors with high water demand. However, a better understanding of key aspects such as technology, logistics, economics, and regulations within UOG wastewater management is needed, specifically at a regional scale. The overall objective of this work was to systematically analyze these key aspects in order to further facilitate increased beneficial reuse within UOG wastewater management.

In the first research objective, the on-site treatment capacity of membrane distillation (MD) powered by waste heat or natural gas was quantified at 20 wells in Weld County, CO. On-site treatment eliminates the costly need for transportation of UOG wastewater either for DWI or off-site treatment. There was a knowledge gap in the body of literature in regards to quantifying the amount of waste heat or natural gas available at a well-pad and if this energy source would meet the treatment demand based on wastewater flow. Our research demonstrated that waste heat from hydraulic fracturing (HF) activity is a valuable energy source for on-site MD treatment during the initial few months of wastewater production. However, the feasibility of waste heat from HF for on-site MD treatment varies among well sites and is dependent on the efficiencies of MD and thermal energy storage. Well-pad natural gas provides a more consistent supply of thermal energy than waste heat and easily meets the treatment demand for the majority of the 20 wells evaluated. A hybrid configuration utilizing both waste heat and natural gas as the energy sources

for MD treatment of UOG wastewater is intriguing, however, its practical implementation may be challenging due to the complexity and economic cost.

For the second research objective, a spatial analysis framework was developed using ArcGIS software for Weld County, Colorado to determine the effect of transportation distance and cost related to UOG wastewater management. Specifically, transportation distance and cost was determined to either transport UOG wastewater from a production well to the nearest disposal well (current predominant UOG wastewater management strategy in Weld County, CO) or to a theoretical centralized wastewater treatment (CWT) facility using MD as its core technology. The centralized wastewater treatment facility is co-located with a natural gas compressor station (NGCS) to take advantage of the waste heat generated at the station to power MD treatment. When evaluating the two options at a county scale, transporting to the nearest disposal well was the more advantageous strategy. However, by removing a small portion of the county (located in northeast Weld County) that overwhelmingly favored DWI, the analysis showed that the two options became comparable. When refining the scale of the analysis further to a smaller area of Weld County, a slight advantage developed for CWT in regards to transportation distance and cost. This demonstrated the importance of the spatial analysis scale when considering logistics such as transportation.

The third research objective built upon the spatial analysis framework developed for Weld County discussed previously. A quantification of the waste heat available at the NGCSs in Weld County was completed followed by analysis to determine the feasibility of treating all UOG wastewater that located closest to each NGCS at a CWT facility. It was determined that for 30 of the 35 NGCS locations MD powered by NGCS waste heat could feasibly treat all the UOG wastewater sent to that location (UOG wastewater would be sent to an NGCS if transportation

distance was less than to the nearest disposal well). The quantification of NGCS waste heat available and spatial analysis showed a better correlation between waste heat quantity and UOG wastewater density in southeast and central Weld County. This analysis emphasized the importance of matching treatment demand with capacity provided by waste heat.

For the fourth research objective, two strategies to mitigate a major constraint of MD treatment of UOG wastewater, surfactant-induced membrane wetting, were compared. The two strategies, pretreatment using coagulation and walnut shell filtration to reduce surfactants and fabrication of an omniphobic membrane to resist wetting, were evaluated based on laboratory-scale MD experiments. UOG wastewater sourced from the DJ Basin in Weld County, CO was used in the MD experiments with MD performance in terms of water flux and permeate conductivity quantified. Both strategies vastly improved performance in regards to salt rejection rate when compared to the control which was MD treatment of raw UOG wastewater with a commercial PVDF membrane. However, MD treatment with an omniphobic membrane was constrained due to fouling/scaling that caused an unacceptable flux decline. To better understand the surfactant composition in the UOG wastewater, ultrahigh pressure liquid chromatography (UHPLC) coupled with quadrupole time-of-flight mass spectrometry (QToF/MS) was implemented to identify surfactants in the UOG wastewater and qualify the effect of pretreatment in reducing surfactants. From the analysis, 192 surfactants were identified in the UOG wastewater with 91 of those being reduced by full pretreatment.

In the final research objective, four main barriers (technology, regulations, economics, and social) for beneficial reuse of UOG wastewater were identified and discussed in-depth. Of these four barriers, the technological barrier receives the majority of the attention in regards to research. However, the other three barriers play an equally or possibly more important role in

future beneficial reuse of UOG wastewater. A systems approach focused on overcoming these barriers is needed for wider implementation of UOG wastewater treatment and reuse in the future. An integrated and interactive treatment system needs to be established based on a combination of technology innovation, regulatory compliance, cost minimization, and public communication. This system will require broad collaborations across multiple disciplines pertaining to technology, policy, legislation, economics, and social science.

8.2 Recommendations for Future Work

The present work provides extensive research into key aspects of UOG wastewater treatment and subsequent beneficial reuse. Specifically, most of the research centers on the use of membrane distillation as the core technology for UOG wastewater treatment. Waste heat integration with MD treatment of UOG wastewater is vital for its future viability. More research is needed in developing a system (either on-site at a well-pad or at centralized facility) that incorporates waste heat capture and its use in powering MD treatment of UOG wastewater. Considerations such as efficiency of waste heat storage and the temporal correlation between waste heat generation and UOG wastewater treatment need further study. A demonstration project involving waste heat capture and storage paired with MD treatment of UOG wastewater would assist in validating the feasibility of using waste heat to power MD for this application.

As MD is only one of multiple treatment technologies with the ability to treat hypersaline UOG wastewater, future research in conducting thorough techno-economic analyses (TEAs) comparing these technologies along with UOG wastewater management strategies (i.e., on-site treatment, centralized wastewater treatment, deep-well injection) in various regions. Aspects such as UOG wastewater salinity and composition, availability of DWI, and water scarcity varies

across UOG regions so TEAs need to be tailored to a region of interest to adequately compare technologies and strategies.

A systems-level approach to implementing UOG wastewater treatment and beneficial reuse that incorporates engineers, various type of scientists to include social, regulators and policymakers, and oil and gas entities is needed. Future research focused on developing a systems-level approach that utilizes expertise in various areas beyond just technology development is essential. Conducting thorough life cycle analyses of UOG wastewater treatment and beneficial reuse along with other management strategies will help inform the development of this approach.

Further, future research is needed at larger scales (i.e., pilot scale) to provide more data and experimental results regarding energy efficiency and performance for MD treatment of UOG wastewater. This research will help determine the viability of MD treatment of UOG wastewater in practical application.

Appendix A

Data collection of well information in Weld County, Colorado

Figure A1 shows the locations of 20 unconventional oil and gas (UOG) wells sampled within Weld County, Colorado for the current study (COGCC, 2019). Each of the 20 wells, as discussed in the main text, has data reported for wastewater production and natural gas production during a 12-month period (shown in Figures A2 and A3). These data were used to determine energy demands for MD treatment of UOG wastewater. The produced water and natural gas for the selected 20 wells were compared to data from 200 wells in the Denver-Julesburg basin (COGCC, 2019). Figure A2 shows that the 20 wells analyzed in detail for the present study are representative of the larger data set.

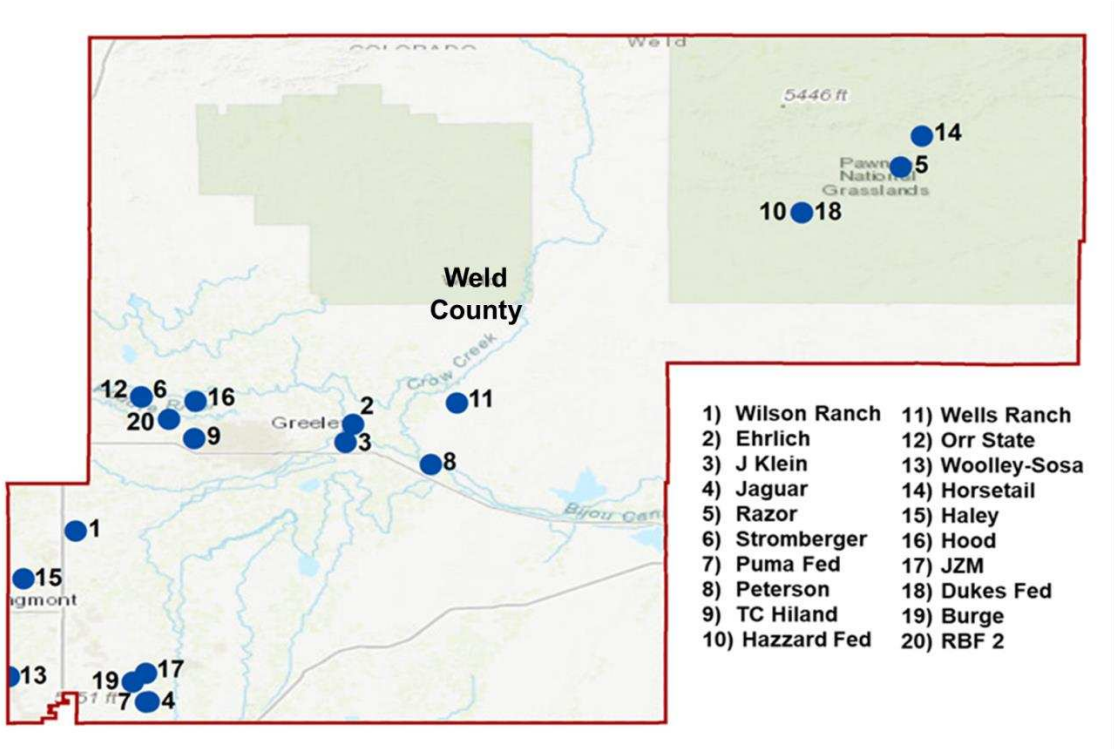

Figure A1. The map of Weld County, CO showing the locations of the 20 wells used in this study.

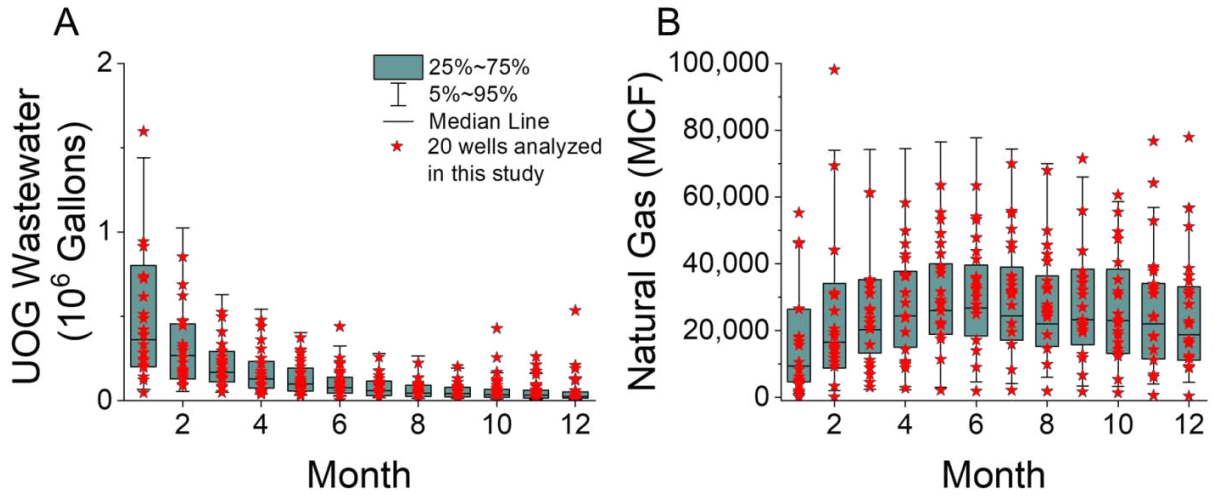

Figure A2. Data of monthly (A) UOG wastewater and (B) natural gas production data for 20 hydraulically fractured wells compared to 200 hydraulically fractured wells in Weld County, CO. The 200 wells are shown using a box-whisker plot. The 25th and 75th quantiles, the 5th and 95th quantiles, as well as the median values are presented. The data for the 20 wells are well distributed when compared to the 200 wells, indicating that the 20 wells analyzed in this study is well representative of hydraulically fractured wells in the investigated region in regards to UOG wastewater and natural gas production.

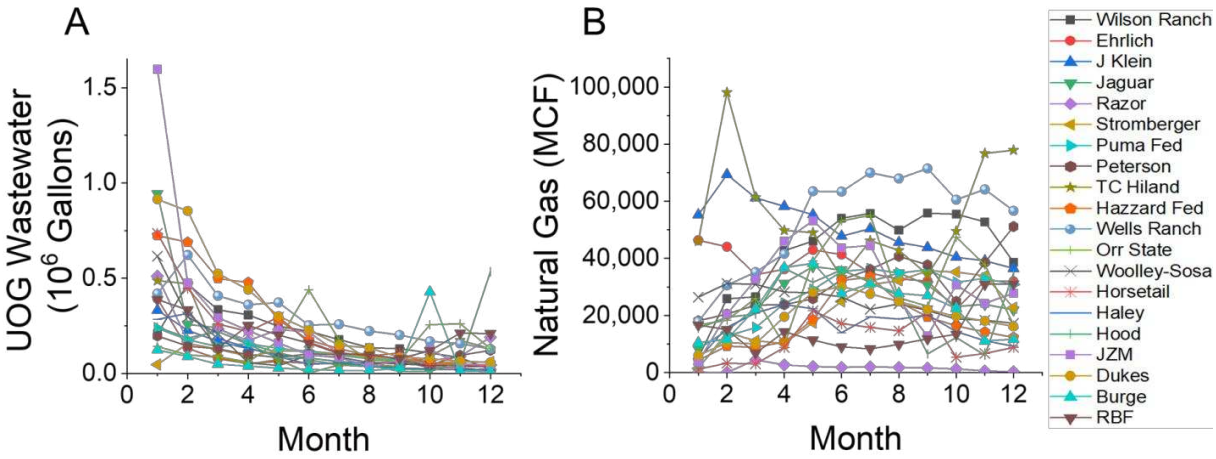

Figure A3. Data of monthly (A) UOG wastewater and (B) natural gas production data for 20 hydraulically fractured wells in Weld County, CO. Data were reported by Colorado Oil and Gas Conservation Commission (COGCC) through the Colorado Oil and Gas Information System (COGIS). Wells were completed between June 15, 2017 and August 26, 2017.

DCMD modeling results for energy consumption by MD

The specific thermal energy consumption attained from our DCMD model simulation ranged from 910 to 2,035 kJ kg^{-1} permeate, corresponding to gained output ratio (GOR) values between ~1.1-2.5 (Figure A4). The feedwater salinity of UOG wastewater in the DJ Basin is typically between 20,000-40,000 mg L^{-1} so the model simulation was run using three different salinities within this range. Additionally, the feedwater temperature was varied between 60-90 °C in the model simulation to investigate the effect of feedwater temperature on MD energy efficiency. The brine salinity was set at 200,000 mg L^{-1} and the distillate temperature was at 20 °C. The results indicate that the energy efficiency of MD improves as the feedwater temperature increases, while feedwater salinity imposes a negligible effect within the salinity range we investigated. Table A1 shows temperatures, mass flow rate, and salinity concentrations at the various nodes in the model.

Table A1. DCMD Model Parameters

	STEC = 910 kJ kg^{-1} permeate Recovery Rate = 90% Flux = 13.02 L m^{-2} h^{-1}			STEC = 2,035 kJ kg^{-1} permeate Recovery Rate = 80% Flux = 3.48 L m^{-2} h^{-1}		
Node	**Temperature**	**Mass flow rate**	**Salinity concentration**	**Temperature**	**Mass flow rate**	**Salinity concentration**
-	**°C**	**kg s^{-1}**	**%**	**°C**	**kg s^{-1}**	**%**
1	20	0.020	2	20	0.0060	4
2	74.11	0.30	18.79	50.52	0.30	19.68
3	90	0.30	18.79	60	0.30	19.68
4	32.34	0.28	20	28.61	0.28	20
5	32.34	0.0020	20	28.61	0.0012	20
6	32.34	0.28	20	28.61	0.29	20
7	77.5	0.28	20	50.95	0.29	20
8	55.01	0.018	0	40.01	0.0048	0
9	20	0.22	0	20	0.22	0
10	80.65	0.24	0	53.66	0.24	0
11	36.78	0.24	0	30.31	0.24	0
12	36.78	0.018	0	30.31	0.0048	0
13	36.78	0.22	0	30.31	0.23	0
14	90.71	0.49	-	60.43	0.49	-
15	83.3	0.49	-	55.8	0.49	-

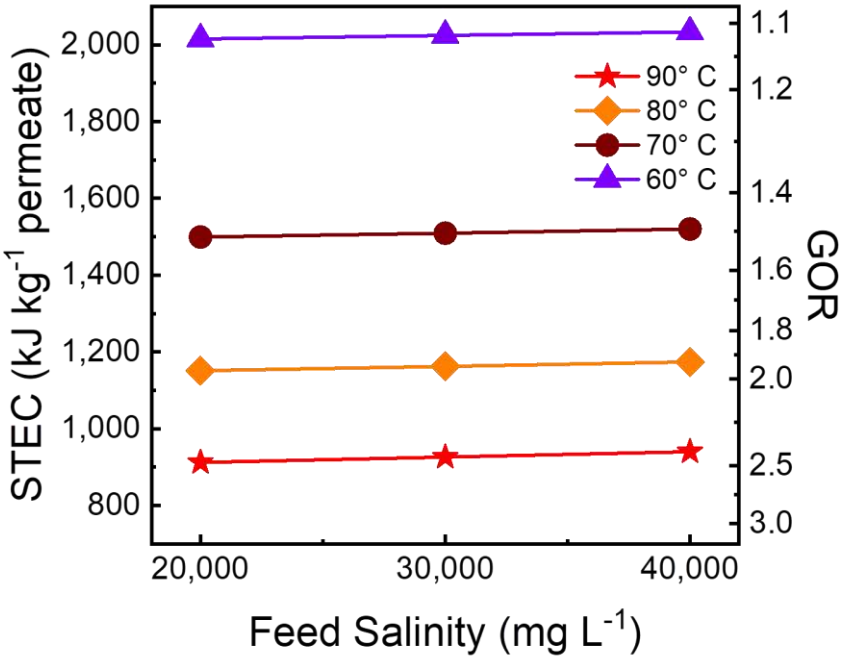

Figure A4. DCMD model simulation results for STEC and GOR at various feed salinities and feedwater temperatures.

Sources of waste heat associated with the UOG production process

Three waste heat sources are available during the typical UOG production process (Figure A5). During the pre-production phase, waste heat is available from the engines powering the hydraulic fracturing (HF) pumps, which is only available during the HF operation. During the production phase, waste heat is available from an engine powering a generator that is required to provide electrical power for on-site services during the well life such as instrumentation, air compressors, and downhole pumps. During the post-production phase, waste heat is available from engines powering natural gas compressor stations (NGCSs) which are installed along the pipeline transmission system. Since this study focuses on waste heat that is able to power on-site UOG wastewater treatment, waste heat from NGCSs is not included in our analysis due to the fact that the wastewater needs to be transported to the stations.

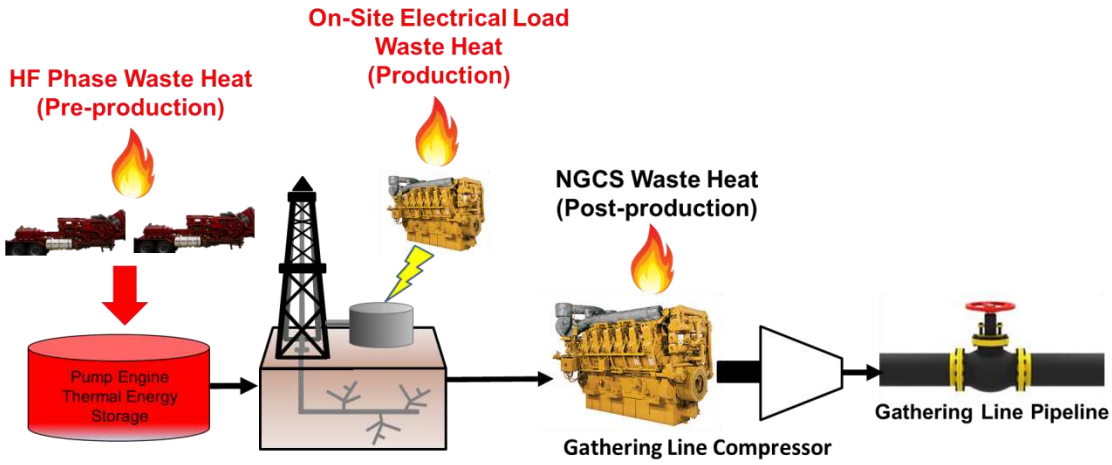

Figure A5. Sources of waste heat available during UOG production process. Waste heat from the HF phase (pre-production) and from the on-site electrical load (production phase) are used for analysis because they are able to power on-site MD treatment of UOG wastewater (highlighted by red).

Calculation of waste heat availability

Tables A2 provides detailed calculations of the waste heat available from the engines powering the HF phase of operation. In the approach used in Table A2, the pump and engine efficiencies are known, but the engine and pump powers are unknown (calculated from the HF water use of each well as reported by Colorado Oil and Gas Conservation Commission, COGCC). A pumping power of 10.7 MW is needed when no safety factor is considered (only considering $\dot{V}_{\text{water}} \times \Delta P$). In this approach, it is assumed that there is one high-powered engine-pump pair, and a safety factor of 1.5 is used to ensure there is extra power supply if needed, resulting in 16.1 MW of pumping power. Different durations (16-91 hours) are needed to achieve the volumes used for HF of the wells investigated in this study.

Table A3 shows the estimation of the waste heat generated from the full-time electrical loads on-site. These electrical loads are supplied by generator sets driven by either natural gas or diesel, with waste heat generated from generator sets that supply 8-10 kW of power when running at 50% load. The value used for waste heat rate was averaged from data shown in Table A4, which has information from several industry data sheets depicting efficiencies and waste heat values for a range of generator sets (supplying 8-10 kW at 50% load), as well as other size ranges with different percent loads for comparison purposes. Waste heat rate was calculated as the sum of coolant and exhaust heat from each generator set. Table A4 also shows that the sum of energy converted to power and available in the engine coolant and exhaust are less than the fuel input energy, with an average of 29.8% loss. The potential differences in the available waste heat might result from radiation losses, heat rejection to lubrication oil or aftercooler air, and mechanical to electrical energy conversion inefficiencies. Even though these are not captured in electrical energy or waste heat, the results in the main text demonstrate that capturing the

additional 11.75 kW of waste heat will not substantially impact the main conclusion: waste heat from engines located at individual wells is insufficient to power MD in nearly all the studied locations.

Table A2. Detailed calculation for waste heat available during HF operation based on theoretical pressures, volumetric flow rates, and operating efficiencies.

Variable	Assumption	Value	Units
Water volume (V_{water})	Typical water volume per well (COGCC, 2019)	4.1-22.5×10^6	gal
Initial pressure (P_i)	Ambient pressure	100	kPa
Pumping pressure (P_{pump})	Typical HF pressure (Kahrilas et al., 2016)	6000	psi
Pump efficiency (η_{pump})	Typical pump efficiency (Caterpillar, 2011; Halliburton, 2012)	89	%
Engine efficiency (η_{eng})	Typical diesel engine efficiency (Caterpillar, 2011)	43	%
Safety factor (SF)	Ensures enough power is provided	1.5	-
HF duration (Δt_f)	HF pump operational time	16-91	Hours
Waste heat capture efficiency (η_{waste})	Assume 100% capture efficiency to represent highest possible energy content	100	%
Variable	**Equation**	**Value**	**Units**
Required volume flow water ($\dot{V}_{water}$)	$\dot{V}_{water} = \frac{V_{water}}{\Delta T_f}$	0.26	$m^3\ s^{-1}$
Required pressure increase (ΔP)	$\Delta P = P_{pump} - P_i$	41.3	MPa
Pump power ($\dot{W}_{pump}$)	$\dot{W}_{pump} = \dot{V}_{water} \Delta P * SF$	16.1	MW
Engine power ($\dot{W}_{eng}$)	$\dot{W}_{eng} = \frac{\dot{W}_{pump}}{\eta_{pump}}$	18.1	MW
Waste heat rate ($\dot{Q}_{waste}$)	$\dot{Q}_{waste} = \frac{\dot{W}_{eng}}{\eta_{eng}} * (1 - \eta_{eng})$	24	MW
Total waste heat available (E_{waste})	$E_{waste} = \dot{Q}_{waste} \Delta t_f * \eta_{waste}$	1.4-7.9×10^9	kJ

Table A3. Detailed calculation for waste heat available from on-site electrical loads based on survey of industry standard data sheets.

Variable	Assumption	Value	Units
Waste heat rate ($\dot{Q}_{\text{waste}}$)	Typical waste heat from engine at 50% load delivering 8 to 10 kW of power	18.95	kW
Duration (Δt)	Total operating time	12	Months
Variable	**Equation**	**Value**	**Units**
Total waste heat available (E_{waste})	$E_{\text{waste}} = \dot{Q}_{\text{waste}} \Delta t$	5.9×10^{8}	kJ

Table A4. Survey of industry standard data sheets (Caterpillar, Cummins, GENERAC, Kohler)

Manufacturer	Model #	Fuel Type	Load	Power	Fuel Input Power	Thermal Efficiency	Coolant Heat	Exhaust Heat	Heat Accounted For
-	-	-	%	kW	kW	%	kW	kW	%
CAT	DE7.5E3S	Diesel	100	8	31.25	26	10	7.16	81%
CAT	DE9.5E3	Diesel	100	8	32.33	25	10	7.16	78%
CAT	DE9.5E3B	Diesel	100	8	31.25	26	10	7.16	81%
CAT	DE11E3S	Diesel	75	9	35.56	25	10.28	8.19	77%
CAT	DE13.5E3	Diesel	75	9	34.48	26	10.17	8.10	79%
CAT	DE13.5E3B	Diesel	75	9	34.48	26	10.17	8.10	79%
KOHLER	15REOZK	Diesel	75	9.75	43.11	23	14.50	2.40	62%
CAT	DE16E3S	Diesel	50	8.8	35.56	25	10.49	7.49	75%
CAT	DE18E3	Diesel	50	8	33.41	24	8.24	5.78	66%
GENERAC	RD020	Diesel	50	10	39.80	25	9.50	7.34	67%
CUMMINS	C20D6	Diesel	50	9.1	35.89	25	13.55	8.59	87%
GENERAC	SD020	Diesel	50	9	43.11	21	11.47	7.84	66%
KOHLER	20REOZK	Diesel	50	8.25	38.09	22	10.96	14.47	88%
CAT	DE22E3B	Diesel	50	9	35.56	25	10.43	7.45	76%
CAT	DE22E3	Diesel	50	9	35.56	25	10.43	7.45	76%
CUMMINS	C35D6	Diesel	25	8	42.78	19	10.02	9.69	65%
GENERAC	SD035	Diesel	25	8	39.10	20	7.68	9.94	66%
GENERAC	SG035	Gas	25	8	67.32	12	11.16	7.31	39%
CUMMINS	C40D6	Diesel	25	9	47.31	19	10.55	10.85	64%
GENERAC	SD040	Diesel	25	9	42.11	21	8.58	11.33	69%
KOHLER	40REOZK	Diesel	25	8.5	49.12	17	8.90	8.66	53%
KOHLER	KG40	Gas	25	9.25	63.72	15	15.00	14.90	61%

Natural gas composition

The composition of natural gas determines its lower heating value (LHV), which represents the amount of thermal energy released from burning/combusting the gas. The composition of natural gas changes significantly throughout regions in the U.S. In order to make a reasonable estimation for the Denver-Julesburg (DJ) Basin, the thermal energy contained in natural gas must be calculated based on the corresponding composition. Once the molecular percentage (*molf*) of each compound is known, the corresponding mass fraction (*mf*) can be calculated using the molecular weight (*MW*). The *mf* is then used to calculate the LHV using Equations A1-A3 as below.

$$MW_i = \sum_i^{elements} MW_{element} * N_{element} \text{(A1)}$$

$$mf_i = {molf_i * MW_i}\Big/{\sum_i^n molf_i * MW_i} \text{(A2)}$$

$$LHV = \sum_i^n mf_i * LHV_i \text{(A3)}$$

Table A5 shows a typical gas composition for the DJ Basin according to the U.S. Geological Survey (Higley and Cox, 2007). Table A6 describes the calculation of LHV for natural gas in the DJ basin based on the composition and compound properties shown in Table A5. Our calculation method resulted in a LHV of 45.8 MJ kg^{-1} in the DJ Basin. This correlates well with the typical LHV of treated natural gas (44-57 MJ kg^{-1}) (Boundy et al., 2011; U.S. EIA, 2019). Because the referenced composition has a variety of compounds that account for the remaining 1.7%, the major compounds are normalized to yield a mole fraction sum of 1.

Table A5. Composition of a typical natural gas mixture in the Denver-Julesburg Basin.

	Composition		Compound Properties			
Compound	**Molar Percentage**	**Normalized $molf_i$**	**LHV_i (kJ kg^{-1})**	**N_{Carbon}**	**$N_{Hydrogen}$**	**N_{Oxygen}**
Methane	82.6%	0.840	50024	1	4	0
Ethane	10.1%	0.103	47509	2	6	0
Propane	2.7%	0.028	46331	3	8	0
Pentane	0.3%	0.003	45717	5	12	0
Carbon Dioxide	2.6%	0.026	0	1	0	2
Totals	**98.3%**	**1**	--	--	--	--

Table A6. Detailed calculation for heat available from burning natural gas.

Variable	**Assumption**	**Value**	**Units**
Molecular Weight CH_4	Chemical formula	16.0	g mol^{-1}
Molecular Weight C_2H_6	Chemical formula	30.1	g mol^{-1}
Molecular Weight C_3H_8	Chemical formula	44.1	g mol^{-1}
Molecular Weight C_5H_{12}	Chemical formula	72.1	g mol^{-1}
Molecular Weight CO_2	Chemical formula	44.0	g mol^{-1}
Variable	**Equation**	**Value**	**Units**
Total Mass per Mole (M)	$M = \sum_i molf_i MW_i$	19.2	g mol^{-1}
Mass Fraction CH_4 (mf_{CH4})	$mf_{CH4} = \frac{molf_{CH4} MW_{CH4}}{M}$	0.70	-
Mass Fraction C_2H_6 (mf_{C2H6})	$mf_{C2H6} = \frac{molf_{C2H6} MW_{C2H6}}{M}$	0.16	-
Mass Fraction C_3H_8 (mf_{C3H8})	$mf_{C3H8} = \frac{molf_{C3H8} MW_{C3H8}}{M}$	0.06	-
Mass Fraction C_5H_{12} (mf_{C5H12})	$mf_{C5H12} = \frac{molf_{C5H12} MW_{C5H12}}{M}$	0.01	-
Mass Fraction CO_2 (mf_{CO2})	$mf_{CO2} = \frac{molf_{CO2} MW_{CO2}}{M}$	0.06	-
Lower Heating Value (*LHV*)	$LHV = \sum_i mf_i LHV_i$	45.8	MJ kg^{-1}

The ratio of energy demand of MD treatment to thermal energy provided by well-pad natural gas

When comparing the thermal energy generated from burning of natural gas to the thermal energy demand of MD treatment of UOG wastewater, a determination can be made on whether wastewater storage is required. The need of wastewater storage will impose a logistical cost of installing UOG wastewater storage tanks on-site. As shown in Figure A6, no wastewater storage would be required for 16 of the 20 wells during all the 12 months analyzed in the study. For the Razor, Hazzard Fed, Horsetail, and JZM wells, wastewater storage within the first two months is needed.

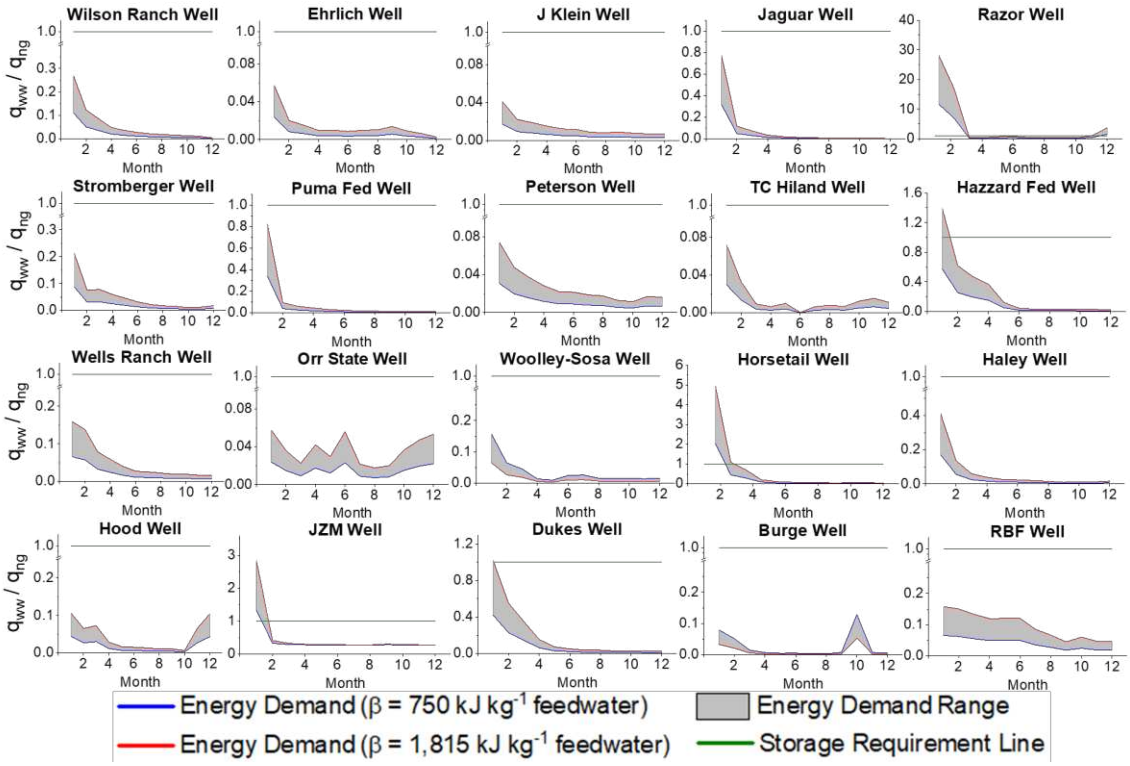

Figure A6. Ratio of thermal energy demand of wastewater treatment (q_{ww}) to thermal energy available from natural gas (q_{ng}) during 12 months for 20 wells in Weld County, CO. A storage required line (q_{ww}/q_{ng} = 1) was created to visually depict in which months there would be a requirement to store UOG wastewater due to insufficient natural gas being produced for MD treatment of wastewater from each well.

References

Boundy, B., Diegel, S., Wright, L., Davis, S., 2011. Biomass Energy Data Book: Edition 4; Oak Ridge National Laboratory: Oak Ridge, TN.

Caterpillar, 3512C HD Petroleum Engine. 2011. Caterpillar Web site. https://s7d2.scene7.com/is/content/Caterpillar/LEHW0056-01 (accessed May 13, 2019).

Caterpillar, Diesel Generator Set DE7.5E3S Data Sheet, 2016a. Caterpillar Web site. https://s7d2.scene7.com/is/content/Caterpillar/CM20160901-16936-26493 (accessed May 13, 2019).

Caterpillar, Diesel Generator Set DE9.5E3 Data Sheet, 2016b. Caterpillar Web site. https://s7d2.scene7.com/is/content/Caterpillar/CM20160901-15630-21889 (accessed May 13, 2019).

Caterpillar, Diesel Generator Set DE9.5E3B Data Sheet, 2016c. Caterpillar Web site. http://s7d2.scene7.com/is/content/Caterpillar/CM20180920-21994-42866 (accessed May 13, 2019).

Caterpillar, Diesel Generator Set DE11E3S Data Sheet, 2016d. Caterpillar Web site. http://s7d2.scene7.com/is/content/Caterpillar/CM20160901-15992-05681 (accessed May 13, 2019).

Caterpillar, Diesel Generator Set DE13.5E3 Data Sheet, 2016e. Caterpillar Web site. http://s7d2.scene7.com/is/content/Caterpillar/CM20160901-15992-08420 (accessed May 13, 2019).

Caterpillar, Diesel Generator Set DE13.5E3B Data Sheet, 2016f. Caterpillar Web site. http://s7d2.scene7.com/is/content/Caterpillar/CM20180920-22251-57947 (accessed May 13, 2019).

Caterpillar, Diesel Generator Set DE16E3S Data Sheet, 2016g. Caterpillar Web site. https://s7d2.scene7.com/is/content/Caterpillar/CM20160901-22292-21046 (accessed May 13, 2019).

Caterpillar, Diesel Generator Set DE18E3 Data Sheet, 2016h. Caterpillar Web site. https://s7d2.scene7.com/is/content/Caterpillar/CM20160901-22721-16587 (accessed May 13, 2019).

Caterpillar, Diesel Generator Set DE22E3B Data Sheet, 2016i. Caterpillar Web site. http://s7d2.scene7.com/is/content/Caterpillar/CM20180918-31801-45503 (accessed May 13, 2019).

Caterpillar, Diesel Generator Set DE22E3 Data Sheet, 2016l. Caterpillar Web site. https://s7d2.scene7.com/is/content/Caterpillar/CM20160901-23279-16986 (accessed May 13, 2019).

Colorado Oil and Gas Conservation Commission, 2019. Colorado Oil and Gas Information System Home Page. https://cogcc.state.co.us/data.html#/cogis (accessed May 4, 2019).

Cummins, C20D6 Diesel Generator Set Data Sheet, 2017a. Cummins Web site. https://powersuite.cummins.com/PS5/PS5Content/SiteContent/en/Binary_Asset/pdf/Commercial/SparkIgnited/NAS-5869-EN.pdf (accessed May 16, 2019).

Cummins, C35D6 Diesel Generator Set Data Sheet, 2017b. Cummins Web site. https://powersuite.cummins.com/PS5/PS5Content/SiteContent/en/Binary_Asset/pdf/KentData/DataSheets/DS96-CPGK.pdf (accessed May 16, 2019).

Cummins, C40D6 Diesel Generator Set Data Sheet, 2017c. Cummins Web site. https://powersuite.cummins.com/PS5/PS5Content/SiteContent/en/Binary_Asset/pdf/KentData/SpecSheets/SS29-CPGK.pdf (accessed May 16, 2019).

GENERAC, RD020 Diesel Generator Set Data Sheet, 2016. GENERAC Web site. http://www.generac.com/Industrial/products/diesel-generators/standard/protector-series-20kw-diesel-generator (accessed May 15, 2019).

GENERAC, SD020 Industrial Diesel Generator Set Data Sheet, 2015. GENERAC Web site. http://www.generac.com/Industrial/products/diesel-generators/configured/20kw-diesel-generator (accessed May 15, 2019).

GENERAC, SD035 Industrial Diesel Generator Set Data Sheet, 2017a. GENERAC Web site. http://www.generac.com/Industrial/products/diesel-generators/configured/35kw-diesel-generator (accessed May 15, 2019).

GENERAC, SG035 Industrial Spark-Ignited Generator Set Data Sheet, 2017b. GENERAC Web site. http://www.generac.com/Industrial/products/gaseous-generators/configured/35kw-gaseous-generator (accessed May 15, 2019).

GENERAC, SD040 Industrial Diesel Generator Set Data Sheet, 2017c. GENERAC Web site. http://www.generac.com/Industrial/products/diesel-generators/configured/40kw-diesel-generator (accessed May 15, 2019).

Gilron, J., Song, L., Sirkar, K.K., 2007. Design for cascade of crossflow direct contact membrane distillation. *Ind. Chem. Eng. Res.* 46, 2324-2334.

Halliburton, HT-2000 Pump Trailer (FPR-I), 2012. Halliburton Web site. https://www.halliburton.com/content/dam/ps/public/pe/contents/Data_Sheets/web/H/H09147-HT-2000-Pump-Trailer-SDS.pdf accessed Apr 7, 2019).

Higley, D. K., Cox, D. O., 2007. *Oil and gas exploration and development along the front range in the Denver Basin of Colorado, Nebraska, and Wyoming*, in Higley, D.K., compiler, Petroleum systems and assessment of undiscovered oil and gas in the Denver Basin Province, Colorado, Kansas, Nebraska, South Dakota, and Wyoming - USGS Province 39: U.S. Geological Survey Digital Data Series DDS-69-P, ch. 2, 41 p.

Kahrilas, G. A., Blotevogel, J., Corrin, E. R., Borch, T., 2016. Downhole transformation of the hydraulic fracturing fluid biocide glutaraldehyde: Implications for flowback and produced water quality. *Environ. Sci. Technol. 50* (20), 11414-11423.

Kohler, Model 15REOZK Diesel Generator Set Data Sheet, 2018a. Kohler Web site. http://www.kohlerpower.sg/onlinecatalog/pdf/g5434.pdf (accessed May 15, 2019).

Kohler, Model 20REOZK Diesel Generator Set Data Sheet, 2018b. Kohler Web site. http://resources.kohler.com/power/kohler/industrial/pdf/g5435.pdf?_ga=2.84671577.1951556154.1565966812-1256517797.1565966812 (accessed May 15, 2019).

Kohler, Model 40REOZK Diesel Generator Set Data Sheet, 2018c. Kohler Web site. http://www.kohlerpower.sg/onlinecatalog/pdf/g5437.pdf (accessed May 15, 2019).

Kohler, Model KG40 Gas Generator Set Data Sheet, 2018d. Kohler Web site. http://www.kohlerpower.sg/onlinecatalog/pdf/KG40.pdf (accessed May 15, 2019).

Kohler, Model 50 REOZK Diesel Generator Set Data Sheet, 2018e. Kohler Web site. http://www.kohlerpower.sg/onlinecatalog/pdf/g5438.pdf (accessed May 15, 2019).

U.S. Energy Information Administration, 2019. Colorado Heat Content of Natural Gas Deliveries to Consumers. U.S. EIA Web site. https://www.eia.gov/dnav/ng/hist/nga_epg0_vgth_sco_btucfa.htm (accessed Jul 29, 2019).

Appendix B

Waste heat estimation from data sheets

A summary of heat balance data from industry standard data sheets is provided for engines located at NGCSs in Weld County, CO (Table B1). Engines located on-site at the 35 NGCSs used in this study were determined from documents found in the Colorado Department of Public Health and Environment (CDPHE) air quality control database (CDPHE, 2020). This allowed for the estimation of waste heat available from engines located at each NGCS.

Table B1. Summary of industry standard data sheets for engines to power natural gas compressor stations for Weld County, CO (Caterpillar 2009a-b, 2010a-d, 2011a-b, 2012, 2013;Waukesha 2011a-d, 2013a-b)

Manufacturer	Model #	Load	Power	Power	Coolant Heat	Exhaust Heat	Waste Heat
-	-	%	kW	HP	kW	kW	kW
CAT	G3508	100	500	670	399.8	481.9	881.7
		75	375	502	338.1	372.8	710.9
CAT	G3512 LE	100	641	860	602.5	503.6	1106.1
		75	481	645	488.3	376.2	864.5
CAT	G3516B LE	100	1029	1380	761.5	1098	1859.5
CAT	G3606 LE	100	1368	1835	590	1334	1924
		75	1026	1376	427	1061	1488
CAT	G3608 LE	100	1767	2370	717	1783	2500
		75	1326	1728	503	1437	1940
CAT	G3612 LE	100	2647	3550	1107	2664	3771
		75	1985	2663	798	2132	2930
CAT	G3616	100	3531	4735	1444	3609	5053
		75	2648	3551	1009	2928	3937
WAUKESHA	5790G	100	550	738	609	365	974
WAUKESHA	7042G	100	764	1025	830	547	1377
		75	668	896	719	460	1179
WAUKESHA	7044GSI	100	1253	1680	1347	1143	2490
		75	1044	1400	1117	868	1985
WAUKESHA	F18	100	330	400	293	237	530
		75	230	335	237	186	423
WAUKESHA	F3524	100	626	840	720	558	1278
		75	522	700	576	420	996
WAUKESHA	L36GSID	100	600	800	662	458	1120

Direct Contact Membrane Distillation model for evaluating energy consumption by MD treatment

To evaluate energy consumption for treating DJ Basin UOG wastewater via direct contact MD (DCMD), an Engineering Equation Solver (EES) model was developed (Figure B1). The detail of this model is fully described in our recent work (Robbins et al., 2020). The specific thermal energy consumption (STEC) range was 910 to 2,035 kJ kg^{-1} permeate (750-1,815 kJ kg^{-1} feedwater) from our DCMD model, corresponding to a GOR range of ~1-2.5. These values are used in the main text to estimate waste heat powered MD treatment capacity at each NCGS.

A thorough literature review was also performed to obtain the reported values of STEC and GOR for MD in literature (Table B2). According to the references in Table B2 (Khayet and Matsuura, 2011; Swaminathan et al., 2011; Summers et al., 2012; Qtaishat and Banat, 2013; Thiel et al., 2015; Lokare et al., 2017; Tavakkoli et al., 2017; Deshmukh et al., 2018; Kim et al., 2018; Schwantes et al., 2018; Ullah et al., 2018), a GOR range of 1-7.5 (or a STEC range of 300-2,260 kJ kg^{-1} permeate) is reported. As shown in Table B2, the GOR of several MD systems has been restrained to less than 4-6. Based on this literature review, a feasible high-end GOR of 5 was used in the current study to represent MD systems possessing well-designed system configuration with high treatment capacities (Deshmukh et al., 2018) and high efficiencies of heat recovery (e.g., multi-stage design (Gilron et al., 2007)). The justification of this GOR upper limit is also explained in the main text.

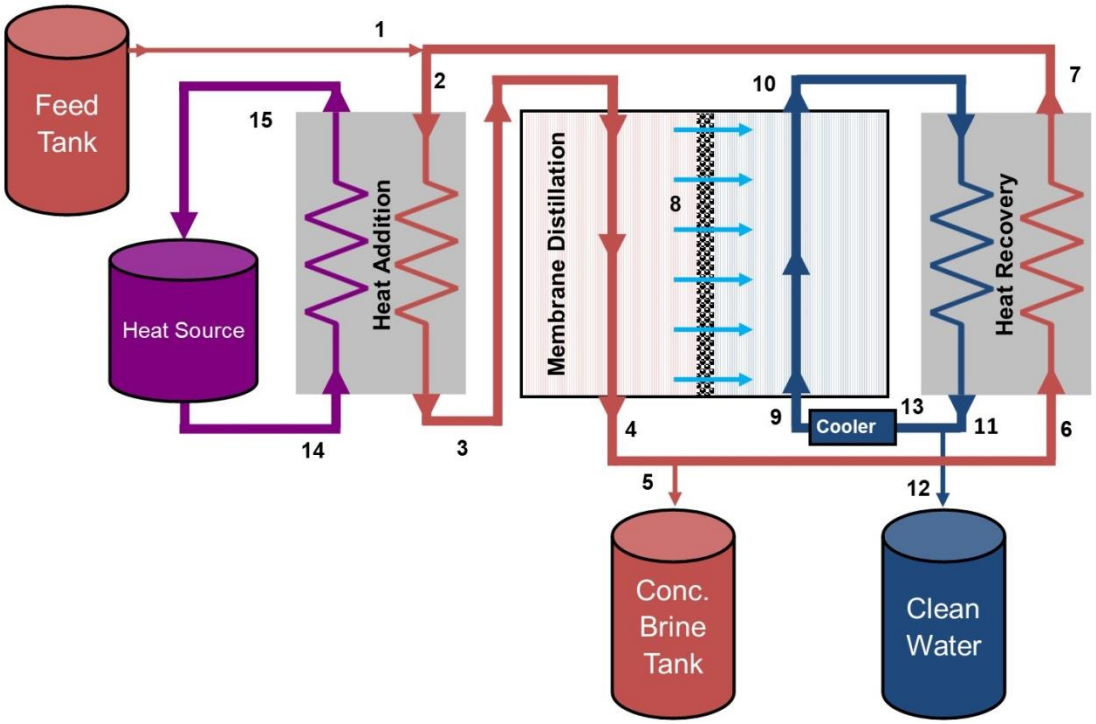

Figure B1. Schematic of our DCMD model flow diagram for treating UOG wastewater (as published in Robbins et al., 2020).

Table B2. Specific thermal energy consumption (STEC) and gain output ratio (GOR) reported in literature for membrane distillation.

Reference	STEC (kJ kg^{-1} of permeate)	GOR	Feed water characteristics	MD type/configuration
Deshmukh et al., 2018, *Energy and Environmental Science*	*550- 2,260* *200 - 750*	1 – 4 (1 m^3/day treatment capacity) 3 – 11 (100 m^3/day treatment capacity)	Not reported	Varying system capacities; no type reported
Lokare et al., 2017, *Desalination*	1,900 – 2,050	*1.1 – 1.2*	Marcellus Shale wastewater; 100,000 mg/L salinity	Direct contact MD (DCMD); 66% water recovery rate
Kim et al., 2018, *Water Research*	300	*7.5*	Eagle Ford Shale wastewater; 30,000 mg/L salinity	DCMD with crystallization; 74% water recovery rate;
Tavakkoli et al., 2017, *Desalination*	975 – 1,550	*1.5 – 2.3*	Marcellus Shale wastewater; 100,000 mg/L salinity	DCMD; 66% water recovery rate
Thiel et al., 2015, *Desalination*	~ 1,800 for feedwater salinity of 15% and brine salinity of 26%	1 – 2	Theoretical UOG wastewater	Permeate gap MD (PGMD); fixed brine salinity of 26%
Khayet and Matsuura, 2011, Elsevier	~ 2,170	*1.04*	Not reported	DCMD pilot plant
Summers et al., 2012, *Desalination*	*500 – 1,500* *565 – 2,260*	~ 1.5 – 4.5 for DCMD ~ 1 – 4 for air gap MD (AGMD)	Not reported	0.1 – 1 m^3 prototypes; based on effective length of membrane from 20 – 100 meters
Qtaishat et al., 2013, *Desalination*	725 - 900	*2.5 – 3.1*	Red Sea seawater	Solar vacuum MD (VMD) plant
Swaminathan et al., 2016, *J Membrane Science*	*375 - 550*	4 – 6 for MD in practice	Not reported	Various MD configurations based on values reported in literature
Schwantes et al., 2018, *Desalination*	*500 – 1,075*	2 – 4.4	Theoretical RO brine (70,000 – 240,000 mg/L salinity)	AGMD; 72% water recovery rate
Ullah et al., 2018, *Desalination*	360	*6.25*	Seawater	Theoretical DCMD plant; 60-80% recovery rate
Winter et al., 2011, *J Membrane Science*	470 - 750	*3 – 4.8*	Synthetic seawater	Spiral-wound PGMD module

Summary of transportation distance and cost at various scales

In this study, analyses of distance and cost associated with wastewater transportation to a CWT facility at an NGCS or for deep-well injection at a disposal well were completed at various scales. Table B3 summarizes the scales used in this study to provide the readers with easier and comparative information on our analyses.

Table B3. Summary of transportation distance and cost at various scales.

Weld County (all)	**# in Analysis**	**Transportation Distance (Miles)**	**Transportation Cost ($ per barrel)**
NGCS	35	5.64 million	$0.62
Disposal Wells	47	4.23 million	$0.57
Weld County (excl. NE Weld County)	**# in Analysis**	**Transportation Distance (Miles)**	**Transportation Cost ($ per barrel)**
NGCS	34	3.71 million	$0.58
Disposal Wells	42	3.84 million	$0.59
Western Weld County (w/o brine)	**# in Analysis**	**Transportation Distance (Miles)**	**Transportation Cost ($ per barrel)**
NGCS	10	945,000	$0.56
Disposal Wells	9	1.92 million	$0.69
Western Weld County (w/ brine)	**# in Analysis**	**Transportation Distance (Miles)**	**Transportation Cost ($ per barrel)**
NGCS	10	1.13 million	$0.56
Disposal Wells	9	1.92 million	$0.69

Cumulative distribution function plot of critical GOR values

Critical GOR values for the 35 CWT facilities at NGCSs are shown with a cumulative distribution function (CDF) plot (Figure B2). The GOR range from our DCMD model is 1.1 to 2.5, while the feasible high-end GOR is selected as 5 according to the literature (see justification in the main text). The dashed lines are shown to provide a visual representation of the probability for a CWT facility at an NGCS to either be below a GOR of 2.5, between a GOR of 2.5 and 5, or greater than a GOR of 5.

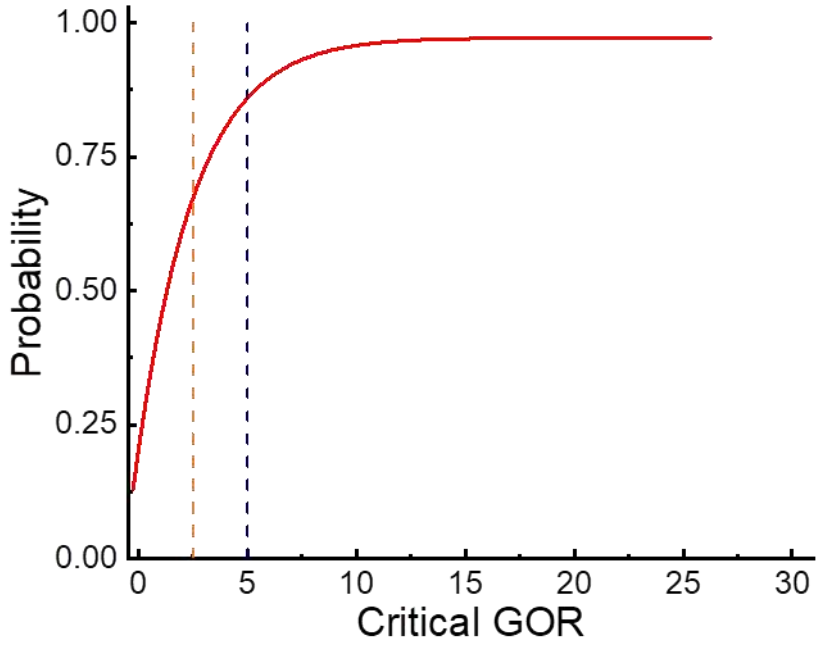

Figure B2. Cumulative distribution function (CDF) plot of critical GOR values required by CWT co-located at NGCSs to meet treatment demands. The high-end feasible value of GOR from our DCMD model and from the literature is represented with the orange (GOR = 2.5) and blue dashed (GOR = 5) lines, respectively.

Transportation distance and cost to NGCSs with a critical GOR less than 5

Analysis was conducted for the 30 NGCSs with a critical GOR less than 5, which is the upper limit of the feasible GOR according to the literature (the justification is described in the main text). The one-way transportation distance to move all UOG wastewater to these NGCSs was 886,000 miles (compared to 2.13 million miles to transport wastewater to the nearest disposal wells). The transportation cost for CWT at NGCSs (not factoring in MD brine transportation to the nearest disposal well) was $12.6 million as compared to $15.5 million for deep-well injection ($2.9 million cost savings for CWT, Figure B3). Considering the transportation of the MD brine to the nearest disposal wells reduced the cost savings for CWT to $700,000.

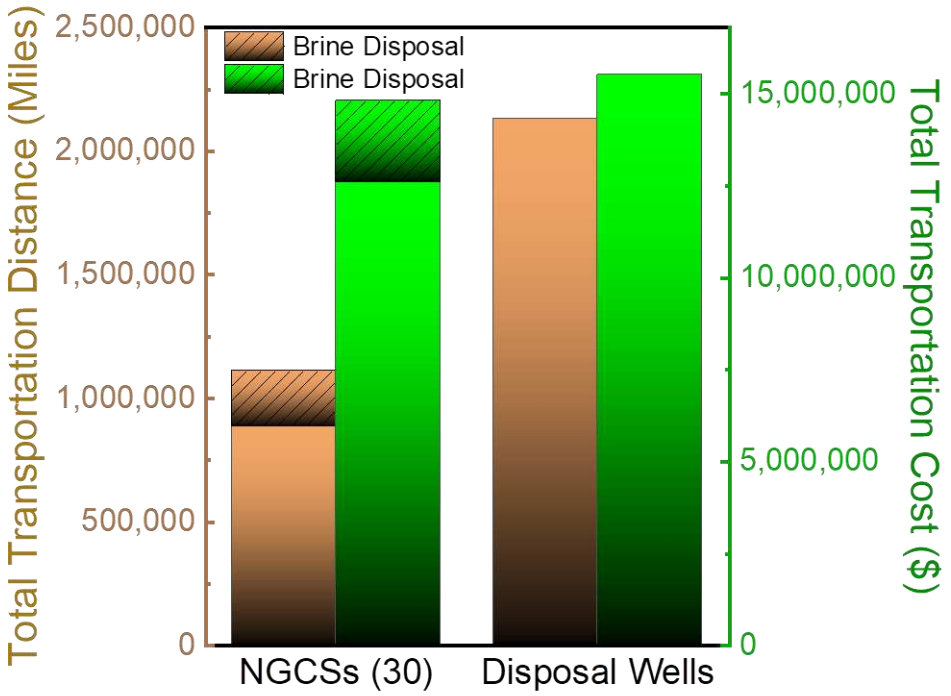

Figure B3. The total transportation distance and cost for transporting UOG wastewater from producing wells to either 30 NGCSs with a critical GOR less than 5 or to a disposal well.

References

Caterpillar, G3516B LE Gas Petroleum Engine. 2009a. Caterpillar web site. https://s7d2.scene7.com/is/content/Caterpillar/LEHW0037-00 (accessed 4/3/2020).

Caterpillar, G3406 Gas Petroleum Engine. 2009b. Caterpillar web site. https://s7d2.scene7.com/is/content/Caterpillar/LEHW0029-00 (accessed 4/3/2020).

Caterpillar, G3606 LE Gas Petroleum Engine. 2010a. Caterpillar web site. https://s7d2.scene7.com/is/content/Caterpillar/LEHW0039-02 (accessed 4/3/2020).

Caterpillar, G3608 LE Gas Petroleum Engine. 2010b. Caterpillar web site. https://s7d2.scene7.com/is/content/Caterpillar/LEHW0040-02 (accessed 4/3/2020).

Caterpillar, G3512 LE Gas Petroleum Engine. 2010c. Caterpillar web site. https://s7d2.scene7.com/is/content/Caterpillar/LEHW0035-01 (accessed 4/3/2020).

Caterpillar, G3612 LE Gas Petroleum Engine. 2010d. Caterpillar web site. https://s7d2.scene7.com/is/content/Caterpillar/LEHW0041-02 (accessed 4/3/2020).

Caterpillar, G3306B Gas Petroleum Engine. 2011a. Caterpillar web site. https://s7d2.scene7.com/is/content/Caterpillar/LEHW0111-01 (accessed 4/3/2020).

Caterpillar, CG137-12 Gas Petroleum Engine. 2011b. Caterpillar web site. https://s7d2.scene7.com/is/content/Caterpillar/LEHW0119-01 (accessed 4/3/2020).

Caterpillar, CG137-8 Gas Petroleum Engine. 2012. Caterpillar web site. https://s7d2.scene7.com/is/content/Caterpillar/LEHW0153-00 (accessed 4/3/2020).

Caterpillar, G3408C LE Gas Petroleum Engine. 2013. Caterpillar web site. https://s7d2.scene7.com/is/content/Caterpillar/LEHW0031-03 (accessed 4/3/2020).

Colorado Department of Public Health and Environment, 2020. CO Environ. Records. https://environmentalrecords.colorado.gov/HPRMWebDrawer/Search (accessed May 20, 2020).

Deshmukh, A., Boo, C., Karanikola, V., Lin, S., Straub, A.P., Tong, T., Warsinger, D.M., Elimelech, M., 2018. Membrane distillation at the water-energy nexus: Limits, opportunities, and challenges. *Energy Environ. Sci. 11* (5), 1177-1196.

Gilron, J., Song, L., Sirkar, K.K., 2007. Design for cascade of crossflow direct contact membrane distillation. *Ind. Chem. Eng. Res.* 46, 2324-2334.

Khayet, M.S., Matsuura, T., 2011. *Membrane Distillation: Principles and Applications*. Elsevier: Amsterdam.

Kim, J., Kim, J., Hong S., 2018. Recovery of water and minerals from shale gas produced water by membrane distillation crystallization. *Water Res.* 129, 447-459.

Lokare, O.R., Tavakkoli, S., Rodriguez, G., Khanna, V., Vidic, R.D., 2017. Integrating membrane distillation with waste heat from natural gas compressor stations for produced water treatment in Pennsylvania. *Desalination* 413, 144-153.

Qtaishat, M.R., Banat, F., 2013. Desalination by solar powered membrane distillation systems. *Desalination* 308, 186-197.

Robbins, C.A., Grauberger, B.M., Garland, S.D., Carlson, K.H., Lin, S., Bandhauer, T.M., Tong, T., 2020. On-site treatment capacity of membrane distillation powered by waste heat or natural gas for unconventional oil and gas wastewater in the Denver-Julesburg Basin. *Environ. Inter.,* 145, 106142.

Schwantes, R., Chavan, K., Winter, D., Felsmann, C., Pfaffereott, J., 2018. Techno-economic comparison of membrane distillation and MVC in a zero liquid discharge application. *Desalination* 428, 50-68.

Summers, E.K., Arafat, H.A., Lienhard, J.H., 2012. Energy efficiency comparison of single-stage membrane distillation (MD) desalination cycles in different configurations. *Desalination* 290, 54-66.

Swaminathan, J., Chung, H.W., Warsinger, D.M., Al-Marzooqi, F.A., Arafat, H.A., Lienhard, J.H., 2011. Energy efficiency of permeate gap and novel conductive gap membrane distillation. *J. Membr. Sci.* 375 (1-2), 104-112.

Tavakkoli, S., Lokare, O.R., Vidic, R.D., Khanna, V., 2017. A techno-economic assessment of membrane distillation for treatment of Marcellus shale produced water. *Desalination* 416, 24-34.

Thiel, G., Tow, E., Banchik, L., Chung, H.W., Leinhard, J., 2015. Energy consumption in desalinating produced water from shale oil and gas extraction. *Desalination* 366, 94-112.

Ullah, R., Khraisheh, M., Esteves, R.J., McLeskey, J.T., Al-Ghouti, M., Gad-el-Hak, M., Vahedi Tafreshi, H., 2018. Energy efficiency of direct contact membrane distillation. *Desalination* 433, 56-67.

Waukesha, 5790G Gas Petroleum Engine. 2011a. S & L Energie web site. http://sl-energie.com/index.php?id=16&L=1 (accessed 4/3/2020).

Waukesha, 7042G Gas Petroleum Engine. 2011b. S & L Energie web site. http://sl-energie.com/index.php?id=16&L=1 (accessed 4/3/2020).

Waukesha, F18 Gas Petroleum Engine. 2011c. S & L Energie web site. http://sl-energie.com/index.php?id=16&L=1 (accessed 4/3/2020).

Waukesha, L36SID Gas Petroleum Engine. 2011d. S & L Energie web site. http://sl-energie.com/index.php?id=16&L=1 (accessed 4/3/2020).

Waukesha, 7044GSI Gas Petroleum Engine. 2013a. S & L Energie web site. http://sl-energie.com/index.php?id=16&L=1 (accessed 4/3/2020).

Waukesha, F3524 Gas Petroleum Engine. 2013b. S & L Energie web site. http://sl-energie.com/index.php?id=16&L=1 (accessed 4/3/2020).

Appendix C

Table C1. Coagulation-flocculation jar test results

$FeCl_3$ Dose (mg/L)	Turbidity (NTUs)	Turbidity Removal (%)	pH
0	266	-	7.36
25	28.5	89.2	7.21
50	14.5	94.5	7.06
75	8.90	96.7	7.03
100	5.04	98.1	6.84
125	6.62	97.5	6.72
150	8.89	96.7	6.30

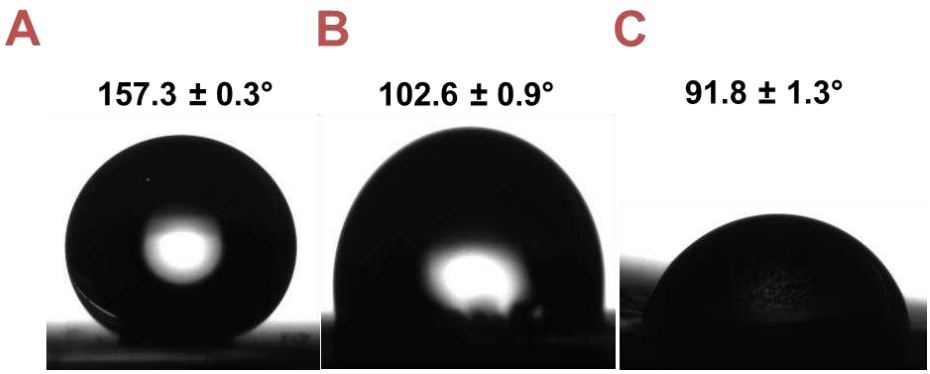

Figure C1. Omniphobicity of PVDF-SiNP-FAS membrane as demonstrated by in-air (A) water contact angle, (B) contact angle with 30% ethanol solution, and (C) contact angle with hexadecane.

Table C2. Surfactants identified as PEGs or within the PEG range reduced by full pretreatment

Time (min)	Measured Mass (*m* / *z*)	Kendrick Mass Defect	Putative Formula	Putative Identification	Error (ppm)	A / A_0 (volume)
2.204	363.1621	0.054	$C_{14} H_{28} O_9$	PEG-COOH-COOH	-1.16	~ 0
2.416	377.1421	0.082	$C_{14} H_{26} O_{10}$	PEG-COOH	0.61	~ 0
2.705	458.2952	-0.022	$C_{20} H_{40} O_{10}$		-1.85	~ 0
2.922	393.2088	0.025	$C_{16} H_{34} O_9$	PEG-EO8	-2.53	~ 0
3.217	407.1883	0.054	$C_{16} H_{32} O_{10}$	PEG-COOH	-1.38	~ 0
3.25	546.3475	-0.022	$C_{24} H_{48} O_{12}$		-1.88	0.24
3.374	421.1683	0.082	$C_{16} H_{30} O_{11}$	PEG-COOH-COOH	0.3	0.35
3.467	502.3212	-0.022	$C_{22} H_{44} O_{11}$		-2.44	~ 0
3.565	437.2349	0.025	$C_{18} H_{38} O_{10}$	PEG-EO9	-2.01	0.47
3.58	590.3739	-0.022	$C_{26} H_{52} O_{13}$		-1.49	~ 0
3.652	451.2148	0.054	$C_{18} H_{36} O_{11}$	PEG-COOH	-0.87	0.20
3.733	465.1946	0.082	$C_{18} H_{34} O_{12}$	PEG-COOH-COOH	0.43	0.37
3.75	634.3998	-0.022	$C_{28} H_{56} O_{14}$		-2.02	~ 0
3.808	481.262	0.025	$C_{20} H_{42} O_{11}$	PEG-EO10	0.52	0.32
3.878	495.2412	0.054	$C_{20} H_{40} O_{12}$	PEG-COOH	-0.3	0.21
3.947	509.221	0.082	$C_{20} H_{38} O_{13}$	PEG-COOH-COOH	0.63	0.42
3.977	520.3319	-0.022	$C_{22} H_{46} O_{12}$	PEG-EO11	-2.02	0.34
4.041	534.312	0.006	$C_{22} H_{44} O_{13}$	PEG-COOH	-0.37	0.21
4.07	678.4252	-0.021	$C_{30} H_{60} O_{15}$		-3.03	~ 0
4.106	548.2917	0.035	$C_{22} H_{42} O_{14}$	PEG-COOH-COOH	0.28	0.61
4.109	564.3582	-0.022	$C_{24} H_{50} O_{13}$	PEG-EO12	-1.73	0.37
4.15	416.7479	-0.5	$C_{42} H_{75} O_{13}$		-4.23	~ 0
4.169	578.3383	0.006	$C_{24} H_{48} O_{14}$	PEG-COOH	-0.29	0.24
4.217	590.3496	-0.021	$C_{26} H_{54} O_{14}$	PEG-EO13	-2.89	0.39
4.221	608.3837	-0.5	$C_{44} H_{79} O_{14}$		-3.6	~ 0
4.22	438.7609	-0.066	$C_{18} H_{36} O_6$		-4.66	0.82
4.277	366.2839	0.007	$C_{26} H_{52} O_{15}$	PEG-COOH	-1.19	0.31
4.287	460.7741	-0.5	$C_{46} H_{83} O_{15}$		-3.36	~ 0
4.311	652.4098	-0.021	$C_{28} H_{58} O_{15}$	PEG-EO14	-2.9	0.42

Table C2 (cont.). Surfactants identified as PEGs or within the PEG range reduced by full pretreatment

Time (min)	Measured Mass (*m / z*)	Kendrick Mass Defect	Putative Formula	Putative Identification	Error (ppm)	A / A_0 (volume)
4.347	287.1463	0.025	C_{12} H_{24} O_6		-0.24	0.37
4.371	666.3894	0.007	C_{28} H_{56} O_{16}	PEG-COOH	-2.34	0.44
4.394	701.392	0.026	C_{30} H_{62} O_{16}	PEG-EO15	-1.33	0.64
4.395	494.3015	-0.007	C_{44} H_{90} O_{23}	PEG-EO22	0.12	~ 0
4.452	710.4151	0.008	C_{30} H_{60} O_{17}		-2.76	0.25
4.469	740.4615	-0.021	C_{32} H_{66} O_{17}	PEG-EO16	-3.85	0.30
4.526	759.396	0.056	C_{32} H_{64} O_{18}	PEG-COOH	-3.78	~ 0
9.625	646.4368	-0.052	C_{30} H_{60} O_{13}	PEG-COOH	-0.97	0.86

Table C3. Surfactants identified as PEGs or within the PEG range unchanged by full pretreatment

Time (min)	Measured Mass (*m / z*)	Kendrick Mass Defect	Putative Formula	Putative Identification	Error (ppm)	A / A_0 (volume)
4.17	453.344	-0.074	C_{23} H_{48} O_8		3.31	> 0.95
4.232	592.3174	0.035	C_{24} H_{46} O_{15}	PEG-COOH-COOH	-0.76	> 0.95
4.338	636.3427	0.036	C_{26} H_{50} O_{16}	PEG-COOH-COOH	-1.94	> 0.95
4.43	680.3681	0.037	C_{28} H_{54} O_{17}		-3.07	> 0.95
4.514	724.3938	0.038	C_{30} H_{58} O_{18}	PEG-COOH-COOH	-3.68	> 0.95
4.604	599.3999	-0.043	C_{29} H_{58} O_{12}		-1.01	> 0.95
4.673	701.4933	-0.076	C_{34} H_{67} O_{13}		2.18	> 0.95
4.674	679.5107	-0.106	C_{38} H_{72} O_8		-1.58	> 0.95

Table C4. Surfactants identified as PPGs or within the PPG range reduced by full pretreatment

Time (min)	Measured Mass (*m / z*)	Kendrick Mass Defect	Putative Formula	Putative Identification	Error (ppm)	A / A_0 (volume)
5.543	387.2347	-0.004	$C_{18}H_{36}O_7$		-1.42	0.71
6.057	445.2761	-0.011	$C_{21}H_{42}O_8$		-2.47	0.71
6.345	505.3344	-0.034	$C_{24}H_{50}O_9$	PPG-8PO	-1.05	0.02
6.534	558.3831	-0.051	$C_{26}H_{52}O_{11}$		-2.86	0.54
6.754	558.4208	-0.088	$C_{27}H_{56}O_{10}$	PPG-9PO	-0.92	0.029
6.827	572.3994	-0.059	$C_{27}H_{54}O_{11}$		-2.16	0.15
6.941	393.3096	-0.075	$C_{20}H_{39}O_6$		2.99	~ 0
6.951	556.4036	-0.072	$C_{27}H_{54}O_{10}$		-3.86	0.72

Table C5. Surfactants identified as PPGs or within the PPG range unchanged by full pretreatment

Time (min)	Measured Mass (*m / z*)	Kendrick Mass Defect	Putative Formula	Putative Identification	Error (ppm)	A / A_0 (volume)
4.273	273.1675	-0.005	$C_{12}H_{26}O_5$	PPG-4PO	0.79	> 0.95
4.911	331.2093	-0.012	$C_{15}H_{32}O_6$	PPG-5PO	0.54	> 0.95
5.441	389.2511	-0.019	$C_{18}H_{38}O_7$	PPG-6PO	-0.17	> 0.95
5.91	447.2929	-0.027	$C_{21}H_{44}O_8$	PPG-7PO	-0.24	> 0.95
5.91	447.2929	-0.027	$C_{21}H_{44}O_8$	PPG-7PO	-0.24	> 0.95
6.433	519.3131	-0.004	$C_{24}H_{48}O_{10}$		-2.05	> 0.95
6.76	602.4454	-0.087	$C_{29}H_{60}O_{11}$		-3.36	> 0.95
7.195	630.4409	-0.066	$C_{30}H_{60}O_{12}$		-2.59	> 0.95
8.661	674.5028	-0.101	$C_{33}H_{68}O_{12}$	PPG-11PO	-3.77	> 0.95
9.099	732.545	-0.109	$C_{36}H_{74}O_{13}$	PPG-12PO	-2.8	> 0.95
9.42	790.5864	-0.116	$C_{39}H_{80}O_{14}$	PPG-13PO	-3.16	> 0.95

Table C6. Surfactants identified as AEOs or within the AEO range reduced by full pretreatment

Time (min)	Measured Mass (*m / z*)	Kendrick Mass Defect	Putative Formula	Putative Identification	Error (ppm)	A / A_0 (volume)
7.537	544.4036	-0.079	$C_{26}H_{54}O_{10}$	C8-EO9	-4.21	0.15
7.579	302.3047	-0.125	$C_{18}H_{36}O_2$		-2.82	0.89
7.975	258.2784	-0.125	$C_{16}H_{32}O$		-3.02	0.93
8.258	748.5396	-0.094	$C_{36}H_{74}O_{14}$	C10-EO13	-2.97	0.93
8.367	630.44	-0.065	$C_{30}H_{60}O_{12}$		-4.45	0.04

Table C7. Surfactants identified as AEOs or within the AEO range unchanged by full pretreatment

Time (min)	Measured Mass (*m / z*)	Kendrick Mass Defect	Putative Formula	Putative Identification	Error (ppm)	A / A_0 (volume)
6.386	588.4296	-0.079	$C_{28}H_{58}O_{11}$	C8-EO10	-4.54	> 0.95
6.433	519.3131	-0.004	$C_{24}H_{48}O_{10}$		-2.05	> 0.95
7.904	690.4975	-0.086	$C_{33}H_{68}O_{13}$		-3	> 0.95
7.916	646.4714	-0.086	$C_{31}H_{64}O_{12}$		-3.88	> 0.95
7.948	514.3935	-0.087	$C_{25}H_{52}O_9$		-3.44	> 0.95
7.974	343.2445	-0.04	$C_{17}H_{36}O_5$		-3.61	> 0.95
8.277	704.5132	-0.094	$C_{34}H_{70}O_{13}$	C10-EO12	-3.65	> 0.95
8.293	660.4869	-0.094	$C_{32}H_{66}O_{12}$	C10-EO11	-4.12	> 0.95
8.331	572.4342	-0.093	$C_{28}H_{58}O_{10}$	C10-EO9	-4.93	> 0.95
8.349	528.4092	-0.095	$C_{26}H_{54}O_9$	C10-EO8	-3.33	> 0.95
8.368	484.3831	-0.095	$C_{24}H_{50}O_8$	C10-EO7	-3.43	> 0.95
8.401	401.2858	-0.047	$C_{20}H_{42}O_6$	C10-EO5	-4.14	> 0.95
8.416	357.26	-0.047	$C_{18}H_{38}O_5$	C10-EO4	-3.79	> 0.95
8.524	848.6285	-0.123	$C_{42}H_{86}O_{15}$		-0.97	> 0.95
8.685	806.5834	-0.103	$C_{39}H_{80}O_{15}$		-0.83	> 0.95
8.707	762.5558	-0.102	$C_{37}H_{76}O_{14}$		-2.49	> 0.95
8.73	718.5293	-0.101	$C_{35}H_{72}O_{13}$		-3.03	> 0.95

Table C8. Surfactants identified as NPEOs or within the NPEO range reduced by full pretreatment

Time (min)	Measured Mass (*m / z*)	Kendrick Mass Defect	Putative Formula	Putative Identification	Error (ppm)	A / A_0 (volume)
8.806	586.4514	-0.102	$C_{29}H_{60}O_{10}$		-2.19	0.90
8.833	542.4255	-0.103	$C_{27}H_{56}O_{9}$		-1.84	0.87
9.051	560.373	-0.039	$C_{59}H_{106}O_{19}$		-1.81	0.87
9.129	954.6539	-0.085	$C_{45}H_{92}O_{19}$		-3.35	0.93
9.16	649.4432	-0.056	$C_{41}H_{60}O_{6}$		-2.77	0.94
9.171	910.6283	-0.086	$C_{43}H_{88}O_{18}$		-3.41	0.92
9.214	670.4544	-0.055	$C_{65}H_{124}O_{25}$		-1.79	~ 0
9.315	868.5976	-0.08	$C_{44}H_{82}O_{15}$		-2.08	0.93
9.317	778.55	-0.086	$C_{37}H_{76}O_{15}$		-2.84	0.94
9.571	690.4621	-0.051	$C_{32}H_{64}O_{14}$		-1.98	0.83
9.682	602.4115	-0.053	$C_{28}H_{56}O_{12}$		-0.33	0.87
9.842	938.6595	-0.101	$C_{45}H_{92}O_{18}$		-3.13	0.73
9.891	894.6338	-0.101	$C_{43}H_{88}O_{17}$		-3	0.66
9.941	850.6096	-0.103	$C_{41}H_{84}O_{16}$		-0.94	0.82
10.018	846.5612	-0.057	$C_{44}H_{76}O_{14}$		-1.12	0.94
10.07	802.5344	-0.057	$C_{42}H_{72}O_{13}$		-0.85	0.90
10.219	685.4671	-0.059	$C_{39}H_{66}O_{8}$		-2.15	0.92
10.259	656.1168	0.274	$C_{32}H_{25}O_{14}$		-0.64	0.92
10.28	641.4413	-0.059	$C_{37}H_{62}O_{7}$		-1.2	0.91
10.322	389.2657	-0.034	$C_{30}H_{21}O_{13}$		-0.76	0.90
10.343	764.5519	-0.097	$C_{35}H_{58}O_{6}$		-2.4	0.91
10.386	685.4671	-0.059	$C_{33}H_{54}O_{6}$		-3.73	0.91
10.387	720.5258	-0.097	$C_{28}H_{17}O_{12}$		-2.08	0.89
10.409	641.4413	-0.059	$C_{78}H_{156}O_{32}$		-0.55	~ 0
10.41	676.4995	-0.097	$C_{33}H_{54}O_{5}$		-2.38	~ 0
10.421	613.4084	-0.043	$C_{43}H_{80}O_{13}$		-1.04	0.76
10.556	569.3813	-0.042	$C_{39}H_{72}O_{11}$		-2.13	0.80
10.623	442.3516	-0.088	$C_{37}H_{68}O_{10}$		-1.38	0.85

Table C8 (cont.). Surfactants identified as NEPOs or within the NPEO range reduced by full pretreatment

Time (min)	Measured Mass (*m / z*)	Kendrick Mass Defect	Putative Formula	Putative Identification	Error (ppm)	A / A_0 (volume)
10.693	646.4881	-0.059	$C_{35}H_{64}O_9$		-1.9	0.90
10.765	1006.722	-0.056	$C_{50}H_{100}O_{18}$		-2.84	0.87
10.766	602.4618	-0.096	$C_{33}H_{60}O_8$		-1.61	0.92
10.792	962.6963	-0.103	$C_{48}H_{96}O_{17}$		-2.16	0.89
10.821	918.6706	-0.096	$C_{46}H_{92}O_{16}$		-1.75	0.87
10.851	874.6451	-0.096	$C_{44}H_{88}O_{15}$		-1.58	0.91
10.881	830.6185	-0.103	$C_{42}H_{84}O_{14}$		-1.68	0.84
10.911	786.5936	-0.096	$C_{40}H_{80}O_{13}$		-0.41	0.89
10.944	742.5672	-0.122	$C_{38}H_{76}O_{12}$		0.24	0.88
10.975	698.5415	-0.103	$C_{36}H_{72}O_{11}$		-0.01	0.80
11.009	654.5139	-0.123	$C_{34}H_{68}O_{10}$		-1.29	0.80
11.043	610.4878	-0.124	$C_{32}H_{64}O_9$		-1.74	0.88
11.079	566.4616	-0.104	$C_{30}H_{60}O_8$		-2.12	0.83

Table C9. Surfactants identified as NPEOs or within the NPEO range unchanged by full pretreatment

Time (min)	Measured Mass (*m / z*)	Kendrick Mass Defect	Putative Formula	Putative Identification	Error (ppm)	A / A_0 (volume)
8.78	630.4768	-0.101	$C_{31}H_{64}O_{11}$		-3.23	> 0.95
8.794	688.4827	-0.073	$C_{33}H_{66}O_{13}$		-1.42	> 0.95
8.842	600.4303	-0.073	$C_{29}H_{58}O_{11}$		-3.69	> 0.95
8.859	498.3992	-0.102	$C_{25}H_{52}O_{8}$		-1.91	> 0.95
8.885	454.3731	-0.103	$C_{23}H_{48}O_{7}$		-1.88	> 0.95
8.914	415.3022	-0.055	$C_{21}H_{44}O_{6}$		-2.02	> 0.95
8.92	898.609	-0.074	$C_{45}H_{84}O_{16}$	NP-EO15	-1.79	> 0.95
8.929	371.2759	-0.055	$C_{19}H_{40}O_{5}$		-2.58	> 0.95
8.944	327.2497	-0.055	$C_{17}H_{36}O_{4}$		-2.51	> 0.95
8.963	854.5808	-0.072	$C_{43}H_{80}O_{15}$	NP-EO14	-3.32	> 0.95
9.012	810.5551	-0.072	$C_{41}H_{76}O_{14}$	NP-EO13	-3.07	> 0.95
9.065	766.5293	-0.073	$C_{39}H_{72}O_{13}$	NP-EO12	-2.86	> 0.95
9.12	722.5033	-0.073	$C_{37}H_{68}O_{12}$	NP-EO11	-2.66	> 0.95
9.178	678.4768	-0.073	$C_{35}H_{64}O_{11}$	NP-EO10	-3.48	> 0.95
9.216	866.6034	-0.087	$C_{41}H_{84}O_{17}$		-1.56	> 0.95
9.239	634.4507	-0.073	$C_{33}H_{60}O_{10}$	NP-EO9	-3.38	> 0.95
9.264	822.5768	-0.087	$C_{39}H_{80}O_{16}$		-1.8	> 0.95
9.265	912.6223	-0.079	$C_{46}H_{86}O_{16}$		-3.42	> 0.95
9.306	590.4248	-0.073	$C_{31}H_{56}O_{9}$	NP-EO8	-3.51	> 0.95
9.369	824.572	-0.081	$C_{42}H_{78}O_{14}$		-1.75	> 0.95
9.376	546.3987	-0.073	$C_{29}H_{52}O_{8}$	NP-EO7	-3.75	> 0.95
9.425	780.5456	-0.081	$C_{40}H_{74}O_{13}$	NP-EO6	-1.8	> 0.95
9.451	502.3731	-0.074	$C_{27}H_{48}O_{7}$		-2.05	> 0.95
9.463	968.6688	-0.092	$C_{46}H_{94}O_{19}$		-3.17	> 0.95
9.484	736.5196	-0.081	$C_{38}H_{70}O_{12}$		-1.7	> 0.95
9.51	924.6441	-0.094	$C_{44}H_{90}O_{18}$		-2.41	> 0.95

Table C9 (cont.). Surfactants within the NPEO range unchanged by full pretreatment

Time (min)	Measured Mass (*m / z*)	Kendrick Mass Defect	Putative Formula	Putative Identification	Error (ppm)	A / A_0 (volume)
9.514	734.4888	-0.051	$C_{34}H_{68}O_{15}$	NP-EO5	-1.98	> 0.95
9.533	458.3463	-0.073	$C_{25}H_{44}O_{6}$		-2.89	> 0.95
9.546	692.4932	-0.081	$C_{36}H_{66}O_{11}$		-2.03	> 0.95
9.555	494.3509	-0.057	$C_{49}H_{92}O_{17}$		0.04	> 0.95
9.556	880.6183	-0.094	$C_{42}H_{86}O_{17}$		-2.3	> 0.95
9.606	926.6399	-0.088	$C_{47}H_{88}O_{16}$		-2.05	> 0.95
9.607	836.5923	-0.094	$C_{40}H_{82}O_{16}$		-1.92	> 0.95
9.614	648.4669	-0.081	$C_{34}H_{62}O_{10}$		-2.17	> 0.95
9.659	792.5661	-0.094	$C_{38}H_{78}O_{15}$		-2.69	> 0.95
9.659	882.6133	-0.088	$C_{45}H_{84}O_{15}$		-1.91	> 0.95
9.684	604.4411	-0.081	$C_{32}H_{58}O_{9}$		-1.71	> 0.95
9.714	838.5878	-0.088	$C_{43}H_{80}O_{14}$		-1.41	> 0.95
9.745	552.3762	-0.047	$C_{59}H_{106}O_{18}$		-3.36	> 0.95
9.758	560.4152	-0.082	$C_{30}H_{54}O_{8}$		-1.32	> 0.95
9.772	794.5619	-0.089	$C_{41}H_{76}O_{13}$		-1.12	> 0.95
9.834	750.5359	-0.089	$C_{39}H_{72}O_{12}$		-0.74	> 0.95
9.838	516.3892	-0.082	$C_{28}H_{50}O_{7}$		-0.92	> 0.95
9.898	706.5094	-0.089	$C_{37}H_{68}O_{11}$		-1.31	> 0.95
9.924	472.3628	-0.082	$C_{26}H_{46}O_{6}$		-1.24	> 0.95
9.941	940.655	-0.095	$C_{48}H_{90}O_{16}$		-2.19	> 0.95
9.995	896.6292	-0.095	$C_{46}H_{86}O_{15}$		-1.88	> 0.95
10.018	428.3363	-0.081	$C_{24}H_{42}O_{5}$		-2.09	> 0.95
10.051	852.6038	-0.096	$C_{44}H_{82}O_{14}$		-1.12	> 0.95
10.11	808.5776	-0.096	$C_{42}H_{78}O_{13}$		-1.07	> 0.95
10.123	389.2657	-0.034	$C_{22}H_{38}O_{4}$		-1.56	> 0.95
10.171	764.5519	-0.097	$C_{40}H_{74}O_{12}$		-0.45	> 0.95
10.202	530.4036	-0.088	$C_{29}H_{52}O_{7}$		-3.39	> 0.95
10.236	720.5258	-0.097	$C_{38}H_{70}O_{11}$		-0.8	> 0.95
10.302	676.4995	-0.097	$C_{36}H_{66}O_{10}$		-0.73	> 0.95
10.32	613.4084	-0.043	$C_{35}H_{58}O_{7}$		-2.92	> 0.95

Table C9 (cont.). Surfactants within the NPEO range unchanged by full pretreatment

Time (min)	Measured Mass (*m / z*)	Kendrick Mass Defect	Putative Formula	Putative Identification	Error (ppm)	A / A_0 (volume)
10.372	632.4732	-0.088	$C_{34}H_{62}O_9$		-0.56	> 0.95
10.395	442.3516	0.274	$C_{25}H_{44}O_5$		0.22	> 0.95
10.446	558.4466	0.274	$C_{32}H_{58}O_8$		-0.95	> 0.95
10.49	778.5665	-0.059	$C_{41}H_{76}O_{12}$		-4.38	> 0.95
10.522	544.4204	-0.097	$C_{30}H_{54}O_7$		-1.03	> 0.95
10.602	500.3939	0.275	$C_{28}H_{50}O_6$		-1.66	> 0.95
10.681	456.3676	-0.074	$C_{26}H_{46}O_5$		-1.79	> 0.95
10.843	558.4361	-0.103	$C_{31}H_{56}O_7$		-0.67	> 0.95
10.92	514.4095	-0.103	$C_{29}H_{52}O_6$		-1.06	> 0.95

Appendix D

Table D1. Produced water reuse standards for slickwater hydraulic fracturing fluids in the Permian basin from 5 different operators (Patton, 2018)

Parameter	A	B	C	D	E
Chlorides (mg/L)	140,000	100,000	N/A	85,000	N/A
Total Hardness (mg/L)	50,000	N/A	N/A	20,000	Ca – 2000 Mg – 2000
Sulfides (mg/L)	0	0	0	0	0
Iron (mg/L)	25	10	10	10	10
Oil (mg/L)	100	50	40	10	N/A
TSS[a] (mg/L or particle size[b])	100	100 μ[b]	50	5 μ[b]	N/A
pH	6.5 – 7.5	6 - 8	6.5 – 7.5	6 - 7	6 - 8
Bacteria (CFU/mL)	100	0	0	1,000 GHB[c] 100 SRB[d] 100 APB[e]	10,000

[a] TSS: total suspended solids;

[b] Some operators required no particles greater than certain particle sizes;

[c] GHB: general heterotrophic bacteria;

[d] SRB: sulfate reducing bacteria;

[e] APB: acid producing bacteria.

Table D2. NPDES Water Quality Standards from 12 NPDES Permits (7 from Colorado, 2 from Pennsylvania, and 3 from Texas) for important parameters in unconventional shale oil and gas wastewater (CDPHE, 2011, 2012a-d, 2015, 2017; PADEP, 2016, 2018; USEPA Region 6, 2018a-c). The number in the parenthesis indicates the number of permits with the regulated value out of the total permits in the corresponding state. Otherwise, the regulated values (including N/A and report) are included in all the permits of the state.

Parameter	Colorado		Pennsylvania		Texas		Reported PW Quality*
General Parameters of Concern	**30 Day Avg.**	**Daily Max.**	**30 Day Avg.**	**Daily Max.**	**30 Day Avg.**	**Daily Max.**	**Range**
Flow (MGD)	0.0072 – 1.3	Report	Report	Report or 0.08	0.019 – 0.030	N/A	N/A
BOD_5 (mg/L)	N/A	N/A	53	163	N/A	N/A	2 – 12,400
COD (mg/L)	N/A	N/A	N/A	N/A	N/A	100	18.7 – 79,000
TSS (mg/L)	30	N/A	11.3 – 61.3	29.6 – 216	N/A	N/A	2 – 21,820
TDS (mg/L)	Report or 3,500 (1/7)	Report	500	1000	Report	Report	1,755 – 398,024
Chlorides (mg/L)	N/A or 250 (3/7)	Report	250	500	Report	Report	16,000 – 188,728
Organic Parameters of Concern	**30 Day Avg.**	**Daily Max.**	**30 Day Avg.**	**Daily Max.**	**30 Day Avg.**	**Daily Max.**	**Range**
Oil and Grease (mg/L)	N/A	10	15 (1/2)	30 (1/2)	10	15	3 – 1,720
Benzene (µg/L)	Report or 2.2 (1/7)	5,300 (6/7)	Report (1/2)	N/A	N/A	Report	1 – 778,000
Toluene (µg/L)	Report or 510 (1/7)	17,500 (6/7)	N/A	N/A	N/A	Report	0.097 – 41,500
Ethylbenzene (µg/L)	Report or 530 (1/7)	32,000 (6/7)	N/A	N/A	N/A	Report	0 – 399,840
Total Xylenes (µg/L)	Report or 10,000 (1/7)	N/A	N/A	N/A	N/A	Report	0.043 – 1,670
o-Cresol (µg/L)	N/A	N/A	561	1920	Report	Report	Not Reported
2,4,6-Trichlorophenol (µg/L)	N/A	N/A	106	155	Report	Report	Not Reported
Phenol (µg/L)	N/A	N/A	1080	3650	Report	Report	Not Reported
Acetone (µg/L)	N/A	N/A	7970	30,200	N/A	N/A	27 – 21,700
Acetophenone (µg/L)	N/A	N/A	56.2	114	N/A	N/A	Not Reported
Bis(2-Ethylexyl) Phthalate (µg/L)	N/A	N/A	101 (1/2)	215 (1/2)	Report	Report	Not Reported
2-Butanone (µg/L)	N/A	N/A	1850	4810	N/A	N/A	Not Reported
Butyl Benzyl Phthalate (µg/L)	N/A	N/A	88.7 (1/2)	188 (1/2)	Report	Report	Not Reported
Carbazole (µg/L)	N/A	N/A	276 (1/2)	598 (1/2)	N/A	N/A	Not Reported
n-Decane (µg/L)	N/A	N/A	437 (1/2)	948 (1/2)	N/A	N/A	Not Reported
n-Octadecane (µg/L)	N/A	N/A	302 (1/2)	589 (1/2)	N/A	N/A	Not Reported
p-Cresol (µg/L)	N/A	N/A	205	698	N/A	N/A	Not Reported
Pyridine (µg/L)	N/A	N/A	182	370	N/A	N/A	Not Reported
Metal Parameters of Concern	**30 Day Avg.**	**Daily Max.**	**30 Day Avg.**	**Daily Max.**	**30 Day Avg.**	**Daily Max.**	**Range**
Aluminum, Total Recoverable (µg/L)	1,438 (4/7)	10,071 (4/7)	Report (1/2)	N/A	Report	Report	10 – 860,000
Antimony (µg/L)	Report	Report	31.2 (1/2)	111 (1/2)	Report	Report	Not Reported
Arsenic (µg/L)	Report	340 (4/7)	19.9 (1/2)	99.3 (1/2)	Report	Report	9 – 151
Barium (µg/L)	Report	Report	10,000	20,000	Report	Report	5 – 2.2 x 10^7
Beryllium (µg/L)	100 (6/7)	Report	N/A	N/A	Report	Report	0.21 – 80
Cadmium (µg/L)	0.77 – 0.97 (6/7)	5.4 – 9.1 (4/7)	52.2 (1/2)	172 (1/2)	Report	Report	0.19 - 100
Chromium, Total (µg/L)	N/A	N/A	10.2 (1/2)	167 (1/2)	Report	Report	0.84 – 2200

Cobalt (µg/L)	N/A	N/A	70.3 (1/2)	182 (1/2)	Report	Report	0.7 – 90,000
Copper (µg/L)	18 – 200 (6/7)	28 – 50 (4/7)	216 – 757	659 – 865	Report	Report	2.5 – 116,000
Iron, Total Recoverable (µg/L)	1,000 (4/7)	N/A	3,000 (1/2)	6,000 (1/2)	N/A	N/A	25 – 1.4 x 10^6
Lead (µg/L)	5.9 – 100 (6/7)	151 – 281 (4/7)	160 (1/2)	350 (1/2)	Report	Report	0.5 – 3,500
Manganese (µg/L)	2,145 – 2,618 (4/7)	3,882 – 4,305 (4/7)	2,000 (1/2)	4,000 (1/2)	N/A	N/A	0.01 – 73
Mercury (µg/L)	0.01 (4/7)	N/A	0.246 (1/2)	0.641 (1/2)	Report	Report	0 – 65
Nickel (µg/L)	101 – 200 (6/7)	912 – 1,513 (4/7)	309 (1/2)	794 (1/2)	Report	Report	1 – 19,200
Selenium (µg/L)	4.6 – 20 (6/7)	Report or 18.4 (4/7)	69.8 (1/2)	176 (1/2)	Report	Report	2.5 – 1,000
Silver (µg/L)	1.2 – 3.5 (4/7)	7.9 – 22 (4/7)	12.2 (1/2)	31.8 (1/2)	Report	Report	0.5 – 100
Strontium (µg/L)	N/A	N/A	10,000 (1/2)	20,000 (1/2)	N/A	N/A	11 – 1.61 x 10^6
Tin, Total (µg/L)	N/A	N/A	36.7 (1/2)	95.5 (1/2)	N/A	N/A	Not Reported
Titanium, Total (µg/L)	N/A	N/A	6.12 (1/2)	15.9 (1/2)	N/A	N/A	Not Reported
Thallium (µg/L)	15 (4/7)	N/A	N/A	N/A	Report	Report	Not Reported
Uranium (µg/L)	3,578 – 6,915 (4/7)	5,728 – 11,070 (4/7)	N/A	N/A	Report	Report	0.08 – 497
Vanadium (µg/L)	N/A	N/A	51.8 (1/2)	62.8 (1/2)	Report	Report	Not Reported
Zinc (µg/L)	243 – 2,000 (6/7)	281 – 467 (4/7)	252 – 420	497-657	Report	Report	0.005 – 247
Radionuclides of Concern	**30 Day Avg.**	**Daily Max.**	**30 Day Avg.**	**Daily Max.**	**30 Day Avg.**	**Daily Max.**	**Range**
Radium 226+228, Total (piC/L)	Report	5 (6/7)	N/A	N/A	N/A	Report	753 – 17,980

* Haluszczak et al., 2013; Esmaeilirad et al., 2015; Xiong et al., 2016; Bell et al., 2017; Lokare et al., 2017; Kim et al., 2018; Chang et al., 2019; Zhang et al., 2019

References

Patton, M. *Cost Effective Produced Water Reuse*. Proceedings of the 7th Annual Rocky Mountains Shale Water Congress, October, 24, 2018, Denver, CO.

Colorado Department of Public Health and Environment, CDPS Permit Number COG840001. Denver, CO, 2012a.

Colorado Department of Public Health and Environment, CDPS Permit Number COG840005. Denver, CO, 2012b.

Colorado Department of Public Health and Environment, CDPS Permit Number COG840007. Denver, CO, 2012c.

Colorado Department of Public Health and Environment, CDPS Permit Number COG840008. Denver, CO, 2012d.

Colorado Department of Public Health and Environment, CDPS Permit Number COG840004. Denver, CO, 2011.

Colorado Department of Public Health and Environment, CDPS Permit Number COG840009. Denver, CO, 2015.

Colorado Department of Public Health and Environment, CDPS Permit Number COG840002. Denver, CO, 2017.

Pennsylvania Department of Environmental Protection, NPDES Permit Number PA0263516. 2016.

Pennsylvania Department of Environmental Protection, NPDES Permit Number PA0232351, 2018.

USEPA Region 6, NPDES Draft Permit Number TX0134061. Dallas, TX, 2018a.

USEPA Region 6, NPDES Draft Permit Number TX0134062. Dallas, TX, 2018b.

USEPA Region 6, NPDES Draft Permit Number TX0134063. Dallas, TX, 2018c.

Bell, E. A.; Poynor, T. E.; Newhart, K. B.; Regnery, J.; Coday, B. D.; Cath, T. Y. Produced water treatment using forward osmosis membranes: Evaluation of extended-time performance and fouling. *Journal of Membrane Science* **2017,** *525*, 77-88.

Chang, H.; Li, T.; Liu, B.; Vidic, R. D.; Elimelech, M.; Crittenden, J. C. Potential and implemented membrane-based technologies for the treatment and reuse of flowback and produced water from shale gas and oil plays: A review. *Desalination* **2019,** *455*, 34-57.

Esmaeilirad, N.; Carlson, K.; Omur Ozbek, P. Influence of softening sequencing on electrocoagulation treatment of produced water. *J Hazard Mater* **2015,** *283*, 721-9.

Haluszczak, L. O.; Rose, A. W.; Kump, L. R. Geochemical evaluation of flowback brine from Marcellus gas wells in Pennsylvania, USA. *Applied Geochemistry* **2013,** *28*, 55-61.

Kim, J.; Kim, J.; Hong, S. Recovery of water and minerals from shale gas produced water by membrane distillation crystallization. *Water Res* **2018,** *129*, 447-459.

Lokare, O. R.; Tavakkoli, S.; Wadekar, S.; Khanna, V.; Vidic, R. D. Fouling in direct contact membrane distillation of produced water from unconventional gas extraction. *Journal of Membrane Science* **2017,** *524*, 493-501.

Xiong, B.; Zydney, A. L.; Kumar, M. Fouling of microfiltration membranes by flowback and produced waters from the Marcellus shale gas play. *Water Res* **2016,** *99*, 162-170.

Zhang, Z. Du, X.; Carlson, K.; Robbins, C.; Tong, T. Effective treatment of shale oil and gas produced water by membrane distillation coupled with precipitative softening and walnut shell filtration. *Desalination* **2019,** *454*, 82-90.